UNIVERSITY OF SOUTHAMPTON

FACULTY OF NATURAL AND ENVIRONMENTAL SCIENCES

School of Biological Sciences

The nematicide, Fluensulfone, alters auxin responses in *Arabidopsis*

Eleanor Kirby

Thesis for the degree of Doctor of Philosophy

January 2021

UNIVERSITY OF SOUTHAMPTON

ABSTRACT

FACULTY OF NATURAL AND ENVIRONMENTAL SCIENCES

School of Biological Sciences

Doctor of Philosophy

THE NEMATICIDE, FLUENSULFONE, ALTERS AUXIN RESPONSES IN *ARABIDOPSIS*

Eleanor Kirby

Plant parasitic nematode (PPN) species are estimated to cause a 12.3% annual yield reduction of economically important crops making it essential that new mechanisms are found to control these pests. The new generation nematicide, fluensulfone (Nimitz®), displays potent nematicidal activity towards PPNs, including root-knot nematode *Meloidogyne* spp. and potato cyst nematode, *G. pallida*. In comparison to phased out nematicides and existing organophosphate- and carbamate-based nematicides, fluensulfone has a significantly reduced environmental impact. The mode of action of fluensulfone remains to be elucidated but preliminary experiments indicated that fluensulfone had biological effects on *Arabidopsis thaliana*, we therefore used *Arabidopsis* as a system to identify the molecular targets of fluensulfone.

Application of exogenous fluensulfone resulted in reduced seedling growth in the light. However, application in the absence of light induced de-etiolation, characterized by inhibition of hypocotyl elongation, cotyledon opening and accumulation of the chlorophyll precursor, protochlorophyllide. Co-treatment with both natural (IAA) and synthetic auxins (1-NAA, 2,4-D) were able to partially rescue this phenotype, but application of other phytohormones did not. RNAseq analysis demonstrated differential expression of 7820 and 2666 genes following fluensulfone treatment in the light and dark, respectively. Functional analysis based on gene ontology (GO) terms indicated enrichment of auxin-associated terms within these differentially expressed gene sets and data set comparisons indicated significant overlap in gene expression profiles after treatment with various auxin related compounds. Three fluorescent reporter lines were also used to demonstrate a reduction in

auxin signalling at the root tip with auxin-induced degradation of the DII::VENUS reporter being prevented following fluensulfone treatment for as little as 15 minutes. Furthermore, comparisons with established auxin receptor antagonist, auxinole, displayed a similar de-etiolated phenotype and inhibition of the DII::VENUS reporter degradation. Together our results suggest that one primary effect of fluensulfone is a rapid alteration of the auxin response in *Arabidopsis*.

Table of Contents

List of figures **1**

List of tables **5**

Acknowledgements **7**

Definitions and Abbreviations **8**

Chapter 1: General introduction **13**

1.1 Nematodes as agricultural burdens **14**

1.1.1 An introduction to the Nematoda phylum 14

1.1.2 Plant parasitic nematode life cycle 16

1.1.2.1 Ectoparasites 18

1.1.2.3 Migratory endoparasites 18

1.1.2.4 Sedentary endoparasites 19

1.2 Plant and sedentary endoparasitic nematode interactions **21**

1.2.1 Stylet aperture 21

1.2.2 Hatching 21

1.2.3 Movement to the host plant 23

1.2.4 Movement into/through the host plant 23

1.2.5 Feeding site establishment 25

1.2.6 Plant parasitic nematode infection in *Arabidopsis* 27

1.3 Plant parasitic nematode control **28**

1.3.1 Chemical control as a means to reduce plant parasitic nematode populations 29

1.3.1.1 Fumigant nematicides 29

1.3.1.2 Non-fumigant nematicides 30

1.3.2 Alternative methods of control 32

1.4 Fluensulfone - A new option for chemical control of plant parasitic nematodes **34**

1.4.1 Efficacy against plant parasitic nematodes 34

1.4.2 Toxicity profile 37

1.4.3 Properties of FLS in the field 37

1.4.5 Mode of action studies 38

1.5 An introduction to *Arabidopsis* **39**

1.5.1 Basic physiology 40

1.5.2 Light detection in *Arabidopsis* 41

1.5.2.1 Phytochromes 42
1.5.2.2 Cryptochromes 44
1.5.2.3 Phototropins 44
1.5.2.4 Light signaling pathways 45
1.5.5 *Arabidopsis* phytohormones 47
1.5.5.1 Gibberellins 47
1.5.5.2 Ethylene 49
1.5.5.3 Brassinosteroids 52
1.5.6 Auxin 54
1.5.6.1 Auxin perception and signaling 55
1.5.6.2 The role of Aux/IAAs 58
1.5.6.3 Crosstalk between phytohormones 61
1.6 Project aims 62
Chapter 2: Materials and Methods 63
2.1 Plant material, growth conditions and treatments 64
2.2 Measurements of pigments 65
2.2.1 Chlorophyll and carotenoid extraction 65
2.2.2 Protochlorophyllide extraction 66
2.3 Forward genetic screen for FLS resistance 66
2.3.2 EMS mutagenesis 66
2.3.3 Determination of mutagen effectiveness 67
2.3.4 Screening M2 generation 67
2.3.5 Isolation of FLS resistant mutants 67
2.3.6 Back-crossing FLS resistant lines to WT 68
2.3.7 Physiological measurements of mature *Arabidopsis* plants 68
2.4 Imaging of auxin signaling by confocal microscopy 68
2.5 Gene expression analysis by quantitative real-time PCR (qPCR) 69
2.5.1 RNA isolation from seedlings 69
2.5.2 First strand cDNA synthesis 70
2.5.3 Quantitative real-time PCR 70
2.6 Transcriptome analysis 72
2.6.1 RNA sequencing 72
2.6.2 Differential Gene Expression Analysis 73
2.7 Quantification of endogenous phytohormones 74
2.7.1 Tissue details and shipping 74

Chapter 3: Characterising the effects of FLS on *Arabidopsis* physiology 75

3.1 Introduction 76

3.2 Results 79

3.2.1 FLS induces phytotoxicity in light conditions 79

3.2.2 FLS-induced phytotoxicity is reversible at low concentrations 84

3.2.3 Investigating the effects of post-germinative application of FLS 84

3.2.4 FLS induces a de-etiolated phenotype in the absence of light and perturbs subsequent chlorophyll accumulation in light 90

3.2.5 The role of HY5, HYH and PIF in FLS-induced de-etiolation 95

3.2.6 Application of exogenous epi-brassinolide and gibberellin was unable to reverse FLS-induced de-etiolation 96

3.2.7 Application of exogenous auxins was able to reverse features of FLS-induced de-etiolation 102

3.2.8 Ethylene precursor ACC can partially rescue FLS-induced de-etiolation 105

3.2.9 Transcriptomic analysis of the effect of FLS treatment 108

3.2.10 Endogenous phytohormone quantification 116

3.3 Discussion 118

3.3.1 FLS has a unique profile of effects under different growth conditions 118

3.3.2 FLS induces de-etiolation that is partially mediated by HY5 and HYH 119

3.3.3 Reversal of FLS induced de-etiolation is auxin specific 125

Chapter 4: The role of auxin in FLS action 129

4.1 Introduction 130

4.2 Results 132

4.2.1 Exogenous IAA displays a more robust rescue of FLS in the dark 132

4.2.2 IAA rescue of FLS-induced de-etiolation is not due to a delay in development 135

4.2.3 Auxin dependent gene expression is variable in light and dark 137

4.2.4 Auxin distribution and quantity is altered following long-term FLS exposure 140

4.2.5 Auxin signaling at the root tip is decreased rapidly upon FLS exposure 145

4.2.6 TIR1 antagonist, auxinole, phenocopies FLS 147

4.2.7 Auxin receptor mutants display de-etiolated phenotypes in the dark 152

4.2.8 Co-treatment with auxins protect seedlings and permits chlorophyll accumulation 153

4.2.9 Pre-treatment with auxins protect seedlings from FLS-induced protochlorophyllide accumulation 155

4.2.10 Seed treatment of FLS is phytotoxic to seedlings and reversible by auxin treatment ... 158

4.3 Discussion **163**

4.3.1 FLS and auxin present a dichotomous relationship dependent on light conditions 163

4.3.2 The role of FLS as an auxin receptor antagonist 166

4.3.3 Auxins may have a role in protecting against FLS phytotoxicity in the field 169

Chapter 5: A forward genetics approach to identify targets that facilitate FLS susceptibility **171**

5.1 Introduction **172**

5.2 Results **174**

5.2.1 Determination of mutagenesis and screening protocol 174

5.2.2 Isolation of FLS resistant mutants 175

5.2.3 Secondary screening of selected resistant lines 178

5.2.4 Characterizing the development of FLS-resistant lines 187

5.3 Discussion **190**

Chapter 6: General Discussion **194**

6.1 FLS acts to stabilize Aux/IAA proteins in *Arabidopsis* 195

6.2 Application of *Arabidopsis* mode of action to plant parasitic nematode species 197

6.3 The role of auxin in ameliorating FLS effects 199

6.4 Auxin and light signaling pathways are closely linked to regulate photomorphogenic growth 201

6.5 Conclusions and future research directions 203

Appendix : Supplementary data **204**

List of references **233**

List of figures

Figure 1.1 Life cycle of *C. elegans*..... 15

Figure 1.2 Phylogeny of the Nematoda phylum..... 17

Figure 1.3 Life cycle of a cyst nematode..... 20

Figure 1.4 Chemical structure of FLS..... 34

Figure 1.5 Phenotypes of (A) Light-grown de-etiolated seedlings and (B) Dark-grown etiolated seedlings..... 42

Figure 1.6 Ethylene biosynthesis pathway..... 51

Figure 1.7 Brassinosteroid signalling pathway..... 52

Figure 1.8 The chemical structures of natural/synthetic auxins and anti-auxins..... 56

Figure 1.9 Subunit structure of an SCF complex..... 57

Figure 1.10 Auxin signalling in plants..... 60

Figure 2.1 Thermal profile of qPCR reactions..... 72

Figure 3.1 FLS reduces growth of *Arabidopsis* seedlings..... 80

Figure 3.2 FLS reduces growth of *Arabidopsis* seedlings under red (RL) and blue light (BL)..... 81

Figure 3.3 Intensity of WL affects growth..... 82

Figure 3.4 FLS has reduced phytotoxicity in the soil environment..... 83

Figure 3.5 The pre-germinative effect of FLS on *Arabidopsis* seedlings..... 85

Figure 3.6 FLS treatment from germination reduces growth that is non-recoverable. 86

Figure 3.7 The post-germinative effect of FLS on *Arabidopsis* seedlings..... 87

Figure 3.8 Low concentrations of FLS treatment 3 days after germination causes a transient increase in growth..... 88

Figure 3.9 Low concentrations of FLS treatment 7 days after germination causes a transient increase in growth..... 89
Figure 3.10 Exogenous FLS induces a de-etiolated phenotype in the dark..... 91
Figure 3.11 FLS induces the expression of light-regulated genes in the dark..... 93
Figure 3.12 FLS perturbs chlorophyll accumulation when seedlings are transferred to light..... 94
Figure 3.13 FLS-induced de-etiolation is partially mediated by HY5/HYH..... 97
Figure 3.14 FLS-induced de-etiolation is not mediated by PIFs..... 98
Figure 3.15 Exogenous epi-brassinolide (EBR) is unable to rescue FLS induced a de-etiolation..... 99
Figure 3.16 Exogenous gibberellic acid (GA) is unable to rescue FLS induced a de-etiolation in the dark..... 100
Figure 3.17 Exogenous gibberellic acid (GA) is able to rescue paclobutrazol (PAC) - induced de-etiolation in the dark..... 101
Figure 3.18 The natural auxin, Indole-3-acetic acid (IAA), can reverse FLS-induced de-etiolation..... 103
Figure 3.19 The synthetic auxins, 1-NAA and 2,4-D, are able to reverse FLS-induced de-
etiolation..... 104
Figure 3.20 Ethylene pre-cursor, ACC cannot reverse FLS-induced de-etiolation..... 106
Figure 3.21 Auxin and ethylene are partially additive in the reversal of FLS-induced de-etiolation..... 107
Figure 3.22 The effect of FLS on the *Arabidopsis* transcriptome..... 109
Figure 3.23 Comparison between transcripts down- and up-regulated by FLS from dark-grown samples and other data sets from mutations or treatments resulting in a de-etiolated phenotype..... 112
Figure 3.24 Comparison between transcripts down- and up-regulated by FLS from light-grown samples and other studies..... 115
Figure 3.25 Effect of FLS on endogenous phytohormones..... 117

Figure 4.1 IAA is able to rescue FLS induced a de-etiolation at sub-µM concentrations..... 133
Figure 4.2 Exogenous IAA partially rescues toxicity of high concentration FLS in the light..... 134
Figure 4.3 IAA rescue of FLS de-etiolation is not due to a delay in development..... 136
Figure 4.4 Auxin biosynthesis genes are not downregulated in response to FLS..... 138
Figure 4.5 Auxin signalling genes are downregulated following FLS exposure..... 139
Figure 4.6 The effect of FLS treatment on auxin signalling is different in light and dark at the root tip..... 142
Figure 4.7 The DII::VENUS reporter is stabilised rapidly at the root tip upon FLS exposure..... 146
Figure 4.8 Comparing phenotypes of FLS-treated seedlings and seedlings treated with auxin inhibitors..... 148
Figure 4.9 Comparing phenotypes of FLS-treated seedlings and seedlings treated with established auxin antagonists, auxinole and PCIB..... 150
Figure 4.10 DII::VENUS stabilisation in seedlings treated with FLS and known auxin antagonists..... 151
Figure 4.11 Auxin receptor mutants are partially de-etiolated..... 152
Figure 4.12 IAA treatment reverses the FLS-induced block of chlorophyll production... 154
Figure 4.13 Pre-treatment of seedlings with IAA reduces Pchlide accumulation and allows chlorophyll biosynthesis..... 156
Figure 4.14 Pre-treatment of seedlings with 2,4-D reduces Pchlide accumulation and allows chlorophyll biosynthesis..... 157
Figure 4.15 24 h seed treatment with FLS is sufficient to induce Pchlide accumulation. 159
Figure 4.16 24 h seed treatment with IAA is able offset the effect of an FLS seed treatment..... 161
Figure 4.17 IAA seed treatment is sufficient to reduce FLS-induced de-etiolation for seedlings grown in the presence of FLS..... 162
Figure 5.1 EMS mutagenesis of *Arabidopsis* seedlings..... 176

Figure 5.2 Schematic of forward genetic screen..... 177

Figure 5.3 Re-screen of 6 lines that show the highest level of FLS-resistance..... 179

Figure 5.4 Performance of FLS-resistant line #22 in 3 growth conditions..... 180

Figure 5.5 Performance of FLS-resistant line #51 in 3 growth conditions..... 181

Figure 5.6 Performance of FLS-resistant line #61 in 3 growth conditions..... 182

Figure 5.7 Performance of FLS-resistant line #69 in 3 growth conditions..... 183

Figure 5.8 Performance of FLS-resistant line #93 in 3 growth conditions..... 184

Figure 5.9 Performance of FLS-resistant line #94 in 3 growth conditions..... 185

Figure 5.10 Developmental characterization of FLS- resistant lines..... 186

Figure 5.11 Reproductive organ measurements in FLS-resistant lines. 188

Figure 5.12 Silique development in FLS-resistant lines..... 189

Figure 5.13 Seed yield and seed size in FLS-resistant lines..... 189

Figure 6.1 Model for FLS action on auxin signalling..... 196

Figure S1 Re-screen of 91 potentially FLS-resistant lines..... 215

List of tables

Table 2.1 Details of primers for qPCR…… 71

Table 3.1 Gene ontology enrichment analysis of biological processes induced by FLS in dark-grown seedlings…….. 110

Table 3.2 Gene ontology enrichment analysis of cellular component affected by FLS in dark-grown seedlings…….. 111

Table 3.3 Experimental treatments for transcriptomic data set comparisons…… 111

Table 3.4 Hormone-related biological processes enriched following FLS treatment in light- and dark- grown samples…….. 114

Table 4.1 Summary table of auxin responsive genes from RNAseq analysis……. 140

Table 5.1 Significant changes in root length of mutant lines compared to WT following a re-screen on 50 µM FLS…….. 178

Table 5.2 Secondary screening of six FLS-resistant mutants…….. 186

Table S1 Gene ontology enrichment analysis of biological processes…….. 208

Table S2 Gene ontology enrichment analysis of cellular component…… 208

Table S3 Gene ontology enrichment analysis of biological processes…….. 209

Table S4 Gene ontology enrichment analysis of cellular component…… 210

Table S5 Gene ontology enrichment analysis of biological processes…….. 211

Table S6 Gene ontology enrichment analysis of cellular component…… 212

Table S7 Hormone quantification of FLS-treated samples…… 212

Table S8 Expression of auxin-related genes in transcriptomic analysis…… 213

Table S9 Details of 94 potentially resistant lines selected from screening on 50 µM FLS. …….. 214

Research Thesis: Declaration of Authorship

Print name:

Eleanor Kirby

Title of thesis:

The nematicide, fluensulfone, alters auxin responses in A*rabidopsis*

I declare that this thesis and the work presented in it are my own and has been generated by me as the result of my own original research.

I confirm that:

1. This work was done wholly or mainly while in candidature for a research degree at this University;
2. Where any part of this thesis has previously been submitted for a degree or any other qualification at this University or any other institution, this has been clearly stated;
3. Where I have consulted the published work of others, this is always clearly attributed;
4. Where I have quoted from the work of others, the source is always given. With the exception of such quotations, this thesis is entirely my own work;
5. I have acknowledged all main sources of help;
6. Where the thesis is based on work done by myself jointly with others, I have made clear exactly what was done by others and what I have contributed myself;
7. Parts of this work have been published as patent:

   4.228 (US PRO) 90977-PRO
   MIXTURES AND COMPOSITIONS OF FLUENSULFONE AND AUXIN, AND USES THEREOF

Signature: Date: 03.01.2021

Acknowledgements

Firstly, I would like to thank my supervisors, Matthew Terry, Lindy Holden-Dye and Vincent O'Connor for all their support and expert guidance throughout this project. You have always been available when I needed assistance and this project would not have been as interesting without your continuous ideas that kept me motivated and excited to see results.

Secondly, I would also like to give huge thanks to ADAMA agricultural solutions Ltd., particularly Ionit Iberkleid, for funding my project and being so generous with their time in discussing results and providing stimulating ideas to further the project.

In addition, I would like to extend a sincere thank you to Stefan Kepinski and Sigurd Ramans Harborough at the University of Leeds for giving me the opportunity to visit their research group and a huge thank you to Malcolm Bennet at the University of Nottingham for his generosity with seed stocks.

I would also like to express my appreciation for all the lab group members past and present I have worked alongside from the MJT, LEW, LHD and VOC labs at the University of Southampton. All groups have not only been excellent colleagues, but also friends.

Last but not least, I would like to thank my family and friends for their continued and unwavering support throughout my studies and writing up period, made more challenging during this pandemic. In particular, a special thank you to my fiancé, Oliver, who has motivated me and kept me smiling.

Definitions and Abbreviations

1,3-D	1,3-dichloropropene
$^1O2$	Singlet oxygen
2,4-D	2,4-dichlorophenoxyacetic acid
4-Cl-IAA	4-chloroindole-3-acetic acid
5-HT	5-Hydroxytryptamine
ABA	Abscisic acid
ABI	ABA-insensitive
ACC	1-aminocyclopropane-1-carboxylic acid
ACN	Acetonitrile
ACS	1-aminocyclopropane-1-carboxylate synthase
ADF	Actin depolymerizing factor
AFB	Auxin Signalling F-Box
AIP	ABI-Interacting Protein
AMT	Ammonium transporter
ANOVA	Analysis of Variance
Arabidopsis	*Arabidopsis thaliana*
ARF	Auxin Response Factor
ASA	Anthranilate Synthase a
ASB	Anthranilate Synthase b
ASK	Arabidopsis SKP1-like
AuxRE	Auxin responsive elements
AXR	Auxin Resistant
BAK	BRI1-associated kinase
BES	bri1-EMS-suppressor1
BH-IAA	Butoxycarbonylaminohexyl-IAA
bHLH	Basic helix-loop-helix
BIN	Brassinosteroid insensitive
BL	Blue Light
BP	Biological Process
BR	Brassinosteroids
BRI	Brassinosteroid-Insensitive
BRZ	Brassinazole
bZIP	Basic Leucine Zipper Domain
BZR	Brassinazole-resistant
C. elegans	*Caenorhabditis elegans*
CAB	Chlorophyll a and b binding proteins
CAD	Collisionally activated dissociation
cAMP	Cyclic adenosine monophosphate
cDNA	Complementary deoxyribonucleic acid
Chl	Chlorophyll
CHLH	Magnesium chelatase subunit H

Chlide	Chlorophyllide
CLE	Clavata3/embryo surrounding region
CM	Chorismate mutase
CN	Cyst Nematode
COI	Coronatine-insensitive protein 1
Col	Columbia ecotype
COP	Constitutively photomorphogenic
CPD	Constitutive photomorphogenic dwarf
CR	Campesterol
cry1	Cryptochrome 1
cry2	Cryptochrome 2
CS	Castasterone
CSR1	Chlorsulfuron/imidazolinone resistant 1
CTR1	Constitutive triple response 1
CUL1	CULLIN
CYP	Cytochrome P450s
cZ	cis-zeatin
DEG	Differentially expressed gene
DET	De-etiolated
DHZ	DL- dihydrozeatin
DII	Domain II
DMSO	dimethyl sulfoxide
DNA	Deoxyribonucleic acid
DRGs	Down-regulated genes
DWF4	Dwarf4
EBR	Epi-brassinolide
EIN	Ethylene insensitive
EMS	Ethyl methane sulfonate
EPA	Environmental Protection Agency
ERF	Ethylene response factor
ESI	electrospray ionization
ETR	Ethylene receptor
FAD	Flavin adenine dinucleotide
FBP	F-box protein
FLS	Fluensulfone
Flu	Fluorescent
FMN	Flavin mononucleotide
FR	Far red light
FW	Fresh weight
g	Gram
G. pallida	*Globodera pallida*
G. rostochiensis	*Globodera rostochiensis*
GA	Gibberellin
GFP	Green fluorescent protein

GGDP	Geranylgeranyl diphosphate
GH3	Gretchen hagen 3
GID1	GA insensitive dwarf
GO	Gene ontology
gof	Gain-of-function
GPA	Guanine nucleotide-binding protein alpha
GSA	Glutamate-1-semialdehyde 2,1-aminomutase
GSs	Glucosinolates
h	Hour
H. schachtii	*Heterodera schachtii*
HDA	Histone deacetylase
HPLC	High-performance liquid chromatography
HY	Long hypocotyl
HYH	Hy5 homolog
IAA	Indole-3-acetic acid
IAN	Indole-3-acetonitrile
IBA	Indole-3-butyric acid
INS	Indole synthase
IPyA	Indole-3-pyruvic acid
JA	Jasmonate
JA-Ile	N-jasmonyl-L-isoleucine
JAZ	Jasmonate zim domain
KEGG	Kyoto Encyclopedia of Genes and Genomes
KNOX	Knotted1-like homeobox
LAX	Like AUX1
LC/MS	Liquid chromatography/mass spectrometry
LD_{50}	Median lethal dose
L*er*	*Landsberg erecta*
LHCB	Light-harvesting chlorophyll a/b-binding protein
LOV	Light, oxygen or voltage domain
LRR	Leucine-rich repeat
LRR-RLK	LRR receptor-like-kinase
M	Molar
M. hapla	*Meloidogyne hapla*
M. javanica	*Meloidogyne javanica*
M. incognita	*Meloidogyne incognita*
MeOH	Methanol
MgCh	Mg chelatase
Min	Minute
mL	Millilitre
mm	Millimetre
mM	Millimolar
MRM	Multiple reaction monitoring
mRNA	Messenger ribonucleic acid

MS	Murashige and Skoog
MTA	Methylthioadenosine
MTT	3-[4,5-dimethylthiazole-2-yl]-2,5-diphenyltetrazolium bromide
N. abberans	*Nacobbus abberans*
1-NAA	Naphthalene acetic acid
NADPH	Nicotinamide adenine dinucleotide phosphate hydrogen
NASC	Nottingham Arabidopsis Stock Centre
NBS	Nucleotide binding site
NEC	Nitrogen enriched compost
NPA	N-1-Naphthylphthalamic Acid
OPDA	12-oxo-phytodienoic acid
P. penetrans	*Pratylenchus penetrans*
P. thornei	*Pratylenchus thornei*
PAA	Phenylacetic acid
PAC	Paclobutrazol
PCA	Principal component analysis
Pchlide	Protochlorophyllide
PCIB	p-Chlorophenoxyisobutyric Acid
PCR	Polymerase Chain Reaction
PFD	Photon fluence density
Pfr	Far-red light absorbing form of phytochrome
PHAN	Phantastica
PHOT	Phototropin
PHR	Photolyase
PHY	Phytochrome
PIF	phytochrome interacting factor
PLB	Prolamellar body
POR	Protochlorophyllide oxidoreductase
PPI	Pre-plant incorporation
PPM	Parts per million
PPN	Plant parasitic nematode
Pr	Red light absorbing form of phytochrome
RAM	Root apical meristem
RBX1	RING BOX1
RFU	Relative fluorescence unit
RKN	Root-knot nematode
RL	Red light
RNA	Ribonucleic acid
RNAseq	RNA sequencing
ROS	Reactive oxygen species
RT	Reverse transcriptase
s	Second
S-AdoMet	S-adenosylmethionine

SA	Salicylic acid
SAM	S-adenosyl-l-methionine/Shoot apical meristem
SAUR	Small auxin upregulated RNA
SAV	Shade avoidance
SCF	Skp1/Cullin/F-box
SD	Standard deviation
SEM	Standard error of the mean
SHY2	Suppressor of hy
SL	Strigolactone
SNP	Single nucleotide polymorphism
SUC	Sucrose transporter
TAA	Tryptophan Aminotransferase
TAIR	The Arabidopsis Information Resource
TIR	Transport inhibitor response
Tm	Melting temperature
TMM	Trimmed mean of M-values
TPS	Terpene synthase
Trp	Tryptophan
Tyr	Tyrosine
tZ	Trans-zeatin
tZR	Trans-zeatin riboside
UPS	Ubiquitin-proteasome system
URGs	Up-regulated genes
UVR-8	Ultra-violet resistance locus
v/v	Volume per volume
w/v	Weight per volume
WL	White light
WT	Wild type
X. index	*Xiphinema index*
YFP	Yellow fluorescent protein
YLS8	Yellow leaf specific
µg	Microgram
µL	Microliter
µM	Micromolar

Chapter 1: General introduction

1.1 Nematodes as agricultural burdens

1.1.1 An introduction to the Nematoda phylum

The phylum Nematoda is extremely diverse, with nematodes inhabiting an extensive range of environments from marine to fresh water, polar to tropical regions and the highest and lowest elevations. Although only 25,000 species have been described (Zhang, 2013), it is estimated there are closer to one million species in existence. Of the 25,000 nematode species identified, around half are free-living and are able to feed on bacteria or microscopic organisms; the other half are parasitic (Maggenti, 1981) and are able to parasitize a huge proportion of animal and plant species (Blaxter et al., 2011).

Animal parasitic nematodes, such as *Anycyclostoma duodenale*, are estimated to infect 1 billion people globally with infection being predominant in tropical regions and developing countries (WHO, 2004). Infestation of nematodes in humans can cause a range of debilitating symptoms from lack of energy and vigor to blindness and even malformation (Bethony et al., 2006). Animal parasitic nematodes can also be prevalent in livestock, causing productivity reduction, which furthers the economic burden (Jasmer et al., 2003). Nematodes also contribute to a reduction in agricultural productivity via infestation of plants and crops, including the economically important cereal crops - wheat and maize. It is known there are over 4000 nematode species that are able to parasitize plants and every crop plant is vulnerable to at least one species of plant parasitic nematode (PPN) (Bridge and Starr, 2007). Therefore, parasitic nematodes present a significant threat to economic development in the world's poorest countries.

Nematodes are typically 5-100μm thick and 0.1-2.5mm long, however, the smallest nematodes are microscopic whilst some parasitic species can reach up to one meter in length (Ruppert et al., 2003). Many nematodes, such as *Caenorhabditis elegans* are free-living, feed on bacteria and undergo four molts of the cuticle during growth. However, other nematodes parasitize plants and animals and have hugely diverse life cycles that exploit a range of biological niches (Lee, 2002).

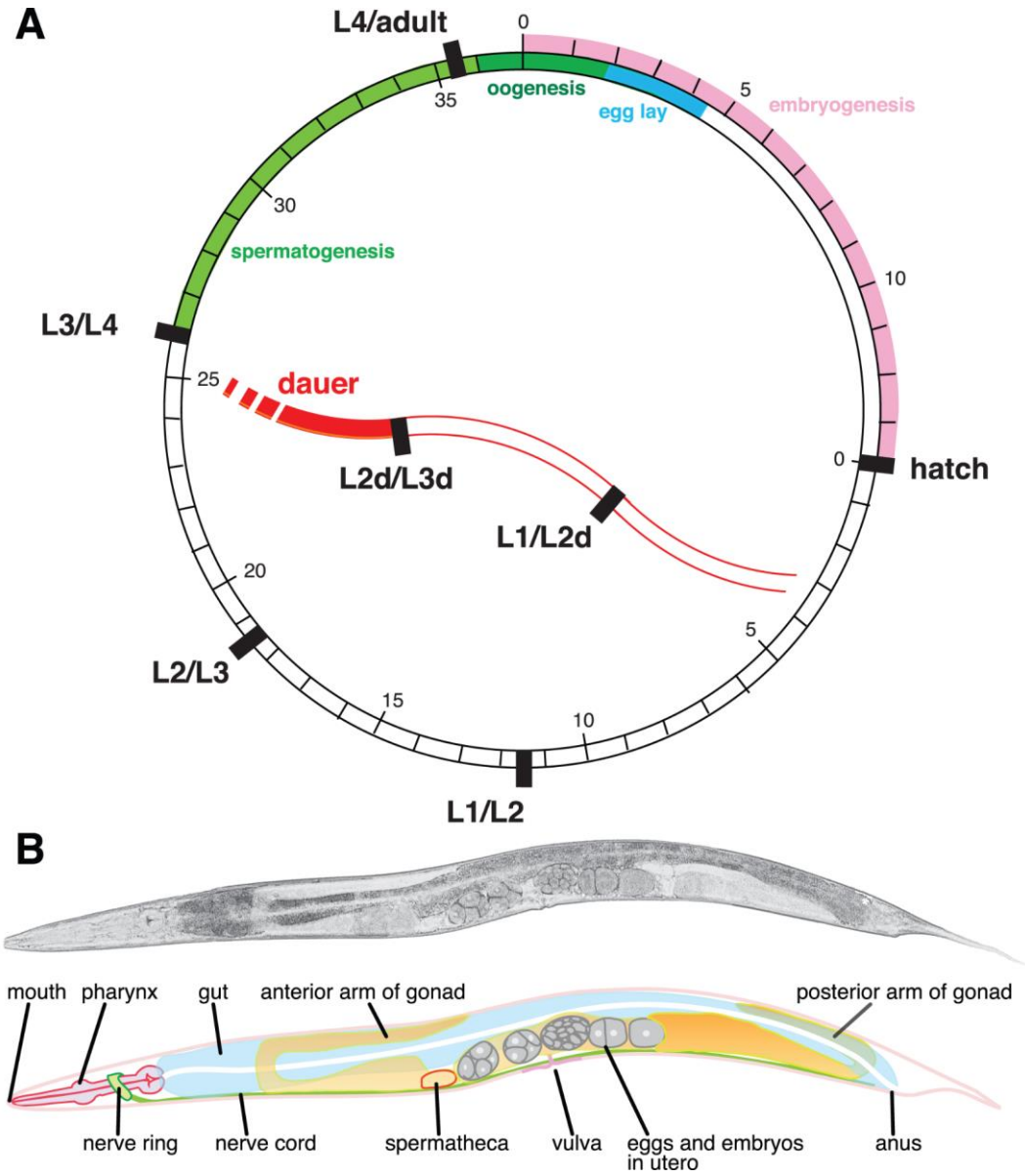

Figure 1.1. Life cycle of *C. elegans.* L refers to 'larval' stages and dauer refers to the period of time in which the larva is in a dormant-like state to survive harsh conditions. (B) Anatomy of *C. elegans* adult. Figure retrieved from Blaxter, 2011.

In contrast to the range of life cycles, the nematode basic body plan is highly conserved across phyla. Nematodes are unsegmented, worm-like animals described as pseudocoelmates with a body consisting of a body wall separated from the inner tube (alimentary system and gonad) by a pseudocoelom (Campbell and Reece, 2008). The body wall consists of musculature, the epidermis and an outer body cuticle (Hyman, 1951) which is molted between larval stages to reach a reproductively viable adult stage (figure 1.1A). The cuticle becomes specialized at each reproductive stage but continues to consist

of 9 layers of proteinaceous fibers (Watson, 1965); despite the cuticle being so complex, it remains permeable to both water and gas, allowing respiration to occur through it. Beneath this cuticle is a layer of longitudinal muscle which, combined with the internal pressure, creates a thrashing action nematodes use to move. At the anterior end, there is a mouth which contains 3 lips – and teeth in predatory species – and behind this is a pharynx which expands and contracts to allow the pumping of food into the intestines (Mapes, 1965). Additionally, the nematode nervous system is well developed, comprised of a circum-pharyngeal nerve ring made of 4 nerve ganglia from which 6 longitudinal nerves extend through the body along the gut and reproductive organs (Bird & Bird, 1991). 6 shorter nerves also extend toward the mouth parts (figure 1.1B). A large majority of nematodes remain worm-like throughout the life cycle, with the exception of sedentary endoparasitic PPNs which swell into a ball shape when they reach adulthood.

1.1.2 Plant parasitic nematode life cycle

Around 15% of all nematodes are obligate parasites of plants and are able to feed on most parts of the host plant, including roots, stems, leaves and seeds (Fuller et al., 2008). Those species that attack the root system of host plants are attributed to the highest level of crop reduction and agricultural burden (Perry & Moens, 2013). PPNs either require a host plant to allow growth or protection from predators/pathogens in the soil or use a host plant to complete their lifecycle or allow reproduction to occur.

PPNs use a specialized organ, the stylet, to feed from the plant and classification of PPNs can be inferred through stylet size and shape as this affects the mode and site of feeding. PPNs tend to induce stunting of growth through diversion of essential nutrients and disruption of osmotic transport (Fuller et al., 2008); this, subsequently, leads to impairment of CO_2 and nitrogen fixation (Bird & Loveys, 1975; Huang, 1987), reducing photosynthesis. PPN and infection of the roots retards root development, leading to diminished nutrient and water uptake (Decker and Sveshnikovam, 1983). Although PPN infection does not typically lead to host plant death, it is the sheer number of nematodes, typically hundreds of thousands on one plant, which cause such a reduction in crop yield. Host death usually occurs following introduction of a pathogen by the parasite. As the

aboveground symptoms of PPN infection are subtle and visible infection signs, such as root galls and cysts, are difficult to determine, infection can go largely unnoticed by growers until infestation has spread - usually aided by farming equipment. A large majority of PPNs are soil dwelling root pathogens and few feed primarily on shoot tissue. Most PPN species belong in the class *Chromoderea*, order *Rhabditida* and are further classified according to feeding strategy (figure 1.2).

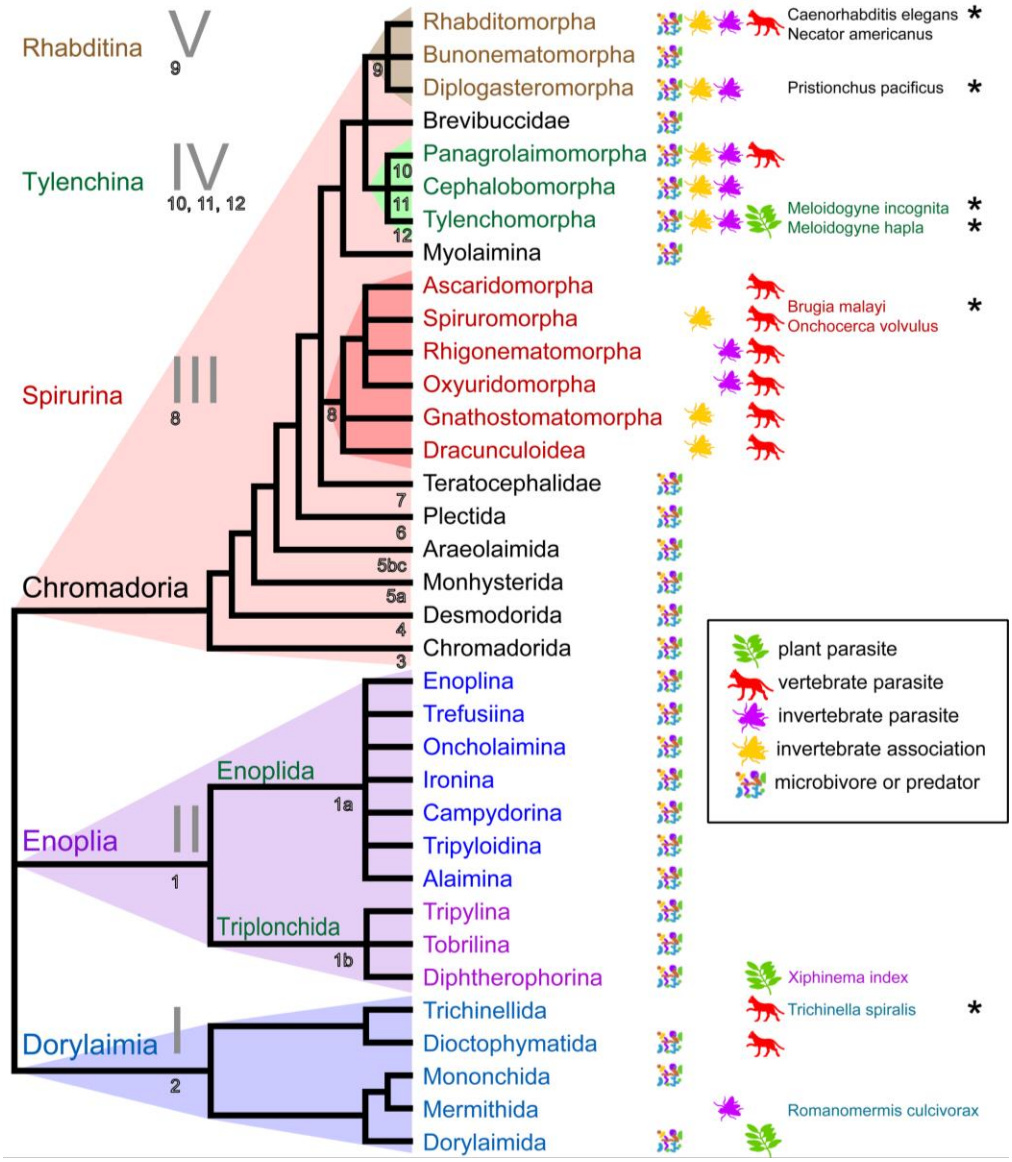

Figure 1.2. Phylogeny of the Nematoda phylum. This phylogenetic tree is based upon phylogenetic analysis of the small subunit ribosomal RNA gene (Blaxter et al., 1998). Clade names introduced by De Ley & Blaxter, 2002, 2004 and, more recently, numerical clade scheme below the branches introduced by Holovachov et al., 2009; Holterman et al., 2006. Icons beside groups represent feeding style and asterisks indicate species with a sequenced genome. Figure retrieved from Blaxter, 2011.

1.1.2.1 Ectoparasites

Ectoparasitic PPNs remain outside of the plant when feeding (Jasmer et al., 2003) and insert their stylet into epidermal cells of the root (Wyss, 1997). Species have variable stylet length allowing them to exploit different plant tissues (Bridge and Starr, 2007) and ectoparasitic nematodes are able to use this feeding strategy to feed on multiple plants, but this also leads to an increased likelihood of predator and/or pathogen attack on the nematode. Species of this classification are vermiform and feeding at all 4 juvenile and adult stages. This group can be further sub-divided by their motility. Migratory ectoparasites feed at numerous sites along the root for a short period of time (Tytgat et al., 2000; Wyss, 1997), whereas, sedentary ectoparasites establish a feeding site on one cell, create an enlarged feeding cell and feed for an extended period (Rhoades and Linford, 1961). Additionally, only ectoparasites in the class *Enoplea* are able to act as vectors and transmit viruses such as tomato ringspot that can continue to be infective for months following initial infection (Chen et al., 2004).

1.1.2.3 Migratory endoparasites

Nematodes with this feeding style, such as *Pratylenchus* (lesion nematode), *Radopholus* (burrowing nematodes) and *Hirschmanniella* (rice root nematode) (Bridge and Starr, 2007), complete their whole lifecycle within the cortex of the host plant. All motile stages are infective and are able to feed, leave the root system (Tytgat et al., 2000) and migrate through the soil to find a new host plant. These nematodes do not make permanent feeding cells. Instead, they are able to migrate through root tissue and cause necrotic lesions which, ultimately, stunts plant growth and leads to host plant death through increased risk of secondary infection by bacteria and fungi (Bridge and Starr, 2007).

1.1.2.4 Sedentary endoparasites

The most economically important group of parasitic nematodes are the sedentary endoparasites which include the cyst nematodes (CNs) (*Heterodera* and *Globodera spp.*) and root-knot nematodes (RKNs) (*Meloidogyne spp.*) (Holden-Dye and Walker, 2011). These groups both have complex plant-pathogen interactions and establish permanent feeding sites. Despite these shared principles there are noticeable differences in their life cycles.

CN J2s enter near the root tip and quickly migrate to the vascular system. The J2 then uses its stylet aperture to inject secretions into the plant cells to break down cell wall components (Smant et al., 1998) and stimulate the formation of a multinucleate syncytium from which they are able to feed through their whole life cycle. These large feeder cells plug the vascular system of the plant making it susceptible to water stress. Once feeding cells are established the juveniles become sedentary and their muscles atrophy. Juveniles then undergo three molts inside the root system to develop to the adult stage. The female cyst nematode then swells considerably into a bulb shape and eggs are laid, but retained inside the body, following an obligate sexual cycle (Jones et al., 2013) (figure 1.3).

The CNs are extremely problematic as they are able to persist in the field for a remarkably long period of time and infect crops such as soybean, potato and rice. This persistence is owed to the hardened, dead body of the female surrounding the eggs and the diapause stage the eggs enter to survive sub-optimal conditions (Bird & Opperman, 1998).

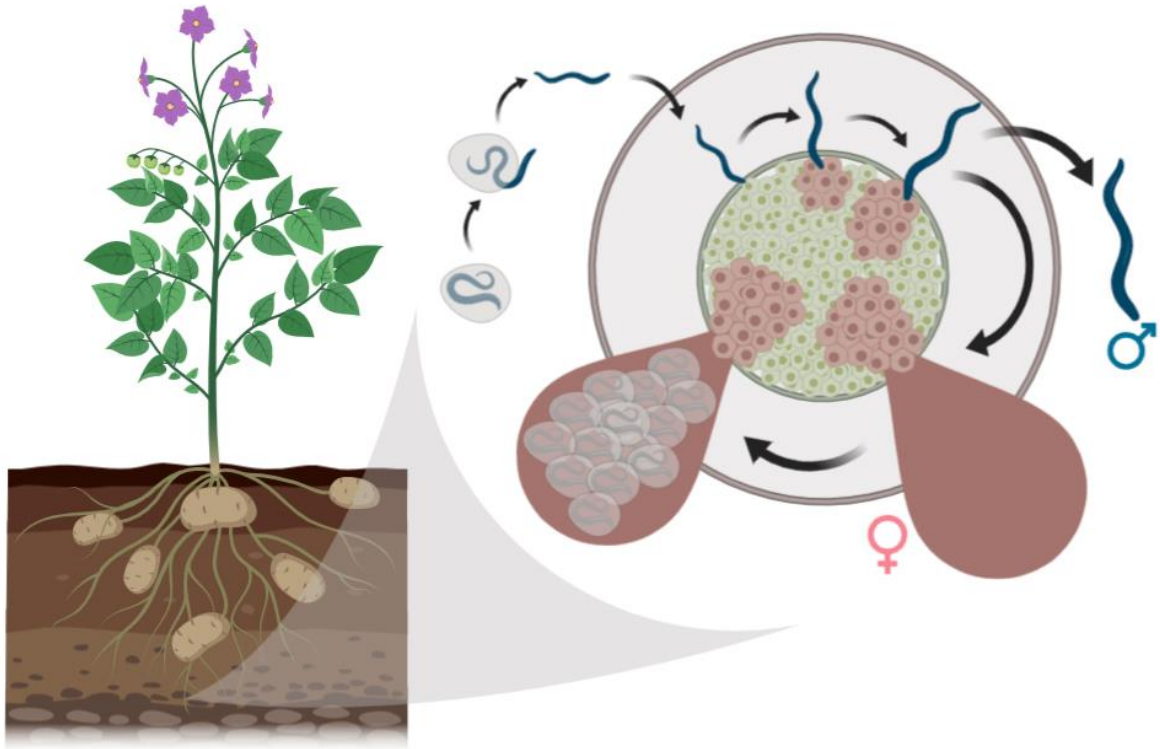

Figure 1.3. Life cycle of a cyst nematode. Cyst nematodes have a sedentary endoparasitic mode of parasitism. The J2s hatch within the protective cyst, migrate toward the root tip and gain entry. The J2s then establish a feeding site and become non-motile; if a large enough site is achieved the nematodes develops into a female and swell to form the visible cysts within potato roots. Eggs are produced within the female body and the body becomes a protective casing for the eggs which remain in a diapause stage until a stimulus is detected.

In contrast, RKN juveniles move intracellularly, down the cortex, towards the root tip after penetrating the elongation zone of the root (Jones et al., 2013). The J2 then enters the base of the vascular cylinder to establish a feeding site in the root differentiation zone. RKNs develop feeding cells, termed giant cells (Jones, 1981), through the induction of nuclear division without cytokinesis. Surrounding cells then divide and swell causing the formation of the characteristic root knots. Nematodes then undergo three molts and develop into pear-shaped, egg-laying females which lay eggs outside the nematode in a gelatinous mass (Jones et al., 2013), following reproduction by parthenogenesis (Chitwood & Perry, 2009). Although RKNs do not have an environmentally resistant stage, they are able to parasitize a broad range of host plants, allowing them to persist and generate high agricultural burden.

1.2 Plant and sedentary endoparasitic nematode interactions

1.2.1 Stylet aperture

The stylet aperture is essential to the PPN life cycle. It is a cuticular appendage which can protract and retract and is vital for hatching, host invasion and feeding. It is cylindrical in shape with a bulb at the posterior end, which is attached to the pharyngeal system. The stylet is hollow allowing movement of nutrients in and secretions out (Perry & Moens, 2013) and is developed at the first molt, from J1-J2. The stylet's first crucial role is piercing the eggshell during hatching, followed by establishment of root invasion (Perry, 2002; Perry & Moens, 2013). Once inside the plant host tissue, the stylet also functions to secrete fluid to create feeding cells and ingest host plant cell cytoplasm. These actions are initiated by the pumping of the metacorpal pharyngeal bulb and the enzymatic secretions are generated by the subventral and dorsal glands.

1.2.2 Hatching

For most sedentary endoparasitic nematodes, the J2 stage is infective. Many RKN J2s are able to hatch in the presence of water, although chemical cues have been shown to induce hatching of *Meloidogyne hapla* juveniles (Perry, 2002). This largely non-specific hatching cue demonstrates the polyphagous nature of many RKN species. In contrast, CN species have a specific host range and are highly dependent upon certain hatching signals from the host plant (Castillo, 2012).

Not only are PPNs host specific, they also synchronize their lifecycle to the host plant allowing them to hatch at the optimum time when the root system has not fully established (Perry & Clarke, 1981). PPNs are able to invade more successfully in younger plants due to ageing plants possessing tougher roots (Wyss, 1992). To allow this synchronicity many CNs are extremely reliant on host plant diffusate to initiate hatching (Forrest & Perry, 1980; Perry, 2002). This diffusate contains hatching factors (Perry, 2002), stimulants and inhibitors and it is thought that inhibitors are released first to allow the root system to be established. Following this hatching factors and stimulants are released, and these compounds then synergize and induce the hatching process. However, it is thought that attracting PPNs is a detrimental, secondary consequence of

root diffusate release and the primary purpose of root diffusate is to potentially enhance interaction between beneficial organisms in the soil and the host plant. Although the majority of these hatching factors and inhibitors have not been isolated, terpenoids and glycinoecleptins have been shown to induce hatching and are present within root diffusate (Masamune et al., 1982). In the event of diffusate absence, CNs, such as *Globodera pallida,* are able to remain in a quiescent state within the eggs for up to 30 years (Spears, 1968). During this quiescent period, juveniles have reduced metabolic activity and are resistant to nematicides (Spears, 1968; Cooper and Van Gundy, 1971a) as they are protected by the eggshell, consisting of the outer vitelline membrane, middle chitinous layer and inner lipid layer. The lipid layer prevents the juvenile from desiccation and also confers resistance to toxins due to its impermeability (Perry & Wharton, 2011).

Although the hatching process has not been fully described yet, it is thought rehydration is a vital step. It has been seen that high levels of trehalose are present in the perivitelline fluid that surround the unhatched nematode and this disaccharide places an osmotic stress on the juvenile, causing partial dehydration (Clarke & Hennessy, 1976; Ellenby, 1968; Perry, 1983; Perry, Clarke, & Hennessy, 1980). This dehydration then limits metabolic activity and movement (Ellenby & Perry, 1976; Perry, 2002; Perry & Clarke, 1981).

Following exposure to root diffusate, it is thought that the juvenile becomes re-hydrated (Ellenby and Perry, 1976). This rehydration is likely to be permitted by permeability changes of the inner lipid layer via calcium flux, allowing trehalose escape and water uptake, thus reducing osmotic pressure on the unhatched juvenile (Atkinson and Ballantyne, 1979; Clarke and Hennessy, 1983; Behm, 1997). Additionally, after diffusate exposure, juveniles are seen to increase oxygen uptake and cAMP levels (Atkinson and Ballantyne, 1977a; Atkinson and Ballantyne, 1977b), which initiates consumption of lipid reserves (Robinson et al., 1985). Juveniles also become more motile and extensive stylet thrusting can be observed which perforates the eggshell at the narrow end, allowing the juvenile to hatch (see Perry, 2002 for review).

1.2.3 Movement to the host plant

As the infective J2s are non-feeding they rely solely on energy reserves, such as lipids and glycogen stores, until a suitable host plant is detected (Cooper and Van Gundy, 1971b; Cooper and Van Gundy, 1971a; Dropkin and Acedo, 1974). The location of a suitable host plant is thought to be dependent on attractant and repellant cues (Reynolds et al., 2011). RKN juveniles have been shown to be attracted to non-specific cues such as CO_2 (Robinson, 2004; Robinson & Perry, 2011), released by living or decaying matter, and repelled by ammonia, released by decaying material (Castro et al., 1991) – this has been thought to modulate movement towards living material, rather than dead material as *Globodera rostochiensis* has been shown to exhibit increased movement in the presence of root diffusate (Devine and Jones, 2003). However, *Heterodera schachtii* (sugar beet nematode) is the only CN to show chemotaxis towards CO_2 and oxygen (Johnson and Vigelierchio, 1961). Similarly, chemical cues that allow host plant detection have not yet been identified. However, when the nematode is within a few millimeters of the root it has been postulated that the rhizosphere may release chemical cues allowing the nematode to orientate itself (Perry, Moens, & Starr, 2009).

1.2.4 Movement into/through the host plant

The entry into the host plant by the RKN *Meloidogyne incognita* has been studied using *Arabidopsis* due to its translucent roots and ease of maintenance (Wyss et al., 1992). After locating the root tip, *M. incognita* will begin to ascertain an invasion site through exploratory behaviors, such as lip rubbing on root epidermal cells and stylet probing (Wyss et al., 1992). As mentioned previously, J2s usually enter via the elongation zone where newly dividing cells are present and it has been seen that, at older regions of the root, invasion and penetration ability of J2s is decreased (Wyss et al., 1992). Upon invasion, lip rubbing and stylet protrusion perforates cells walls and the median bulb pulsates, facilitating the release of enzymatic secretions from the subventral oesophageal glands. Once inside the root, the nematode moves intercellularly, in the middle lamella (Taiz and Zeiger, 2006) – a pectin rich layer joining neighboring cells. Due to this mode of migration, RKNs cause relatively little damage to the host plant. The movement of CNs

are significantly more destructive as their migratory path is intracellular and involves constant stylet thrusting to rupture cells (Wyss et al., 1992).

Although stylet movements are known to be important for penetration and migration through plant tissue, enzymatic secretions from the stylet have also been shown to be essential to achieve parasitism. Genes encoding a β-1,4-endoglucanase and cellulase has been found in stylet secretions from CN esophageal glands and homologous genes have been identified in RKNs (Smant et al., 1998; De Meutter et al., 2001). Immunolocalisation in tobacco roots also localized this nematode cellulase to the migratory path, but it was not present in the feeding cells (Goellner et al., 2000), suggesting it has role in the infective process. Other genes encoding pectate lyse and polygalacturonase have also been identified and transcripts have been localized to sub-ventral glands in PPNs (Popeijus et al., 2000; Doyle and Lambert, 2002; de Boer et al., 2002). These enzymes allow the softening of the cell wall to enable nematode migration through the plant tissue.

The chorismate mutase gene – *MjCM-1,* has also been identified in RKN esophageal glands. Transgenic expression of *MjCM-1* in roots suppresses lateral root formation and vascular system development (Lambert et al., 1999; Doyle and Lambert, 2003). This abnormal phenotype can be rescued through exogenous application of the auxin, indole-3-acetic acid (IAA), suggesting expression of this gene reduces auxin levels (Doyle and Lambert, 2003). The conversion of chorismate to anthranilate is the first committed step in the synthesis of tryptophan, the pre-cursor of auxin. Therefore, as *MjCM-1* catalyzes the conversion of chorismate to prephenate, this ultimately reduces tryptophan synthesis in favour of phenylalanine and tyrosine synthesis, thus tryptophan derived compounds, such as auxins, are reduced (Mobley et al., 1999). Homologs of this gene have also been identified in CNs (Popeijus et al., 2000; Bekal et al., 2003) and *Arabidopsis* (Mobley et al., 1999). Interestingly, the genes that encode cell-wall degrading enzymes and chorismate mutase are not present in *C. elegans* or most animals and have a high level of similarity to genes encoded by microorganisms. Root diffusate has also been shown to stimulate stylet secretions from PPNs and analyses of these secretions have identified many cellulases, proteases (Smant et al., 1998; Rosso et al., 1999; Popeijus et al., 2000) and other

enzymes, such as thioredoxin peroxidase which is suggested to suppress reactive oxygen mediated host defense (Curtis et al., 2011).

1.2.5 Feeding site establishment

After entering the vascular cylinder, CNs and RKNs select a parenchymous cell adjacent to the vascular elements to develop into a feeding cell which will act to sustain the nematode throughout the *in planta* part of its life cycle (Golinowski et al., 1996; Golinowski & Magnusson, 1991; Magnusson & Golinowski, 1991). Once the stylet has been inserted into a cell and secretions begin, CNs induce cell enlargement and proliferation of organelles (Hussey & Grundler, 1998). This process also begins in neighboring cells that extends to cell wall degradation and, ultimately, joins hundreds of cells to form a large syncytium on which the nematode can feed. In contrast, RKNs cause formation of giant cells through induction of karyokinesis in the absence of cytokinesis (Jones & Payne, 1978). Similarly, to syncytia, organelle proliferation occurs (Bleve-Zacheo and Melillo, 1997). Both of these feeding sites develop dense cytoplasm (Goverse et al., 2000) and specialized cell wall ingrowths which allow easier extraction of nutrients from the vascular element (Bird, 1961). These feeding structures are essential for the survival of both CNs and RKNs as they function as metabolic sinks that funnel plant resources and blocking their development using cell cycle inhibitors has been shown to cause developmental arrest of the nematode (de Almeida Engler et al., 1999).

Upon inoculation with PPNs and subsequent development of feeding structures, it is known that complex changes in gene expression are induced to allow extensive alterations in the cell wall morphology of plant cells. These changes are brought about by stylet secretions originating from the dorsal oesophageal glands (Hussey, 1989) that have been shown to upregulate cell wall degrading enzymes, such as endoglucanase and polygalacturonase. For example, *H. schachtii* has cellulose binding proteins that are able to interact with the host plant's pectin methylesterase, which is thought to promote its activity and allow modification to the cell wall (Hewezi et al., 2008). Although cell wall modifying enzymes are known to be released by nematodes, it has also been seen that plant-derived cell wall modifying compounds, such as endo-β-1,4-glucanses (Goellner et

al., 2001), pectin acetylesterases (Vercauteren et al., 2002), polygalacturonases, expansins (Jammes et al., 2005) and actin depolymerizing factors (ADFs) (Fuller et al., 2007) are upregulated during feeding cell formation. This allows the rearrangement of the plant cytoskeleton to permit the penetration of the juvenile and feeding cell formation.

Genes that function in cell cycle progression and water transport (Hammes et al., 2005; Opperman et al., 1994) are also upregulated in and around feeding cells and the phytohormones, auxin and ethylene, are thought to be a positive regulator of PPN susceptibility, as ethylene- and auxin- insensitive mutants display reduced PPN-infection compared to wild-type (WT) (Gutierrez et al., 2009).

Interestingly, it has also been seen that the *Arabidopsis* sucrose transporter genes *AtSUC1* and *AtSUC2* show high expression levels in syncytia, suggesting a possible role in maintenance of the metabolic sink (Juergensen et al., 2003; Hammes et al., 2005). However, *AtSUC2* expression is not seen in giant cells which also act as metabolic sinks. Stylet secretions from RKNs have been found to induce similar structures within the host root to endosymbiotic rhizobia, stimulating comparative gene studies between the two processes (Koltai et al., 2001). Orthologous genes to those encoding the transcriptional regulators PHAN and KNOX were co-localized in RKN feeding sites and Rhizobium-induced nodules (Koltai et al., 2001). However, similarities between feeding site and nodule formation may be limited as analysis of 192 nodule genes only displayed upregulation of two upon nematode infection. On the other hand, several genes with roles in defense responses display downregulation following RKN inoculation suggesting the nematode acts to suppresses host plant defense (Kyndt et al., 2012).

It is also thought that the presence of auxin is important in feeding site development as both CNs and RKNs fail to develop in an auxin-insensitive tomato mutant (Goverse et al., 1998). Additionally, following infection by *G. rostochiensis,* higher expression of the auxin-binding protein is observed and silencing this gene reduces feeding site establishment (Dąbrowska-Bronk et al., 2015). *G. rostochiensis* is also known to secrete the protein CLE1 which allows syncytia formation as it is cleaved by plant proteases to its active form,

which mimics receptor ligands within the plant (Guo et al., 2011). Once the feeding site has been established, the juvenile is able to insert its stylet and develop a feeding tube. The feeding tube is visible close to the stylet just before feeding begins and it thought to prevent ingestion of whole organelles into the stylet structure which may cause a blockage (Razak & Evans, 1976).

1.2.6 Plant parasitic nematode infection in *Arabidopsis*

Arabidopsis is able to act as a host plant for the agriculturally important sedentary endoparasitic nematodes (CNs and RKNs) in monoxenic conditions. This system allows plant-pathogen interactions to be studied in detail and gene expression to be monitored following infection. *H. schachtii,* a cyst nematode, is able to penetrate the root tissue and migrate through the cortical cells in a destructive fashion with their stylet to the vascular cylinder. Here, an initial syncytial feeding cell was formed and the juvenile began feeding 7 hours after initial infection. By 3 days post infection, the formation of a large syncytium and the appearance of cell wall fragments could be observed (Sijmons et al., 1994). These observations of *H. schachtii* infection in *Arabidopsis* roots closely mirror those following *H. schachtii* infection in rape seed (Wyss and Zunke, 1986). This would allow future interactions seen between *Arabidopsis* and *H. schachtii* to be comparable to commercial crops.

In contrast remarkable disparities were seen when observing infection of *M. incognita,* a root knot nematode, in *Arabidopsis* relative to cyst nematode infection. Following exploration of the root surface, the infective juveniles entered the root close behind the root tip and used their stylets to move between cells, limiting damage in this phase. Initial movement was towards the meristematic tissue at the root tip, but once the nematode arrived there, movement became acropetal within the vascular cylinder accompanied by continuous stylet thrusting. After 2 days, multinuclear giant cells were observed from which the juvenile fed and root galls could be seen (Sijmons et al., 1991). These feeding structures act as metabolic sinks and increased root metabolism can be seen directly in the syncytium and at the regions immediately above the syncytium (Sijmons et al., 1991). Parallels cannot be drawn from the observations of *M. incognita* on *Arabidopsis* as their

movements have not been fully described in crop host species; although, the characteristic root galling and giant cell formation was observed in *Arabidopsis* suggesting infection strategy would be comparable.

Following *M. incognita* infection, microarrays have been utilized to determine gene expression changes in *Arabidopsis.* Global analysis determined downregulation of plant defense mechanisms and upregulation of genes encoding 40S and 60S ribosomal proteins, cell cycle genes (Jammes et al., 2005) and aquaporins (Jammes et al., 2005; Hammes et al., 2005). These gene expression changes were selectively seen in root galls suggesting increased levels of protein synthesis, cell division and enhanced water transport to the feeding site. *AtAMT1;2*, an ammonium transporter, was also seen to be consistently downregulated in the giant cells formed by *M. incognita* (Fuller et al., 2007), however, expression of this same gene was previously reported to be up-regulated in cells following infection alongside a number of others transporters: *AtAUX4* and *AtSUC1* (Hammes et al., 2005). The ammonium transporter family mediates the uptake of ammonium ions from the soil, which is the most abundant source of nitrogen for plants. It is known that ammonia-based compounds have nematicidcal activity and can be used to control the root knot nematode population in the soil (Oka and Pivonia, 2002) and in culture conditions (Sudirman and Webster, 1995) during tomato plant cultivation. Therefore, this suggests local repression of ammonium transporters could act to decrease levels of inhibitory substances. Initial infection of the juvenile induces global gene expression changes and subsequent formation of feeding cells which block the vascular system and divert essential nutrients and water away from the host plant tissue. This then causes water stress and nutrient deficiency, which ultimately reduces their ability to utilize materials for flower and grain production, creating huge yield loss of major crop plants.

1.3 Plant parasitic nematode control

It has been estimated that yield losses in a variety of crop plants due to parasitic nematodes was 12.3% and this corresponds to a $157 billion loss globally (Singh et al., 2015). However, some species can cause yield losses in excess of 70% following long-term monoculture (Zawislak and Tyburski, 1992). Due to restricted use and phasing out of

nematicides previously used in the 1980s it is more than likely these figures have risen and as an anticipated increase of 75% in food demand in 2050 is predicted (Keating et al., 2010), it is essential new mechanisms are found to maximize food resources.

The global distribution of PPNs varies greatly between species; some *Meloidogyne* species are able to live in many locations while *Naccobus* species are geographically restricted and some *Heterodera* species are host restricted. The genus *Globodera* are of most concern in the UK with *G. rostochiensis* and *G. pallida* causing an estimated 9% loss in potato yield (DEFRA, 2010) and a £50 million loss per annum (Wale et al., 2011). *Globodera* is also an issue throughout Europe with yield losses reaching 50% (Trudgill et al., 2003).

1.3.1 Chemical control as a means to reduce plant parasitic nematode populations

1.3.1.1 Fumigant nematicides

Chemical control has remained the most widely used method to increase crop yield following infestation (Perry & Moens, 2013). Chemical control agents (nematicides) act against PPNs to either kill or paralyze nematodes in the crop plant or soil, and thus reduce damage to the root system (Eisenhauera et al., 2010).

Nematicides can be subdivided into fumigant and non-fumigant based upon their mode of application to the soil; fumigant nematicides are generally applied directly to the soil and display a gaseous dispersion (Chen et al., 2004). Fumigant nematicides, such as methyl bromide and 1,3-dichloropropene, are extremely efficacious due to their high volatility at ambient temperatures and perform best in soils that have adequate moisture and temperature to aid dispersal and low levels of organic matter as this de-activates the toxicant. Fumigant nematicides are usually based on halogenated hydrocarbons in a liquid or gaseous form for ease of application and are thought to perturb a number of vital biochemical paths in the nematodes including those crucial for protein synthesis and respiration (Chitwood, 2003).

In the late 19th century the first known fumigant nematicide used was carbon disulphide (Haydock et al., 2006) and shortly after, in the first half of the 20th century, methyl bromide and 1, 3-dichloropropene (1,3-D) were developed. Due to its ability to control a number of PPN species methyl bromide was widely used as a nematicide throughout the 20th century; however, its usage is now banned as it has high leaching properties and has been implicated in the depletion of the ozone layer (Fuller et al., 2008). Methyl bromide also displays a broad, non-selective toxicity and is able to act against non-target insects, rodents and plants (Duniway, 2002). Cases of epilepsy and severe disability in humans have also been documented following high levels of exposure to methyl bromide (Rathus and Landy, 1961) and this contributed to its use being terminated. The only fumigant nematicide currently used in agriculture is 1, 3-D although its usage was banned in the EU in 2011. Like methyl bromide, 1, 3-D has phytotoxic effects towards plants, in particular seeds, so it can only be used as a pre-plant treatment in the soil (Chen et al., 2004).

Although fumigant nematicides are highly effective in reducing PPN numbers in the soil and are shown to dramatically enhance crop yield as a result, their non-target toxicity and high volatility have caused a number to be withdrawn from use. To achieve a similar level of control fumigant nematicides are required to be mixed with non-fumigant alternatives which is costly.

1.3.1.2 Non-fumigant nematicides

Non-fumigant nematicides are less volatile than their fumigant counterparts and are active at doses of 2-10 kg a.i./ha compared to 200-300 liters/ha of liquid fumigants. When developed in the 1960s most non-fumigant nematicides were in granulated form and tilled into the top 10cm of soil to release the active compound to spread through the soil via irrigation or rainfall. Non-fumigant nematicides can also be applied via foliar spray and can have systemic effects as the chemical can be translocated through the plant tissue and exert its toxicity to PPNs already within the host (Oka et al., 2012).

Organophosphates and carbamates are two chemical groups within the non-fumigant nematicide group and they both act as nematostatics, causing paralysis of the nematode

via inhibition of cholinesterases (Husain et al., 2010). Cholinesterases act to break down the neurotransmitter acetylcholine which acts as one of the major excitatory neurotransmitters across the animal kingdom (Holden-Dye and Walker, 2011). It plays a significant role in regulation of neuromuscular transmission. In nematodes this is particularly important in the body wall muscle that controls motility and the pharyngeal structure that controls stylet and feeding function and elicits muscle activity. Organophosphates are able to phosphorylate cholinesterases and cause an irreversible inhibition of their activity (Costa, 2006) while carbamate causes a reversible inhibition (Alfonso et al., 1993). This inhibition of cholinesterases causes a buildup of acetylcholine within the synaptic cleft and hyper stimulation of receptors, which leads to hypercontracted muscle, resulting in paralysis (Opperman and Chang, 1991; Husain et al., 2010).

Field relevant concentrations of non-fumigants have been shown to elicit reversible paralysis (Oka et al., 2009) and impairment of chemoreception (Winter et al., 2002) making application time crucial to reduce crop loss. This becomes a practical issue with these chemicals as the recommended dose does not ensure nematode death (Oka et al., 2012) so when treatment is discontinued the PPN population in the soil may recover, resulting in delayed infestation. It has even been suggested that PPN infectivity is prolonged as low doses of cholinesterase inhibitors reduce energy and lipid consumption (Perry & Moens, 2013). Another issue with non-fumigant nematicides is that they lack selectivity and possess high non-target organism toxicity due to acetylcholine being highly conserved across the animal kingdom. For example, aldicarb and carbofuran display high toxicity towards birds and fish (Stenersen, 1979; Van Straalen and Van Rijn, 1998) and high exposure to organophosphates in humans can lead to seizures and even death (Husain et al., 2010). Chronic exposure to low levels of organophosphates is also shown to cause long-term health issues such as delayed neuropathy in non-target organisms (Costa, 2006) and behavioral defects in humans (Steenland, 1996).

High leaching properties of non-fumigant nematicides also present an issue as many, such as aldicarb, oxamyl and fenamiphos (Zaki et al., 1982; Bilkert and Rao, 1985), are highly mobile in the soil causing movement away from the initial site of application and

environmental damage. Additionally, as mentioned before, non-fumigant nematicides can be systemic and taken up by the crop plant; this then poses a risk to humans as residues may remain inside the plant tissue post-harvest (Chen et al., 2004). Furthermore, extended treatment using chemicals like fenamiphos results in more rapid biodegradation of the compound by bacteria in the soil (Smelt et al., 1996), which results in a more frequent treatment regime. The increased application frequency then increases the risk of PPN resistance which has been displayed in *M. incognita* following continuous exposure to sub-lethal doses of carbofuran (Meher et al., 2009).

As a result of these disadvantages, many non-fumigant nematicides have been phased out and chemicals such as aldicarb, carbofuran and parathion have all been banned in most countries. Although there are a number of issues and prohibition surrounding the use of nematicides, they still remain the most effective way of reducing the number of PPNs and are widely used in integrated pest management strategies (Sikora and Fernandez, 2005; Westphal, 2011). As such, nematicides with a more specific toxicity profile and non-chemical approaches are in demand more than ever.

1.3.2 Alternative methods of control

Non-chemical based methods such as biological control and host resistance offer an alternative way to reduce PPN numbers and have fewer damaging effects on the environment. Biological control uses other living organisms to manage plant disease or pathogens, including PPNs (Stirling, 2011) and potential organisms can be natural predators, parasites and pathogens of the pest. Unfortunately, organisms for biological control, such as predatory nematodes, are not widely used as a viable control mechanism (Viaene et al., 2013) due to issues in growing sufficient numbers (Salinas and Kotcon, 2005); however, fungi and bacteria offer a more encouraging alternative (Stirling, 2011). Both CNs and RKNs numbers have been successfully controlled using the fungus *Pupureocillium lilcacinus* (Parajuli, Kemerait, & Timper, 2014; Wilson & Jackson, 2013) but the effectiveness of these biological agents is dependent upon abiotic factors, such as soil moisture content and pH (Roberts et al., 1981; Cayrol, 1983), which are not easily predicted. Therefore, biological control alone, in most cases, is not sufficient to control

PPN populations but can be a vital part of integrated pest management strategies (Viaene et al., 2013).

Utilizing or engineering host resistance into crop plants can also be exploited as a control mechanism to reduce PPN number. Resistant plants can grow more efficiently in the presence of harmful PPNs or act to completely stop the life-cycle by not supporting PPN growth (Fuller et al., 2008; Starr, Mcdonald, & Claudius-Cole, 2013). There are many genes that confer resistance to PPNs and several have been characterized. The first nematode resistance (Nem-R) gene to be cloned was $Hs1^{pro-1}$ from sugar beet and confers resistance against the sugar beet cyst nematode (Cai et al., 1997). This gene has no similarities to other known plant genes but most cloned nematode-resistant genes resemble other resistance genes from plants in their protein domain structure, with a leucine-rich repeat (LRR) domain (Ellis and Jones, 1998). The most studied of them is the tomato gene, *Mi*, which provides resistance against 3 species of RKN (Williamson, 1998). The encoded protein has a nucleotide binding site (NBS) and a leucine rich repeat (LRR) region and belongs to a distinct class of plant resistance genes that do not contain an N-terminal toll-interleukin receptor-like (TIR) domain. Other members of the NBS-LRR family include the nematode resistance genes *Gpa2, Hero* and *Gro1-4.* The tomato genes *Mi* and *Hero* are known to have a broad-spectrum resistance against several RKN species and a few pathotypes of potato CNs, respectively. In contrast, the potato genes *Gpa1* and *Gro1-4* confer resistance to a select few pathotypes of one potato CN species (Leister et al., 1996; van der Voort et al., 1999). There is also evidence to suggest the phytoalexins produced by plants act as PPN repellents (Harborne, 1990; Mazid, Ta, & Mohammad, 2011).

Although biological control systems have potential as an alternative to chemical control, there is an issue with resistance breakdown and PPN strains overcoming host resistance (Ornat and Verdejo-Lucas, 2001; Aubertot et al., 2006). At present, all methods of PPN control come with disadvantages and it is widely accepted that the best route to nematode control is through integrated pest management strategies using a combination of chemical and non-chemical approaches alongside agricultural practices, such as crop rotation (Hillocks and Cooper, 2012).

1.4 Fluensulfone - A new option for chemical control of plant parasitic nematodes

Fluensulfone (FLS), full name: 5-chloro-2-(3,4,4-trifluorobut-3-ene-1-sulfonyl)-1,3-thiazole, also known as MCW-2 and Nimitz™ is a member of the heterocyclic fluoroalkenyl sulfone group (figure 1.8). This is a relatively new true nematicide which exerts its effects on a number of PPN species to protect a range of crop plants. Following its discovery, it has been developed into an agricultural product by ADAMA, which has quickly become approved for use in the U.S, Mexico, Israel, Australia and, most recently, Brazil.

1.4.1 Efficacy against plant parasitic nematodes

FLS has shown to be effective against a number of PPN species including *Meloidogyne spp., Pratylenchus spp., Xiphinema index, Nacobbus abberans* and *Globodera pallida* (Calvo-araya et al., 2016; Norshie et al., 2016; Oka, 2014; Oka et al., 2009; 2012). In these pot experiments, application of FLS reduced *M. incognita*-induced root galling of pepper seedlings and the number of eggs in the soil (Oka et al., 2012). Soil drenching with FLS was carried out after initial inoculation with *M. incognita* to determine if the chemical can act systemically and it was found that prevention of root galling was less effective over time suggesting the chemical may be more effective at the juvenile stages. Foliar spray of FLS was also used on pepper plants and it was determined that pre-plant application was most effective in reducing root damage as opposed to post-plant spraying (Oka et al., 2012).

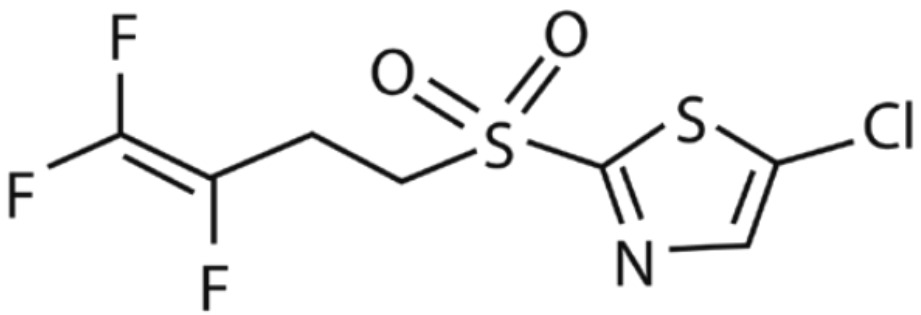

Figure 1.4. Chemical structure of FLS.

In a similar study by Oka et al., (2009) root galls were reduced in tomato seedlings following FLS treatment and it was observed that root galls increased with length of time between inoculation and treatment, suggesting early developmental stages are more susceptible to the chemical. In this same study, 48-hour exposure to FLS reduced egg hatching and 12-hour exposure also caused immobility. Even after rinsing, the percentage of immobilized nematodes increased after 5 days suggesting an irreversible paralysis compared to fenamiphos, which allowed J2 recovery. This proved that FLS has a role as a true nematicide as opposed to a nematostatic, which simply acts to paralyze. Interestingly, the morphology of immobile J2s was distinct to that of J2s exposed to organophosphates and carbamates, which display a shrunken, 'wavy' paralysis. FLS elicited a paralysis characterized by a straight, rod-shape worm suggesting its mode of action is distinct from these current nematicides.

FLS also reduces penetration ability of *M. javanica* after only 24-hour exposure to sub-lethal doses (Oka et al., 2013). Only 12% of juveniles became immobile after treatment with 3.4μM FLS but root penetration was reduced by 90%. This is distinct from fenamiphos which did not reduce root penetration and, once again, suggests FLS had a different mode of action as its effects are longer lasting than nematostatic organophosphates. In another study by Oka- (2014) a number of migratory PPNs were treated with FLS to determine if it elicited the same inhibitory effects across species. Motility of *Ditylenchus dispaci, Bursaphelenchus xylophilus* and *Aphelenchoides besseyi* were all unaffected after 48-hour exposure to 54.4 μM FLS and displayed a low susceptibility compared to *Meloidogyne* species which are adversely affected at extremely low concentrations. It has been noted previously that *Ditylenchus dispaci, Bursaphelenchus xylophilus* and *Aphelenchoides besseyi* species are less sensitive to nematicides (Lee et al., 1972; Voss & Speich, 1976). However, some migratory species, such as *X. index, Pratylenchus penetrans* and *Pratylenchus thornei,* displayed immobilization after FLS treatment and *P. penetrans* root invasion capacity was reduced in pot experiments, albeit at concentrations that exceeded those needed for *M. javanica.*

Recently, more studies on application methods of FLS have been carried out to determine its effects in the field. Pre-plant application of 5.6 kg/ha FLS via a backpack sprayer, tilling

and irrigation was not effective in reducing the population density of nematodes in the soil and did not increase growth of blueberry plants (Noe and Brannen, 2015). However, post-plant trials using a single application of 1.96 kg/ha FLS through drip tubes dramatically decreased nematode population in the soil and increased plant growth by 44%. This effect was enhanced following dual treatment (Noe and Brannen, 2015).

FLS was also used as a pre-plant treatment in a tomato-cucumber double cropping system, a practice used in agriculture regularly, to determine its effects. Resistant cultivars and 1, 3-D treatments were also used alongside for comparison. Tomato gall rating was lower in FLS-treated plots, however, resistant cultivars had significantly fewer galls compared to chemical treatment (Morris et al., 2015). The number of *Meloidogyne spp.* J2s were reduced in the soil following FLS treatment compared to the untreated control also. Pre-plant application of FLS to cucumber plots significantly increased plant vigor 14-days post-treatment and gall rating was also reduced, however, J2 numbers were not lower in this soil (Morris et al., 2015).

In another study by Morris et al., (2016) a number of application methods were evaluated for efficacy against RKNs on a range of vegetables. Pre-plant incorporation (PPI) application of FLS, post-plant drip irrigation and post-plant foliar application of FLS was carried out before inoculation with 1500 *M. incognita* J2 individuals. It was seen PPI treatment did not reduce galling compared to untreated control plots, but drip irrigation reduced galling in all vegetables. Foliar application only reduced galls in tomato roots but also reduced vigor and dry weight of tomato and eggplants suggesting moderate phytotoxic effects. However, cucumber and squash plants did not display this reduced vigor. Similarly, following pre-plant drip irrigation, vine length and fresh root weight of cucumbers were no different to untreated plots (Calvo-araya et al., 2016). Gall index and RKN *N. abberans* population size were also decreased compared to untreated and oxamyl-treated plots, suggesting higher efficacy of FLS.

A field evaluation of FLS ability to control the cyst nematode *G. pallida* was also carried out (Norshie et al., 2016). Two sites received FLS tilled into soil at 5 concentrations- 1.95, 3, 4.05, 5.05 and 6 kg/ha, and; root infection decreased in all treatments 29-days post-

plant and 44-days post-plant (with the exception of 1.95 kg/ha at 44 days). FLS was also seen to increase shoot fresh weight and yield at 42 days and displayed no phytotoxic effects (Norshie et al., 2016). These studies demonstrate the efficacy of FLS, both in lab and field conditions, suggesting it could be a new, viable method of reducing PPN numbers.

1.4.2 Toxicity profile

Due to the high levels of non-specific toxicity of a number of nematicides, including fumigant and non-fumigant chemicals (see section 1.3.1), a new alternative with low non-target organism toxicity would be hugely beneficial to the agricultural industry. FLS shows a favourable toxicity profile compared to organophosphates and carbamates with toxicity to vertebrates being 1000-fold lower than organophosphates (Dewhurst and Tasheva, 2013). The LD_{50} value for oral entry of FLS in rats was 671 mg.kg compared to 2.7 mg.kg for fenamiphos (organophosphate) and 0.8 mg.kg for aldicarb (carbamate) (Oka et al., 2009) showing that FLS only has a moderate acute toxicity. Additionally, it was determined that an increased incidence of tumors in humans was unlikely as no increase in carcinomas were found in the lungs of mice in an 18-month bioassay (Strupp et al., 2012). Environmental Protection Agency (EPA) eco-toxicity studies also show low toxicity towards a number of bird and fish species. FLS also shows low toxicity towards non-target insect species, including the economically important honeybee, compared to current nematicides in use (Oka et al., 2008). Interestingly, a study also determined FLS did not have a negative impact on the soil microbial community (Rousidou et al., 2013). This favourable toxicity profile shows the specificity of FLS, however non-target toxicity still remains against algae at field relevant concentrations suggesting a potential issue if leaching were to occur.

1.4.3 Properties of FLS in the field

In addition to its favourable toxicity profile, FLS also exhibits low leaching properties due to it being a fluoroalkenyl compound and, thus, being non-polar (Phillion et al., 1999). It exhibits low solubility and these properties reduce the risk of damaging nearby non-target ecosystems and also increases the period in which FLS remains effective (Oka et al.,

2008). The low leaching nature of FLS provides an advantageous difference compared to carbamate- and organophosphate-based nematicides, like aldicarb and fenamiphos, which have a long half-life (Oka et al., 2008) and high leaching properties (Zaki et al., 1982; Bilkert and Rao, 1985). Biodegradation of agricultural products is also of particular concern. If a product is applied frequently to the same site and soil-borne microorganisms are able to degrade it, this can reduce its toxicity (Smelt et al., 1987; Smelt et al., 1996; Suett & Jukes, 1988). The nematicidal activity of FLS was not impaired following repeated application to the same site in comparison to fenamiphos that showed reduced efficacy (Oka et al., 2013). This suggests FLS is less susceptible to biodegradation than other nematicides available for use.

1.4.5 Mode of action studies

Up until recently most of the work on FLS has been conducted to determine its effectiveness as a nematicide in the field. Early observation with *M. incognita* compared paralysis profiles relative to cholinesterase inhibitors, such as carbamates and organophosphates and suggested that its mode of action is distinct (Oka et al., 2009). Although it is known FLS acts to paralyze some PPN species, it has also been seen that sub-lethal concentrations, which do not elicit paralysis, reduce root penetration (Oka et al., 2012) implying paralysis is not the only method this compound works through to reduce infectivity.

Work by Kearn et al. (2014) and Feist et al. (2020) has further confirmed FLS mode of action to be distinct from anticholinesterases and macrolytic lactones. This work involved using *C. elegans* as a model for intoxication. Exposure to high concentrations of FLS (100-300μM) elicited reversible paralysis and inhibition of pharyngeal pumping rate while exposure to aldicarb only caused reduced motility without the inhibition of pharyngeal pumping. Additionally, a characteristic hypercontraction and shortening of body length of *C. elegans* caused by aldicarb was not observed when exposed to FLS. Kearn et al. (2014) used the *unc-17 C. elegans* mutant which has a marked resistance towards cholinesterase inhibitors and showed that, although it was resistant to aldicarb, FLS could still elicit similar levels of paralysis compared to a WT worm, suggesting FLS is not targeting

cholinesterases. Ivermectin, a macrolytic lactone, also exhibited a similar paralysis profile to FLS and elicits its action through glutamate-gated chloride channels. Kearn et al. (2014) also determined that FLS could still cause an inhibition of thrashing and pharyngeal pumping in an ivermectin-resistant mutant. This gave an indication that FLS is not working through the same mechanisms as anticholinesterases or macrolytic lactones. It has also been established the mode of action of FLS is distinct from the succinate dehydrogenase inhibitor, fluopyram, following evaluation of hatching inhibition capabilities in *G. pallida* (Feist et al., 2020).

Further mode of action studies by Kearn et al. (2017) on *G. pallida* have suggested FLS mode of action is through a progressive metabolic impairment. *G. pallida* exhibited impaired motility and reduced stylet thrusting at concentrations significantly lower than *C. elegans* and metabolic activity, determined through tetrazolium dye (MTT) staining, showed a concentration dependent reduction. This suggested that FLS reduces PPN infectivity via metabolic impairment. Furthermore, FLS induces a gradual shift in MTT staining from the head region to the tail region suggesting alterations in metabolism in the posterior of *G. pallida*. Nile red staining of lipids also supports this hypothesis as exposure to 10μM FLS for 10 days caused reduced staining, consistent with a gradual metabolic insult as a result of altered lipid metabolism (Kearn et al., 2017) . The large difference in sensitivity between *C. elegans* and PPN species suggests FLS may be acting on key elements of PPN metabolism not present in non-parasitic worms. Interestingly, it seems *Arabidopsis* also has a higher sensitivity towards FLS than *C. elegans,* suggesting the possibility that PPNs and *Arabidopsis* have a conserved target.

1.5 An introduction to *Arabidopsis*

Arabidopsis is a small, dicotyledonous, flowering winter annual, native to Eurasia (Hoffmann, 2002; Mitchell-Olds, 2001; Sharbel et al., 2000) with a relatively short life cycle of 6 weeks from germination to mature seed, making it a popular model organism in molecular biology and genetics. *Arabidopsis* is a member of the *Brassicaceae* family and was first described by physician Johannes Thal in 1577. Over 750 naturally occurring accessions of *Arabidopsis* have been collected from around the globe (Koornneef et al., 2004) and these display extensive genetic and phenotypic variation in terms of form,

development and physiology (e.g. leaf shape, flowering time) enabling studies to be conducted to determine complex genetic interactions that confer adaptation to different environments.

Although *Arabidopsis* is not an economically important plant, it has remained at the core of vigorous genetic, biochemical and physiological study for almost 50 years as it exhibits many traits suitable for laboratory studies. Laibach (1943) first chose this organism as a genetic model, followed by Redei (1975), who studied it in more detail. Due to its nature as a photosynthetic organism, *Arabidopsis* only requires light, air, water and minerals to complete its life cycle and produce a prolific number of seeds via self-pollination.

Arguably one of the most valuable traits *Arabidopsis* possesses is a relatively small, diploid, sequenced genome that can be genetically engineered easily and significantly faster than any other plant genome. A detailed genetic map was released by Koornneef et al. (1983), which acted to increase the popularity of this organism as a genetic model. The whole genome is made up of 5 chromosomes with 25,498 genes encoding proteins from 11,000 families with 125-megabase pairs, 115.4 of which are sequenced (Cheng et al., 2017).

1.5.1 Basic physiology

Arabidopsis is an annual plant. The leaves at the base of the mature plant have a serrated margin and form a rosette and a few leaves also develop on the flowering stem which are smaller and have a smoother margin. All leaves are covered in fine, unicellular hairs named trichomes (Larkin et al., 1996). *Arabidopsis* has provided considerable insight into the genetics of leaf morphogenesis – specifically in dicotyledonous plants, through the use of leaf development mutants. Three stages of leaf development have been determined: initiation of leaf primordium, dorsiventrality establishment and marginal meristem development (Tsukaya, 2013). *Arabidopsis* roots are simple in structure with a single primary root that grows vertically and later produces smaller lateral roots (Esau, 1977). The primary root is initiated from the root apical meristem (RAM) (Steeves and Sussex, 1989) as opposed to the shoot apical meristem (SAM) which acts as the source for

all above ground tissue such as the flowers and leaves. The RAM produces a specialized area of tissue, named the root cap, which covers the distal tip of the developing root to protect the tip as it grows through the soil. The root cap functions to perceive and respond to environmental stimuli such as gravity, temperature and humidity and acts to facilitate direction of root growth accordingly (Raven and Edwards, 2001).

1.5.2 Light detection in *Arabidopsis*

The importance of light signals in plant development is well established, with observations noting developmental processes of an etiolated seedling grown in the dark when moved into the light as far back as the 1880s (Darwin and Darwin, 1880). This phenomenon, now termed photomorphogenesis, involves 4 families of photoreceptors that detect different wavelengths of light: the phytochromes, cryptochromes, phototropins and UVR-8 (Kong and Okajima, 2016). Phytochromes A, B, C, D, and E mediate red/far-red (R/FR) light-based phototropic responses while cryptochromes and phototropins modulate UV-A/blue light influenced processes (Schäfer and Nagy, 2006). These sophisticated light sensing mechanisms allow the plant to detect the quantity and quality of light to maximize photosynthetic ability (Schäfer and Nagy, 2006) and aid survival.

When no light is detected, a young seedling undergoes skotomorphogenic development in which the seedling extends its growth to increase the chance of finding light. Phenotypically, the hypocotyl becomes elongated and the apical hook, protecting the cotyledons, remains closed. Chlorophyll biosynthesis is also inhibited causing a pale colour and root development is reduced. An etiolated phenotype has also been described in photoreceptor mutants under different light conditions and in mutants which are deficient or insensitive to hormones (Chory et al., 1991; Deng et al., 1991; Nagpal et al., 2000; Tian et al., 2003b). When a seedling is then exposed to white light (WL) the seedling transitions to a photomorphogenic growth pattern and the seedling becomes de-etiolated. De-etiolation involves opening of the apical hook and expansion of the cotyledons to maximize surface area for light capture. It also involves the biosynthesis of chlorophyll pigments that causes greening and allows photosynthesis. Development of the below-ground root structure is also activated (figure 1.5).

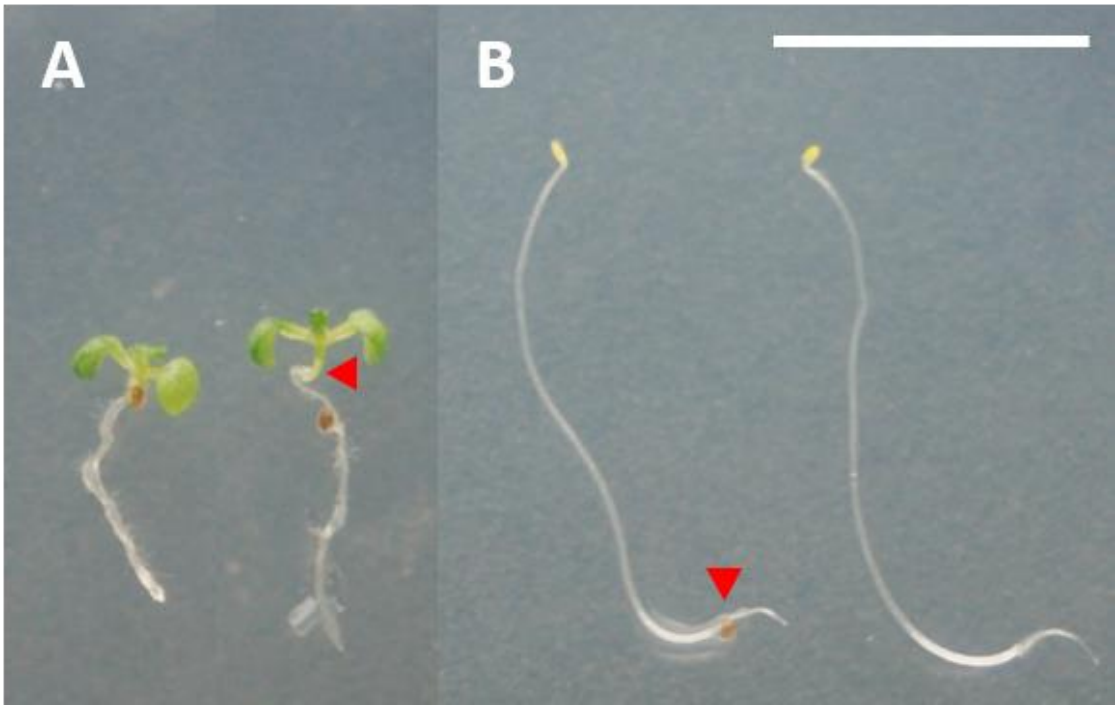

Figure 1.5. Phenotypes of (A) Light-grown de-etiolated seedlings and (B) Dark-grown etiolated seedlings. Red arrows denote hypocotyl-root boundary. Scale bar represents 1cm.

1.5.2.1 Phytochromes

The phytochrome system allows plants to grow towards the light and move out of shaded areas (Franklin and Whitelam, 2005). Plants in direct sunlight are exposed to high levels of red light (RL) compared to far-red (FR), while plants in the shade are exposed to FR-enriched light as other plants have absorbed a high proportion of the RL (reviewed in Smith & Whitelam, 1997).

The phytochrome family are reversibly photochromic proteins which exist as dimers. Each monomer is composed of an apoprotein covalently attached to phytochromobilin, a linear tetrapyrrole (Lagarias and Rapoport, 1980). Plants possess multiple phytochromes defined by their apoprotein-encoding genes. Three (*PHYA-PHYC*), are conserved in angiosperms while additional genes have been identified in dicotyledonous plants as a result of recent gene duplication events (Mathews & Sharrock, 1997; Mathews et al., 1995); specifically, *Arabidopsis* has 5 apoprotein-encoding genes (*PHYA-PHYE*) that have been sequenced and characterized (Clack et al., 1994; Sharrock & Quail, 1989). Phytochromes have two photo-convertible forms – Pr and Pfr. Pr, the biologically inactive

form, absorbs RL at around 667nm, while Pfr, the active form, absorbs FR light at 730nm. Phytochromes are produced in the inactive Pr form, with activity being acquired upon photoconversion to Pfr following exposure to RL. Photoconversion of Pfr to Pr is then optimized at FR wavelengths (Rockwell et al., 2006). This results in a dynamic photoequilibrium in natural light conditions. After conversion to Pfr, phytochromes translocate to the nucleus (Kircher et al., 1999; Sakamoto & Nagatani, 1996) and physically interact with phytochrome interacting factors (PIFs) – a subfamily of bHLH transcription factors (reviewed in Duek & Fankhauser, 2005). Therefore, the plants in shaded areas convert Pfr into Pr and growth is increased. In contrast, plants in full sunlight are able to convert Pr into Pfr which inhibits growth. This system allows plants with the fastest and most efficient growth to survive in dense populations.

The phytochrome system is also utilized by the seedling to determine presence or absence of light to regulate timing of germination (Casal and Sánchez, 1998). This regulation is vital in maintaining food reserves within seeds as, if germination occurs below the soil surface, a seedling would deplete food resources and die before breaching the surface. Therefore, the phytochrome system allows germination to occur only when the seed is exposed to light at the soils surface which causes Pr conversion to Pfr allowing photomorphogenesis and germination to ensue. In dark-grown seedlings or seedlings below soil, the Pr form of phytochrome is present and seed germination will be inhibited.

In addition, the phytochrome system is used to adjust a plants growth patterns according to the seasons. This is termed photoperiodism and is classified as a biological response to the duration and timing of dark and light periods in relation to a 24-hour cycle (Thomas and Vince-Prue, 1997). As unfiltered sunlight is rich in RL and lacking FR light, all the phytochrome molecules convert to the Pfr form at dawn and persist in this conformation until sunset. During darkness hours Pfr converts to Pr, therefore, if the night is long there will be no Pfr remaining at sunrise; whereas, if the night is short Pfr molecules will still be present. Presence of Pfr then stimulates flowering and vegetative growth as shortening nights indicate springtime and lengthening nights signify autumn.

1.5.2.2 Cryptochromes

Cryptochromes are a class of flavoproteins involved in blue-light mediated responses in plants. Cryptochrome 1 (*cry1*) in *Arabidopsis* was not discovered until 1993 by Ahmad and Cashmore who indicated considerable amino acid sequence similarity to prokaryotic DNA photolyases, although later work determined the protein had no photolyase activity and included a unique C-terminal extension (Ahmad and Cashmore, 1993). All members of the flavoprotein superfamily have an N-terminal photolyase homology (PHR) domain able to bind two chromophores, flavin adenine dinucleotide (FAD) cofactor and pterin (Brautigam et al., 2004) which allows cryptochrome responsivity at two different wavelengths (Hoang et al., 2008). This flavin chromophore acts to inhibit elongation of the stem through alteration of cell turgor pressure after it has been reduced by blue-light. Mutation at the CRY1 locus produces plants with reduced growth inhibition when exposed to blue-light. Mutants also exhibit depleted levels of blue-light induced genes (Ahmad et al., 1995). Following the discovery of *cry1*, *cry2* was identified and, like *cry1*, it is similar to photolyases and has a C-terminal extension variable from *cry1* (Lin et al., 1996). Mutations in *cry2* also cause inhibition of hypocotyl elongation and is also responsible for blue-light-mediated cotyledon and leaf expansion (Lin et al., 1998). Overexpression of *cry2* in transgenic plant lines has been seen to increase blue-light-stimulated cotyledon expansion, resulting in numerous broad leaves and no flowers as opposed to a flower with few primary leaves in a WT plant (Lin et al., 1998).

1.5.2.3 Phototropins

The phototropin photoreceptors are also involved in blue-light mediated phototropism responses, allowing plants to alter their growth in response to the light environment. Phototropins have two PAS domains, LOV domains and a classical Ser/Thr kinase domain downstream (Huala et al., 1997). Each LOV domain is able to bind flavin mononucleotide (FMN) as a chromophore to create the holoprotein (Christie et al., 1999). These FMN molecules can then undertake a photocycle which forms a cysteinyl adduct following blue-light activation and experiences break down in dark conditions. Phototropins 1 (phot1) and 2 (phot2) have roles in phototropism, chloroplast migration, stomatal

opening, inhibition of stem growth and calcium uptake, all in response to blue-light (Briggs and Christie, 2002).

1.5.2.4 Light signaling pathways

Plants are continuously monitoring light conditions to optimize their growth through photoreceptors and the signaling pathways stemming from them. A striking morphological change can be observed after etiolated seedlings are transferred to light and begin to undergo photomorphogenesis, or de-etiolation. This developmental change involves large scale gene expression changes in around one third of *Arabidopsis* genes (Ma et al., 2001) and analysis of temporal gene expression changes have shown the majority of the very early response genes expressed during phyA signaling are transcription factors (Tepperman et al., 2001). In contrast, many of the genes known to induce photomorphogenic development are expressed later suggesting photoreceptors are able to propagate a signal to a number of essential transcription factors which are then able to stimulate expression of a second set of transcriptional regulators that promote photomorphogenic development.

One of the principal factors interacting with phytochromes A and B are PIF (phytochrome interacting factor) proteins, which are bHLH transcription factors that bind to the G-box in the promotor region of several genes and negatively regulate photomorphogenesis (Martínez-García et al., 2000; Huq and Quail, 2002; Huq et al., 2004). Co-localisation studies discovered the distribution of PIF3 varied under different light conditions; in the dark, PIF3 is present in the nucleus and undergoes light-induced degradation via phyA, phyB and phyD (Bauer et al., 2004). In the same study, it was determined that the dark-induced accumulation of PIF3 in the nucleus is COP1 dependent, whereas, the light-induced PIF3 degradation was COP1 independent. It was suggested that PIF3 accumulation in the dark is the result of a COP1-mediated degradation of a PIF3 repressor, this would be consistent with the knowledge that light induces the exclusion of COP1 from the nucleus.

COP1 is an ubiquitin E3 ligase, required for the activity of the COP9 signalosome, which targets proteins for degradation and acts as a central repressor of photomorphogenesis (Osterlund et al., 1999) and mutations within COP1 give seedlings a light-grown-like phenotype in the absence of light. Genetic screens have enabled the COP1 (constitutively photomorphogenic) locus (Deng et al., 1991) and a number of other loci, COP9 (Wei & Deng, 1992), 2, 3, 4 (Hou et al., 1993), 8, 10 and 11 (Wei et al., 1994) to be characterized. Alongside this, mutations in DET loci – encoding nuclear localized DET1 (de-etiolated) proteins (Pepper et al., 1994) were discovered that generate the same light-grown-like morphology in darkness (Cabrera y Poche et al., 1993; Chory et al., 1989; Chory et al., 1991). Their morphology shows shortened hypocotyls and expanded cotyledons and, due to the recessive nature of the *cop/det* mutations, it suggests photomorphogenesis is the default developmental pathway. In the same manner, genetic screens have also been instrumental in the discovery of effectors of photomorphogenesis such as HY5 and HYH; mutations within these proteins cause plants to develop long hypocotyls when germinated in the light (Holm et al., 2002; Koornneef et al., 1980). HY5 is a bZIP transcription factor localized in the nucleus (Oyama et al., 1997) which is able to bind to the G-box in the promotor region of light-inducible genes and induce their expression (Chattopadhyay et al., 1998).

Together with epistasis studies looking into the interactions between *det1, cop8, cop10, cop11* and *hy5-1* mutants (Chory, 1992; Wei et al., 1994), it was determined that COP1 was epistatic to HY5 (Ang and Deng, 1994). However, further studies reveal a COP1 specific degradation of HY5 and HYH in dark conditions (Holm et al., 2002; Osterlund et al., 2000) This information, alongside the knowledge that abundance of nuclear localized COP1 decreases following exposure to light (von Arnim and Deng, 1994), suggests a model in which COP/DET proteins act to degrade key transcriptional regulators such as HY5 to prevent photomorphogenic development in the dark.

1.5.5 *Arabidopsis* phytohormones

As plants have a sessile lifestyle they are required to regularly adjust their developmental growth according to external stimuli. A number of small molecules, termed plant hormones (phytohormones), allow the coordination of many extracellular signals to regulate appropriate responses and are also essential for implementing the developmental program. Using extracellular signals to communicate between cells is also seen in animals; these signals are classically small proteins or peptides, like insulin, or organic-based hormones, like steroids. In plants the signaling molecules usually signal throughout the organism to promote growth, development and defense. Interestingly, although some plant hormones share similar structures to a number of animal hormones, plant hormones have a significantly larger range in function (Chow and McCourt, 2006). One plant hormone is able to induce effects in many different cells and one cell has the potential to be able to respond to all plant hormones.

The five 'classic' plant hormones: auxin, gibberellin (GA), cytokinin, abscisic acid (ABA) and ethylene were discovered earliest, whereas other molecules such as brassinosteroid (BR), jasmonate (JA) and strigolactone (SL) were later described as new families of plant hormones (Davies, 1987). Biosynthesis and signaling of plant hormones are extremely complex but recent advances have uncovered receptors and key signaling molecules underpinning their pathways and perception. In this chapter GA, auxin and BR signaling will be focused on, see Shan et al., (2012) for a review of all hormone signaling.

1.5.5.1 Gibberellins

Biologically active gibberellins, such as GA_1, GA_3 and GA_4, control a number of aspects of plant development including germination, stem elongation, leaf expansion and seed development. Of over 100 gibberellins in total, only a small number function as biologically active hormones (MacMillan, 2001), this leaves many GAs to exist in plants as precursors or deactivated metabolites. GAs are synthesised from geranylgeranyl diphosphate (GGDP), which is a precursor for diterpenoids (Yamaguchi, 2008) and three enzyme classes, terpene synthase (TPSs), cytochrome P450 monooxygenases (P450s) and 2-oxoglutarate-dependent dioxygenases (2ODDs), have a crucial role in GA biosynthesis.

In higher plants the methylerythritol phosphate pathway in the plastid has been shown to provide the majority of the isoprene units for GA biosynthesis, while the cytosolic mevalonate path only has a minimal contribution (Kasahara et al., 2002). GA signalling involves targeted protein turnover and ubiquitination to exert its effects; the GA receptor, GID1, was identified in a signalling mutant screen in rice and confers complete insensitivity to GA treatment (Ueguchi-Tanaka et al., 2005). GID1 is a nuclear localised protein which can bind biologically active GAs.

Physiological data also demonstrates a role for DELLA proteins in negatively regulating GA. Interestingly, DELLA proteins have been shown to directly interact with PIF3 and PIF4 proteins, sequestering them in an inactive state (de Lucas et al., 2008; Feng et al., 2008) displaying an integration of light and hormone signalling within plants. GA also functions to destabilise DELLAs, allowing PIF3 and PIF4 to begin transcription of target genes (de Lucas et al., 2008; Feng et al., 2008). The receptor GID1 is also able to interact with DELLAs in a GA-dependent manner (Griffiths et al., 2006; Willige et al., 2007) and GID1 expression has been shown to enhance the interaction between DELLAs and the F-box proteins SLY1/GID2 (Griffiths et al., 2006). This would support the notion that DELLAs are ubiquitinated and degraded by $SCF^{SLY/GID2}$ only when in a complex with GA bound GID1, allowing the transcription of GA responsive genes by PIF proteins. This model has been supported by the structures of rice GID1 and *Arabidopsis* GID1a (Murase et al., 2008; Shimada et al., 2008).

Regulated protein turnover is also seen in both ABA and ethylene signalling. ABA-insensitive 3 and 5 (ABI3 and ABI5) protein levels are controlled by the RING E3 ligases ABI3-Interacting Protein (AIP2) and Keep on Going (KEG), respectively, and ABA promotes ubiquitination of ABI3 while inhibiting ubiquitination of ABI5 to allow ABA responses (Stone et al., 2006; Zhang, Garreton, & Chua, 2005). In ethylene signalling, the presence of ethylene causes SCF^{ETP1} and SCF^{ETP2} levels to decrease (Guo & Ecker, 2003; Potuschak et al., 2003), which subsequently increases Ethylene-Insensitive 2 and 3 (EIN2 and EIN3) levels and ethylene responsive gene expression (Qiao et al., 2009).

1.5.5.2 Ethylene

Ethylene is a simple gaseous hormone involved in regulating a number of key developmental stages including seed germination, root hair development and fruit ripening. Endogenous production of ethylene is controlled through abiotic and biotic stressors such as wounding, hypoxia and chilling. Applying exogenous ethylene or a precursor 1-aminocyclopropane-1-carboxylic acid (ACC) to etiolated seedlings induces the 'triple response' which includes the hallmarks of an exaggerated apical hook, shortening of the hypocotyl and radial swelling of the hypocotyl (Plinio Guzman and Ecker, 1990). This response has been exploited over the years using mutant screens and physiological studies to understand ethylene biosynthesis, signal transduction and regulation, allowing this hormones role in plant function to be discovered (Shan et al., 2012).

S-adenosylmethionine (S-AdoMet) is a precursor of ethylene (see Yang & Hoffman, 1984 for review) and 80% of cellular methionine is converted to S-AdoMet by S-AdoMet synthetase (Ravanel et al., 1998). S-AdoMet acts as one of the major methyl donors in plants and is involved in a number of biochemical pathways and in methylation reactions which modify lipids, proteins and nucleic acids. S-AdoMet is converted to ACC by ACC synthase (ACS) in the first committed step of the ethylene biosynthesis path and 5'-methylthioadenosine (MTA) is produced in this reaction. MTA can then be recycled to create methionine, allowing the preservation of the methyl group for future ethylene production (Bleecker and Kende, 2000). This allows the continued production of ethylene without the need for an increased methionine pool. Following this, ACC is oxidized by ACC oxidase to form ethylene, cyanide and CO_2 which is then detoxified to stop cyanide accumulation during times of high ethylene production (Wang et al., 2002) (Figure 1.6).

ACC synthase genes encode the rate limiting step in ethylene biosynthesis and there is significant evidence to suggest these enzymes are both positively and negatively regulated by various external and internal signals. For example, *ACS2* is induced by cyclohexamide, wounding and 2 h ethylene treatment (Liang et al., 1996; Van der Straeten et al., 1992), *ACS4* is induced by cyclohexamide, IAA and wounding; *ACS5* is induced by lithium chloride and cytokinin in etiolated seedlings (Abel et al, 1995; Liang et

al., 1996) and *ACS6* can be specifically induced by cyanide treatment and exposure to ozone (Smith & Arteca, 2000; Overmyer et al., 2000; Vahala et al., 1998).

After synthesis, ethylene is perceived by a family of five membrane-localised receptors: ETR1, ETR2, ERS1, ERS2, and EIN4 (Chang et al., 1993; Hua et al., 1995; Hua and Meyerowitz, 1998; Sakai et al., 1998). These receptors consist of two proteins: a histidine kinase as the receiver that autophosphorylates an internal histidine residue and a response regulator that activates downstream responses when an aspartate residue receives a phosphate from the histidine residue. Ethylene binding happens at the N-terminal transmembrane domains of the receptors and requires a copper co-factor provided by the copper transporter RAN1 (Hirayama et al., 1999).

In the absence of ethylene, the receptors activate CTR1, a Raf-like kinase, which is thought to negatively regulate the downstream ethylene pathway through a MAP-kinase cascade. In the presence of ethylene, the receptors are inactivated, causing deactivation of CTR1, which allows EIN2, a membrane protein, to function as a positive regulator (Alonso et al., 1999) and signal to the EIN3 family transcription factors in the nucleus. EIN3 is able to bind to the promotor region of the ERF1 gene and induce its transcription to then activate the transcription of target genes and downstream ethylene responses (Chao et al., 1997).

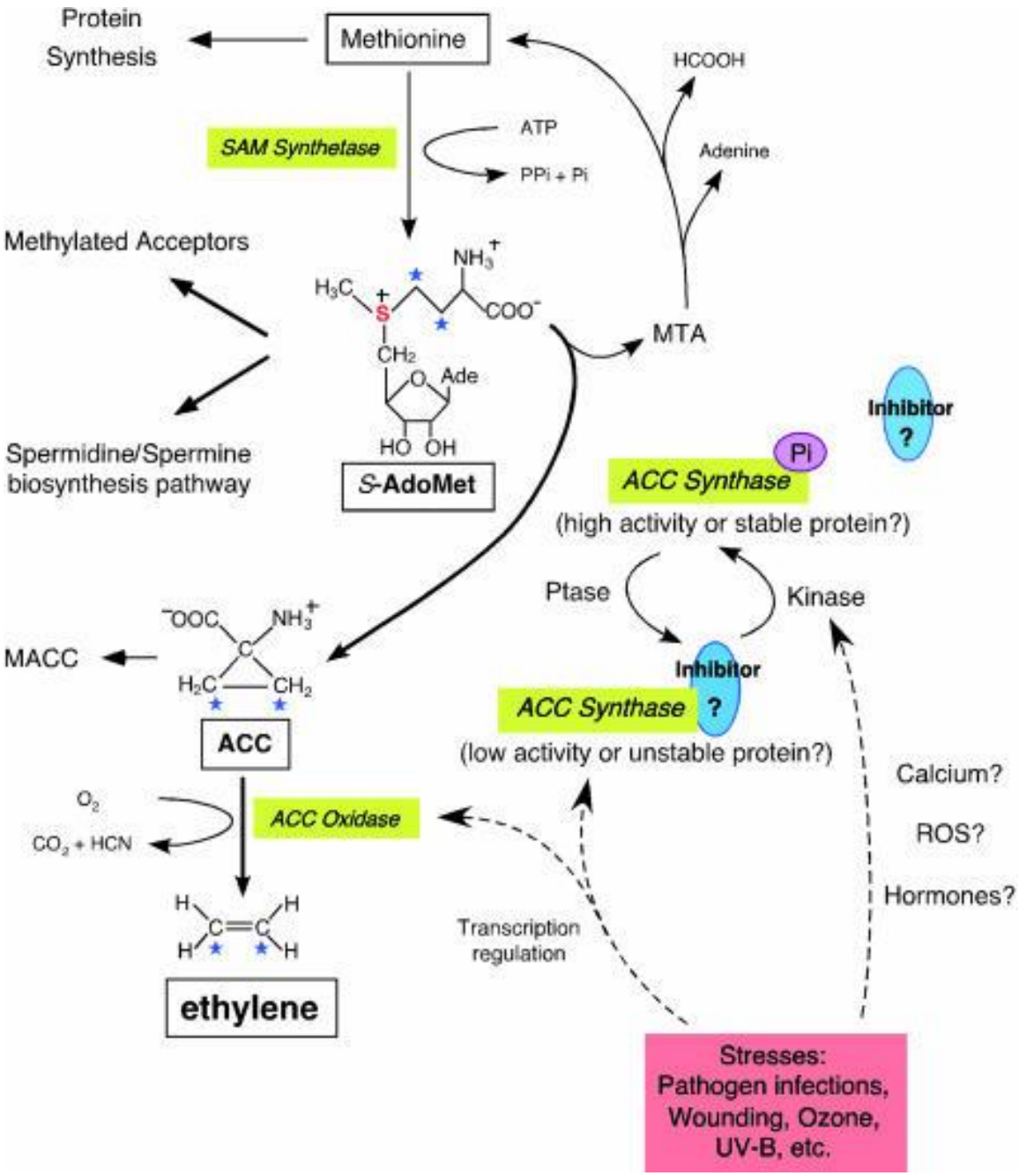

Figure 1.6. Ethylene biosynthesis pathway. S-AdoMet (SAM) is formed via the catalysis of methionine by SAM synthase, using one ATP molecule per molecule of SAM synthesised. ACC, the immediate pre-cursor of ethylene, is formed through the conversion of SAM to ACC by ACC synthase and this is the rate limiting step in ethylene synthesis. 5'-methylthioadenosine (MTA) is the by-product of this reaction and can be recycled back to methionine to preserve the methylthio group. The final step in is the conversion of ACC to ethylene via ACC oxidase. This step generates CO_2 and cyanide. Dashed arrows represent transcriptional regulation of ACC synthase and ACC oxidase. Reversible inhibition of ACC synthase has been hypothesised to occur following stresses. Figure from Wang et al., (2002).

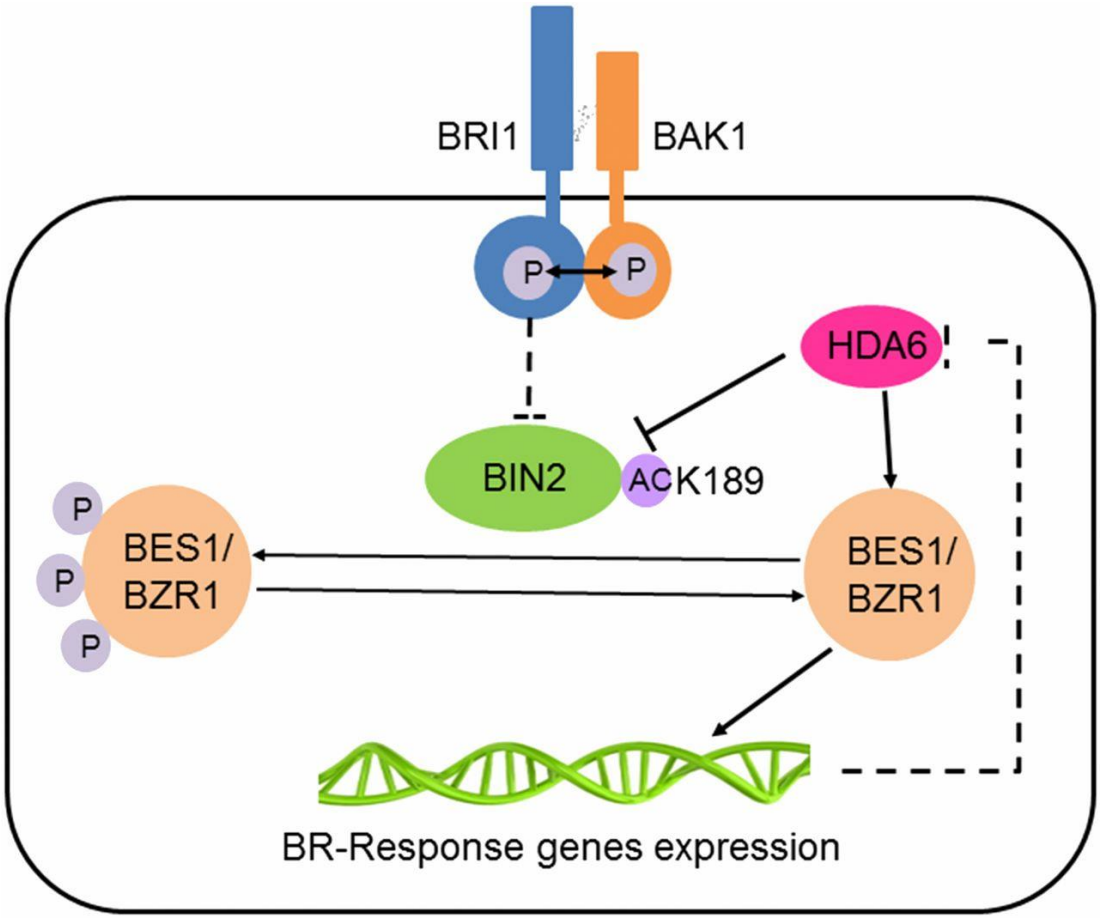

Figure 1.7. Brassinosteroid signalling pathway. BR signalling begins with BR binding to the BRI1 receptor to allow transphosphorylation of BAK1. BR signalling also inhibits an important negative regulator, BIN1, which acts to phosphorylate transcription factors BES1/BZR1 to inhibit BR signalling. Recently it has been shown that, in low energy conditions, a histone deacetylase (HDA6) is also able to inhibit BIN2 activity and may interact with BES1 to regulate its transcriptional activity. Figure from Hao et al (2016).

1.5.5.3 Brassinosteroids

In animals, steroid hormones are essential for embryonic development and homeostasis (Evans, 1988) and, in plants, one class of steroids – brassinosteroids (BRs) – has a role in growth promotion. Physiological studies have shown BRs are able to induce events including stem elongation, root inhibition, ethylene biosynthesis and proton pump activation (Clouse & Sasse, 1998; Mandava, 1988). BRs role in plant growth was observed through a genetic screen of constitutively photomorphogenic mutants (Chory et al., 1989); mutant *Arabidopsis* seedlings showing a light grown phenotype in the dark. One mutant identified was the *de-etiolated2* (*det2*) mutant which was deficient in an early

step in brassinosteroid biosynthesis (Fujioka et al., 1997) . Exogenous application of BR rescued these growth deficits in both dark and light conditions (Li et al., 1996; Fujioka et al., 1997).

The discovery of this BR biosynthetic mutant and others, such as *CPD* and *DWF4* (Szekeres et al., 1996; Choe et al., 1998), alongside gas chromatography-mass spectrometry analyzing intermediates, has allowed the BR biosynthetic pathway to be established. It is now known that campesterol (CR) is a predominant BR precursor and is first converted to campestanol (CN) and subsequently to BR via two pathways: the early and late C-6 oxidation pathway (Zhao & Li, 2012). These two pathways converge on castasterone (CS). However, there is also an additional CN-independent pathway which has been suggested to be the dominant BR biosynthesis path (Fujioka et al., 1997; Ohnishi et al., 2012).

BR mutants were also found that displayed normal root growth on exogenous BR (Fujioka et al., 1997). The mutants showing these qualities displayed mutations in *BRI1*, which was found to encode a plasma membrane-associated LRR receptor-like kinase (LRR-RLK) (Li & Chory, 1997). This family consists of over 200 genes in the *Arabidopsis* genome (Shiu and Bleecker, 2003) and has a role in a number of signaling pathways; however, it was unexpected that BR could bind directly to the extracellular domain of the LRR. The 25 leucine repeats in the BRI1 LRR have a unique 70-amino-acid island domain between repeats 21 and 22 (Li & Chory, 1997) and this was determined to be the site at which BR binds (Kinoshita et al., 2005; Li & Chory, 1997). Binding of BR to BRI1 homodimers allows auto-phosphorylation of its cytoplasmic kinase domain which, subsequently, induces an interaction between another LRR-RLK named BAK1 in which BAK1 is trans-phosphorylated (Wang et al., 2008). Additionally, BR signaling deactivates brassinosteroid insensitive 2 (BIN2) (Li & Nam, 2002) which leads to the activation of two transcription factors, brassinazole-resistant 1 and 2 (BZR1 and BZR2) (Wang et al., 2002) (figure 1.7).

1.5.6 Auxin

In 1880, it was suggested there was a plant-organ forming substance that moved directionally within the plant to produce roots and induce bending of grass coleoptiles towards the sun (Darwin, 1880). Later characterisation determined these substances were a class of compounds called auxins (Went, 1937; Went, 1927) that have been shown to underpin key processes such as tropic responses (Friml et al., 2002; Abas et al., 2006), embryo/vascular patterning (Möller & Weijers, 2009; Scarpella et al., 2010; Weijers et al., 2006), organ initiation (Benková et al., 2003), root/shoot elongation (Perrot-Rechenmann, 2010) and apical dominance (McSteen and Leyser, 2005). The predominant auxin in higher plants is indole-3-acetic acid (IAA) which is present in cells at picogram per milligram fresh weight concentrations (Ljung et al., 2002) and is a small tryptophan derived compound. Auxin biosynthesis is complex and it is known there are multiple paths that contribute to *de novo* auxin production (Zhao, 2010); however, IAA is also known to be released from IAA conjugates (Bartel, 1997). It is widely accepted that tryptophan is a precursor to IAA and the predominant pathway is tryptophan-dependent as many studies have confirmed the conversion of tryptophan to IAA in plants (Nonhebel et al., 1993). However, plants blocked in the final steps of tryptophan synthesis still display WT levels of IAA but with an over-production of IAA conjugates and potential different precursors, such as indole-3-acetonitrile (IAN) (Normanly et al., 1993). This suggests the presence of alternative Trp-independent pathways which have been discovered more recently (Nonhebel, 2015), giving a role to cytosol-localized indole synthase (INS) (Wang et al., 2015) in the initiation of Trp-independent IAA synthesis.

Other compounds have also been reported to show auxinic activity, including the natural endogenous auxins: 4-chloroindole-3-acetic acid (4-Cl-IAA), indole-3-butyric acid (IBA) and phenylacetic acid (PAA) (Ludwig-Muller and Cohen, 2002; Simon and Petrášek, 2011). At concentrations below cellular toxicity, auxins stimulate growth in shoots, growth inhibition in roots and the induction of adventitious and lateral roots in a number of species (Woodward and Bartel, 2005). For example, exogenous application of IAA at $3x10^{-8}$ M causes a 50% inhibition in root growth (Wilson et al. 1990).

In addition to their physiological effects, these auxins all contain structural similarities; they all share a carboxyl group and aryl ring structure which is also found in a number of synthetic auxins such as 2,4-dichlorophenoxyacetic acid (2,4-D) and naphthalene acetic acid (1-NAA) (figure 1.8). These compounds, along with derivates like dicamba and picloram, have a long history of use as herbicides. Their function is to elicit the same cellular responses as IAA, but due to their higher stability in the plant, their auxinic action is longer lasting and more intense. One reason for their stability is that these compounds are not subject to rapid inactivation via conjugation and degradation in the same way as natural auxins, like IAA (Grossmann, 2010), therefore these compounds can illicit uncontrolled cell elongation and ultimately lead to plant death. While all auxinic compounds cause similar physiological responses in plants, they also have unique modes of action characterised by distinct, but overlapping, changes in gene expression following exposure (Pufky et al., 2003). The variation in gene expression likely reflects differences in metabolism, transport or signalling (De Rybel et al., 2009; Woodward & Bartel, 2005).

1.5.6.1 Auxin perception and signaling

As mentioned previously, auxin induces a number of responses within a plant and underlying these responses are rapid changes in gene expression within minutes, characterised by an almost immediate perception and transduction of a signal from outside of the cell to the nucleus. Auxins are able to enter the cell either by passive diffusion or active uptake via the AUX1/LIKE AUX1 (AUX1/LAX) family of carriers (Bennett et al., 1996; Swarup et al., 2008) and once inside, IAA is small enough to enter the nucleus through nuclear pores where it acts on the ubiquitin-proteasome system (UPS), thus linking auxin perception and a fast transcriptional response.

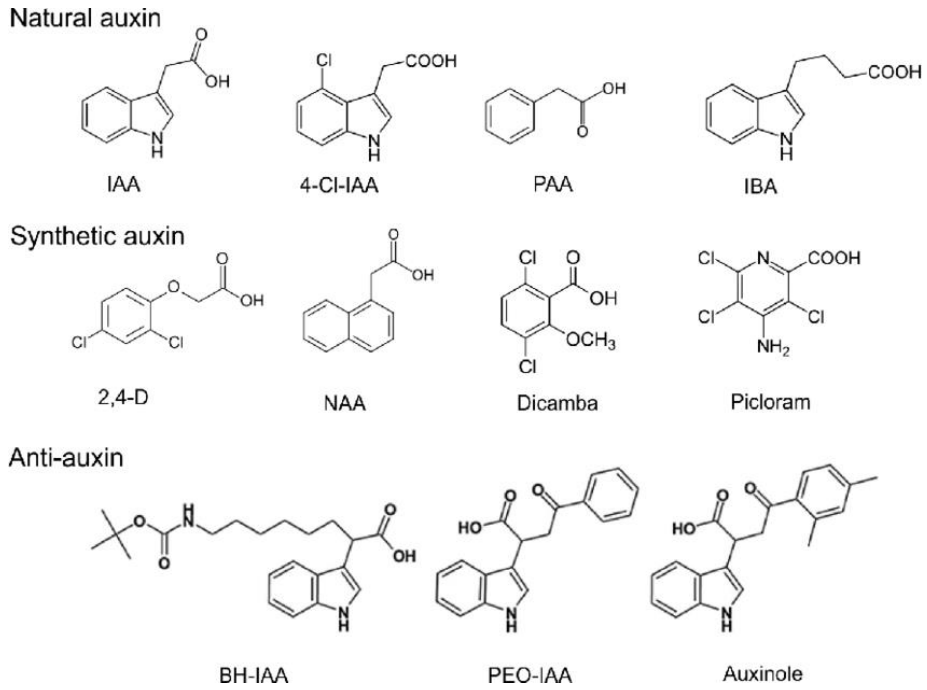

Figure 1.8. The chemical structures of natural/synthetic auxins and anti-auxins. Natural auxins include indole-3-acetic acid (IAA), 4-chloroindole-3-acetic acid (4-Cl-IAA), phenylacetic acid (PAA) and inactive auxin precursors indole-3-butyric acid (IBA). Synthetic auxins include: 2,4-dichlorophenoxyacetic acid (2,4-D), naphthalene acetic acid (1-NAA), 3,6-dichloro-2-methoxybenzoic acid (dicamba) and 4-amino-3,5,6-trichloro-2pyridinecarboxylic acid (picloram). Anti-auxins include: tert-butoxycarbonylaminohexyl-IAA (BH-IAA), α-(phenylethyl-2-oxo)-IAA (PEO-IAA) and α-(2,4-dimethylphenylethyl-2oxo)-IAA (auxinole). Figure retrieved from Chandrasekaran, 2015.

The auxin receptors were discovered through mutant screens looking for *Arabidopsis* seedlings with a reduced response to auxin. Interestingly, many mutants found were impaired in the components of the Skp1/Cullin/F-box (SCF) ubiquitin ligases (E3) or in proteins that regulate the activity of the SCF (Dharmasiri & Estelle, 2002). The E3 ligases confer the substrate specificity to the ubiquitin-proteasome pathway as the F-box protein directly interacts with the substrate (Moon et al., 2004). There are estimated to be over 1000 plant E3 ligases (Chen & Hellmann, 2013) but, SCF E3 ligase complexes specifically recognise targets for ubiquitin transfer. SCF complexes consist of 4 protein subunits with various functions; CULLIN (CUL1) has a role as a scaffold protein, binding RING BOX1 (RBX1) at its C-terminus and a SKP1 / F-box protein (FBP) complex to its N-terminus (Patton et al., 1998; Skowyra et al., 1997; figure 1.9). The FBP family consists of >700 proteins in *Arabidopsis* and is the subunit that confers specificity to the SCF complex. While all FBPs contain a domain for ASK protein docking, they have variable target

recognition domains (Gagne et al., 2002). The SCFs were first linked with a role in canonical auxin signalling when the FBP, TRANSPORT INHIBITOR RESPONSE 1 (TIR1) was found to degrade negative regulators of auxin responsiveness and mutants in *TIR1* displayed auxin resistance (M Ruegger et al., 1998). Additionally, the discovery that TIR1 is directly linked to auxin-regulated transcription was key in the characterization of the signalling pathway (Gray et al., 2001). TIR1 and its 5 close homologs AUXIN SIGNALING F-BOX 1-5 (AFB1-5) are soluble, nuclear localised proteins that interact with ASKs through their N-terminus to form an $SCF^{TIR1/AFB}$ complex (Dharmasiri et al., 2005; Gray et al., 1999).

The C-terminal region of TIR1/AFB is comprised of 18 leucine rich repeats (LRRs; Gagne et al., 2002) that is able to physically interact with auxin/indole-3-acetic acid (Aux/IAA) transcriptional repressor proteins in an auxin-dependent manner to promote Aux/IAA protein degradation (Gray et al., 2001b). Subsequently, Aux/IAA protein degradation de-represses AUXIN RESPONSE FACTOR (ARF) transcriptional activator proteins and auxin-responsive genes can be transcribed.

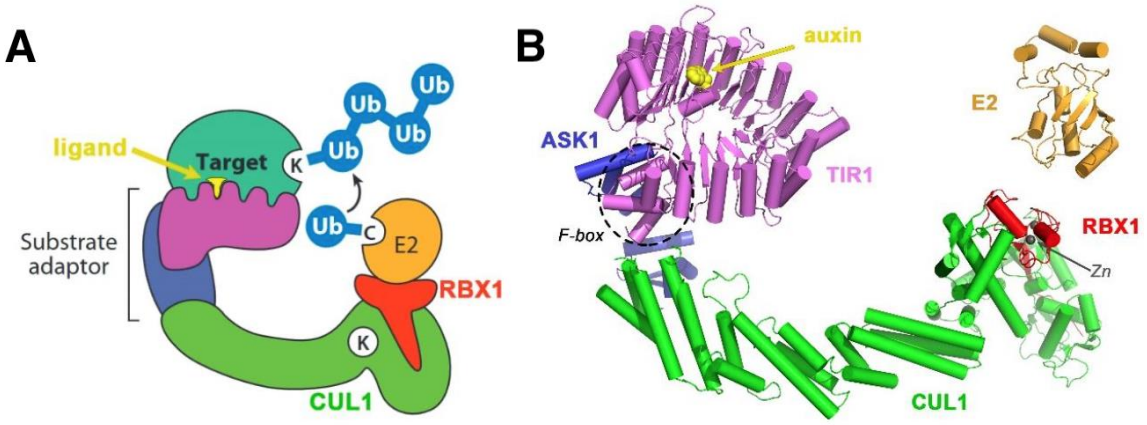

Figure 1.9. Subunit structure of an SCF complex. (A) Organisation of SCF complexes. The CUL1 scaffold protein binds a substrate adaptor or target receptor and an RBX1 protein for E2 docking. The K represents the acceptor sites for Ub and complex modifiers; C represents the active-site cysteine that binds activated Ub. (B) Ribbon model of the SCF^{TIR1} in complex with auxin. ASK1 and the FBP TIR1 bind via the F-box domain (black dashed circle) to create the substrate adaptor that then complexes with CUL1 and RBX1. Auxin (yellow) binds to TIR1 in a pocket to enhance the interaction with its targets, the Aux/IAAs. Modified from Hua & Vierstra (2011).

Auxin enhances the degradation of Aux/IAAs by $SCF^{TIR1/AFB}$ and TIR1 has been shown to bind auxin directly *in vitro* (Dharmasiri et al., 2005; Kepinski & Leyser, 2005). The crystal structure of a TIR1:ASK heterodimer alone and in complex with IAA, 1-NAA or 2,4-D and an Aux/IAA protein displays a 'mushroom-like' structure with TIR1:ASK forming the 'stem' and the 18 LRRs forming the 'cap'. The auxin and Aux/IAA target can then bind to this concave surface referred to as the auxin binding pocket (Tan et al., 2007) (figure 1.10). The carboxyl group of an auxin is anchored to the bottom of the auxin binding pocket and the aromatic ring has less selective interactions with the sides of the pocket. Docking of the Aux/IAA then occurs atop the bound auxin which led to the proposal that auxin acts as a 'molecular glue' to enhance the interaction between the receptor and Aux/IAA targets (Tan et al., 2007). This is the canonical auxin signalling pathway thought to mediate the majority of auxin responses in plants (Badescu and Napier, 2006; Leyser, 2018); however, recently, a non-canonical pathway dependent of TIR1/AFBs, involving ARF3 (ETTIN) and protein kinases has been suggested (Kubeš and Napier, 2019).

Interestingly, it is not only auxin-signalling that requires F-box proteins. CORONATINE INSENSITIVE1 (COI1) is an F-box protein that it closely related to TIR1 (Xie et al., 1998) and it acts to degrade jasmonate response repressors to allow jasmonate signal transduction. Recently the transcriptional regulators, and substrates, for COI1 have been identified: the JAZ protein family (Thines et al., 2007; Chini et al., 2007). These pathways highlight the importance of the ubiquitin-proteasome pathway in hormone signalling.

1.5.6.2 The role of Aux/IAAs

Aux/IAA transcriptional repressors are small proteins encoded by a family of 29 genes in *Arabidopsis* (Remington et al., 2004), that, upon translation, localise rapidly to the nucleus. *Aux/IAAs* genes are classified as primary-auxin responsive genes as their expression increases rapidly upon auxin application (Abel & Theologis, 1996). Therefore, degradation of Aux/IAA proteins leads to de-repression of these genes and a rapid control over the auxin response. However, induction kinetics do vary from a few minutes after auxin application (*IAA1-6*) to 30 minutes (*IAA9-10*) (Abel et al., 1995).

23 of the 29 members of the Aux/IAA family are canonical due to them sharing 4 regions of highly conserved sequence, named domains I, II, III and IV (Abel et al., 1995; Oeller et al., 1993). One essential feature of rapid auxin signalling is the quick degradation of Aux/IAAs which is mediated by a degron located in domain II. The degron consists of a conserved sequence with a core amino acid group VGWPP (Ramos et al., 2001) that is recognised by the $SCF^{TIR1/AFB}$ E3 ligase. It has been shown that after compromising the degron sequence, Aux/IAA proteins become stabilised, accumulate and cause constitutive repression of auxin signalling resulting in auxin resistant phenotypes. A number of gain-of-function (gof) mutations consisting of a single amino acid change in the degron have been isolated; for example, roots of *auxin-resistant* (*axr*) mutants are resistant to growth inhibition by exogenous auxin, have stunted growth, reduced etiolation response, agravitropism and lack of root hairs (Nagpal et al., 2000; Timpte et al., 1994; Yang et al., 2004). In addition, the *suppressor of hy2 mutation 2* (*shy2/iaa3*) gof mutant displays a strong de-etiolated phenotype in the dark suggesting an overlap between auxin and light signalling (Kim et al., 1998a; Tian et al., 2003a). Mutations within the key degron of Aux/IAAs not only stabilize the protein but also alter the degradation rates in response to auxin (William M. Gray et al., 2001). Canonical Aux/IAAs have basal half-lives from 6-80 minutes, while gof mutants are stable (Ramos et al., 2001; William M. Gray et al., 2001).

Aux/IAA proteins repress ARF transcription factors. ARFs have a similar structure to Aux/IAAs and through the PB1 domain (domains III/IV), Aux/IAAs and ARFs can have homo- and heterotypic interactions. *ARFs* in *Arabidopsis* are encoded by a family of 23 genes (Guilfoyle and Hagen, 2007) and the role of ARF transcription factors is to bind to auxin responsive elements (*AuxREs*) to increase or decrease transcription of downstream auxin-responsive genes. These genes include members of the *Aux/IAA, GRETCHEN HAGEN3 (GH3),* and *SMALL AUXIN UPREGULATED RNA (SAUR)* gene families (Hagen and Guilfoyle, 2002).

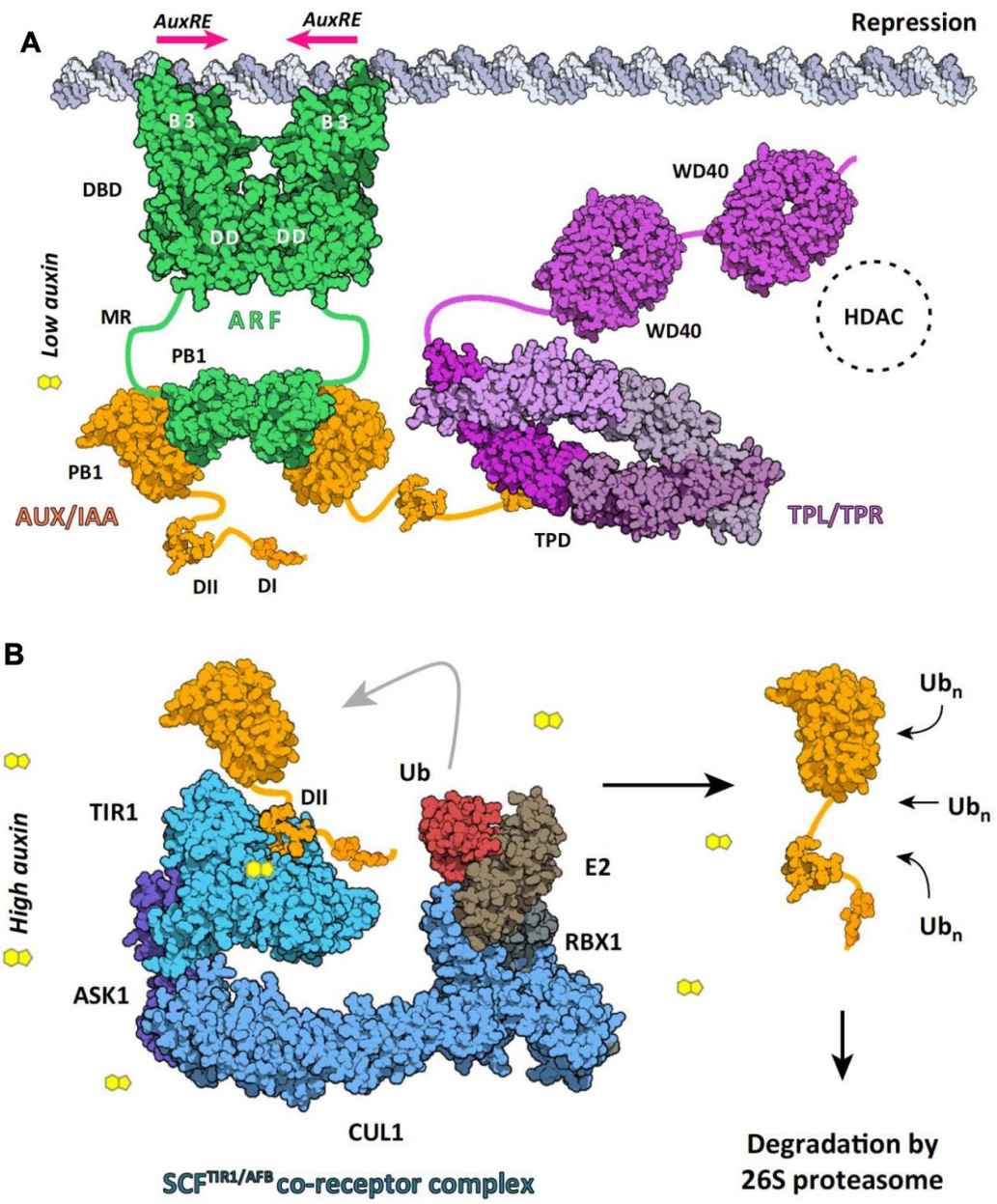

Figure 1.10. Auxin signalling in plants. The structures are represented as green: ARF5, orange: Aux/IAA repressors (IAA17 PB1 domain, IAA7 degron peptide, IAA1 EAR motif), purple: TPL/TPR co-repressors (OsTPR2), cyan/blue: SCF^{TIR1}, yellow: auxin. (A) In low auxin conditions, ARF activators are repressed and, thus, transcription of primary auxin-responsive genes is reduced. The ARF dimer binds *AuxRE* motifs, while they interact with Aux/IAAs via the PB1 domains, which, in turn, interact with TPL/TPR via the EAR and TPL domains. (B)In high auxin conditions, ARFs are derepressed due to Aux/IAAs being degraded via their DII degron peptide by the SCF^{TIR1} complex. Modified from Dinesh et al. (2016).

1.5.6.3 Crosstalk between phytohormones

Previously, it was discussed how plant hormones signal in a number of different ways and how complex their signalling pathways are; however, pathways become even more complex as crosstalk between hormones occurs. Our understnading of interaction between hormone pathways is largely the result of mutant phenotype analysis. For example, the *tir1* and *aux1* auxin-related mutants display altered responsiveness toward ethylene and ABA (Roman et al., 1995; Wilson et al., 1990). Ethylene is able to transcriptionally control the expression of tryptophan aminotransferases, which are crucial in the auxin biosynthetic pathway (Tao et al., 2008; Stepanova et al., 2008). Conversely, auxin is able to effect ethylene biosynthesis through the regulation of 1-aminocyclopropane-1-carboxylate synthase (ACS) genes (Tsuchisaka and Theologis, 2004) and jasmonate biosynthesis (Nagpal et al., 2005). Auxin also has an opposing action with cytokinin and jasmonate as cytokinin and jasmonic acid inhibits lateral root initiation by reducing the expression of auxin-efflux carrier genes, which act to establish auxin gradients in roots (Laplaze et al., 2007; Ishimaru et al., 2018).

It has also been seen that there is a distinct overlap in the auxin and brassinosteroid responsive gene sets (Goda et al., 2004) and targets induced/repressed by brassinosteroids are also induced/repressed by auxin. This convergence of signalling was suggested to be a result of BIN2 kinase phosphorylating and inactivating ARF2 activity which causes an increase in auxin-responsive gene transcription (Vert et al., 2008). DELLA proteins have also been identified as a common 'crosstalk node' between GA signalling and auxin, ethylene and ABA paths (Weiss and Ori, 2007). More recently it has been suggested that DELLAs directly interact with BZR1 to reduce growth (Li et al., 2012) and BRs can influence GA biosynthesis (Tong et al., 2014; Unterholzner et al., 2015). Due to recent advances in the knowledge of hormone signalling components we have discovered interactions at the gene levels, however, we must now begin to understand how these pathways are utilised during plant growth under environmental control. For example, mutants deficient or insensitive to auxin, GA or BR are known to display a skotomorphogenic phenotype in the light as these hormones promote elongation of

hypocotyl in *Arabidopsis.* However, the contribution of each of these hormones towards this response to light is unknown.

1.6 Project aims

The action of fluensulfone (FLS) is distinct from other nematicides currently on the market, but its mode of action remains unknown. Its remarkable efficacy, partnered with a favourable toxicity profile, makes the mode of action desirable to determine as other compounds with similar properties could be developed. Knowing the molecular target of FLS could also aid in safe and appropriate application methods of chemicals with similar actions in field conditions. *Arabidopsis* displays a higher susceptibility towards FLS compared to a *C. elegans* model suggesting the possibility that plant parasitic nematodes (PPNs) and *Arabidopsis* may have a conserved target.

The primary aim of this project is to investigate the phytotoxic effects of FLS on the model organism *Arabidopsis* with the aim to determine the molecular target(s) of FLS. To achieve this a detailed characterization of the response to FLS at the physiological and molecular level will be carried out. As FLS is a novel nematicide, its effects on plants have not been characterised fully and, due to its susceptibility, *Arabidopsis* provides a good system to study the effects of FLS in more depth. Such an analysis could indicate a distinct mode of action. Furthermore, understanding plant responses to FLS will aid in safe application, use and development of this novel nematicide for a range of crop species. The effect of FLS on gene expression will be studied using transcriptome sequencing and q-PCR analysis of specific genes of interest.

In addition, a genetic screen will be carried out to identify *Arabidopsis* mutants that have resistance to FLS. Screening mutated seedlings for herbicide resistance and drug targets is routinely carried out and *Arabidopsis* provides an excellent model for this type of study to allow identification of a key gene that is essential for a compound to work. A screen for FLS-resistant seedlings has the potential to indicate a single gene that mediates FLS phytotoxicity and from this, orthologous genes in PPN species could be identified. The screen will be carried out on seedlings treated with the mutagen, EMS, and grown on FLS with the aim to select resistant individuals.

Chapter 2: Materials and Methods

2.1 Plant material, growth conditions and treatments

pifQ (Leivar et al., 2008)*, tir1-1* (Ruegger et al., 1998)*; tir1-1, afb2-3* (Parry et al., 2009)*; tir1-1, afb2-3, afb4-8; tir1-1, afb2-3, afb5-5* (Prigge et al., 2016) seed material purchased from Nottingham Arabidopsis Stock Centre (NASC). DR5::VENUS, DII::VENUS and IAA2::GFP auxin response reporter lines (Bishopp et al., 2011) were kindly gifted by Professor Malcolm Bennett (University of Nottingham). *hy5/hyh* double mutant was a gift from Professor Christian Hardtke (University of Lausanne).

All *Arabidopsis* seeds were surface sterilized in 15% (v/v) bleach solution for 20 minutes and washed 5 times with 1mL of sterile water. For experiments in which plants were grown to maturity, *Arabidopsis* seeds were sown to a depth of approximately 0.5cm in compost containing equal volumes of Levingtons F+S modular compost, John Innes No 1 and Vermiculite. Plants were grown under a 16-hour photoperiod provided by SON-T 400W sodium lamps giving a fluence rate of 400-1000 µmol m^{-2} sec^{-1}.

Fluensulfone (FLS) (Batch numbers: 93867518 and 21004, provided by ADAMA agricultural solutions) was stored in darkness at 4oC with desiccant silica granules. FLS stock solutions were prepared in 100% dimethyl sulfoxide (DMSO), stored at -20°C, and added into the plant growth medium solution (half strength Murashige and Skoog (MS) basal medium (Murashige and Skoog, 1962) supplemented with 0.8% (w/v) agar to a final concentration of 0.1% (v/v). Stock solutions were added to plant growth medium on day of use after autoclaving, at temperatures below 45oC. Vehicle control plates followed the same protocol with omission of FLS and addition of 0.1% (v/v) DMSO.

For seedling phenotype studies seeds were grown on 0.8% (w/v)agar plates containing half strength MS medium in which stock solutions of FLS at 1000x final concentration were added to achieve final concentrations of 5 µM, 10 µM, 20 µM, 50 µM, 100 µM, 150 µM and 200 µM FLS with a total of 0.1% (v/v) DMSO. For hormone rescue experiments all hormones were added to 0.8% (w/v) agar plates containing half strength MS medium. Epi-brassinolide (EBR), Gibberellic acid (GA_3), IAA, 1-NAA, 2,4-D and ACC stock solutions of 1000x working concentrations were made up in 100% ethanol and added to autoclaved

media at a temperature below 45oC to a final concentration indicated in each experiment. All hormones were purchased from Merck (formerly Sigma-Aldrich) and added to autoclaved media at temperature below 45°C. Sucrose was omitted from all growth media, unless stated otherwise and plates were sealed with parafilm for the entirety of growth.

For light grown seedlings, the growth conditions used were continuous WL (100±10 μmol m^{-2} s^{-1}) at 22±1°C after 24 h stratification at 4°C in darkness to synchronise germination and break dormancy. For etiolation experiments, seeds were stratified at 4°C for 24 h in the dark, followed by a 2 h WL (100±10μmol m^{-2} s^{-1}) treatment at 22±1°C before 5d growth in constant darkness at 22±1°C. Fresh weight of seedlings was recorded following blotting on filter paper. Root length, cotyledon opening angle and hypocotyl length was also recorded using ImageJ programme (https://imagej.nih.gov/ij/, 1997-2018).

For the WL source Philips MASTER TL-D lamps (type 18W, light colour 840) were set to emit light at photon fluence density (PFD) of 100±10μmol m^{-2} s^{-1}. For the low light experiments, plates were covered with neutral density filters to reach desired the PFD (Lee Filters, Andover, UK). For high light experiments plates were raised above shelf-height of the light cabinet to reach desired PFD without the use of filters. For red and blue light (RL and BL, respectively) experiments WL was passed through red and blue filters (Lee Filters, Andover, UK #106 and #161, respectively) resulting in a fluence rate of 60±5μmol m^{-2} s^{-1}.

2.2 Measurements of pigments

Unless stated otherwise, all chemicals used in the creation of solutions, buffers, media etc. were purchased from Merck Ltd. (formerly Sigma Aldrich Ltd.).

2.2.1 Chlorophyll and carotenoid extraction

400 µL of 80% acetone was added to ~15 whole *Arabidopsis* seedlings which were ground using a hand pestle and centrifuged at 16,000 x g for 5 minutes. Supernatant was collected and the process repeated again, resulting in a final volume of 800µL from two

extraction steps. Absorbance was measured at 470, 647 and 663nm with a U-2001 spectrophotometer (Hitachi, Tokyo, Japan) and chlorophyll and carotenoid concentrations determined using equations from Lichtenthaler (1987) and expressed as μg per gram of fresh weight or ng per seedling.

Chlorophyll *a* = 12.25 A_{663} – 2.79 A_{647}

Chlorophyll *b* = 21.50 A_{647} – 5.10 A_{663}

Total chlorophyll = 7.15 A_{663} + 18.71 A_{647}

Carotenoids = (1000 A_{470} – 1.82 Chl *a* – 85.02 Chl *b*) / 198

2.2.2 Protochlorophyllide extraction

400 µL of 100% acetone:0.1M NH_4OH (9:1) was added to ~30 excised whole seedlings, the tissue was then ground using a hand pestle and centrifuged at 16,000 x g for 5 minutes. Supernatant was collected and the process repeated again resulting in a final volume of 800 µL. All extraction steps were carried out in darkness with green safety light. Fluorescence emission spectra was recorded on F-2000 spectrofluorometer (Hitachi, Tokyo, Japan) following excitation at 440nm. Relative amounts of protochlorophyllide (Pchlide) were calculated from the emission peak at ~636nm and expressed as relative fluorescence unit (RFU) per gram of fresh weight or per seedling (Terry and Kacprzak, 2019).

2.3 Forward genetic screen for FLS resistance

2.3.2 EMS mutagenesis

Preliminary mutagenesis was conducted using 4 concentrations of ethyl methanesulfonate (EMS) (0.25, 0.5, 0.75 and 1%) to determine concentration for final, large-scale mutagenesis. WT Col-0 ecotype seeds were imbibed in 0.1% potassium chloride solution for 12 h at 4°C then soaked in 100 mM sodium phosphate, 5% (v/v) DMSO and EMS for 4 h and agitated every 30 minutes – 1mL of this solution was used per ~1000 seeds. 1.5mL microfuge tubes were sealed with parafilm and contained in a 50mL falcon tube during treatment to reduce the potential release of the mutagen. Following this, seeds were washed twice with 100 mM sodium thiosulfate for 15 min and twice with distilled water for 15 minutes. Seeds were dried on filter paper (Whatman, UK) and

stored in fresh 1.5mL microfuge tubes. All steps were carried out in a fume hood. Following a drying out period, seeds were planted on soil at a density of around 1cm^2 per seed with ~10 plants per pot for pooling, this was the M_1 generation. M_1 generation were grown until seed could be harvested from pools of ~10, this was termed the M_2 generation.

2.3.3 Determination of mutagen effectiveness

900 M2 generation seeds from one pool of each EMS concentration were sown on 0.8% (w/v) agar plates containing half strength MS medium for 7d in continuous light (100±10µmol m^{-2} s^{-}1) alongside 900 WT Col-0 seeds for comparison. After 7d the number of seeds germinated, bleached and reduced in stature was recorded to give final percentages for comparison. Reduced growth was defined by cotyledon breadth at 7d <2mm.

2.3.4 Screening M2 generation

A small sample of M2 seeds from each M1 pool were surface sterilized in 15% (v/v) bleach solution for 20 minutes and washed 5 times with 1mL of sterile water. Using a glass pipette, seeds were individually sown on 0.8% (w/v) agar plates containing half strength MS medium and 50µM FLS and grown in continuous WL (100±10µmol m^{-2} s^{-}1) for up to 28d after 48 h stratification.

2.3.5 Isolation of FLS resistant mutants

Potential resistant mutants were identified via visual parameters, such as improved growth and/or increased root length and/or increased greening compared to the rest of the population grown on 50µM FLS. These individuals were removed from the plates containing FLS and moved to 0.8% (w/v) agar plates containing half strength MS medium with the addition of 1% (w/v) sucrose to encourage further growth. Once these plants had developed at least 2 true leaves the plant was then transferred to soil (described in section 2.1) and grown to maturity in a growth room.

Once individuals had reached maturity their seed was collected and re-screened on 0.8% agar plates containing half strength MS medium and 50µM FLS alongside WT seed for comparison. Seed was screened for 7 d in continuous WL following 48 h stratification at 4°C in darkness. Fresh weight, chlorophyll and root length measurements were recorded to determine if resistance was retained in that generation.

2.3.6 Back-crossing FLS resistant lines to WT

From the maternal plant (resistant line or WT), mature siliques and open flower buds were removed with forceps. Anthers were removed from 3-5 buds prior to flower opening and pollen release to stop self-fertilization and the emasculated buds were left for 1-2 days to mature. The emasculated buds were then subsequently pollinated using anthers from the male donor plant (WT or resistant line). Seeds from successful back-crosses were allowed to mature prior to harvesting.

2.3.7 Physiological measurements of mature *Arabidopsis* plants

Development of each FLS-resistant line was recorded after sowing lines on soil (described in section 2.1) and monitoring growth each day and recording days to germination, bolting and flowering. Once flower buds and siliques had reached maturity they were imaged on an optical light microscope (model:SDZ-PL; Kyowa, Tokyo, Japan) and quantification of stigma, stamen and silique length was measured using the Image J programme.

2.4 Imaging of auxin signaling by confocal microscopy

Imaging of DR5::VENUS, DII::VENUS and IAA2::GFP seedlings was performed on an SP8 confocal microscope (Leica, Wetzlar, Germany) using the x20 air objective. For visualization of the root organization, the roots were stained with 10µg/mL propidium iodide for 10 minutes in the dark with regular agitation. Seedlings were stained following a 3 h 1µM IAA or 3 h mock treatment and mounted in water between slide and coverslip. IAA treatment and staining for each condition were staggered to allow time for imaging and to reduce propidium iodide entering cells if samples were not imaged immediately. The Z-axis was adjusted for each sample to ensure maximal fluorescence within the whole

root tip was represented. For fluorescence quantification, the GFP (ex: 488 nm, em: approx..500-550 nm) and VENUS (ex: 514 nm, em: approx..520-560 nm) was used to remove any activity of the propidium iodide staining; the area within 200µM of the root tip was selected and a mean grey value was given and expressed relative to control. For the VENUS lines, each image was split and the VENUS channel was analysed. The image was then made binary with a threshold value of 30 to remove background. Particle analysis was carried out using a minimum particle size just below that of the smallest nuclei in each image to extract nuclei that had high levels of reporter activity and remove any nuclei that were not fully in the plane of focus. 4 individuals per condition were analysed. All quantification carried out on ImageJ software.

2.5 Gene expression analysis by quantitative real-time PCR (qPCR)

2.5.1 RNA isolation from seedlings

All plastic ware and buffers were autoclaved prior to extraction to ensure sterilisation and all steps were performed on ice. Around 200-400mg of *Arabidopsis* whole seedling tissue was harvested into 1 mL tubes (Eppendorf, Hamburg, Germany), immediately frozen and stored at -80°C until extraction began. 500 µL of 'RNA Miniprep' buffer (100 mM NaCl; 10 mM Tris pH 7.0; 1 mM EDTA and 1 % (w/v) SDS) was added to frozen tissue and tissue was ground carefully using a hand pestle. 150 µL phenol pH 4.8 and 250 µL chloroform was added to samples and they were vortexed for 30 s. Following vortexing, samples were centrifuged at 16,000 x *g* for 5 min at 4°C which allowed phase separation. Approximately 450-500 µL of the upper phase was transferred to a new tube, combined with 450 µL LiCl and precipitated for approximately 12 h at 4°C. Precipitate was recovered by a centrifugation at 16,000 x *g* for 10 min at 4°C. To avoid contamination by genomic DNA, 300 µL DNase buffer (10mM Tris HCl pH 7.5; 2.5mM $MgCl_2$; and 0.5mM $CaCl_2$) and 1 µL DNase 1 (Promega, Wisconsin, USA) were added and samples were incubated at 37°C for 25 min using a thermomixer. 500 µL of phenol:chloroform:isoamyl alcohol (25:24:1, v/v/v; Thermo Fisher Scientific, USA) was added and samples were vortex for 30 s and centrifuged at 16,000 x *g* for 5 min at 4°C. The upper phase was then transferred to a new tube and combined with 750 µL of ethanol containing 5% (w/v) 3 M sodium acetate (pH 5.5). Samples were vortex briefly and incubated for 1 hour at -20°C to precipitate. The

supernatant was removed following centrifugation for 10 min at 16,000 x *g*, at 4°C, leaving an RNA pellet which was left to air dry at room temperature for approximately 10-15 minutes. The final RNA pellet was resuspended in 30-60 µL TE buffer (10 mM Tris HCl (pH 8), 1 mM EDTA). The concentration and purity of the RNA samples were determined using 'Nano-Drop' ND-1000 spectrophotometer (Thermo Fischer Scientific). When possible, RNA was directly subjected to cDNA synthesis. RNA samples were stored at -80°C.

2.5.2 First strand cDNA synthesis

cDNA was synthesized from a 1 µL of total RNA using the Precision nanoScript 2 Reverse Transcription Kit (PrimerDesign, Chandler's Ford, UK). In brief, 1 µL of RNA was added to a mixture of 1 µL random primers and 1 µL oligo-dT primers and made up with RNase/DNase free water to a final volume of 10 µL. Samples were vortexed and incubated at 65°C for 5 minutes and immediately transferred to ice for a further 5 minutes. Following cooling of the samples, 10 µL of reverse transcription mix (5 µL of nanoScript2 4x Buffer, 1 µL of 10mM dNTP, 3 µL RNAse/DNAse free water, 1 µL of nanoScript2 enzyme) was added to each sample. Samples were vortexed and briefly spun to collect the solution at the bottom of the tube. Samples were placed in the peqSTAR thermocycler (Peqlab, Delaware, USA) and cDNA synthesis was performed under the following conditions: 25°C for 5 min, 42°C for 20 min and 75°C for 10 min. cDNA samples were stored at -20°C until required.

2.5.3 Quantitative real-time PCR

The final volume for each quantitative real-time PCR (qPCR) reaction was 10 µL. Each reaction was comprised of: 5 µL PrecisionFAST-SY 2x MasterMix premixed with SYBRgreen (Primerdesign, UK), 0.5 µL cDNA template, 2 µL MQ water and 2.5 µL primer mix, containing 2 µM gene specific primers re-suspended in milli-Q (MQ) water (see table 2.1 for primer details). For negative controls MQ water was used in place of cDNA template. The qPCR was conducted using white plastic 96-well plates and sealing film (both Starlab, Milton Keynes, UK) and monitored using the Step One Plus Real Time PCR System (Thermo Fisher Scientific, USA). The summary of thermal cycling conditions is

represented in Figure 2.1**.** Melting curves were also generated for each sample, to ensure no non-target products were amplified. Each reaction was performed in two technical replicates with 3 biological replicates.

Table 2.1. Details of primers for qPCR. List of primers used in qPCR analyses including sequence details, melting temperature and amplicon size.

Primer name	Primer sequence 5'-3'	T_m (°C)	Product size (bp)
YLS8_F	AAGGACAAGCAGGAGTTCATT	57	93
YLS8_R	AGTAATCTTTTGGAGCAATCACC	57	
HEMA1_F	GCTTCTTCTGATTCTGCGTC	55	128
HEMA1_R	GCTGTGTGAATACTAAGTCCAATC	56	
CHLH_F	CATTGCTGACACTACAACTGC	54	145
CHLH_R	CTTCTCTATCTCACGAACTCCTTC	57	
PORA_F	GTTCGGTGTTTCACTTTCGG	58	74
PORA_R	TCTGTTCCCTCTTGCATCTCA	58	
LHCB1.2_F	CTCCGCAAGGTTGGTGTATC	55	60
LHCB1.2_R	CGGTTAGGTAGGACGGTGTAT	55	
ASA1_F	CCTTATACCAATTTACCGCTGT	56	115
ASA1_R	ACGCTATAACGACCAACGC	56	
CYP79B2_F	ATCAAGTGCGATTATGGACAAG	57	139
CYP79B2_R	TTACAAGCTCCTTAATGGTGG	55	
CYP79B3_F	CCAACCATTAAGGAACTTGT	52	181
CYP79B3_R	GACGGGATGAAGACGGAA	56	
TAA1_F	GTATTGGGTGGGCATTGGT	58	118
TAA1_R	CTCAGACTCGGACTCGCTCT	57	
YUCCA1_F	ACCGTTCATGTGTTGCCAAG	59	147
YUCCA1_R	CATTTTTCAGCTCAAGCGGA	59	
IAA1v2_F	GCTCCTCCTCCTGCAAAA	56	75
IAA1v2_R	GAGCTCCGTCCATACTCAC	52	
IAA2_F	GAGCTATGTCTTGGATTACCCG	58	90
IAA2_R	GAGTTTTGGTAGGAGGTGTAGATT	56	
IAA3_F	TCCTCGAAAGGCTCAGATT	55	68
IAA3_R	CACATAGATTCCTTGACCCTCA	57	
IAA19_F	GAAAGATGGTGACAACTGC	50	91
IAA19_R	CACTCGTCTACTCCTCTAGG	49	
IAA29_F	AGATGGATGGTGTGGCAATAG	57	77
IAA29_R	GTATCTTCTCTGTCGCAATCTTC	56	

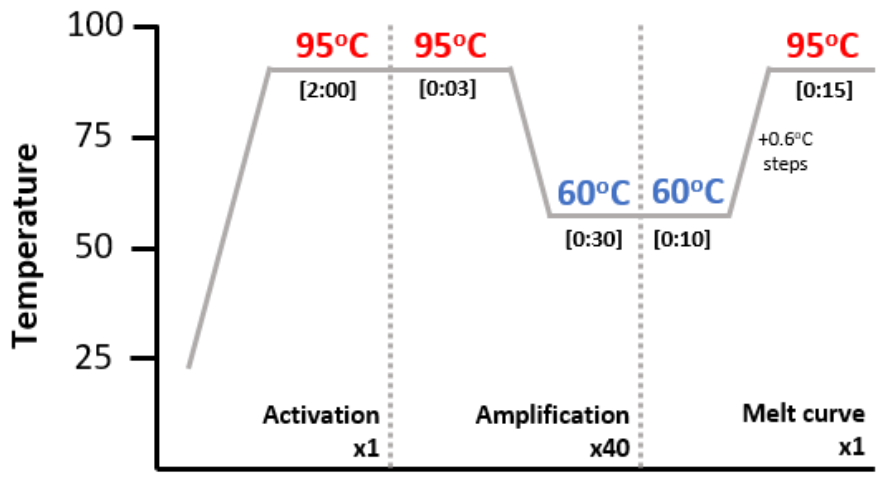

Figure 2.1. Thermal profile of qPCR reactions. The activation step requires 95°C for 2 minutes followed by amplification for 40 cycles consisting of denaturation for 3 seconds at 95°C and annealing for 30 seconds at 60°C. A melt curve was created by measuring fluorescence following every 0.6°C increase in temperature until 95°C was reached.

2.6 Transcriptome analysis

Dr Alison Baylay (National Oceanography Centre, Southampton) is kindly acknowledged for the contribution in library preparation and initial data analysis.

2.6.1 RNA sequencing

Arabidopsis seedlings were grown on media containing 0.1% (v/v) DMSO or 50µM FLS in 22±1°C WL (100±10µmol m^{-2} s^{-1}) for 7 days or for 5 days in constant darkness. They were then snap frozen in liquid nitrogen and RNA was extracted as described in section 2.5.1. Three replicates were used for RNAseq.

Paired end libraries for Illumina sequencing were prepared using the NEBNext Poly(A) mRNA Magnetic Isolation Module (E7490) Library Prep Kit for Illumina, following the manufacturer's protocol. Libraries were pooled and sequenced on an Illumina MiSeq platform (Illumina, California, USA) using paired-end sequencing, with a read length of 151 bp.

The quality of the raw reads was inspected using FASTQC software v0.11.6 (Andrews, 2010) and raw sequence reads were pre-processed with CutAdapt v1.8.1 (Martin, 2011) to remove TruSeq universal adapter sequences and low quality bases from the 3' end of

reads, using a quality threshold of 20 and minimum read length of 50 bp. Trimmed reads were mapped against the *Arabidopsis* TAIR10 reference genome assembly using HiSAT2 v2.0.5 (Kim et al., 2015), and reads mapping to annotated genes in TAIR10 were counted using StringTie v1.3.4, (Pertea et al., 2015). Libraries were normalized in the Bioconductor package DESeq2 v1.20.0 (Love et al., 2014), running on R v3.5.0, using the 'trimmed mean of M-values' (TMM) method. This transforms the count data to the log2 scale in a way that minimizes differences between samples for rows with small counts and also normalizes the data with respect to library size implemented. Initial inspection of the samples was done using principal component analysis (PCA) and a Pearson's correlation heat map using DESeq2 functions and R package 'pheatmap' (Kolde, 2015), respectively.

2.6.2 Differential Gene Expression Analysis

Differential gene expression analysis was carried out using DESeq2 (Love et al., 2014), running on R v3.5.0. A list of genes with expression significantly affected by growth condition was identified using an ANODEV approach carried out in the DESeq2 package. The fit of read count data against a one-factor negative binomial general linear model, where replicates were grouped by growth condition, was compared to a reduced model where condition information was removed using likelihood ratio testing. Pairwise contrasts between conditions were calculated using a Wald test. In both cases, genes with an adjusted P-value of < 0.05 following Benjamini–Hochberg correction for multiple testing were classed as significantly differentially expressed. MA plots and heatmaps for differentially expressed genes were generated in DEseq2 for visualisation.

Using the GO enrichment analysis tool (Mi et al., 2017) biological process gene ontology (GO BP) term (Ashburner et al., 2000; Carbon et al., 2019) term and Kyoto Encyclopedia of Genes and Genomes (KEGG) pathway term (Kanehisa and Goto, 2000) overrepresentation analysis was performed on differentially expressed genes (DEGs). The analysis determined whether any terms are annotated to a list of specified genes, in this case a list of DEGs, at a frequency greater than what would be expected by chance, and calculated a p-value using the hypergeometric distribution. The minimum number of DEGs required to be annotated by a given ontology term was set to 2. The p-values of enrichment analysis

were corrected for multiple testing using Benjamini-Hochberg multiple testing adjustment. Thresholds for adjusted p-value and q-value of the enrichment were set to default values 0.05 and 0.2, respectively.

Comparisons to publicly available microarrays and RNAseq data sets was carried out using a log fold-change cut-off of 1 to identify DEGs and compare the number of shared genes expected to number of shared genes observed to give a quantitative value for overlap between FLS-treated samples and other data sets. The value of expected genes shared was calculated: (up/down regulated genes by FLS*up/regulated genes by data set X)/total genes sequenced in RNAseq.

2.7 Quantification of endogenous phytohormones

2.7.1 Tissue details and shipping

WT *Arabidopsis* seedlings were grown on plant growth media +/- 50 μM FLS for 7 days in white light 22±1°C WL (100±10μmol m^{-2} s^{-1}) or 5 days dark and material was collected in liquid nitrogen and stored at -80^{oC} until samples were shipped on dry ice. Extraction and hormone quantification was performed by The Proteomics & Mass Spectrometry Facility at the Danforth Plant Science Center using full details provided in the appendix

Chapter 3: Characterising the effects of FLS on *Arabidopsis* physiology

3.1 Introduction

Plant parasitic nematodes (PPNs) are obligate parasites that infest crops and cause average yield losses of 12.3% on the world's major food staples, leading to an estimated financial burden of $125 billion per year (Singh et al., 2015). Due to restricted use and phasing out of chemical nematicides previously used it is more than likely these figures have risen and as an anticipated increase food demand is predicted, and it is essential new mechanisms are found to maximize food resources. The fumigant nematicide, methyl bromide, was widely used as a nematicide throughout the 20th century; however, its usage is now banned due to its implications in ozone layer depletion (Fuller et al., 2008). Carbamate-and organophosphate-based nematicides, acting as anti-cholinesterases, now serve as alternatives to methyl bromide and although they are less volatile, many have restricted use due to non-target organism toxicity (Costa, 2006; Pope et al. , 2005).

The unacceptable environmental impact of widely used nematicides has prompted the development of new chemicals with improved toxicology profiles. Recently, a novel nematicide has been developed named FLS, full name: 5-chloro-2-(3,4,4-trifluorobut-3-ene-1-sulfonyl)-1,3-thiazole, also known as MCW-2 and Nimitz® and it is a member of the heterocyclic fluoroalkenyl sulfone group. FLS has strong nematicidal action (Oka et al., 2008; Oka et al., 2009; Phillion et al., 1999) while retaining low non-target organism toxicity (Oka et al., 2009; Rousidou et al., 2013; Strupp et al., 2012). Early observation of FLS effect on the PPN *Meloidogyne incognita* compared paralysis profiles relative to cholinesterase inhibitors, such as carbamates and organophosphates and suggested that its mode of action is distinct (Oka et al., 2009). Further work confirmed FLS mode of action to be distinct from anticholinesterases and macrolytic lactones using *Caenorhabditis elegans* as a model for intoxication (Kearn et al., 2014). Using anticholinesterase-resistant and ivermectin-resistant mutants it was determined FLS could still elicit similar levels of paralysis compared to a WT worm, suggesting FLS is not working through the same mechanisms as anticholinesterases or macrolytic lactones. Mode of action studies on the PPN *Globodera pallida* also demonstrated reduced egg hatching, stylet thrusting and impaired motility as observed in *C. elegans,* but at

significantly lower concentrations of FLS (Kearn et al., 2017). It has also been shown that at low concentrations of FLS, inhibition of hatching is reversible, although the majority of juveniles that hatch demonstrate a reduction in mobility that is distinct from other nematicides (Feist et al., 2020). The large difference in sensitivity between *C. elegans* and PPN species suggests FLS may be acting on key elements of PPN metabolism not present in non-parasitic worms. Interestingly, previous studies looking into the effects of FLS on *Arabidopsis* show a profound effect on root development and showed that *Arabidopsis* has a higher sensitivity towards FLS compared to *C. elegans*.

In multiple field trials it was established FLS did not exert any phytotoxic effects on a number of crop plants when applied via drip irrigation and tilling into the top-soil (Morris et al., 2015; Noe et al., 2015; Oka, 2014; Oka et al., 2009, 2012). However, foliar application of FLS on tomato and eggplant reduced plant vigor following application of FLS at rates higher than used commercially (Giannakou et al., 2019; Morris et al., 2016). This suggested FLS could be acting systemically, translocating through the plant and exerting phytotoxicity.

The model plant *Arabidopsis* is used as a species for testing the phytotoxicity of chemicals on non-target plants. *Arabidopsis* has been used to recognize the developmental phytotoxic effects of a number of chemicals, including metal oxide nanoparticles (Lee et al., 2010), sulfanilamides (Schreiber et al., 2012) and herbicides such as sulfometuron methyl (Olszyk et al., 2008). Understanding the potential phytotoxic effects of a chemical, either directly applied to the field or used in medicine and subsequently entering the field, is essential to alleviate concerns of harmful effects.

Early studies on FLS and its metabolites also showed that *Arabidopsis* displayed low-level phytotoxicity towards FLS and determined that this came from the chloro-thiazole-sulfone scaffold (personal communication, ADAMA). FLS and three of its metabolites, 5-chloro-thiazole-2-sulfonic acid, 5-chloro-2-methylsulfonyl thiazole and butane sulfonic acid (referred to as metabolite 25, 26 and 27, respectively) were added to plant growth media at different concentrations to determine the effect on *Arabidopsis* seedling growth. Metabolites 25 and 27 did not alter primary root growth with the exception of

136μM (40ppm) which increased growth. In contrast, FLS and metabolite 26 decreased root length in a dose dependent manner although FLS was more effective; 5ppm FLS induced the same decrease in root length as 68μM (20ppm) of metabolite 26. Similar patterns were observed when analyzing total lateral root length and fresh weight of aerial tissue. The loss of fresh weight at high chemical concentration of FLS and metabolite 26 was suggested to be a result of retardation in leaf development as true leaves failed to form at high concentrations and bleaching was observed on cotyledons. Therefore, this study showed the phytotoxic effects of FLS are associated with the chloro-thiazole-sulfone scaffold structure shared by FLS and metabolite 26 (personal communication, ADAMA). However, phytotoxicity was not observed at field relevant concentrations of 3.4μM (1ppm) suggesting phytotoxicity is unlikely to be an issue when used in the field.

In a similar study, *Arabidopsis* primary root length was reduced in a concentration dependent manner following exposure to 6.8μM (2ppm) and 34μM (10ppm) FLS. Total lateral root length was also decreased when treated with 10ppm FLS (personal communication, ADAMA). After 14 days of growth on 10ppm FLS, aerial tissue fresh weight decreased by 47.7%, whereas, 2ppm did not alter this. Interestingly it was noted that exposure to 10ppm FLS caused plants to bolt at 14 days while 2ppm-treated and untreated plants were still at the vegetative stage. Cellular metabolic activity and mortality was also analyzed using fluorochromes; 2ppm-treated plants did not show any differences in metabolic activity or mortality of root or shoot cells compared to the untreated control while 10ppm-treated plants displayed a lower metabolic activity in root and shoot cells alongside higher mortality in cells located above the root apical meristem (personal communication, ADAMA). These studies have showed that FLS has significant effects on the physiology and development of *Arabidopsis* at concentrations above that used in the field while metabolic activity was not greatly perturbed. It was suggested that these physiological and developmental changes could be due to a disruption in the biosynthesis of phytohormones as these molecules are crucial in regulating shoot and root development.

This chapter aims to investigate the effect of FLS on *Arabidopsis* as a model plant to probe into the mode of action of FLS.

3.2 Results

3.2.1 FLS induces phytotoxicity in light conditions

To understand the effect of FLS on *Arabidopsis* physiology, WT Col-0 *Arabidopsis* seedlings were grown on media containing increasing concentrations of FLS, from 0-200µM, under three light conditions. This concentration range was chosen as it would elicit low- and high-level toxicity and thus a low-level and high-level response. In continuous WL (WL) FLS induced a dramatic phenotypic change in seedlings (figure 3.1), however, germination was not affected even at the highest concentration of 200 µM. Growth was quantified through fresh weight (FW) and total chlorophyll (Chl) measurements. Following growth in continuous WL it was shown that 50µM FLS significantly reduces FW by almost 50% compared to control and total Chl levels were also significantly reduced from 50 µM FLS. However, FLS inhibition of primary root elongation was evident from 10µM FLS where a 26% reduction in primary root length was measured. This concentration is five times lower than that required to reduce fresh weight and chlorophyll, suggesting FLS has a more potent effect on primary root elongation; although, as the root tissue is in direct contact with FLS in the media, this could explain the increase in sensitivity. From concentrations above 20 µM it was also observed that the formation of true leaves and lateral root development was inhibited. The reduction in growth coupled with no effect on germination suggests FLS is primarily acting to inhibit post-germination development of seedlings.

The effect of FLS on growth in monochromatic red (RL) and blue light (BL) was also studied to determine if FLS phytotoxicity would be influenced by different light environments. Interestingly, under RL and BL, FLS caused a significant reduction in fresh weight at lower concentrations than in WL; 10µM and 5µM, respectively (figure 3.2). In WL, total chl levels were reduced from 50µM; however, in RL total chl levels were only reduced following FLS treatment of 100µM and above. In BL, total chl levels were reduced from only 10µM, suggesting FLS treatment is more phytotoxic under BL (figure 3.2).

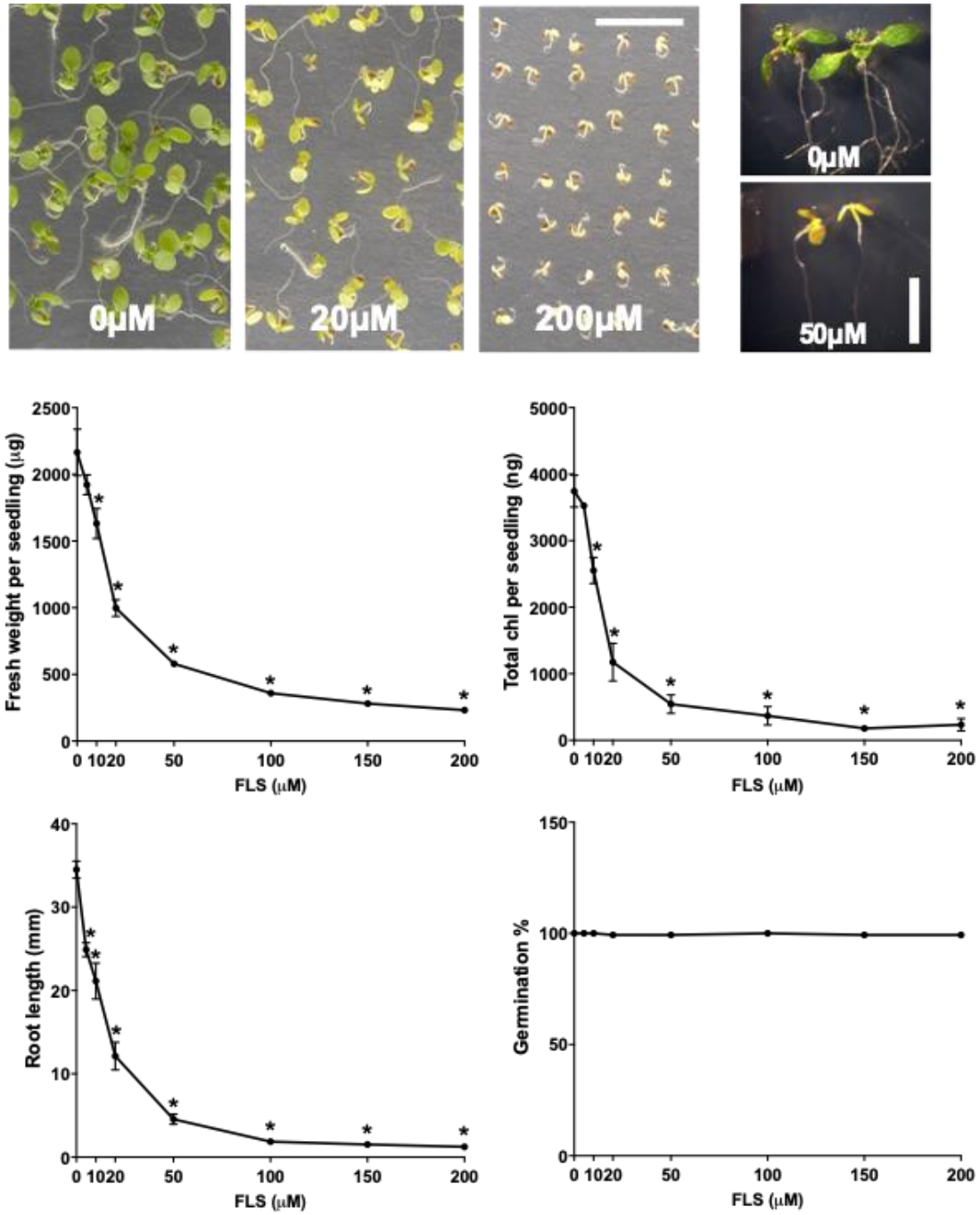

Figure 3.1. FLS reduces growth of *Arabidopsis* seedlings. Col-0 seedlings grown for 7 days on ½ MS 0.8% agar media with addition of FLS to give a final concentration of FLS at indicated concentrations (µM). Vehicle control condition included addition of 0.1% DMSO to media. Data points represent the mean ± SEM of five biological replicates. Asterisks indicate significant difference ($p<0.05$) compared to control conditions by Tukey's post-hoc multiple-comparison test. Scale bar represents 10mm.

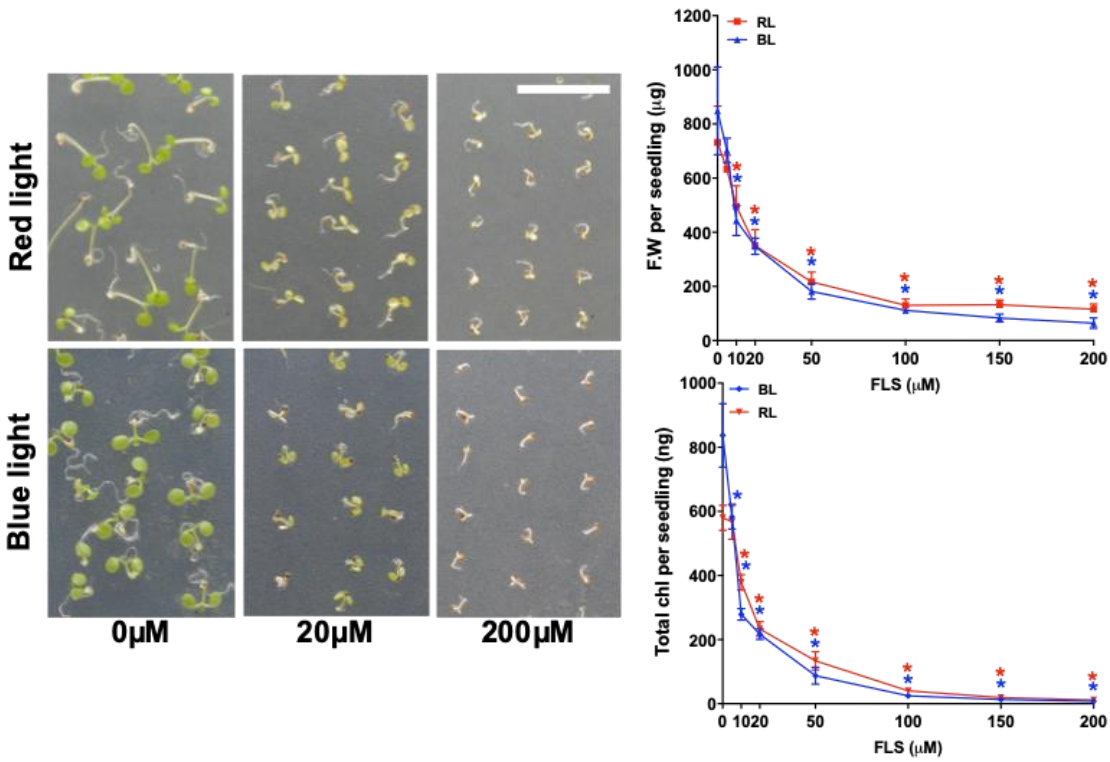

Figure 3.2. FLS reduces growth of *Arabidopsis* seedlings under red (RL) and blue light (BL). Col-0 seedlings grown for 7 days on ½ MS 0.8% agar media with addition of FLS to give a final concentration of FLS at indicated concentrations (µM). Vehicle control condition included addition of 0.1% DMSO to media. Data points represent the mean ± SEM of five biological replicates. Asterisks indicate significant difference ($p<0.05$) compared to control conditions by Tukey's post-hoc multiple-comparison test.

To further understand the basis of FLS phytotoxicity in WL, Col-0 seedlings were grown in three intensities of WL to investigate the effect of fluence rate on FLS action. In all light experiments, previously and hereafter, WL has been 100 ±10 µmol m^{-2} s^{-1} – a moderate intensity, sufficient for seedling growth. For this experiment 15 µmol m^{-2} s^{-1} represents very low light, 40 µmol m^{-2} s^{-1} low light and 200µmol m^{-2} s^{-1} high light due to constraints of the light cabinet. In control seedlings fresh weight was increased by 62% at high light compared to very low light, while total Chl was highest in low light. Similarly, at 20µM FLS a >3-fold an increase in fresh weight was evident when comparing very low light and high light, but the highest Chl levels were at very low light. Different responses were seen for seedlings treated with 200µM FLS as high light reduced fresh weight by 52% compared to very low light; however, very low light-grown seedlings displayed the most Chl accumulation (figure 3.3). These results suggest FLS diminishes the high-light advantage of control seedlings.

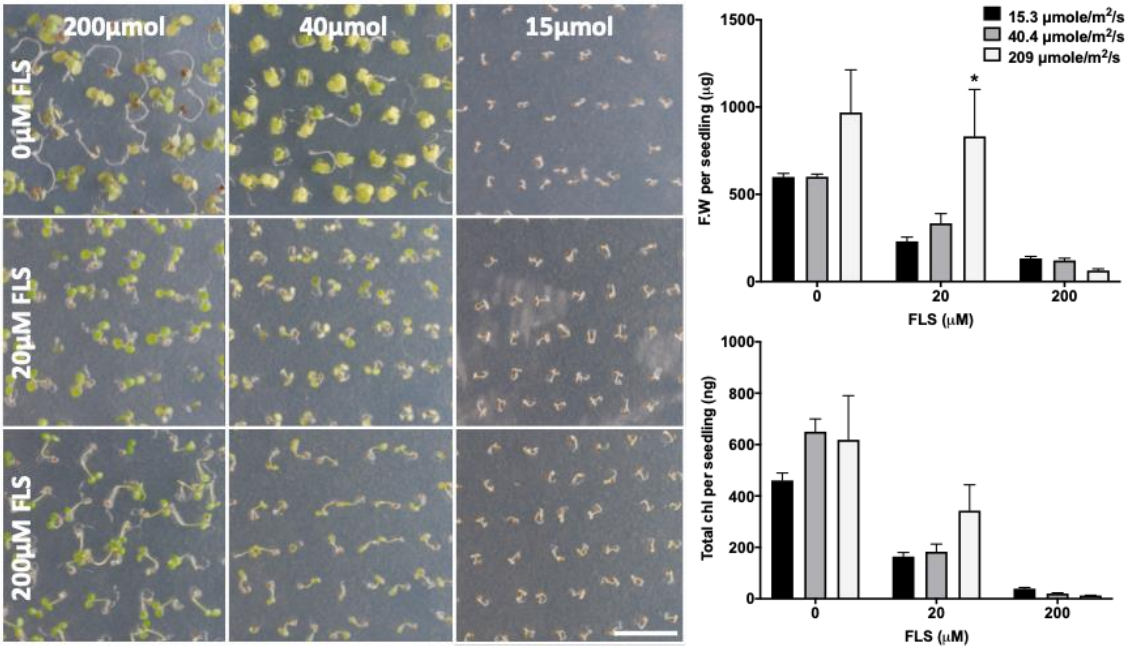

Figure 3.3. Intensity of WL affects growth. Col-0 seedlings grown for 7 days on ½ MS 0.8% agar media with addition of FLS to give a final concentration 20µM and 200µM. Vehicle control condition included addition of 0.1% DMSO to media. Varying fluence rates were achieved through the use of neutral density filters. Data points of fresh weight (FW) and total chlorophyll (chl) represent the mean ± SEM of three biological replicates. Asterisks indicate significant difference ($p<0.05$) compared to lowest light condition by Tukey's post-hoc multiple-comparison test.

Agar plates provide a good, controlled system for seedling studies; however, growing on soil replicates an environment closer to field conditions where this chemical is applied, potentially making the results more transferable to crop environments. Interestingly, after 7 days of growth on soil, *Arabidopsis* seedlings appeared to display no phytotoxicity, even at the highest concentration tested of 200 µM FLS. FW, total Chl and primary root length were not negatively affected by FLS, in fact, at the lower concentrations of 5 and 20 µM FLS there was an increase in FW, total Chl and root length by 149%, 181% and 53%, respectively (figure 3.4A). Following 14 days growth on soil, *Arabidopsis* seedlings started to display phytotoxicity, although not to the same extent as seedlings grown on agar plates. For concentrations below 200 µM FLS, FW, total chlorophyll and root length were not altered; however, at the highest concentration of 200 µM FW, total chlorophyll and root length decreased by 52%, 57% and 43%, respectively (figure 3.4B).

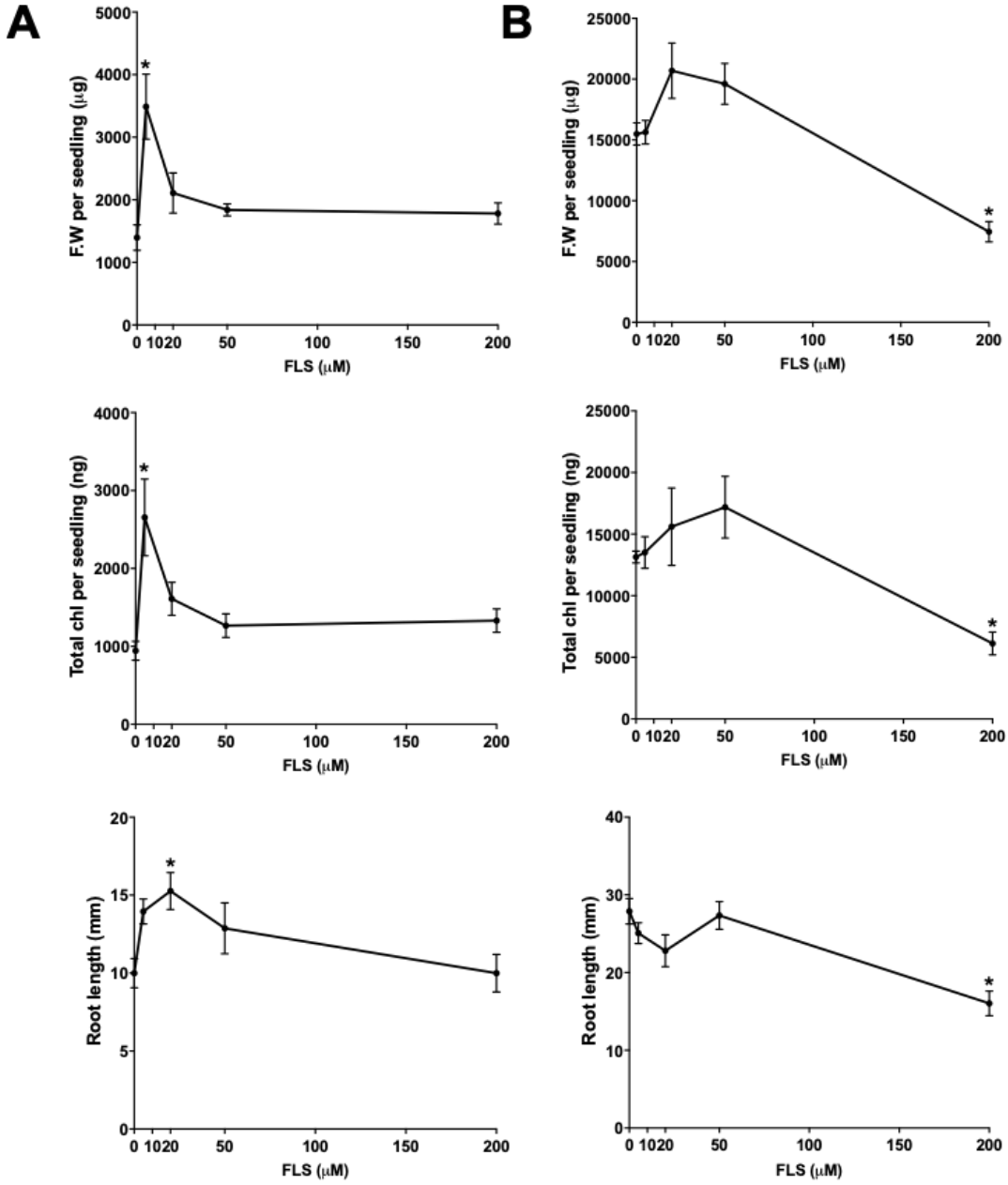

Figure 3.4. FLS has reduced phytotoxicity in the soil environment. Col-0 seedlings grown for (A) 7 and (B) 14 days on soil (1:1:1 transport vermiculite:John Innes No.2 compost:Levington M2 soil) watered with FLS to give a final concentration of FLS at indicated concentrations (µM) every 2 days. Vehicle control condition watered with 0.1% DMSO. Fresh weight (FW) and total chlorophyll (chl) data points represent the mean ± SEM of three biological replicates, primary root length data points represent mean ± SEM of 12-17 individuals. Asterisks indicate significant difference ($p<0.05$) compared to control conditions by Tukey's post-hoc multiple-comparison test.

3.2.2 FLS-induced phytotoxicity is reversible at low concentrations

To investigate the effects of FLS further, recovery experiments were carried out to determine if, after FLS exposure, *Arabidopsis* seedlings were able to recover to control seedling levels or if there was a sustained, long term reduction in growth. Following 5 and 7 days of growth on FLS a dose-dependent reduction in fresh weight, total chlorophyll and root length was measured (figure 3.5). After transferring seedlings to plates omitting FLS, seedling progress was tracked. After 1 day off FLS seedlings were not able to recover; however, after 4 and 6 days off FLS, seedlings exposed to low concentrations (<20μM FLS) were able to continue to accumulate fresh weight, total Chl and elongate the primary root, although 10μM FLS did cause reduced growth compared to WT at all time points (figure 3.6). After 20μM FLS exposure there was a partial recovery as fresh weight, Chl and root length were all able to increase in the recovery period; although, due to the previous FLS exposure, seedling growth remained lower than control seedlings. In contrast, no recovery was observed after the higher concentrations of FLS (50 and 200μM). At these concentrations seedling growth is irreversibly inhibited and no significant increases in fresh weight, total Chl or root length could be measured (figures 3.5 and 3.6).

3.2.3 Investigating the effects of post-germinative application of FLS

It has been established that pre-germinative application of FLS on agar plates causes a significant reduction in fresh weight, total chlorophyll and root length. However, the effect of FLS on *Arabidopsis* seedlings post-germination has not been considered. In the field, crop plants are usually exposed to FLS after they are established; FLS is tilled into the top-soil and the crop is subsequently planted. Looking at the post-germination effect of FLS mimics this practise more closely and could expose the mechanism of action further.

Seedlings were permitted to grow on agar plates omitting FLS for 3 days and subsequently transferred to plates containing increasing concentrations of FLS. Interestingly, it seemed low concentrations (<20 μM FLS) were able to transiently increase root length after 1 day of exposure to FLS (figures 3.7A and 3.8C).

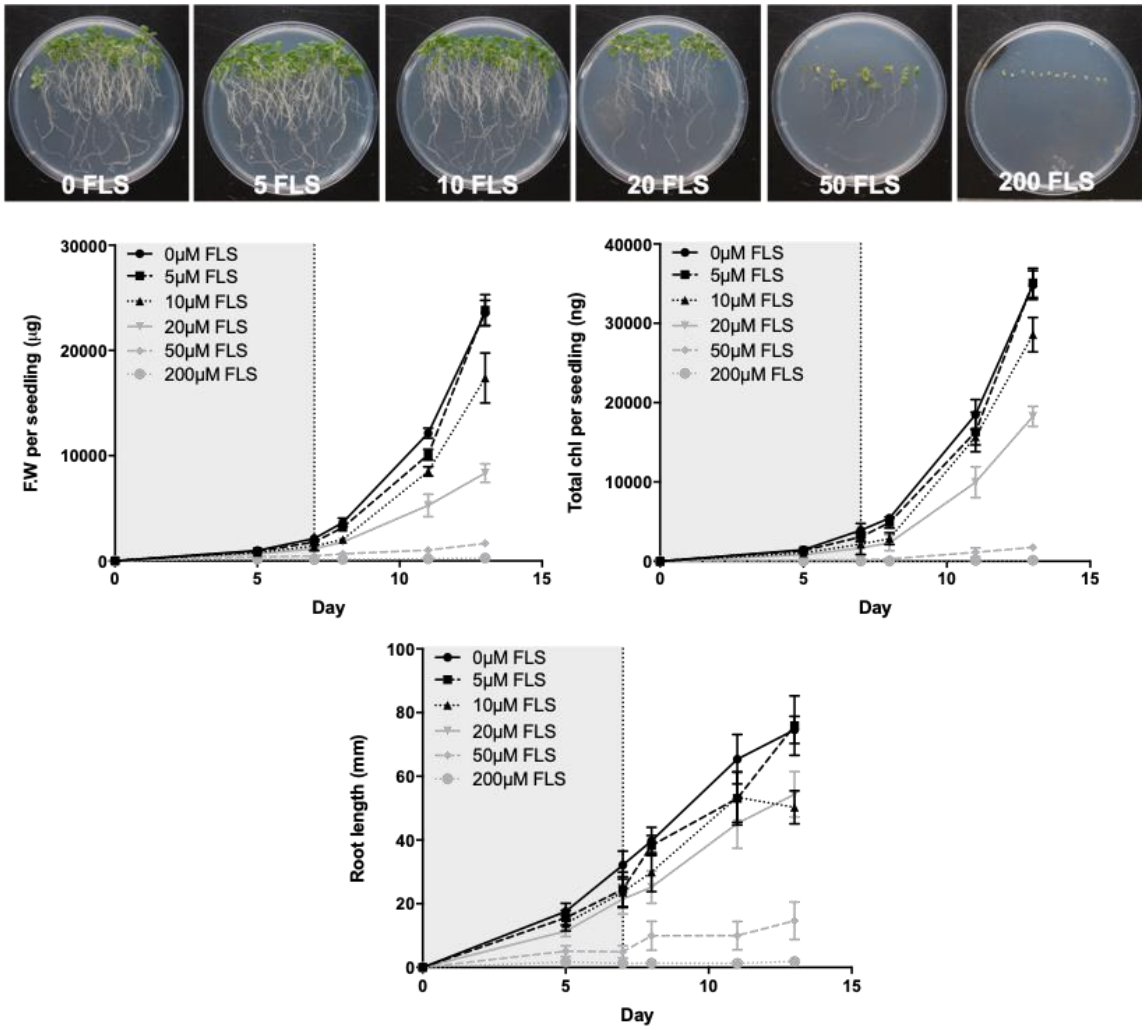

Figure 3.5. The pre-germinative effect of FLS on *Arabidopsis* seedlings. Col-0 seedlings grown for 7 days on ½ MS 0.8% agar media with addition of FLS to give a final concentration of FLS at indicated concentrations (µM). Vehicle control condition included addition of 0.1% DMSO to media. Seedlings were subsequently transferred to plates omitting FLS for a further 6 days to track progress. Dotted line represents point of transfer and grey background represents presence of FLS. Fresh weight (FW) and total chlorophyll (chl) data points represent the mean ± SEM of three biological replicates, primary root length data points represent mean ± SEM of 9-21 individuals.

This transient increase in growth was also seen in fresh weight and total chlorophyll, although the differences were not statistically significant. However, when focusing on the lowest concentration of FLS tested (5 µM) we saw a sustained increase in growth throughout the FLS exposure period. At 200 µM FLS there was an almost immediate reduction in growth after 1 day exposure and at the end of the testing period seedlings were not able to accumulate any further fresh weight, chlorophyll or root length (figures 3.7A and 3.8).

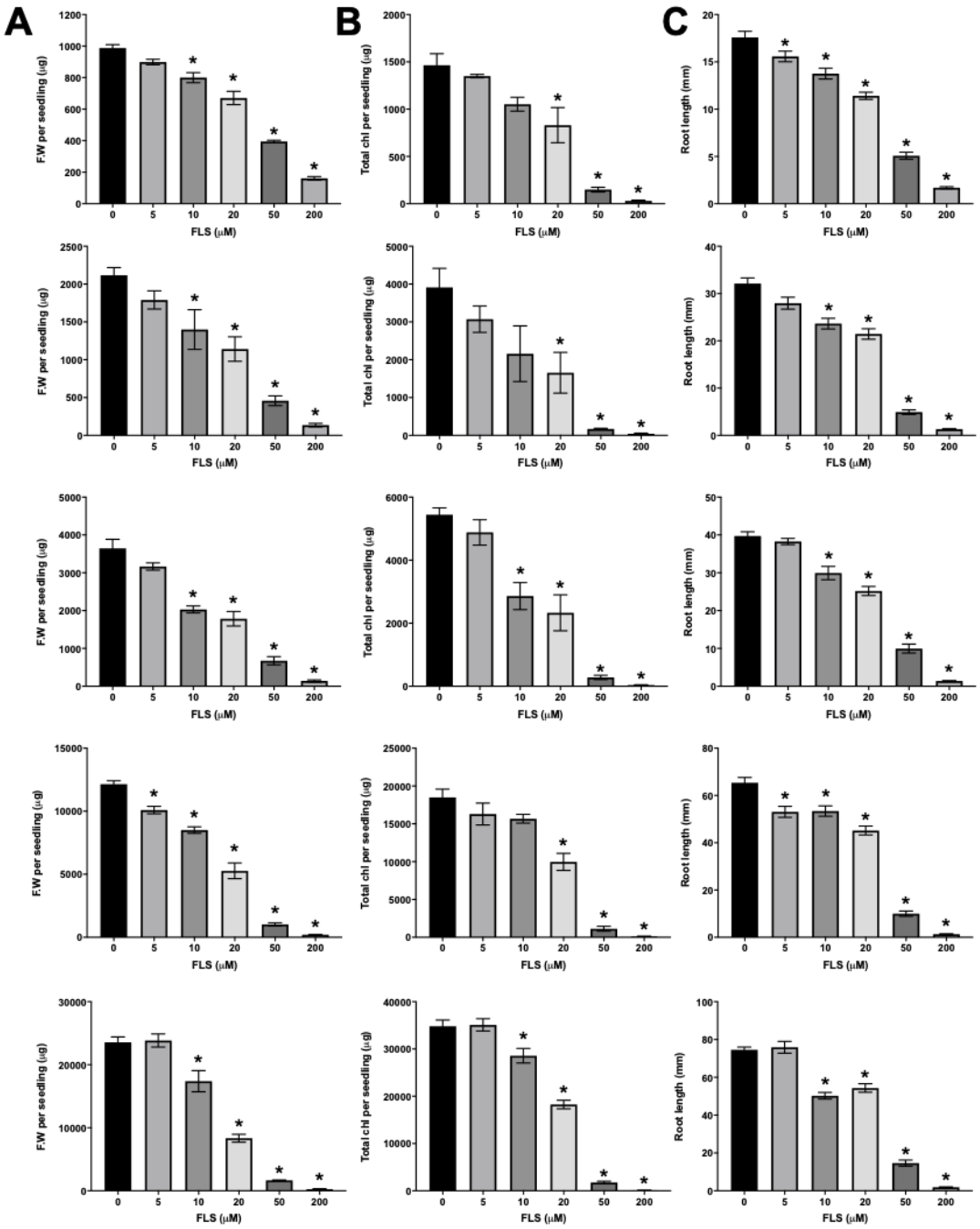

Figure 3.6. FLS treatment from germination reduces growth that is non-recoverable. Col-0 seedlings grown for 7 days on ½ MS 0.8% agar (w/v) media with addition of FLS to give a final concentration of FLS at indicated concentrations (µM). Vehicle control condition included addition of 0.1% DMSO to media. Seedlings are subsequently transferred to plates omitting FLS for a further 6 days to track progress. Graphs represent (A) fresh weight (FW), (B) total chlorophyll (chl) and (C) root length measurements from 5 and 7 days on FLS (top two graphs) and 1, 4 and 6 days off FLS (bottom three graphs). Fresh weight (FW) and total chlorophyll (chl) data points represent the mean ± SEM of three biological replicates, primary root length data points represent mean ± SEM of 9-21 individuals. Asterisks denote P<0.05 in control seedlings compared to FLS treated seedlings by Tukey's post-hoc multiple-comparison test.

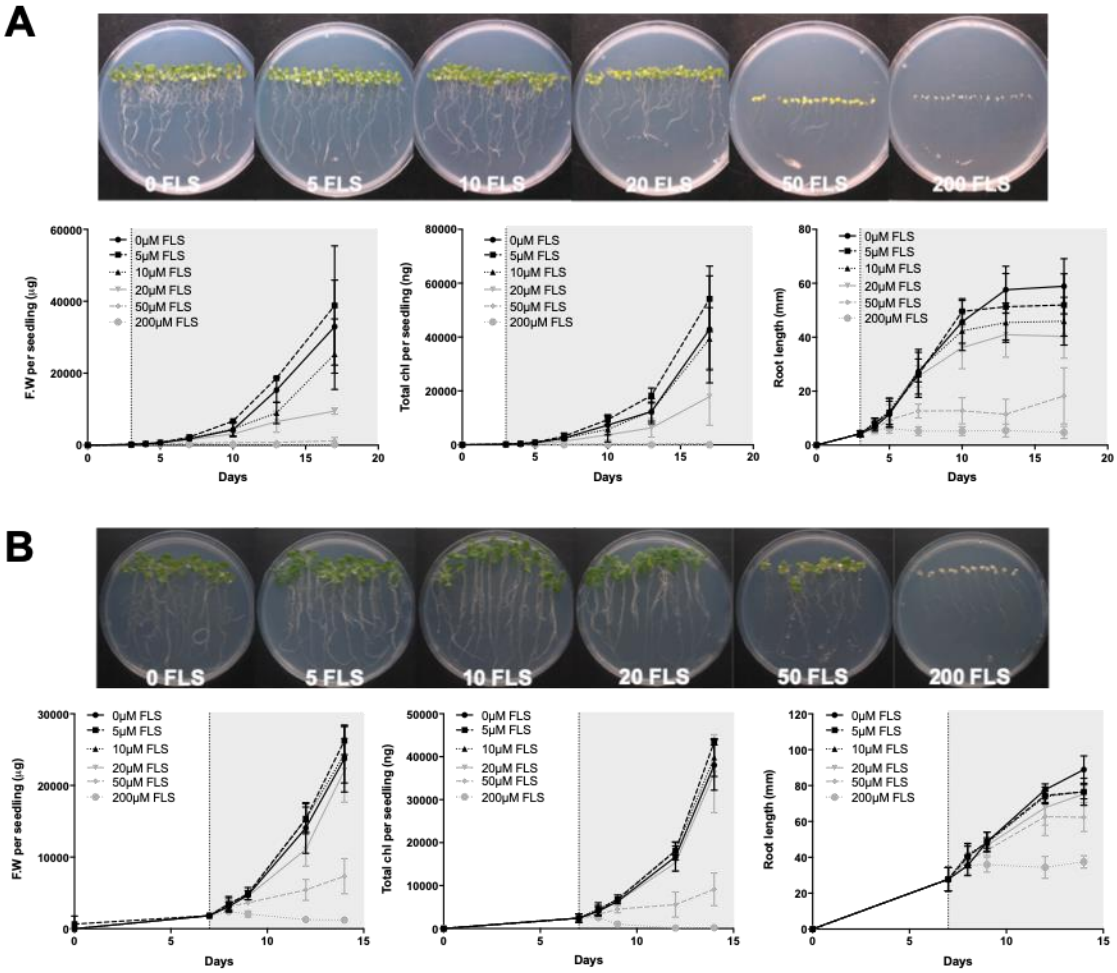

Figure 3.7. The post-germinative effect of FLS on *Arabidopsis* seedlings. Col-0 seedlings were grown on media omitting FLS for (A) 3 and (B) 7 days then subsequently transferred to plates containing the indicated concentrations of FLS for a further 14/7 days. Dotted line represents point of transfer and grey background represent presence of FLS. Fresh weight (FW) and total chlorophyll (chl) data points represent the mean ± SEM of three biological replicates, primary root length data points represent mean ± SEM of 8-56 individuals.

A similar experiment was carried out looking at more established seedlings; following 7 days growth off FLS, seedlings were transferred to plates containing FLS for a further 7 days. A similar pattern was observed. There was a transient increase in root length at lower concentrations (figure 3.9C) and at 200 µM a decrease in growth was observed after only 2 days exposure (figures 3.7B and 3.9). Due to the seedlings being significantly more established at 7 days, compared to 3, they are able to buffer the effects of FLS more successfully leading to a subtler growth enhancing effect of FLS at low concentrations.

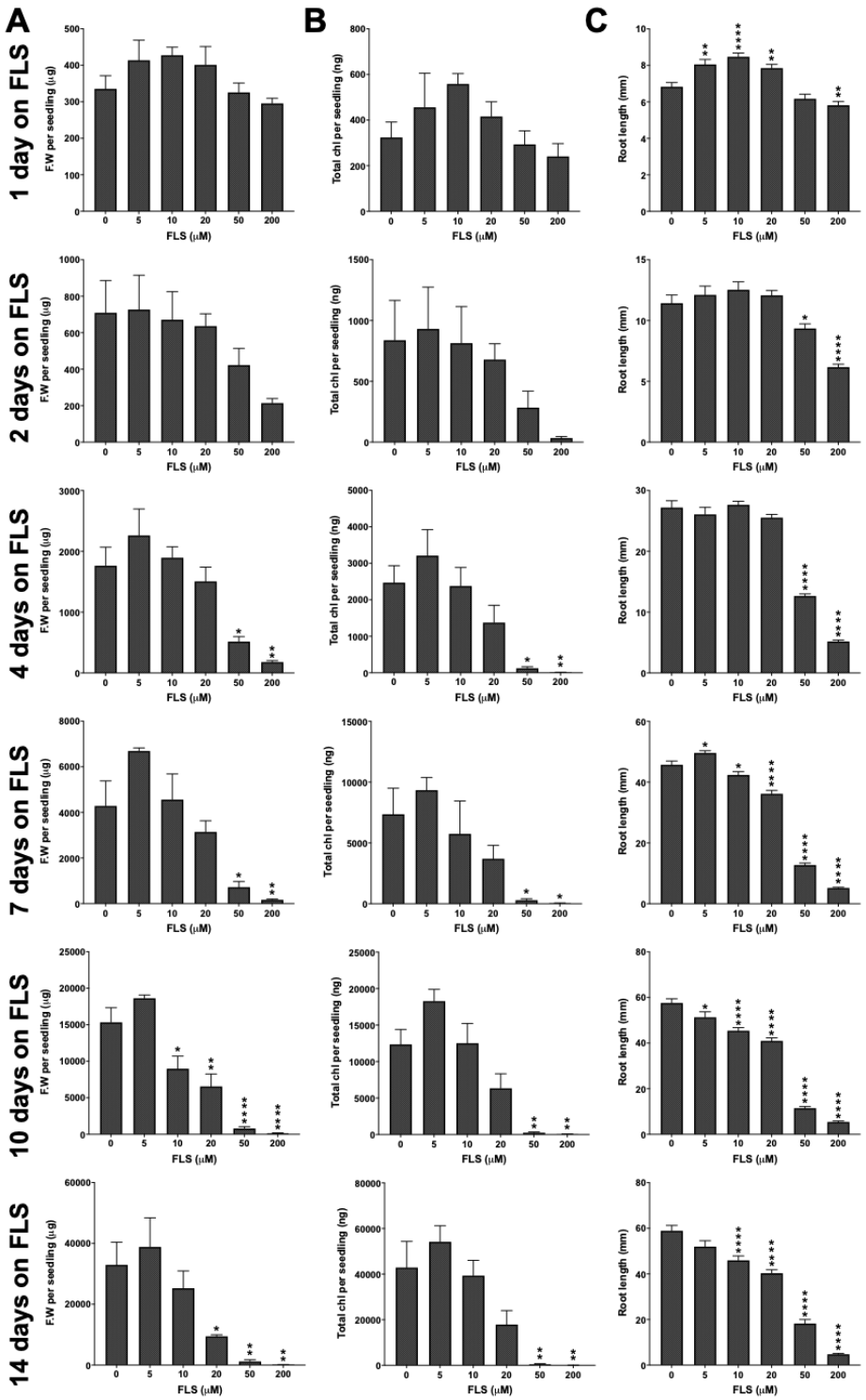

Figure 3.8. Low concentrations of FLS treatment 3 days after germination causes a transient increase in growth. Col-0 seedlings were grown on media omitting FLS for 3 days then subsequently transferred to plates containing the indicated concentrations of FLS for a further 14 days. Graphs represent (A) fresh weight, (B) total chlorophyll and (C) root length measurements from 1, 2, 4, 7, 10 and 14 days on FLS (top-bottom). Fresh weight (FW) and total chlorophyll (chl) data points represent the mean ± SEM of three biological replicates, primary root length data points represent mean ± SEM of 19-56 individuals. Asterisks denote P<0.05 in control seedlings compared to FLS treated seedlings by Tukey's post-hoc multiple-comparison test.

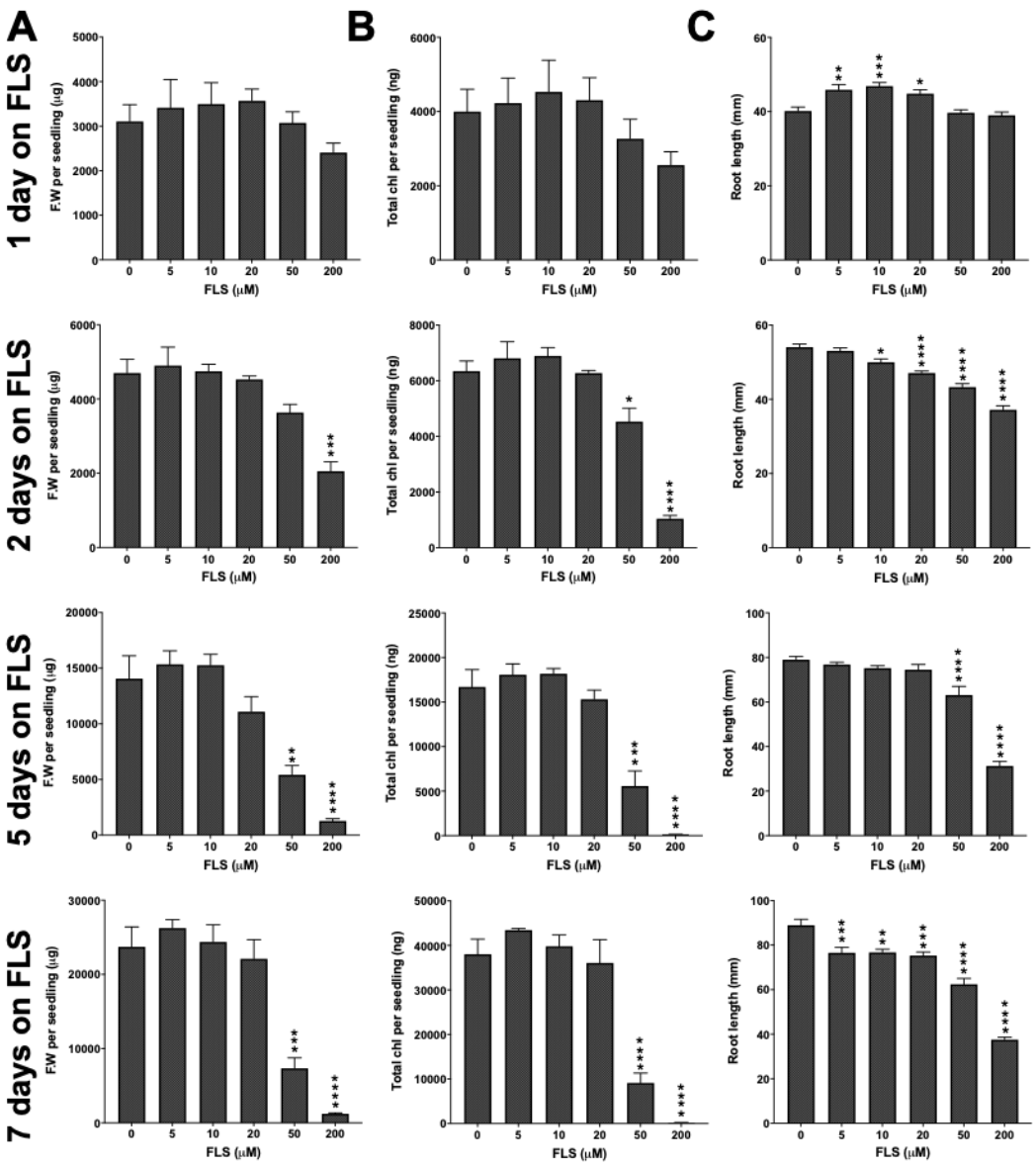

Figure 3.9. Low concentrations of FLS treatment 7 days after germination causes a transient increase in growth. Col-0 seedlings were grown on media omitting FLS for 7 days then subsequently transferred to plates containing the indicated concentrations of FLS for a further 14 days. Graphs represent (A) fresh weight, (B) total chlorophyll and (C) root length measurements from 1, 2, 5 and 7 days on FLS (top-bottom). Fresh weight (FW) and total chlorophyll (chl) data points represent the mean ± SEM of three biological replicates, primary root length data points represent mean ± SEM of 8-31 individuals. Asterisks denote P<0.05 in control seedlings compared to FLS treated seedlings by Tukey's post-hoc multiple-comparison test.

3.2.4 FLS induces a de-etiolated phenotype in the absence of light and perturbs subsequent chlorophyll accumulation in light

Seedling development in the dark is considerably different to development in light and as seeds in contact with FLS in a field setting may be below the soil it was thought that FLS effect on dark-grown seedling development would be an important factor to consider.

In the absence of FLS (figure 3.10) seedlings undergo skotomorphogenesis and display an etiolated phenotype characterised by hypocotyl elongation and apical hook formation. Upon addition of exogenous FLS, seedlings become de-etiolated and display shorter hypocotyls and expanded cotyledons. These features were quantified and show significant inhibition of hypocotyl elongation from 10 µM FLS and expansion of cotyledons from 20µM FLS (figure 3.10) suggesting FLS has prevented normal skotomorphogenic growth in the dark. Elongation of the primary root is a feature of photomorphogenic growth and it is well established that when a WT seedling is grown in darkness root elongation is inhibited but when transferred to light elongation occurs. FLS treatment in the dark had no effect on root length up to concentrations of 150µM and only a slight reduction was observed at 200µM (figure 3.10). This initially would suggest FLS is not inducing photomorphogenic growth in the dark; however, primary root elongation is not dependent upon activation of photomorphogenic development. *Arabidopsis cop1* mutants display photomorphogenic growth in darkness and the gene expression profile is similar to that of light-grown plants; however, primary root elongation is not activated (Kircher & Schopfer, 2012) indicating this is not regulated by photoreceptors in the same way. Chlorophyll synthesis is an essential part of photomorphogenic growth but it is unable to be synthesised in the dark as the penultimate biosynthesis step requires the light dependent protochlorophyllide oxidoreductase (POR) enzymes to convert protochlorophyllide (Pchlide) to chlorophyllide. Therefore, chlorophyll cannot be quantified as in previous experiments; but it is possible to measure Pchlide levels to give further indication of the developmental path of seedlings. In control seedlings Pchlide was detectable at minimal levels; however, as FLS concentration was increased, Pchlide levels also rose with over a 3-fold increase at only 20 µM (figure 3.10).

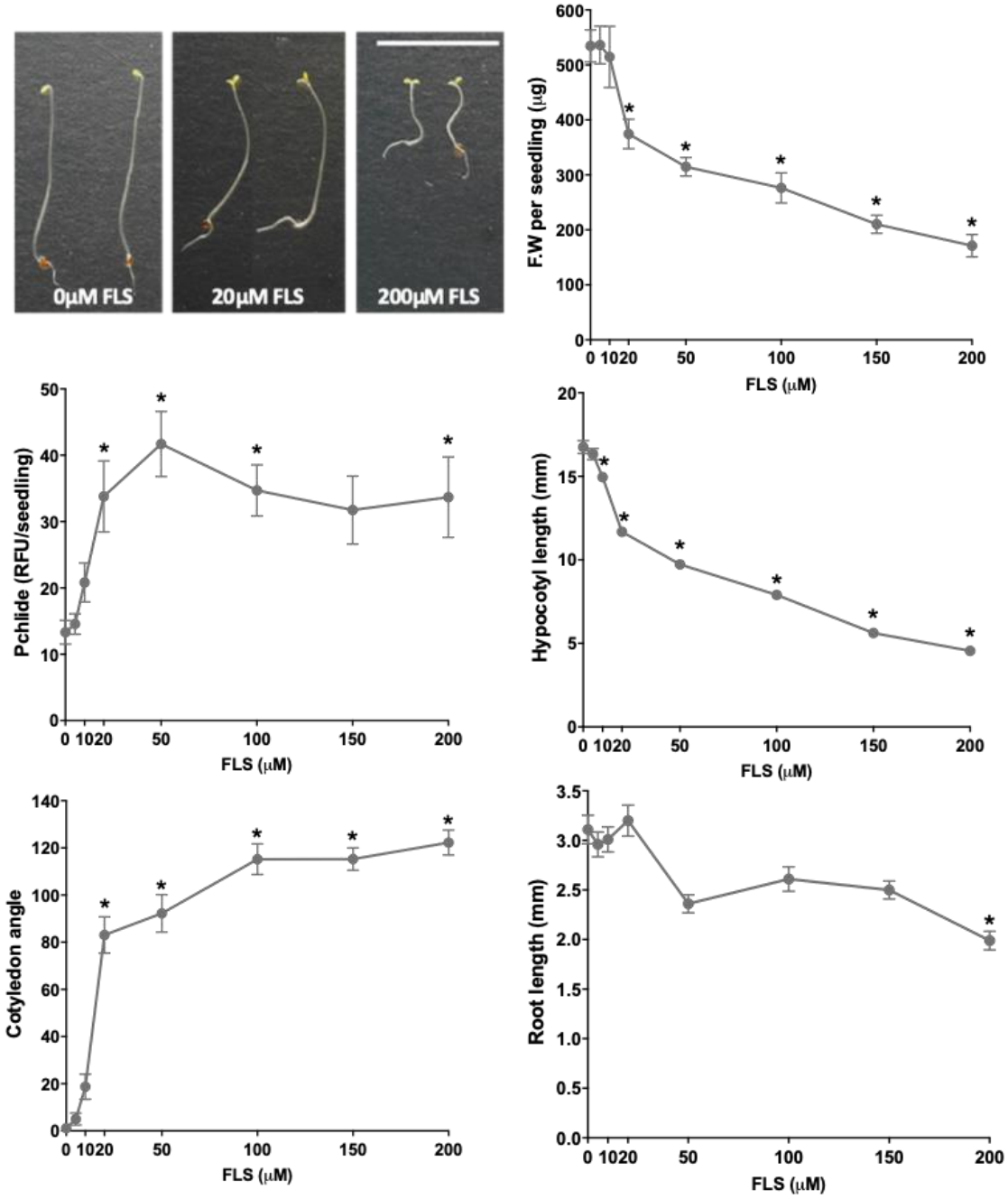

Figure 3.10. Exogenous FLS induces a de-etiolated phenotype in the dark. Col-0 seedlings grown for 5 days in the dark on ½ MS 0.8% agar media with addition of FLS at indicated concentrations (µM). Vehicle control condition included addition of 0.1% DMSO to media. Data points represent the mean ± SEM of four biological replicates, hypocotyl length and cotyledon angle data points represent the mean ± SEM of 60 individuals per condition. Hypocotyl length and cotyledon angle measured on ImageJ software. Asterisks indicate significant difference ($p<0.05$) compared to control conditions by Tukey's post-hoc multiple-comparison test.

Activity of the chlorophyll biosynthesis pathway was also studied through gene expression via qPCR on key genes involved in chlorophyll synthesis, chloroplast biogenesis and light-dependent signalling (Stephenson et al., 2009; Stephenson & Terry, 2008). Following 5 days growth in the dark exposed to 50µM FLS, *PORA* expression in FLS-treated seedlings was unchanged relative to control. However, *HEMA1* and *CHLH* expression was increased up to 9-fold, respective to control, suggesting upregulation of the chlorophyll biosynthesis pathway and also providing an explanation of the accumulation of Pchlide in the dark by FLS. The expression of *LHCB1.2* was also increased following FLS treatment to almost 40-fold of control (figure 3.11A) suggesting chloroplast biogenesis is initiated in response to FLS. Confirmation of FLS-induced changes in gene expression came from RNAseq analysis of dark-grown, 50µM FLS-treated tissue – data explored further in section 3.2.9. Comparing log2Fold change values of the four genes studied using qPCR to the same four genes identified in the RNAseq study, a strong relationship was observed (figure 3.11B).

It is known from the *Arabidopsis flu* mutant that an excessive accumulation of Pchlide in the dark generates singlet oxygen ($^1O2$) which leads to oxidative damage and inhibition of chlorophyll production when dark-grown seedlings are transferred into the light (McCormac & Terry, 2002, 2004; Meskauskiene et al., 2001; Page et al., 2017). To determine if FLS-induced Pchlide accumulation is sufficient to cause oxidative damage, Col-0 seedlings were grown in the dark for 5 d on increasing concentrations of FLS and exposed to WL for 24 h. Following 24 h exposure to light, control seedlings were able to produce chlorophyll, however, seedlings treated with 50µM or more FLS and above had significantly reduced chlorophyll content (figure 3.12A). FLS also significantly reduced fresh weight of seedlings from 20µM FLS in a dose dependent manner.

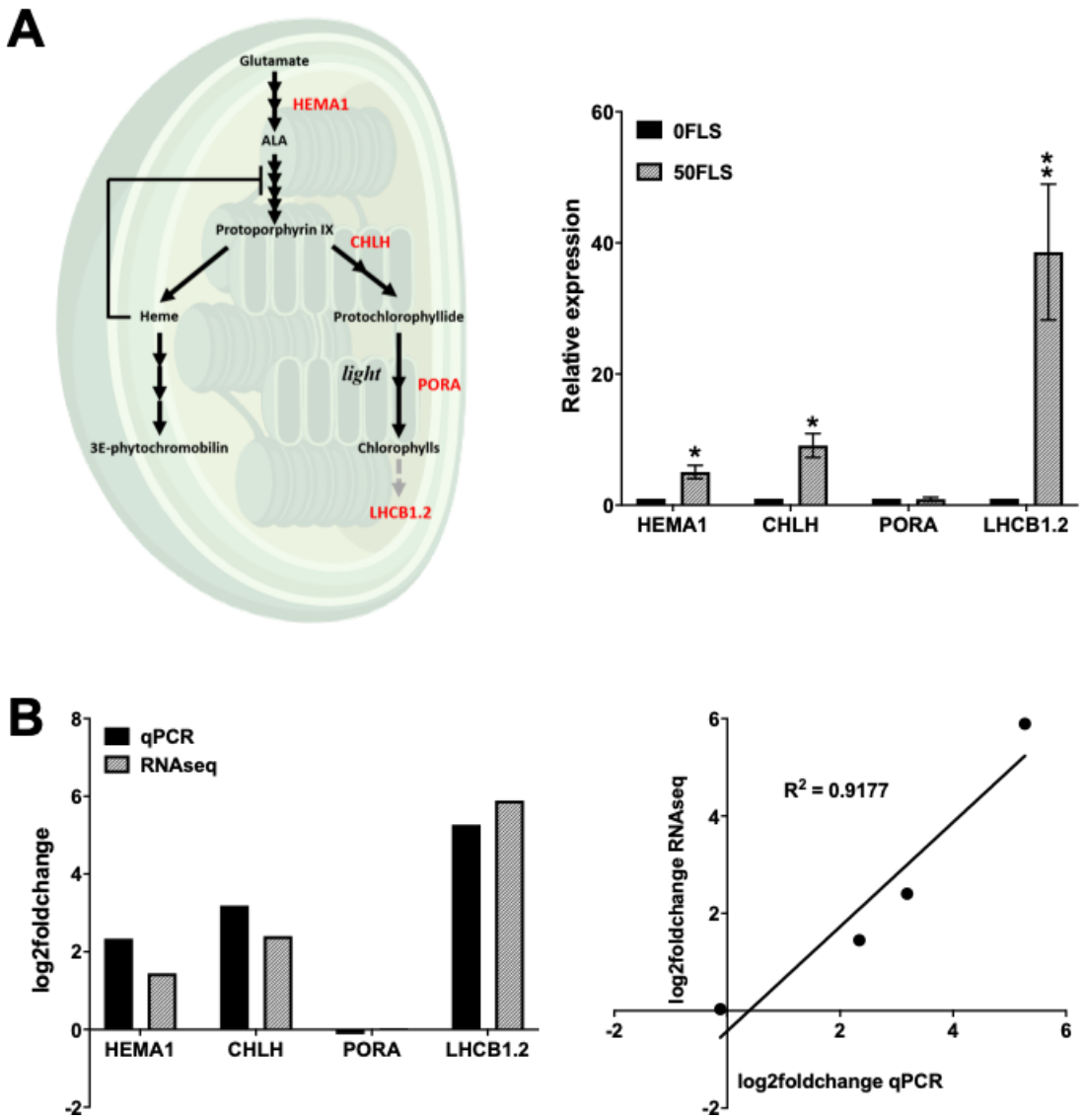

Figure 3.11. FLS induces the expression of light-regulated genes in the dark. (A) Simplified chlorophyll biosynthesis pathway indicating the step in which each protein product of the quantified genes acts. Col-0 seedlings grown for 5 days in the dark on ½ MS 0.8% agar media with addition of 50µM FLS. Gene expression in whole seedlings was measured by quantitative RT-PCR relative to seedlings grown on 0.1% DMSO and normalised to *YELLOW LEAF SPECIFIC* (*YLS8*). Data represents mean ±S.E of three biological replicates. * $p<0.05$, ** $p<0.01$, *** $p<0.001$ in one-way ANOVA test. (B) Comparison of gene expression in qPCR and RNAseq, expressed as log2fold change.

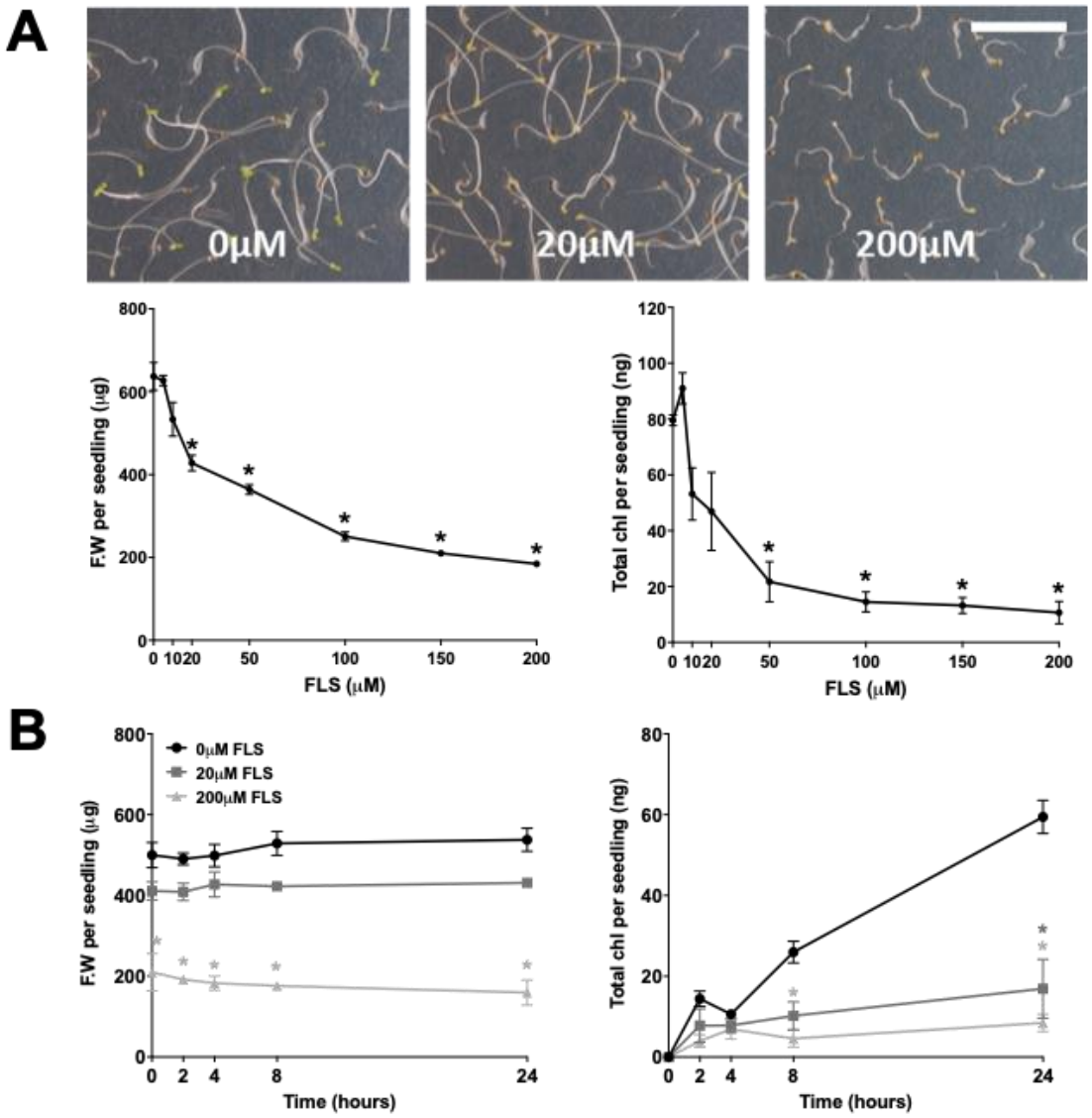

Figure 3.12. FLS perturbs chlorophyll accumulation when seedlings are transferred to light. Col-0 seedlings grown for 5 days on ½ MS 0.8% agar media with addition of FLS at indicated concentrations. Plates were then moved into WL for 24 h (A) or 0-24 h (B) and harvested to assess chlorophyll levels. Vehicle control condition included addition of 0.1% DMSO to media. Data points represent the mean ± SEM of four biological replicates. Asterisks denote P<0.05 in control seedlings compared to FLS treated seedlings by Tukey's post-hoc multiple-comparison test. Scale bar represents 10mm.

In a similar experiment, seedlings were grown in the dark for 5 d +/- FLS and subsequently moved to WL for an increasing number of hours (figure 3.12B). Unsurprisingly, fresh weight was significantly lower in 200µM FLS seedlings at all time points and none of the conditions resulted in the accumulation of a significant increase in fresh weight over the 24 h WL period (figure 3.12B). If the experiment was continued, control seedlings would be expected to show an increase. FLS treatment of both 20 and 200µM displays an inhibition of total chlorophyll accumulation over the testing period. The control seedlings are able to accumulate 2- and 5-fold more chlorophyll at the 8- and 24-hour time points, respectively. In contrast, FLS treated seedlings display a perturbed response and are not able to accumulate chlorophyll.

3.2.5 The role of HY5, HYH and PIF in FLS-induced de-etiolation

The bZIP transcription factors LONG HYPOCOTYL 5 (HY5) and HY5 HOMOLOG (HYH) are key to control light-induced gene expression, downstream of photoreceptors, and are essential in the transition from dark- to light-grown development (Holm et al., 2002). Loss of function *hy5* mutants display a dark-grown phenotype in the light identifying this gene as a positive regulator of light signaling. Therefore, treating the *hy5 hyh* double mutant with FLS in the dark would determine if these proteins are required for FLS-induced de-etiolation or if FLS is activating a separate parallel pathway.

L*er* WT seedlings display the same de-etiolated phenotype as Col-0 seedlings with an increase in Pchlide, cotyledon opening and reduction in hypocotyl length after treatment with FLS (figure 3.13). Although FLS was still able to induce aspects of de-etiolation in the double mutant, a reduced response was observed. WT and mutant seedlings accumulated a similarly low level of Pchlide in the absence of FLS, but, WT seedlings accumulated significantly more Pchlide at 50µM FLS, whereas mutant seedlings require 150µM FLS to elicit a significant increase in Pchlide accumulation. A similar response was evident when looking at cotyledon angle. From this it can be determined HY5 and HYH may partially mediate, but are not absolutely required for, FLS-induced de-etiolation. As these proteins are such key mediators in light-signaling, many pathways and molecules

act upstream; therefore, studying the effect of FLS on pathways that converge on HY5 and HYH could provide more insight into FLS mode of action.

PIF (phytochrome interacting factor) proteins are bHLH transcription factors that bind to the G-box in the promotor region of several genes and negatively regulate photomorphogenesis in a number of ways, including repression of chlorophyll biosynthesis genes (Stephenson et al., 2009; Leivar et al., 2009). Phytochromes in their active state are able to de-stabilize these proteins to allow photomorphogenesis. The quadruple mutant (*pifq*) displays a phenotype similar to FLS in the dark and has a gene expression pattern similar to that of a red-light grown WT (Leivar et al., 2009) potentially suggesting FLS could be targeting this pathway. To investigate this, *pifq* seedlings were treated with increasing concentrations of FLS and grown in the dark. As expected, *pifq* seedlings treated with no FLS display a de-etiolated phenotype characterized by significantly increased Pchlide and reduced hypocotyl length. When FLS is added de-etiolation is exaggerated, with Pchlide accumulation and hypocotyl length changing by similar ratios to the WT seedlings (figure 3.14). From this, it is clear FLS is able to exert it's effects in the *pifq* mutant and therefore that FLS-induced de-etiolation is not dependent on the four PIF proteins lacking in the *pifq* mutant.

3.2.6 Application of exogenous epi-brassinolide and gibberellin was unable to reverse FLS-induced de-etiolation

It is well documented that light signaling intersects with hormone signaling and biosynthesis paths and, specifically, that HY5 is implicated (Alabadí et al., 2008; Chen et al., 2008; Cluis et al., 2004; Sibout et al., 2006; Vandenbussche et al., 2007; Weller et al., 2009). In addition, a number of hormone-deficient or insensitive mutants display de-etiolated phenotypes in the dark – similar to FLS treatment. For this reason, pre-cursors of hormones or hormones themselves were added to the plant growth media alongside FLS to determine if supplementation could alleviate FLS effects in the dark. This would give an indication of whether FLS was acting to reduce endogenous hormone signaling to cause de-etiolation in the dark.

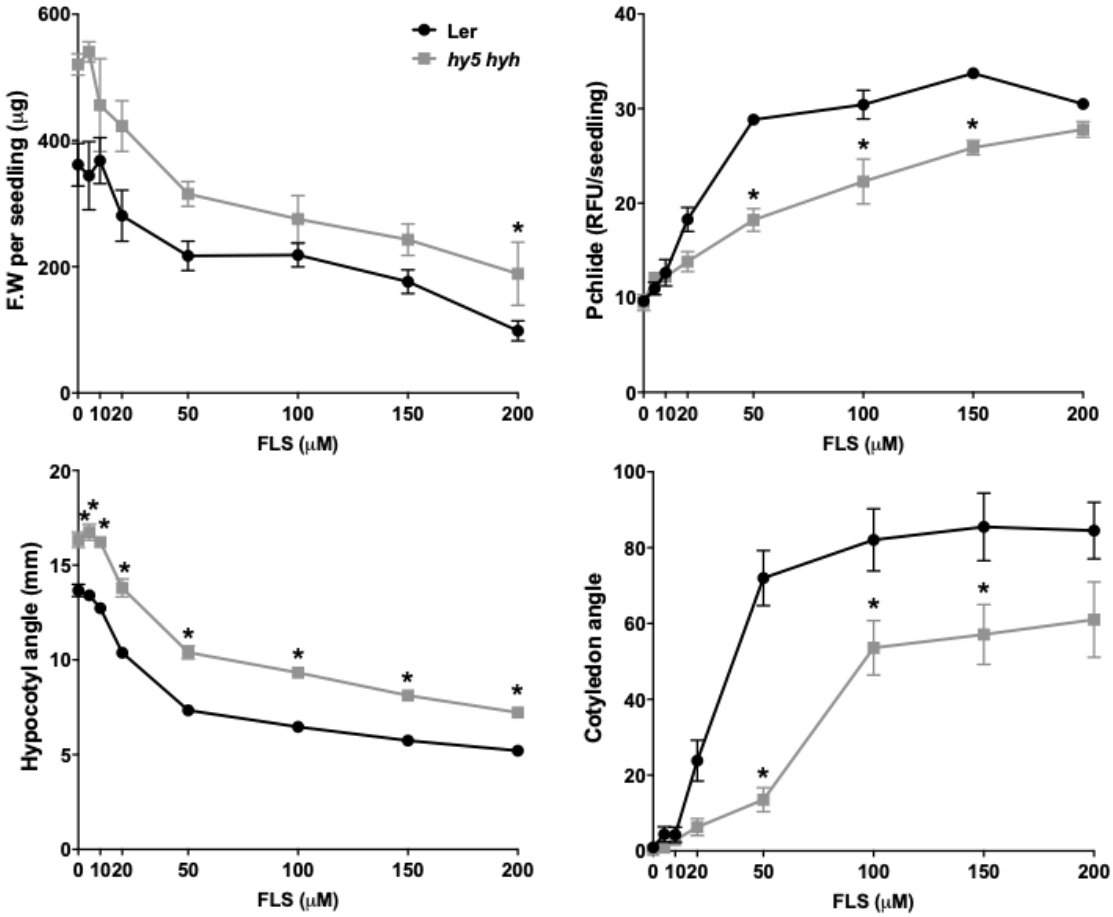

Figure 3.13. FLS-induced de-etiolation is partially mediated by HY5/HYH. L*er* control (black line) and *hy5/hyh* double mutant (grey line) seedlings grown for 5 days on ½ MS 0.8% agar media with addition of FLS to give a final concentration of FLS as indicated (µM). Fresh weight and Pchlide data points represent the mean ± SEM of four biological replicates, hypocotyl length and cotyledon angle data points represent the mean ± SEM of 27-69 individuals per condition. Hypocotyl length and cotyledon angle measured on ImageJ software. Asterisks indicate significant difference ($p<0.05$) compared to *Ler* by Tukey's post-hoc multiple-comparison test.

Brassinosteroids (BRs) within *Arabidopsis* play a key role in photomorphogenesis and a number of deficient mutants (e.g. *det2*) or insensitive mutants (e.g. *bri*) display de-etiolation in the dark indicating BR is a negative regulator of photomorphogenesis. Seedling were exogenously fed 5 and 10µM epi-brassinolide (EBR) in the presence and absence of FLS and displayed no reversal of de-etiolation. Exogenous EBR did not have an effect on fresh weight; but induced Pchlide accumulation in the presence of FLS. Application of EBR reduced hypocotyl length in control seedlings and 20µM FLS-treated seedlings and also induced cotyledon opening in control seedlings (figure 3.15).

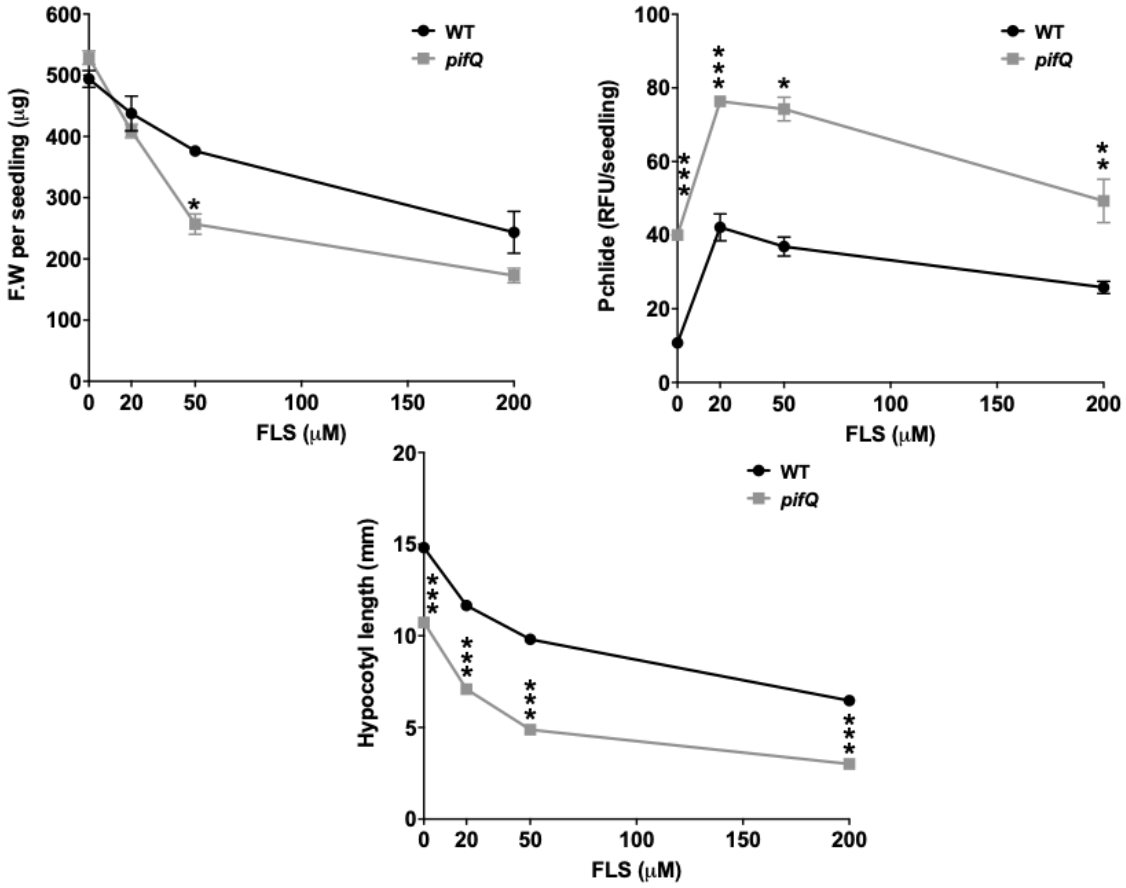

Figure 3.14. FLS-induced de-etiolation is not mediated by PIFs. Col-0 control (black line) and *pifq* mutant (grey line) seedlings grown for 5 days on ½ MS 0.8% agar media with addition of FLS to give a final concentration of FLS as indicated (µM). Fresh weight and Pchlide data points represent the mean ± SEM of three biological replicates, hypocotyl length data points represent the mean ± SEM of 16-22 individuals per condition. Hypocotyl length measured on ImageJ software. Asterisks indicate significant difference ($p<0.05$) compared to Col-0 by Tukey's post-hoc multiple-comparison test.

Additionally, in all cases, application of EBR caused hypocotyl swelling and twisting. This is characteristic of excess EBR due to a defect in normal patterning of cell elongation and has been documented before (Tanaka et al., 2003). The inability of EBR to reduce FLS-induced Pchlide accumulation and the abnormal hypocotyl phenotype, suggests that FLS does not induce de-etiolation via a perturbation of BR biosynthesis. As the EBR at these concentrations was having such a profound effect on hypocotyl growth the experiment was repeated using 10nM and 100nM EBR to check if any effects were being masked by EBR toxicity (data not shown). Even at these low concentrations the results were similar with no reduction in Pchlide and the abnormal hypocotyl phenotype was still observed.

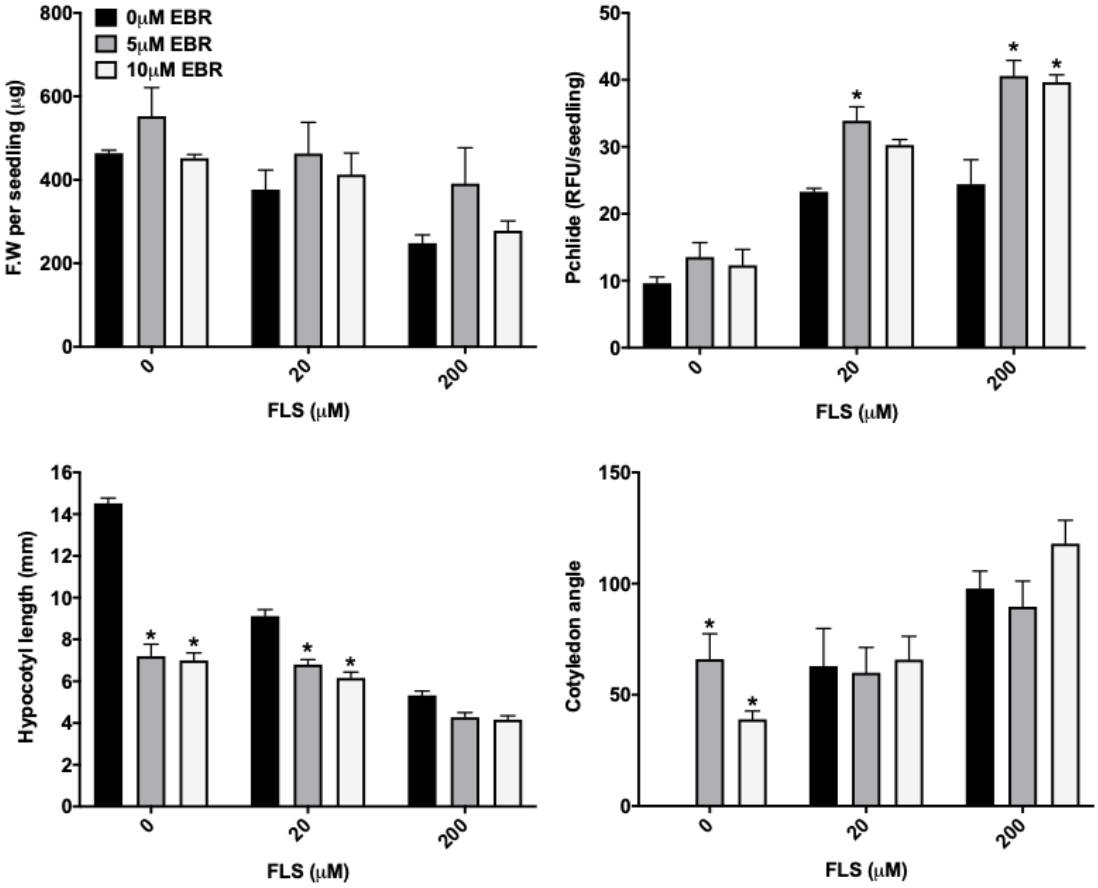

Figure 3.15. Exogenous epi-brassinolide (EBR) is unable to rescue FLS induced a de-etiolation. Col-0 seedlings were grown for 5 days in the dark on ½ MS 0.8% agar media with addition of FLS and epi-brassinolide (EBR) at indicated concentrations (µM). Vehicle control conditions included addition of 0.1% DMSO and 0.1% ethanol to media. Fresh weight and Pchlide data points represent the mean ± SEM of three biological replicates, hypocotyl length and cotyledon angle data points represent the mean ± SEM of 12-25 individuals per condition. Asterisks indicate significant difference ($p<0.05$) compared to 0µM EBR treatment by Tukey's post-hoc multiple-comparison test

It is known that gibberellins (GAs) also repress photomorphogenesis in the dark through studies using a GA biosynthesis inhibitor, paclobutrazol (PAC), and GA-deficient mutant (*ga1-3*) that both display de-etiolation in the dark (Alabadí et al., 2004; Cheminant et al., 2011). Therefore, exogenous GA was applied alongside FLS to determine if GA biosynthesis was affected by FLS treatment. Exogenous GA had no effect on any parameters measured (figure 3.16) with seedlings having the same phenotype regardless of GA application.

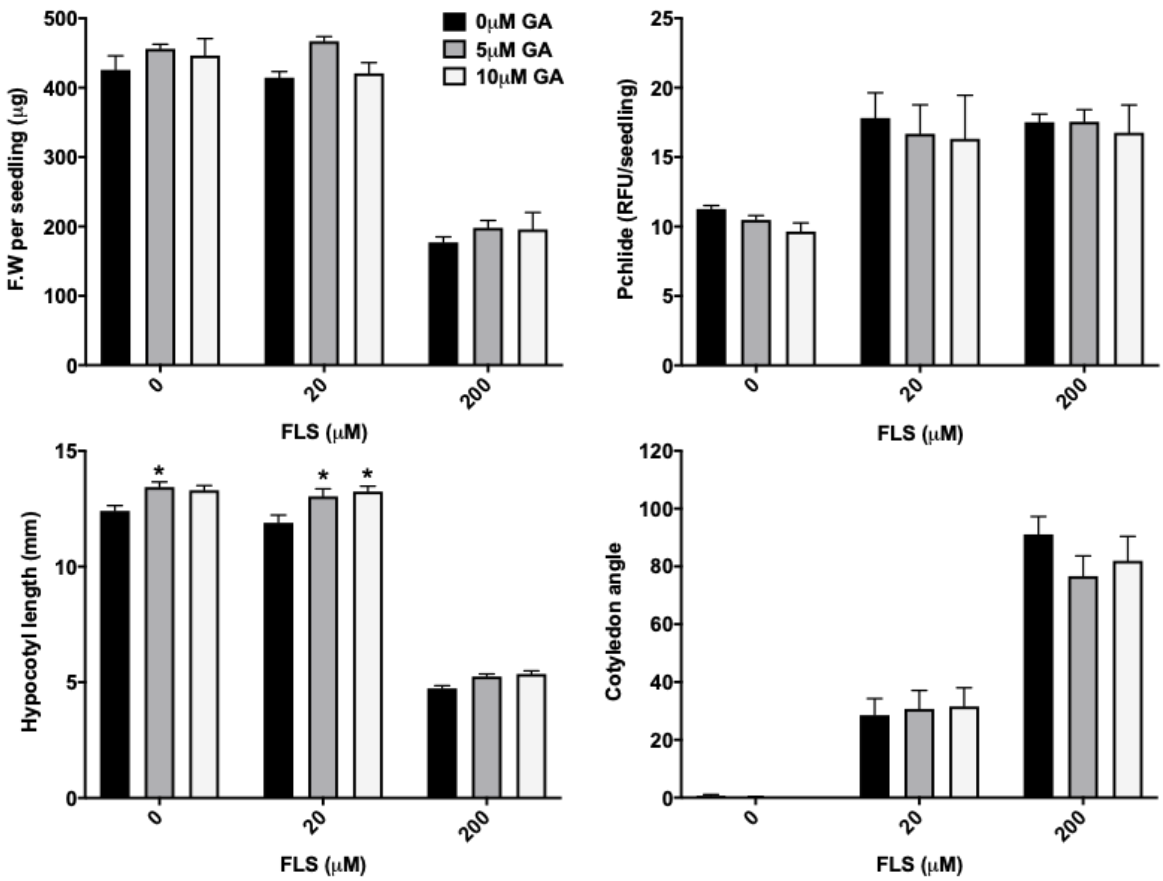

Figure 3.16. Exogenous gibberellic acid (GA) is unable to rescue FLS induced a de-etiolation in the dark. Col-0 seedlings were grown for 5 days in the dark on ½ MS 0.8% agar media with addition of FLS and gibberellic acid (GA) at indicated concentrations (µM). Vehicle control conditions included addition of 0.1% DMSO and 0.1% ethanol to media. Fresh weight and Pchlide data points represent the mean ± SEM of four biological replicates, hypocotyl length and cotyledon angle data points represent the mean ± SEM of 34-51 individuals per condition. Asterisks indicate significant difference ($p<0.05$) compared to 0µM GA treatment by Tukey's post-hoc multiple-comparison test.

To show that 5 and 10µM are biologically relevant concentrations of GA and that the results are not due to lack of GA entering the seedlings, 10µM GA was shown to be sufficient to rescue PAC induced de-etiolation. 1µM PAC was able to induce a de-etiolated phenotype similar to FLS – an accumulation of Pchlide, reduction in hypocotyl length and opening of the cotyledons (figure 3.17); however, these features can be completely reversed by 10µM GA. Through this study it is evident 10µM GA is sufficient to overcome an inhibition of GA biosynthesis; therefore, as it is unable to reverse FLS-induced de-etiolation, it can be concluded that FLS is not affecting GA biosynthesis.

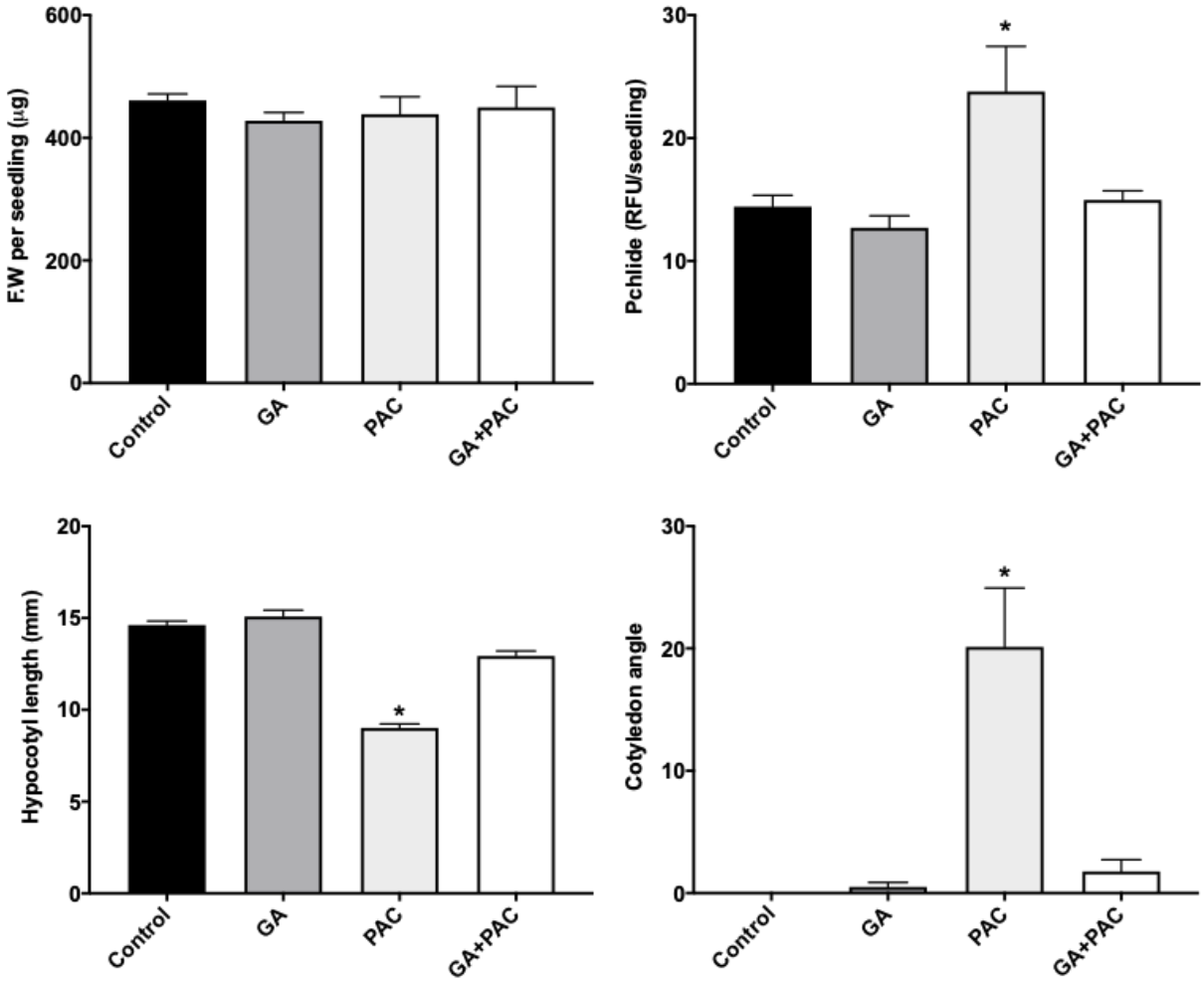

Figure 3.17. Exogenous gibberellic acid (GA) is able to rescue paclobutrazol (PAC) - induced de-etiolation in the dark. Col-0 seedlings were grown for 5 days in the dark on ½ MS 0.8% agar media with addition of paclobutrazol (PAC) and gibberellic acid (GA) at indicated concentrations (µM). Fresh weight and Pchlide data points represent the mean ± SEM of three biological replicates, hypocotyl length and cotyledon angle data points represent the mean ± SEM of 28-45 individuals per condition. Asterisks indicate significant difference ($p<0.05$) compared to control treatment by Tukey's post-hoc multiple-comparison test.

3.2.7 Application of exogenous auxins was able to reverse features of FLS-induced de-etiolation

In comparison to EBR and GA, application of the naturally occurring auxin, indole acetic acid (IAA), was able to significantly reduce a number of de-etiolated features caused by FLS. Most notably, Pchlide accumulation of 20- and 200 µM FLS treated seedlings was reduced by up to 49%, back to control levels, following co-application with IAA and following IAA treatment FLS-induced cotyledon opening was completely reversed. The fresh weight of 20µM FLS-treated seedlings was significantly increased following 5µM exogenous IAA application; however, hypocotyl length was not reversed by exogenous IAA. Additionally, there was no significant effects of IAA on control seedlings suggesting these concentrations were appropriate (figure 3.18).

In a similar experiment, the synthetic auxins naphthaleneacetic acid (1-NAA) and 2,4-Dichlorophenoxyacetic acid (2,4-D) were applied to determine if the response seen with IAA was specific. 1-NAA was used in the same concentration range as IAA; however, as 2,4-D is more metabolically stable, lower concentrations were used. In a similar way to IAA, 1-NAA and 2,4-D reduced Pchlide accumulation and cotyledon opening in the presence of 20 and 200µM FLS; however, IAA remained more effective at the concentrations used.

Additionally, 1-NAA and 2,4-D application had impacts upon seedlings in the absence of FLS; 2,4-D significantly decreased fresh weight of control seedlings while 1-NAA and 2,4-D both reduced hypocotyl length in control and FLS-treated individuals (figure 3.19A & B). Overall, these results suggest that rescue of FLS-induced de-etiolation is specific to auxin, but, IAA displays a more robust rescue than 1-NAA and 2,4-D. Therefore, in all future experiments, IAA will be used as the exogenous auxin unless stated otherwise.

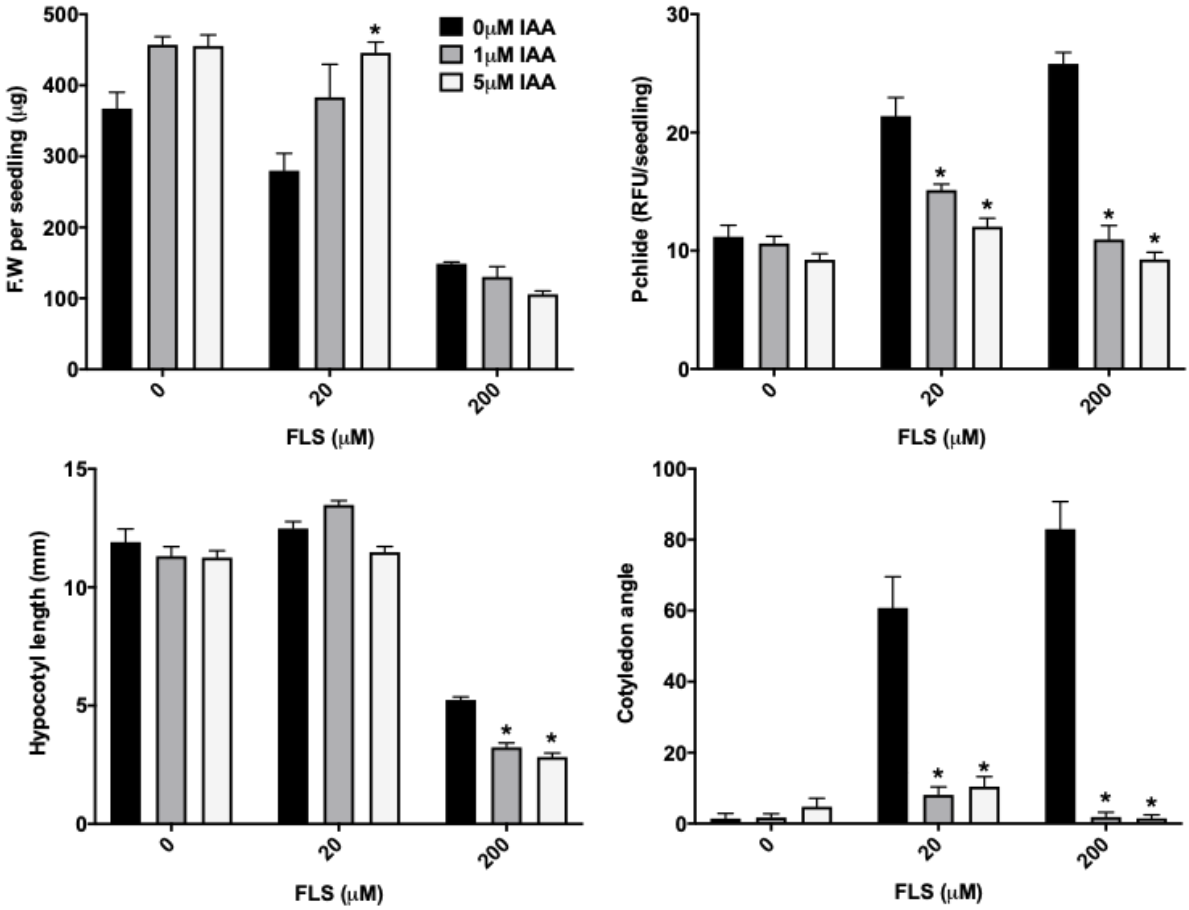

Figure 3.18. The natural auxin, Indole-3-acetic acid (IAA), can reverse FLS-induced de-etiolation. Col-0 seedlings were grown for 5 days on ½ MS 0.8% agar media with addition of FLS and IAA to indicated concentrations. Vehicle control conditions included addition of 0.1% DMSO and 0.1% ethanol to media. Pchlide data points represent the mean ± SEM of four biological replicates, cotyledon data points represent the mean ± SEM of 27-108 individuals per condition. Cotyledon angle measured on ImageJ software. Asterisks indicate significant difference ($p<0.05$) compared to 0μM IAA treatment by Tukey's post-hoc multiple-comparison test.

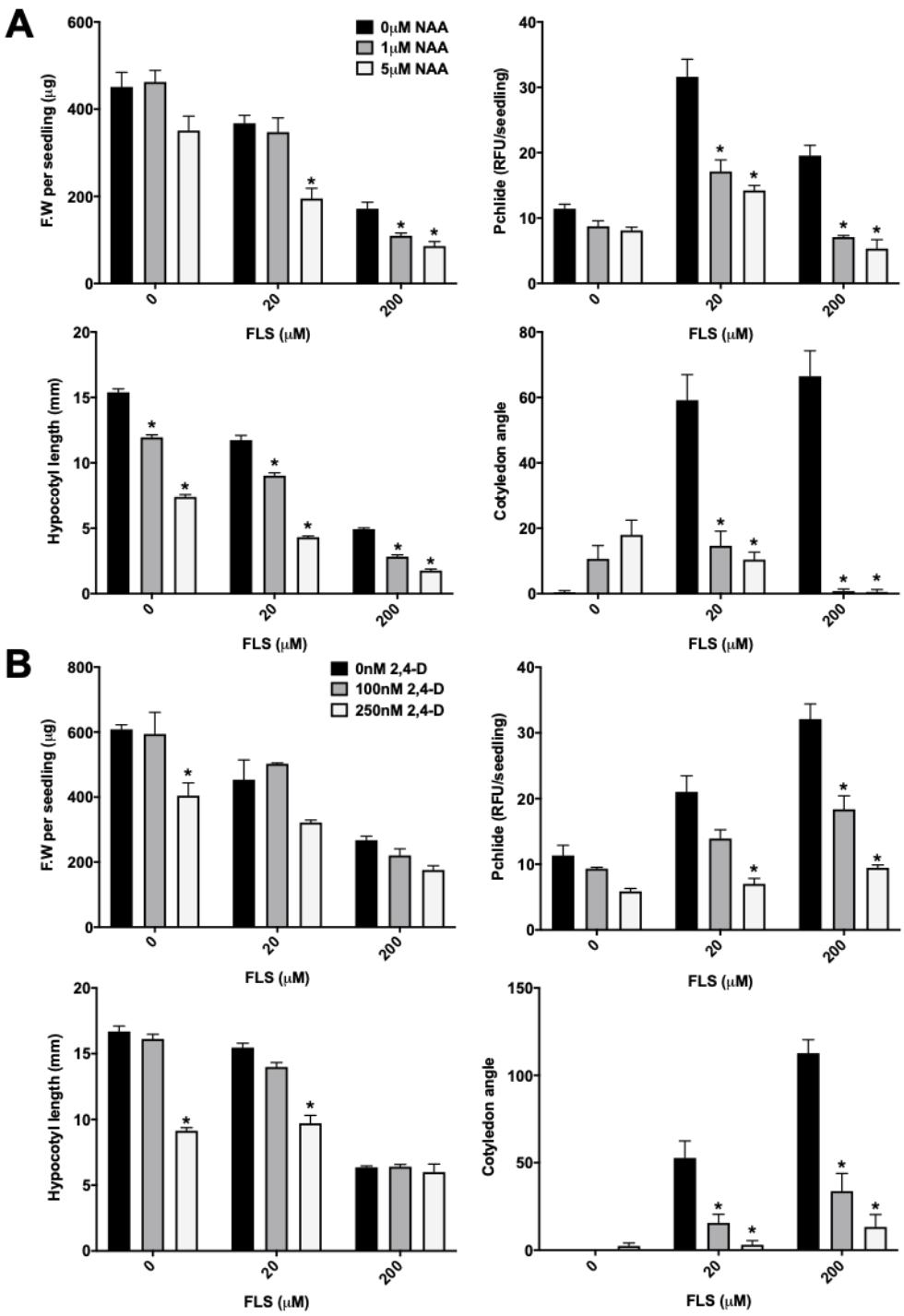

Figure 3.19. The synthetic auxins, 1-Naphthaleneacetic acid (1-NAA) and 2,4-dichlorophenoxyacetic acid (2,4-D), are able to reverse FLS-induced de-etiolation. Col-0 seedlings were grown for 5 days in the dark on ½ MS 0.8% agar media with addition of FLS and (A) 1-NAA or (B) 2,4-D to indicated concentrations. Vehicle control condition included addition of 0.1% DMSO and 0.1% ethanol to media. Fresh weight and Pchlide data points represent the mean ± SEM of three biological replicates, hypocotyl length and cotyledon data points represent the mean ± SEM of 9-57 individuals per condition. Cotyledon angle measured on ImageJ software. Asterisks indicate significant difference ($p<0.05$) compared to 0μM treatment by Tukey's post-hoc multiple-comparison test.

3.2.8 Ethylene precursor ACC can partially rescue FLS-induced de-etiolation

To determine if exogenous ethylene application is able to rescue FLS-induced de-etiolation, the ethylene precursor 1-aminocyclopropane-1-carboxylic acid (ACC) was supplemented to media with FLS at the same concentrations used for auxins. ACC reduced Pchlide accumulation and cotyledon opening induced by 20µM FLS, but not 200µM FLS (figure 3.20). There was no increase in fresh weight, aside a slight increase at the highest doses, or hypocotyl length; in fact, ACC treatment reduced hypocotyl length significantly with a 51% and 43% decrease in control and 20µM FLS-treated seedlings, respectively. This effect was unsurprising as ethylene treatment induces the characteristic 'triple response' (Guzman & Ecker, 1990). In seedlings without FLS, ethylene causes radial swelling, inhibition of hypocotyl elongation and an exaggerated apical hook; this 'triple response' is observable in seedlings treated with 20µM FLS, but not 200µM, suggesting low concentrations of FLS does not impair ethylene signaling. This response seems to be reduced in 200µM FLS seedlings, with only a 14% decrease in hypocotyl length and no significant change in cotyledon opening (figure 3.20), indicating ethylene signaling is altered.

Auxin and ethylene act both antagonistically and synergistically in processes like fruit abscission and root elongation, respectively; they also reciprocally regulate each other's biosynthesis, signaling pathways and have a number of the same gene targets (Zemlyanskaya et al., 2018). It is also evident in auxin mutants that there are strong defects in ethylene responses. As ethylene is able to induce auxin biosynthesis, it was thought that auxin and ethylene could demonstrate an additive effect. 1µM IAA and/or ACC was supplemented into the media in the presence or absence of FLS as these concentrations were sufficient to produce a response. There was no significant effect of IAA or ACC on fresh weight of seedlings, except a reduction when 1µM IAA + 1µM ACC + 200µM FLS were all present (figure 3.21). IAA and ACC were able to reduce Pchlide accumulation in 20µM FLS seedlings to similar levels; however, the effect wasn't additive when applied together. Interestingly, 1µM IAA was the only treatment able to reduce Pchlide accumulation in 200µM FLS seedlings, by 59%; ACC alone or in combination with IAA displayed no significant decrease in Pchlide (figure 3.21).

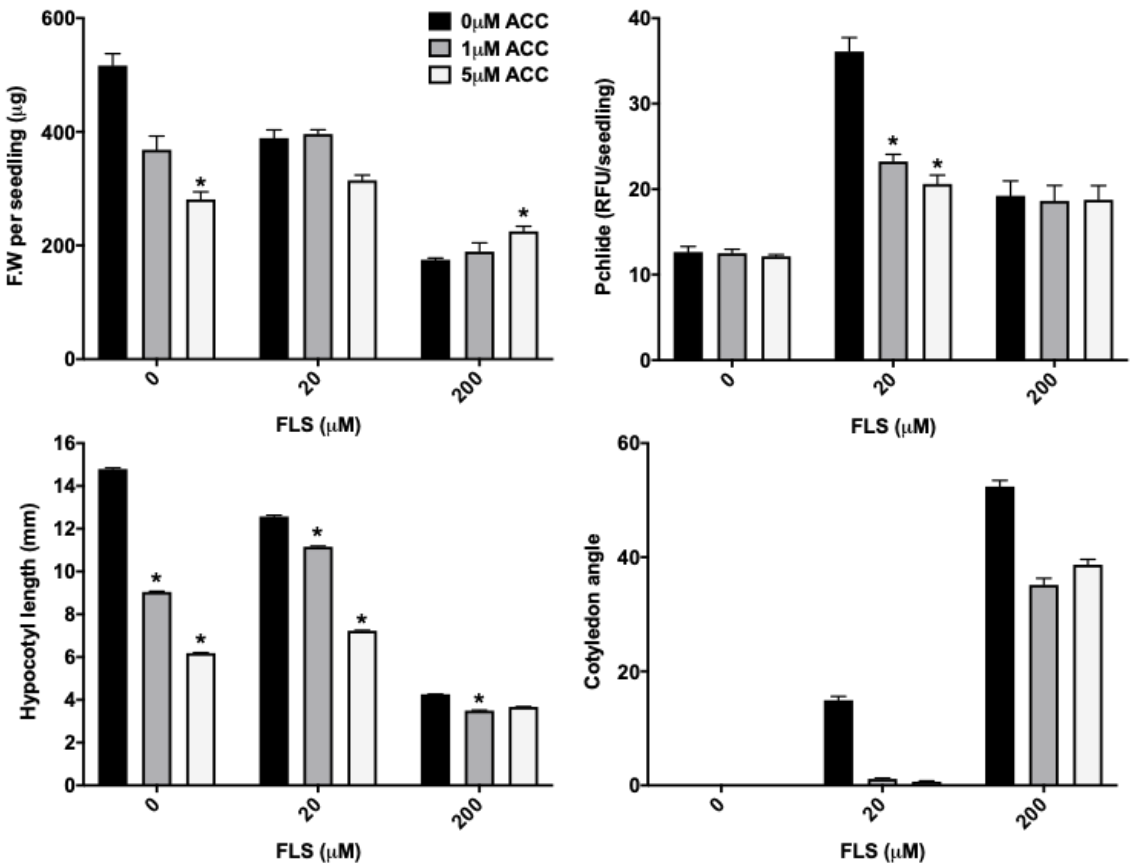

Figure 3.20. Ethylene pre-cursor 1-aminocyclopropane-1-carboxylate (ACC) cannot reverse FLS-induced de-etiolation. Col-0 seedlings were grown for 5 days in the dark on ½ MS 0.8% agar media with addition of FLS and ACC to indicated concentrations. Vehicle control conditions included addition of 0.1% DMSO and 0.1% ethanol to media. Fresh weight and Pchlide data points represent the mean ± SEM of three biological replicates, hypocotyl length and cotyledon data points represent the mean ± SEM of 31-44 individuals per condition. Cotyledon angle measured on ImageJ software. Asterisks indicate significant difference ($p<0.05$) compared to 0μM ACC treatment by Tukey's post-hoc multiple-comparison test.

Only in the presence of ACC, regardless of IAA, was hypocotyl length reduced in control and 20μM seedlings, 1μM IAA alone had no effect. The opposite effect was observed in 200μM FLS seedlings in which hypocotyl length was only reduced in the presence of IAA, whereas ethylene alone had no effect. This is consistent with the results seen in figure 3.20. Both IAA and ACC alone were able to reduce cotyledon opening on FLS treated seedlings; however, at low concentrations of FLS co-treatment with IAA + ACC was not able to reduce cotyledon opening. At high concentrations IAA + ACC treatment looked additive; although, germination and overall growth was greatly reduced in this treatment.

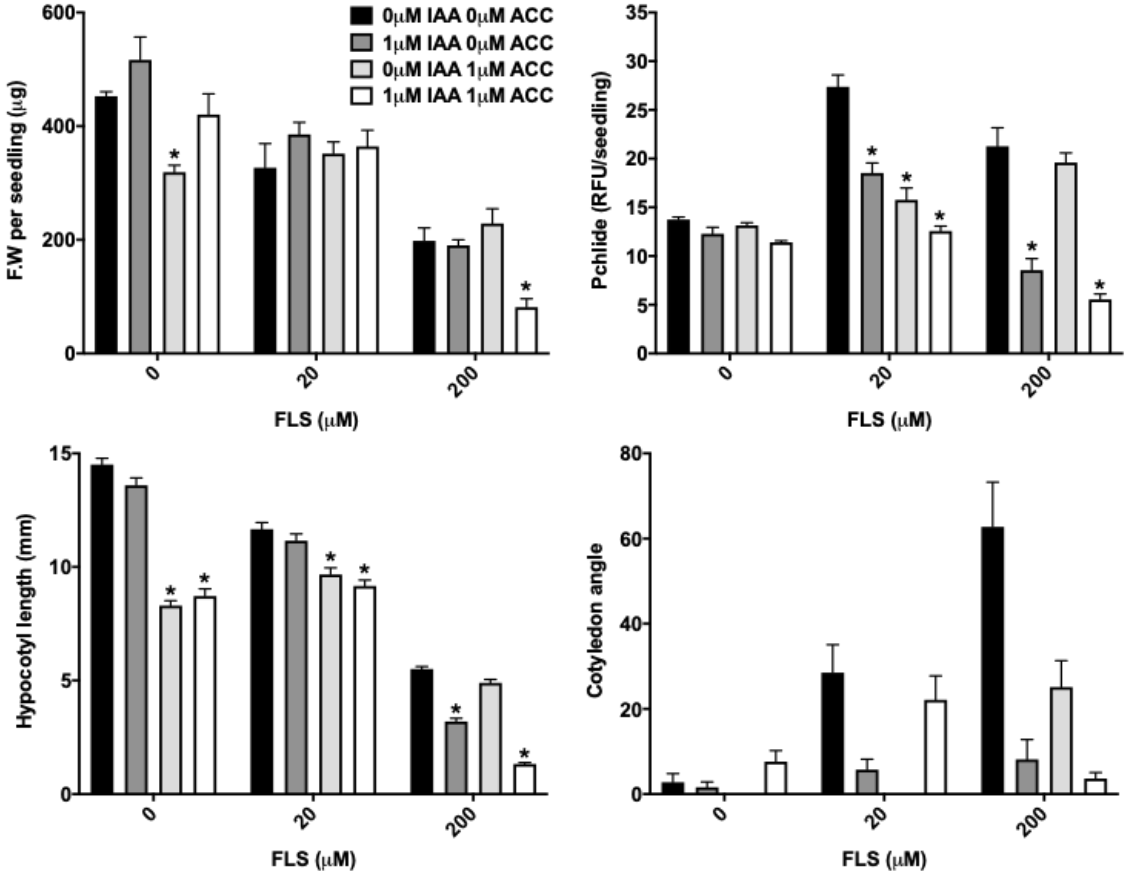

Figure 3.21. Auxin and ethylene are partially additive in the reversal of FLS-induced de-etiolation. Col-0 seedlings were grown for 5 days in the dark on ½ MS 0.8% agar media with addition of FLS, Indole-3-acetic acid (IAA) and 1-aminocyclopropane-1-carboxylate (ACC) to indicated concentrations. Vehicle control conditions included addition of 0.1% DMSO and 0.1% ethanol to media. Fresh weight and Pchlide data points represent the mean ± SEM of three biological replicates, hypocotyl length and cotyledon data points represent the mean ± SEM of 25-35 individuals per condition. Cotyledon angle measured on ImageJ software. Asterisks indicate significant difference ($p<0.05$) compared to 0μM IAA/ACC treatment by Tukey's post-hoc multiple-comparison test.

3.2.9 Transcriptomic analysis of the effect of FLS treatment

In order to understand the global gene expression effect of FLS on both light- and dark-grown *Arabidopsis,* seedlings were treated +/- 50µM FLS and grown for 5/7 days in the dark/light, respectively, subsequently RNA was extracted from these samples and sequenced. This experiment was designed to identify classes of genes preferentially altered by FLS treatment to indicate where FLS may be targeting. RNA was extracted from seedlings from 3 biological replicates of each condition which clustered together in a principal component plot, displaying similar read counts between replicates (figure 3.22A). Following analysis using DESeq, differentially expressed gene (DEG) sets were calculated comprised of 3679 up- and 4141 down-regulated genes and 1403 up- and 1263 down-regulated, in light- and dark-grown FLS treated samples, respectively (figure 3.22B). [Raw data files to be submitted, available on request].

Gene ontology (GO) term enrichment analysis of significantly up-regulated genes from dark-grown FLS-treated seedlings provided further support for FLS induction of a de-etiolated phenotype. 72 biological processes were significantly enriched in these samples with the majority of processes being involved in photosystem assembly and chloroplast biogenesis (table 3.2). In addition, significantly enriched cellular component classes included genes that perform functions in the chloroplast ribulose bisphosphate carboxylase complex, photosystem I and photosystem II (table 3.2).

Comparisons of DEGs in treatments/mutants that induce photomorphogenesis from publicly available microarray data sets were also carried out to determine if FLS induced a response similar to well characterised mutants. Comparing the significantly up- and down-regulated DEGs between 3 data sets from Arabidopsis grown in the dark it was shown that there was the most overlap in FLS treatment and *pifq* seedling data sets (figure 3.23A & B). *pifq* seedlings, which have mutations in the four major *PIFs, PIF1, PIF3, PIF4 and PIF5*, have a well-documented de-etiolated phenotype in the dark and a strong overlap in expressed genes is consistent with the observed phenotype after FLS treatment in the dark.

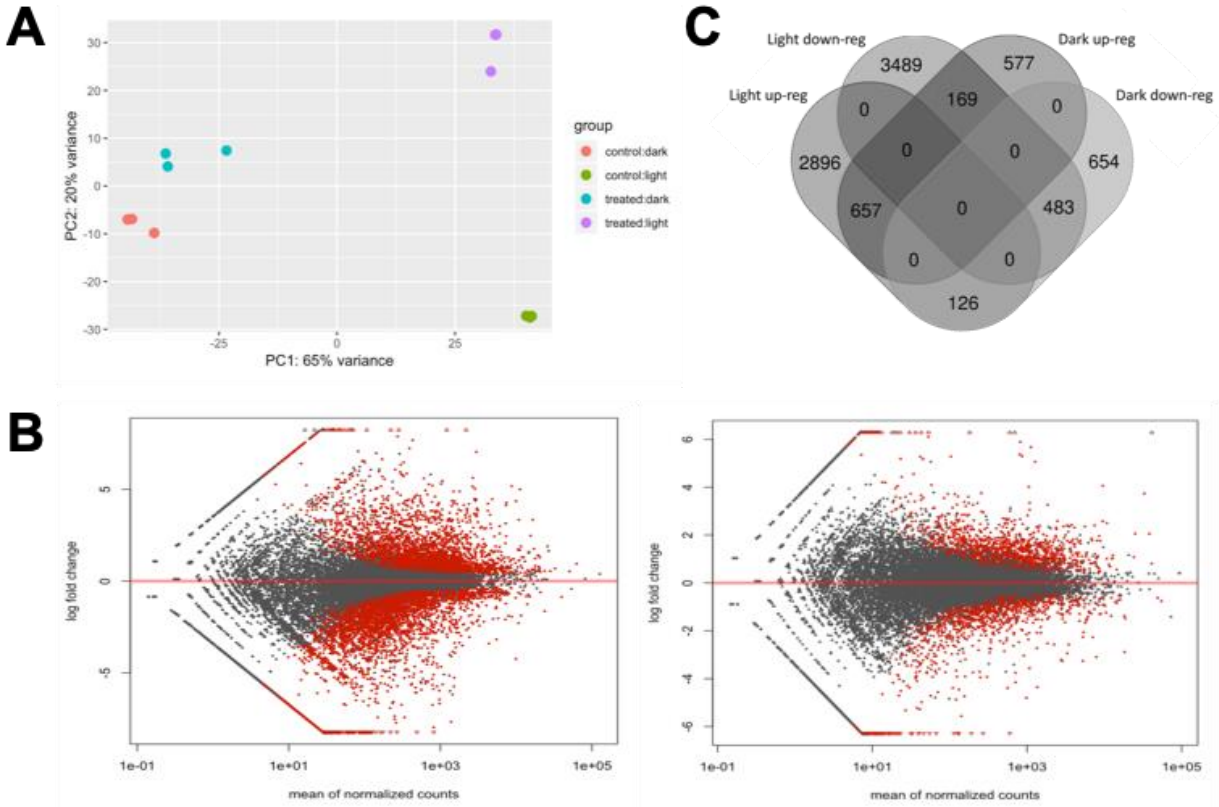

Figure 3.22. The effect of FLS on the *Arabidopsis* transcriptome. RNA was extracted from whole seedlings treated with 50 µM FLS and grown under WL (100±10µmol m^{-2} s^{-1}) or dark conditions. (A) Principal component plot displaying the relationships between 3 biological replicates in each growth condition. Control: 0 µM FLS, Treated: 50 µM FLS. (B) MA-plots displaying 7820 and 2666 significantly differentially expressed genes (DEGs) in light- and dark-grown samples, respectively ($p<0.05$ following Benjamini–Hochberg correction). Red points represent significantly differentially expressed genes (DEGs). (C) Venn diagram displaying DEGs shared between all conditions.

GO term enrichment analysis of the shared up-regulated genes (URGs) between FLS-treated and *pifq* seedlings display significant enrichment in photosynthesis-related genes, including a >40-fold enrichment in genes involved in chloroplast ribulose bisphosphate carboxylase complex and photosystem II stabilisation. Shared down-regulated genes (DRGs) included genes involved in triterpenoid metabolism, cell-junction assembly and response to various stresses (figure 3.23C).

Table 3.1. Gene ontology enrichment analysis of biological processes induced by FLS in dark-grown seedlings. This table represents the top 50 most highly enriched biological processes from 1403 significantly upregulated genes.

GO biological process	Genes in reference genome	Genes in sample	Expected genes	Fold Enrichment	P-value	False Discovery Rate
sulfate reduction (GO:0019419)	4	4	0.2	19.7	3.25E-04	7.13E-03
chloroplast ribulose bisphosphate carboxylase complex assembly (GO:0110102)	5	5	0.25	19.7	5.37E-05	1.51E-03
plastid translation (GO:0032544)	14	11	0.71	15.48	7.66E-09	4.76E-07
photosystem II stabilization (GO:0042549)	7	5	0.36	14.07	1.56E-04	3.75E-03
chloroplast rRNA processing (GO:1901259)	16	11	0.81	13.54	2.05E-08	1.16E-06
reductive pentose-phosphate cycle (GO:0019253)	15	10	0.76	13.13	1.13E-07	5.73E-06
protein import into chloroplast thylakoid membrane (GO:0045038)	6	4	0.3	13.13	9.01E-04	1.75E-02
negative regulation of photosynthesis, light reaction (GO:0043155)	14	9	0.71	12.66	6.17E-07	2.94E-05
photoinhibition (GO:0010205)	14	9	0.71	12.66	6.17E-07	2.91E-05
photosynthesis, dark reaction (GO:0019685)	16	10	0.81	12.31	1.75E-07	8.76E-06
photosystem II repair (GO:0010206)	15	9	0.76	11.82	9.44E-07	4.26E-05
xanthophyll biosynthetic process (GO:0016123)	7	4	0.36	11.26	1.36E-03	2.51E-02
regulation of photosynthesis, light reaction (GO:0042548)	25	14	1.27	11.03	1.71E-09	1.19E-07
regulation of response to oxidative stress (GO:1902882)	9	5	0.46	10.94	3.63E-04	7.87E-03
isoleucine metabolic process (GO:0006549)	9	5	0.46	10.94	3.63E-04	7.85E-03
isoleucine biosynthetic process (GO:0009097)	9	5	0.46	10.94	3.63E-04	7.82E-03
protoporphyrinogen IX biosynthetic process (GO:0006782)	11	6	0.56	10.75	9.82E-05	2.57E-03
protoporphyrinogen IX metabolic process (GO:0046501)	11	6	0.56	10.75	9.82E-05	2.55E-03
negative regulation of photosynthesis (GO:1905156)	17	9	0.86	10.43	2.07E-06	8.72E-05
regulation of generation of precursor metabolites and energy (GO:0043467)	28	14	1.42	9.85	5.23E-09	3.43E-07
carbon fixation (GO:0015977)	20	10	1.02	9.85	8.29E-07	3.80E-05
cellular response to light intensity (GO:0071484)	10	5	0.51	9.85	5.22E-04	1.07E-02
cellular response to superoxide (GO:0071451)	12	6	0.61	9.85	1.41E-04	3.49E-03
cellular response to oxygen radical (GO:0071450)	12	6	0.61	9.85	1.41E-04	3.48E-03
valine biosynthetic process (GO:0009099)	8	4	0.41	9.85	1.96E-03	3.47E-02
PSII associated light-harvesting complex II catabolic process (GO:0010304)	8	4	0.41	9.85	1.96E-03	3.46E-02
removal of superoxide radicals (GO:0019430)	12	6	0.61	9.85	1.41E-04	3.46E-03
superoxide metabolic process (GO:0006801)	13	6	0.66	9.09	1.98E-04	4.59E-03
regulation of chlorophyll biosynthetic process (GO:0010380)	18	8	0.91	8.76	2.08E-05	6.71E-04
aldehyde biosynthetic process (GO:0046184)	9	4	0.46	8.76	2.73E-03	4.65E-02
protein targeting to chloroplast (GO:0045036)	39	17	1.98	8.59	6.30E-10	4.77E-08
establishment of protein localization to chloroplast (GO:0072596)	39	17	1.98	8.59	6.30E-10	4.71E-08
photosynthesis, light harvesting (GO:0009765)	46	20	2.33	8.57	2.03E-11	1.79E-09
chlorophyll biosynthetic process (GO:0015995)	37	16	1.88	8.52	2.20E-09	1.50E-07
cellular oxidant detoxification (GO:0098869)	21	9	1.07	8.44	7.94E-06	2.90E-04
response to oxygen radical (GO:0000305)	14	6	0.71	8.44	2.71E-04	6.14E-03
response to superoxide (GO:0000303)	14	6	0.71	8.44	2.71E-04	6.12E-03
regulation of tetrapyrrole biosynthetic process (GO:1901463)	19	8	0.96	8.29	2.83E-05	8.62E-04
photosynthesis, light harvesting in photosystem I (GO:0009768)	24	10	1.22	8.21	3.03E-06	1.19E-04
protein localization to chloroplast (GO:0072598)	41	17	2.08	8.17	1.16E-09	8.35E-08
protein import into chloroplast stroma (GO:0045037)	17	7	0.86	8.11	1.01E-04	2.60E-03
photosystem II assembly (GO:0010207)	22	9	1.12	8.06	1.07E-05	3.77E-04
cellular detoxification (GO:1990748)	25	10	1.27	7.88	4.06E-06	1.56E-04
protein refolding (GO:0042026)	26	10	1.32	7.58	5.38E-06	2.02E-04
photosystem I assembly (GO:0048564)	13	5	0.66	7.58	1.32E-03	2.46E-02
maturation of LSU-rRNA from tricistronic rRNA transcript (GO:0000463)	13	5	0.66	7.58	1.32E-03	2.45E-02
regulation of tetrapyrrole metabolic process (GO:1901401)	26	10	1.32	7.58	5.38E-06	2.01E-04
protein repair (GO:0030091)	29	11	1.47	7.47	2.03E-06	8.64E-05
regulation of chlorophyll metabolic process (GO:0090056)	24	9	1.22	7.39	1.88E-05	6.16E-04
photosynthetic electron transport in photosystem I (GO:0009773)	16	6	0.81	7.39	4.81E-04	1.00E-02

Table 3.2. Gene ontology enrichment analysis of cellular component affected by FLS in dark-grown seedlings. This table represents the most highly enriched cellular component classes from 1403 significantly upregulated genes.

GO biological process	Genes in reference genome	Genes in sample	Expected genes	Fold Enrichment	P-value	False Discovery Rate
chloroplast ribulose bisphosphate carboxylase complex (GO:0009573)	3	3	0.15	19.7	2.02E-03	1.85E-02
TAT protein transport complex (GO:0033281)	3	3	0.15	19.7	2.02E-03	1.83E-02
chloroplast photosystem I (GO:0030093)	3	3	0.15	19.7	2.02E-03	1.80E-02
chloroplastic endopeptidase Clp complex (GO:0009840)	8	6	0.41	14.78	2.70E-05	3.06E-04
magnesium chelatase complex (GO:0010007)	4	3	0.2	14.78	3.40E-03	2.99E-02
photosystem I reaction center (GO:0009538)	11	7	0.56	12.54	1.20E-05	1.49E-04
ribose phosphate diphosphokinase complex (GO:0002189)	5	3	0.25	11.82	5.25E-03	4.43E-02
nascent polypeptide-associated complex (GO:0005854)	5	3	0.25	11.82	5.25E-03	4.39E-02
Stromule (GO:0010319)	35	19	1.78	10.69	3.21E-12	6.09E-11
Glyoxysome (GO:0009514)	10	5	0.51	9.85	5.22E-04	5.29E-03
plastid chromosome (GO:0009508)	18	8	0.91	8.76	2.08E-05	2.51E-04
light-harvesting complex (GO:0030076)	25	11	1.27	8.67	6.32E-07	8.62E-06
photosystem II oxygen evolving complex (GO:0009654)	23	10	1.17	8.57	2.24E-06	2.94E-05
Plastoglobule (GO:0010287)	79	32	4.01	7.98	1.02E-16	2.40E-15
chloroplast photosystem II (GO:0030095)	19	7	0.96	7.26	1.77E-04	1.88E-03
cytosolic large ribosomal subunit (GO:0022625)	147	54	7.46	7.24	1.31E-25	3.49E-24
plastid large ribosomal subunit (GO:0000311)	15	5	0.76	6.57	2.20E-03	1.95E-02
chloroplast thylakoid lumen (GO:0009543)	81	27	4.11	6.57	1.10E-12	2.17E-11
cytosolic small ribosomal subunit (GO:0022627)	108	35	5.48	6.38	1.03E-15	2.28E-14
chloroplast nucleoid (GO:0042644)	20	6	1.02	5.91	1.26E-03	1.18E-02
organellar small ribosomal subunit (GO:0000314)	27	7	1.37	5.11	1.03E-03	9.80E-03
chloroplast inner membrane (GO:0009706)	80	19	4.06	4.68	2.35E-07	3.34E-06
Preribosome (GO:0030684)	84	14	4.26	3.28	2.58E-04	2.69E-03
Apoplast (GO:0048046)	452	74	22.94	3.23	1.42E-16	3.29E-15
mitochondrial ribosome (GO:0005761)	56	9	2.84	3.17	3.90E-03	3.37E-02
Nucleolus (GO:0005730)	453	62	22.99	2.7	4.70E-11	8.48E-10
cell wall (GO:0005618)	773	82	39.24	2.09	3.39E-09	5.64E-08
Plasmodesma (GO:0009506)	1006	100	51.06	1.96	1.81E-09	3.10E-08
vacuolar membrane (GO:0005774)	637	60	32.33	1.86	1.52E-05	1.85E-04
mitochondrial envelope (GO:0005740)	395	34	20.05	1.7	4.43E-03	3.80E-02

Table 3.3. Experimental treatments for transcriptomic data set comparisons. Details of experimental set-up and analysis of data used to compare to FLS-treated RNAseq data.

	Accession No.	Geno-type	Organism Part	Seedling Age	Light condition	Temp.	Treatment	Reference
6 h WL	**GSE60835**	Col-0	Whole plant	4 days	Continuous dark	-	4 days dark, 6 h WL	(Dong et al., 2014)
pifq	**GSE60835**	Col-0	Whole plant	4 days	Continuous dark	-	4 days dark	(Dong et al., 2014)
det1-1	**GSE60835**	Col-0	Whole plant	4 days	Continuous dark	-	4 days dark	(Dong et al., 2014)
Dicamba	**GSE24052**	Col-0	Whole plant	4 days	16:8 L:D	22oC	7mM Dicamba 40 mins	(Gleason et al., 2011b)
IAA	**E-MEXP-1256**	Col-0	Whole plant	7 days	16:8 L:D	23oC	20µM IAA 120 mins	(Lee et al., 2009)
***axr3-1* -IAA**	**GSE630**	*axr3-1*	Whole plant	7 days	16:8 L:D	22oC	0µM IAA 120 mins	(Okushima et al., 2005)
***axr3-1* +IAA**	**GSE630**	*axr3-1*	Whole plant	7 days	16:8 L:D	22oC	5µM IAA 120 mins	(Okushima et al., 2005)
4-thiazolidione	**GSE1491**	Col-0	Whole plant	7 days	16:8 L:D	25oC	10µM 4-thiazolidione 60 mins	(Armstrong et al., 2004)
Furyl acrylate	**GSE1491**	Col-0	Whole plant	7 days	16:8 L:D	25oC	10µM Furyl acrylate 60 mins	(Armstrong et al., 2004)
ga3-1	**GSE26848**	*ga3-1*	Shoots	18 days	16:8 L:D	18-23oC	18 days light	(Archacki et al., 2013)
Uniconazole-P	**GSE11852**	Col-0	Whole plant	40.8-43.2 hours	Continuous light	-	10nM uniconazole-P	(Zhang et al., 2008)
Brassinolide	**GSE862**	Col-0	Whole plant	9 days	Continuous light	-	1µM brassinolide 150 mins	(Nemhauser et al., 2004)
bri1-5	**GSE46456**	*bri1-5*	Whole plant	7 days	Continuous RL	-	7 days RL	-
Jasmonate	**E-MEXP-883**	Col-0	Whole plant	4 weeks	16:8 L:D	20:24oC	0.1µM MeJA 6 hours	(Dombrecht et al., 2007)
ABA	**GSE65016**	Col-0	Whole plant	12 days	16:8 L:D	22oC	50µM ABA 6 hours	(Kim et al., 2019)
Cytokinin	**GSE102713**	Col-0	Whole plant	10 days	Continuous light	22oC	5µM N-benzyladenine 120 mins	(Shanks et al., 2018)
Norflurazon	**GSE12887**	Col-0	Whole plant	5 days	Continuous light	-	5µM norflurazon	(Koussevitzky et al., 2007)
100m NaCl	**GSE16765**	Col-0	Leaves	20 days	10:14 L:D	23:18oC	100mM NaCl 6 days	(Chan et al., 2011)
140mM NaCl	**GDS3216**	Col-0	Root	6 days	Continuous light	-	140mM NaCl 32 hours	(Dinneny et al., 2008)
PPN 14 days	**GSE37553**	Col-0	Root cells	14 days	Continuous light	-	M. incognita infection 14 days	-
PPN 21 days	**GSE37553**	Col-0	Root cells	21 days	Continuous light	-	M. incognita infection 21 days	-
Cold	**E-TABM-52**	Col-0	Rosette	14 days	16:8 L:D	4oC	14 days 4oC	(Hannah et al., 2006)
2 h drought	**E-MEXP-2435**	Col-0	Whole plant	7 days	16:8 L:D	22oC	2 h drought stress	(Abdeen et al., 2010)
24 h drought	**E-MEXP-2435**	Col-0	Whole plant	8 days	16:8 L:D	22oC	24 h drought stress	(Abdeen et al., 2010)
96 h drought	**E-GEOD-35258**	Col-0	Whole plant	11 days	Continuous light	25oC	96 h low water potential	(Bhaskara et al., 2012)

A

DRG		50µM FLS
	DRG no	819
6hr WL	1158	133
pifq	369	70
det1-1	1973	299

URG		50µM FLS
	URG no	978
6hr WL	1276	309
pifq	532	150
det1-1	3921	612

B

	50uM FLS
6hr WL	3.2
pifq	5.3
det1-1	4.3

	50uM FLS
6hr WL	5.7
pifq	6.6
det1-1	3.7

C

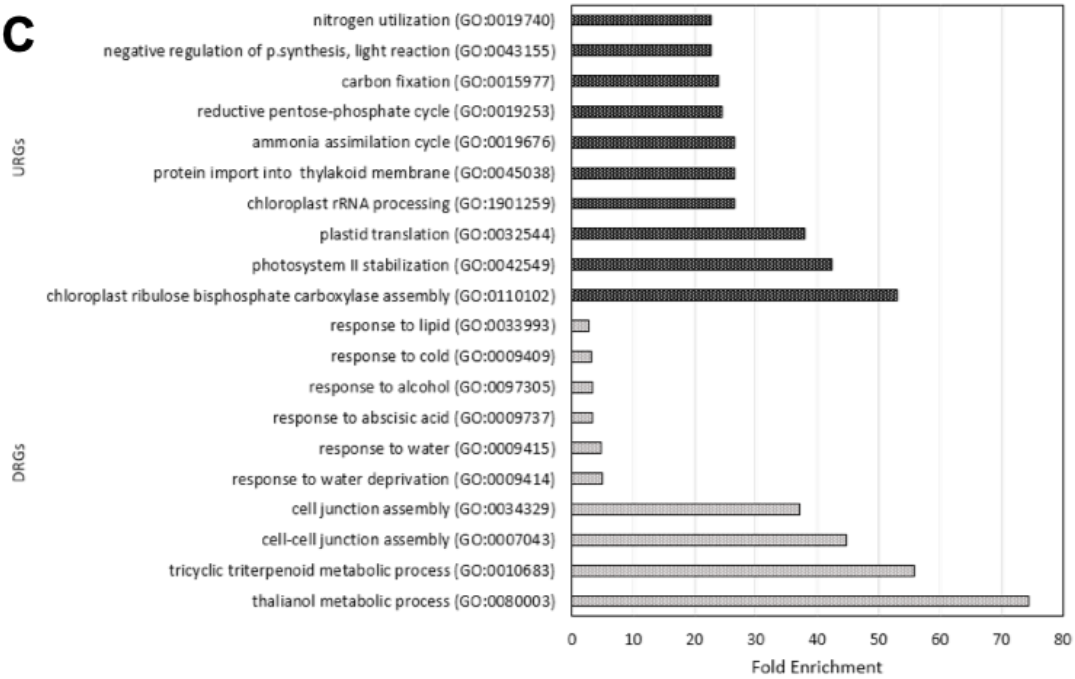

Figure 3.23. Comparison between transcripts down- and up-regulated by FLS from dark-grown samples and other data sets from mutations or treatments resulting in a de-etiolated phenotype. (A) Number of genes overlapping between data sets tested. A log fold change cut-off 1 was applied to define differently regulated genes. (B) Significance of the overlap between FLS treatment and indicated data set. Numbers represent ratios between the number of overlapping genes and the number of genes that would be expected by chance and are additionally depicted in a colour scale. Green indicates low overlap, red indicates high overlap. (C) Top 10 highly enriched GO terms from up- and down-regulated genes (URG and DRGs) shared between dark-grown FLS-regulated genes and gene expression changes in dark-grown *pifq* seedlings.

GO term enrichment analysis on significantly downregulated DEGs in both light- and dark-grown samples displayed an increased frequency of auxin related biological processes when comparing all explicit hormone classes (table 3.4). In light-grown samples, out of 86 enriched classes, from 4141 significantly downregulated genes, 9 classes were explicitly hormone-related from which the majority included auxin-related classes such as auxin efflux and auxin activated signalling pathway. Similarly, in dark-grown samples, out of 24 enriched classes, from 1263 significantly down regulated genes, 7 classes were explicitly hormone-related with 5 of these directly associated with auxin (table 3.4).

Data set comparisons on available microarray data also indicated similarities in the DEGs between light-grown FLS-treated samples and studies applying auxin-related compounds. In comparison, other biotic and abiotic treatments displayed lower levels of similarity (figure 3.24A & B). Interestingly, inhibitors of auxin transcription 4-thiazolidione and furyl acrylate ester, had high DEG similarity in the DEGs to FLS treatment in the light; however, GO term analysis of the shared DEGs did not indicate enrichment in auxin classes (figure 3.24C).

Table 3.4. Hormone-related biological processes enriched following FLS treatment in light- and dark- grown samples. Genes regulated in response to FLS were analysed by GO term enrichment and filtered to display hormone-related biological processes in both up- and down-regulated DEGs from light- and dark-grown FLS-treated samples.

Light/ Dark grown	Up/down regulated DEGs	GO biological process	Genes in reference genome	Genes in sample	Expected genes	Fold Enrichment	P-value	False Discovery Rate
Light	Up	cellular response to SA stimulus (GO:0071446)	49	17	6.45	2.64	1.44E-03	2.50E-02
Light	Up	response to salicylic acid (GO:0009751)	203	70	26.71	2.62	1.21E-10	1.01E-08
Light	Up	response to abscisic acid (GO:0009737)	572	148	75.25	1.97	3.41E-12	3.73E-10
Light	Up	response to jasmonic acid (GO:0009753)	214	53	28.15	1.88	1.05E-04	2.70E-03
Light	Up	response to hormone (GO:0009725)	1720	380	226.27	1.68	2.04E-19	5.02E-17
Light	Up	cellular response to ABA stimulus (GO:0071215)	242	52	31.84	1.63	2.39E-03	3.71E-02
Light	Up	cellular response to hormone stimulus (GO:0032870)	860	157	113.14	1.39	2.24E-04	5.20E-03
Light	Down	auxin efflux (GO:0010315)	13	9	1.93	4.67	1.01E-03	1.93E-02
Light	Down	hormone transport (GO:0009914)	91	30	13.5	2.22	3.40E-04	7.84E-03
Light	Down	auxin polar transport (GO:0009926)	78	25	11.57	2.16	1.66E-03	2.81E-02
Light	Down	cellular response to auxin stimulus (GO:0071365)	183	57	27.14	2.1	4.11E-06	1.62E-04
Light	Down	auxin transport (GO:0060918)	87	27	12.9	2.09	1.75E-03	2.94E-02
Light	Down	auxin-activated signaling pathway (GO:0009734)	164	50	24.32	2.06	3.33E-05	1.03E-03
Light	Down	regulation of hormone levels (GO:0010817)	409	107	60.66	1.76	5.74E-07	2.93E-05
Light	Down	response to auxin (GO:0009733)	401	103	59.47	1.73	2.34E-06	9.81E-05
Light	Down	hormone metabolic process (GO:0042445)	259	60	38.41	1.56	2.46E-03	3.75E-02
Dark	Up	response to cytokinin (GO:0009735)	253	61	12.84	4.75	8.62E-21	1.89E-18
Dark	Up	salicylic acid metabolic process (GO:0009696)	30	7	1.52	4.6	1.74E-03	3.13E-02
Dark	Up	response to hormone (GO:0009725)	1720	160	87.31	1.83	2.09E-12	2.10E-10
Dark	Up	response to abscisic acid (GO:0009737)	572	49	29.03	1.69	8.46E-04	1.66E-02
Dark	Down	auxin polar transport (GO:0009926)	78	12	3.52	3.41	4.83E-04	2.62E-02
Dark	Down	hormone transport (GO:0009914)	91	14	4.1	3.41	1.69E-04	1.20E-02
Dark	Down	auxin transport (GO:0060918)	87	13	3.92	3.31	3.67E-04	2.17E-02
Dark	Down	cellular response to auxin stimulus (GO:0071365)	183	22	8.25	2.67	8.31E-05	6.30E-03
Dark	Down	auxin-activated signaling pathway (GO:0009734)	164	19	7.39	2.57	3.76E-04	2.16E-02
Dark	Down	response to abscisic acid (GO:0009737)	572	55	25.79	2.13	7.27E-07	1.23E-04
Dark	Down	response to auxin (GO:0009733)	401	38	18.08	2.1	6.95E-05	5.55E-03

A

DRG		50µM FLS
	DRG no	3239
Diacamba	844	395
IAA	40	21
axr3-1 -IAA	223	106
axr3-1 +IAA	172	75
4-thiazolidione	173	49
Furyl acrylate	14	7
ga3-1	288	69
Uniconazole-P	105	16
Brassinolide	7	0
bri1-5	122	54
Jasmonate	10	1
ABA	816	239
Cytokinin	31	9
Norflurazon	1551	283
100m NaCl	899	200
140mM NaCl	777	123
PPN 14 days	1899	540
PPN 21 days	1596	431
Cold	664	140
2hr drought	161	45
24hr drought	496	139
96hr drought	1085	215

URG		50µM FLS
	URG no	2186
Diacamba	1013	382
IAA	131	13
axr3-1 -IAA	218	44
axr3-1 +IAA	165	50
4-thiazolidione	322	142
Furyl acrylate	429	183
ga3-1	175	45
Uniconazole-P	205	14
Brassinolide	16	0
bri1-5	282	23
Jasmonate	201	39
ABA	1291	276
Cytokinin	218	16
Norflurazon	1032	250
100m NaCl	1642	296
140mM NaCl	825	133
PPN 14 days	1186	98
PPN 21 days	1116	105
Cold	438	128
2hr drought	599	227
24hr drought	757	237
96hr drought	954	167

B

	50µM FLS		50µM FLS
Diacamba	3.4	Diacamba	4.1
IAA	3.8	IAA	1.1
axr3-1 -IAA	3.5	*axr3-1* -IAA	2.2
axr3-1 +IAA	3.2	*axr3-1* +IAA	3.3
4-thiazolidione	2.1	4-thiazolidione	4.8
Furyl acrylate	3.7	Furyl acrylate	4.6
ga3-1	1.7	*ga3-1*	2.8
Uniconazole-P	1.1	Uniconazole-P	0.7
Brassinolide	0.0	Brassinolide	0.0
bri1-5	3.2	*bri1-5*	0.9
Jasmonate	0.7	Jasmonate	2.1
ABA	2.1	ABA	2.3
Cytokinin	2.1	Cytokinin	0.8
Norflurazon	1.3	Norflurazon	2.6
100m NaCl	1.6	100m NaCl	2.0
140mM NaCl	1.2	140mM NaCl	1.7
PPN 14 days	2.1	PPN 14 days	0.9
PPN 21 days	2.0	PPN 21 days	1.0
Cold	1.5	Cold	3.2
2hr drought	2.0	2hr drought	4.1
24hr drought	2.0	24hr drought	3.4
96hr drought	1.4	96hr drought	1.9

C

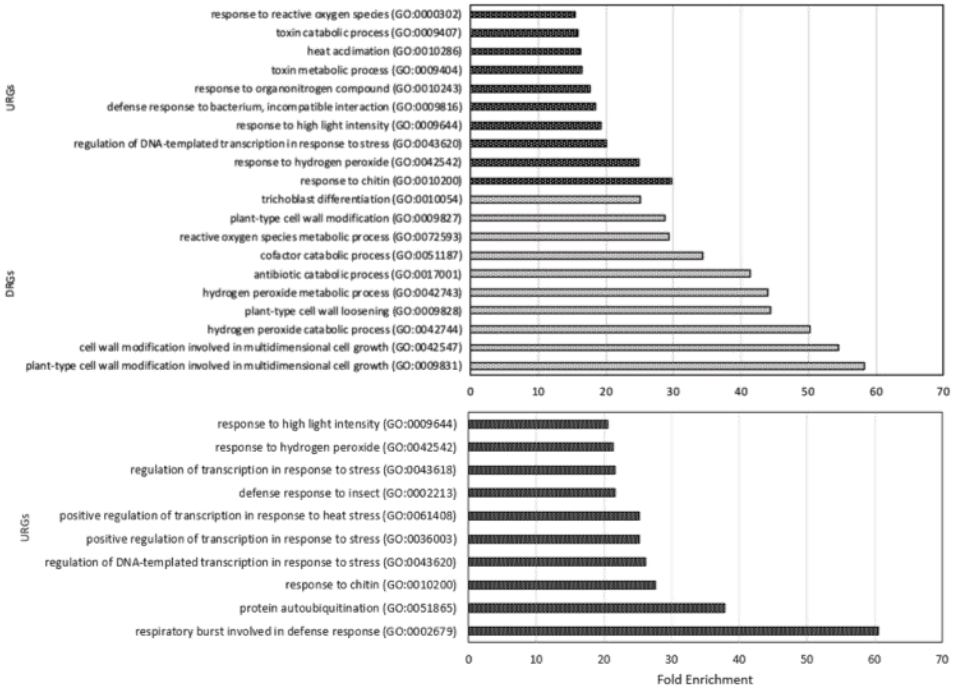

Figure 3.24. Comparison between transcripts down- and up-regulated by FLS from light-grown samples and other studies. (A) Number of genes overlapping between data sets tested. A log fold change cut-off 1 was applied to define differently regulated genes. (B) Significance of the overlap between FLS treatment and indicated data set. Numbers represent ratios between the number of overlapping genes and the number of genes that would be expected by chance and are additionally depicted in a colour scale. Green-red indicating low-high similarity. (C) Top 10 highly enriched GO terms from up- and down-regulated genes (URG and DRGs) shared between light-grown FLS treated samples and samples treated with 4-thiazolidione appended with derivatized acetic acid (top) and furyl acrylate ester of thiadazole heterocycle (bottom).

3.2.10 Endogenous phytohormone quantification

The results to date indicate that the primary effect of FLS might be to inhibit the auxin response. To determine whether the effect was on auxin biosynthesis we determined the effect of FLS on the levels of various endogenous auxins by sending samples for hormone quantification. We also took the opportunity to determine the impact of FLS on other hormones. Light- and dark-grown FLS-treated samples were subject to liquid chromatography mass spectrometry (LC/MS) analysis to determine endogenous hormone levels within seedlings. It was shown, that FLS treatment in the light had a more significant effect on phytohormone levels than in the dark. Focusing on IAA and IAA-Asp conjugate levels, in the light, endogenous IAA was reduced by 54% (figure 3.25A), while there was no difference in the dark. Additionally, the IAA-Asp conjugate was unaffected by FLS treatment in light and dark. Looking at other endogenous hormones, it was shown JA and DHZ levels increased by 1031% and 192% (figure 3.25D&J) in the light, respectively; however, in the dark, JA levels were reduced by 50% (figure 3.25D), demonstrating FLS has light-dependent effects on endogenous hormone signalling.

Looking into the effect of light on endogenous hormones, the data indicates a number of phytohormone levels were higher in un-treated, light-grown samples. IAA, OPDA and SA levels were largely decreased in dark-grown samples by 70%, 99% and 88%, respectively (figure 3.25A,C&G), whilst JA and ABA displayed an increase in the dark by 166% and 83%, respectively (figure 3.25D&F). A number of hormones and/or related conjugates displayed no notable changes in light- and FLS-treatment, particularly the cytokinins tZR, cZ and the auxin conjugate IAA-Asp.

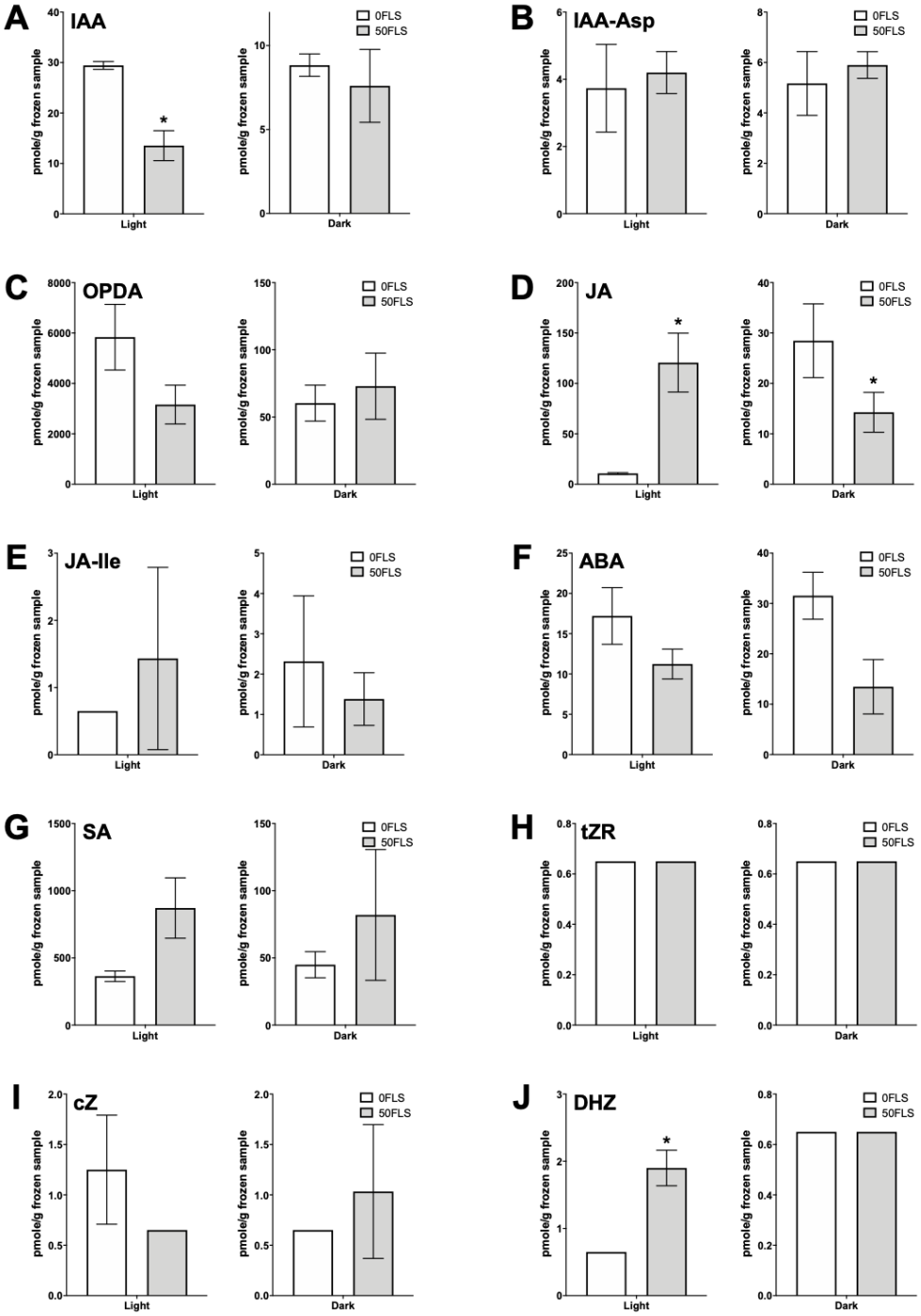

Figure 3.25. Effect of FLS on endogenous phytohormones. Phytohormones (A) Indole-3-acetic acid (IAA), (B) IAA-Asp amide conjugate, (C) 12-oxophytodienoic acid (OPDA), (D) Jasmonic Acid (JA), (E) jasmonoyl isoleucine conjugate (JA-Ile), (F) Abscisic acid (ABA), (G) Salicylic acid (SA) and active cytokinins (H) trans-zeatin riboside (tZR), (I) cis-zeatin (cZ), (J) dihydrozeatin (DHZ) and trans-zeatin (tZ) were quantified using liquid chromatography mass spectrometry analysis (LC/MS) from plant tissue treated +/- 50 µM FLS for 7 days in continuous WL or for 5 days dark. Quantification was based upon comparison with internal standards. tZ levels were too low to be detected in any samples and samples with low (<1.3 pmole/g) were plotted with the value of 0.65. Data represents mean ± SEM of 3 biological replicates; asterisks denote significant difference ($p<0.05$) between FLS treated and untreated samples in paired t-test.

3.3 Discussion

3.3.1 FLS has a unique profile of effects under different growth conditions

FLS application via foliar spray has resulted in mild phytotoxicity toward tomato and eggplants during field trials (Morris et al., 2016) and preliminary studies have demonstrated a reduction in fresh weight and root length in *Arabidopsis* seedlings when FLS was applied to the media. Characterising the effects of FLS on plant growth may, not only help to elucidate this chemical's mode of action, but also provide information on how best to protect crop plants grown in FLS-treated soil.

When applied exogenously, FLS induced a reduction in fresh weight and chlorophyll content of seedlings when grown under white, red and blue light (WL, RL and BL). Overall growth was affected more under RL and BL, compared to WL; this was expected as plant growth is relatively poor in these conditions compared to WL. At field relevant concentrations of <5µM FLS it was shown that *Arabidopsis* seedlings were not negatively affected by FLS. This is in contrast to its effects on the PPN *Globodera pallida*; in *G. pallida* as little as 1µM FLS is sufficient to inhibit hatching from the cyst (Feist et al., 2020) suggesting FLS remains more efficacious to its target, PPNs. When studying the recovery of FLS exposure, seedlings were able to continue growth at a similar rate to control seedlings after exposure to concentrations lower than 20µM FLS. 20µM FLS exposure caused a partially reversible inhibition of growth, while 50 and 200µM FLS irreversibly inhibited growth. A similar pattern of recovery is observed in PPN populations; cysts previously treated with very low concentrations (< 5µM FLS) began hatching after 7 days in solution omitting FLS with the total cumulative hatch of 65% compared to the control of 78%. Following 50µM FLS exposure, hatching from cysts only began 12 days after transfer off FLS and total hatch only reached 40% at the end of the testing period; 500µM FLS-treated cysts showed no recovery (Feist et al., 2020). Comparing the recovery between *Arabidopsis* and *G. pallida* it is noted that, when FLS is present, PPNs are susceptible to very low doses compared to *Arabidopsis;* however, both models display robust recovery at low concentrations and an irreversible inhibition of development at high doses.

PPNs remain more susceptible to FLS following initiation of growth in the absence of FLS. In a similar experimental set up to the post-germination treatment, hatching of *G. pallida* juveniles was initiated and after 16 days, eggs were exposed to increasing concentrations of FLS (Feist et al., 2020). At concentrations of <1 µM hatching was significantly inhibited, although this inhibition was not seen in cysts. Comparatively, exposing *Arabidopsis* seedlings to FLS after germination resulted in a dichotomy; at low concentrations, FLS transiently increased the growth of seedlings, while a rapid inhibition of growth was observed at high concentrations. This effect was seen even in established seedlings suggesting FLS could be acting as a growth enhancer at low concentrations.

The transient enhancement in growth coupled with the phytotoxicity following long term exposure to FLS indicates FLS could be promoting an uncontrolled growth pattern within seedlings. Synthetic auxins such as 2,4-D and 1-NAA act as selective herbicides through a similar mode of action; providing dicot weed control in cereal crops (Grossmann, 2003). 2,4-D was one of the first synthetic auxin herbicides to be commonly used and due to its selectivity to dicots and stability compared to IAA (Ljung et al., 2002) over 600 2,4-D based products are currently on the market (Song, 2014). The effects of auxinic herbicides are similar to that induced by high doses of the natural auxin, IAA; at low doses plant growth is promoted but at high doses excessive and unsustainable growth occurs subsequently causing plant death. Characteristics of auxinic herbicide induced death include upregulation of ABA and ethylene biosynthesis genes, reactive oxygen species (ROS) production, disruption of chloroplasts and tissue necrosis (Grossmann, 2003). ROS production following 2,4-D application promotes excessive cell expansion and tissue proliferation and is thought to be the main toxic effect of this herbicide. Interestingly, the phenotype observed in FLS-treated seedlings in a greening assay is also indicative of excessive ROS production potentially suggesting a conserved mode of action.

3.3.2 FLS induces de-etiolation that is partially mediated by HY5 and HYH

Information on the impact of FLS on dark-grown seedlings is beneficial as crop seeds may be planted into soil with FLS, and therefore their initial growth period until they emerge from the soil would be in the dark. This initial period of growth is extremely important for

plants as the nutrients within the seed are only able to support growth for a short period of time and most of the nutrients are invested in hypocotyl elongation and maintenance of the apical hook. When the seedling reaches light, the growth pattern changes to inhibit hypocotyl elongation, expand cotyledons and elongate the primary root (Kircher & Schopfer, 2012).

When applied exogenously, FLS induced a de-etiolated phenotype in the dark, including the inhibition of hypocotyl elongation, promotion of cotyledon expansion and accumulation of protochlorophyllide (Pchlide). Pchlide is the penultimate step in chlorophyll biosynthesis and its conversion to chlorophyllide (Chlide) requires the light-activated enzyme protochlorophyllide oxidoreductase (POR). POR catalyses transfer of a hydride from NADPH to position C17 on Pchlide, followed by proton transfer from a conserved Tyr residue to position C18 (Heyes et al., 2011) to synthesise Chlide. Under normal conditions in the dark, chlorophyll biosynthesis is halted and Pchlide synthesised is bound to POR proteins to avoid ROS production. This means when the seedling is exposed to light all molecules of Pchlide can bind to POR proteins and NADPH to form Chlide. However, if Pchlide is in excess, not all can bind to the limited POR proteins and the unbound Pchlide results in cell death through the production of singlet oxygen ($^1O_2$) (Triantaphylidès et al., 2008). There are no enzymatic means to detoxify $^1O_2$ so when the seedling is transferred into light, cell death occurs and growth is inhibited.

FLU acts as a negative regulator of chlorophyll biosynthesis through the inhibition of glutamyl-tRNA reductase and the fluorescence (*flu*) mutant, generated in an EMS mutant screen, is not able to restrict Pchlide accumulation in the dark, causing bleaching upon exposure to WL (Meskauskiene et al., 2001). Feeding the tetrapyrrole precursor ALA also causes a similar accumulation of Pchlide and bleaching when transferred to light due to a $^1O_2$ burst (McCormac and Terry, 2002a; McCormac and Terry, 2004; Page et al., 2017). Interestingly, in the greening experiment conducted with FLS, bleaching also occurred. Untreated seedlings were able to accumulate chlorophyll after 5d growth in the dark and 24h in WL; whereas, FLS-treated seedlings did not display any indication of chlorophyll accumulation suggesting a $^1O_2$ burst similar to the *flu* mutant/ALA feeding as a result of Pchlide accumulation. Although a similar result was observed, the *flu* mutant and ALA

feeding do not display a phenotype similar to FLS in the dark or light; the mutant and ALA-fed seedlings grow as normal under continuous WL and do not display de-etiolation in the dark (Meskauskiene et al., 2001).

The accumulation of Pchlide coupled with a de-etiolated phenotype following FLS treatment suggest its synthesis is increased and FLS is inducing photomorphogenesis in the dark. The initial step of Pchlide synthesis involves glutamate in the form of glutamyl-tRNA (Glu) which is reduced to glutamate-1-semialdehyde (Schön et al., 1986) by glutamyl-tRNA reductase and glutamate-1-semialdehyde-2,1-aminomutase, encoded by the *HEMA1* and *GSA* genes, respectively. An amino group from C2 of glutamate-1-semialdehyde is then transferred to a neighbour carbon to synthesise ALA (Smith et al., 1991). ALA is then converted through a sequence of reactions to protoporphyrin IX which marks the branch point between heme or chlorophyll synthesis. In the first step of the chlorophyll synthesis path, a Mg^{2+} ion is inserted into the backbone of protoporphyrin IX by Mg chelatase (MgCh); an enzymatic complex consisting of CHLH, CHLI and CHLD (Jensen et al., 1999), to give Mg-protoporphyrin IX. The last step to Pchlide is then the transfer of a methyl group to a carboxyl group on Mg-protoporphyrin IX to create a Mg-protoporphyrin IX monomethyl ester, on which oxygen is incorporated to form Pchlide (Tanaka, 2007), reviewed in (Mochizuki et al., 2010).

Following FLS treatment in the dark the expression of two key genes, *HEMA1* and *CHLH*, are increased significantly; which, coupled with the Pchlide accumulation measured under FLS treatment, demonstrates FLS is able to induce this pathway to a higher extent than usual in the dark. These genes are also induced in *pifq* mutants, which display a similar phenotype (Stephenson et al., 2009). Expression levels of these genes are relatively low in the dark so as not to over accumulate the photosensitiser intermediate, Pchlide; however, upon FLS treatment the increase in the expression of these genes would suggest FLS is inducing a light-response in seedlings, independent of light. FLS also induces a large increase in the expression of the light-harvesting chlorophyll a/b-binding (LHCB) gene *LHCB1.2* which is, classically and most strongly, induced by light. LHCB proteins are associated with chlorophyll to create the antennae complex that absorbs light and transfers the energy to photosystem II and has a role in protecting against

photo-oxidative damage (Dall'Osto et al., 2015). In addition, *PORA* gene expression is not altered following FLS treatment in the dark. *PORA* expression is high in etiolated seedlings as it has a role in maintaining the crystalline structure of the prolamellar body (PLB) in etioplasts before their light-induced conversion to photosynthetically active chloroplasts (Sperling et al., 1997); however, upon exposure to light *PORA* expression and proteins levels are rapidly decreased due to proteolysis of the enzyme in the absence of Pchlide (Kay and Griffiths, 1983). Due to FLS treatment not affecting *PORA* expression in the dark, this assumes FLS action is not to reduce POR levels to induce toxicity; although, protein levels have not been investigated.

In conclusion, FLS induces phytotoxic effect on *Arabidopsis* seedling growth in the light; but, in the dark, FLS induces de-etiolation. This de-etiolation was characterised by an induction in Pchlide, coupled with inhibition of hypocotyl elongation, cotyledon opening and expression of classically light-regulated genes. Shared de-etiolated phenotypes such as increased Pchlide, short hypocotyls and expanded cotyledons are observed in a number of light-signalling mutants, including *pif* mutants (Stephenson et al., 2009), *cop* mutants (Deng et al., 1991) and *det1* (Pepper et al., 1994). Observing such a large increase in *LHCB* gene expression under FLS treatment, alongside an increase in *HEMA1, CHLH* and Pchlide suggests FLS could be acting to induce photomorphogenesis via inhibition of a negative regulator, like COP1. As mentioned previously, COP1 is an E3 ubiquitin ligase that targets HY5 for degradation to prevent photomorphogenic growth and the *cop1* mutant displays a similar phenotype to FLS in the dark, with an increase in Pchlide (Sperling et al., 1998), inhibition of hypocotyl elongation and expanded cotyledons (Deng et al., 1991). On the other hand, the photomorphogenic growth promoting proteins such as HY5 could be stabilised by FLS meaning an active COP1 protein is unable to ubiquitinate its target for degradation and the pool of these positive regulators is not diminished, allowing light-regulated growth to be induced. De-etiolation in the dark is also seen in a number of mutants that are deficient or insensitive to phytohormones (Alabadí et al., 2004; Barrero et al., 2008; Choe et al., 1998; Chory et al., 1991; Hsieh & Okamoto, 2014; Nagpal et al., 2000; Sinclair et al., 2017; Sineshchekov et al., 2004; Spíchal et al., 2004; Szekeres et al., 1996; Vogel et al., 1998) suggesting FLS

could be interfering with hormone biosynthesis or signalling pathways to induce this phenotype in the dark.

In lieu of the fact that FLS induced a de-etiolated phenotype in the dark and increased the expression of a number of light regulated genes, the first question raised was to ask if FLS-mediated de-etiolation is caused by modulation of the light signalling pathway. HY5 and HYH bZIP transcription factors are positive regulators of light signalling as they are able to induce the expression of light-regulated genes when seedlings are exposed to light (Lee et al., 2007; Zhang et al., 2011). These genes indicate the start of photomorphogenic growth and the seedling can begin to synthesise chlorophylls and expand the cotyledons for light capture. However, in the dark, the COP9 signalosome mediates the degradation of proteins targeted by the E3 ubiquitin ligase, COP1. COP1 localises in the nucleus, and targets HY5 and HYH proteins for degradation via the 26s proteasome; ultimately inhibiting the subsequent expression of light-inducible genes and photomorphogenesis (Yi and Deng, 2005). The HY5 and HYH proteins are essential in photomorphogenesis, with their expression being induced following light treatment (Zhang et al., 2017); therefore, the loss-of-function double mutant has a reduced response to light and displays an elongated hypocotyl phenotype in the light (Holm et al., 2002). As FLS was able to 'bypass' the requirement for light and cause de-etiolation in the dark, the double *hy5 hyh* mutant was treated with FLS to determine if FLS-mediated de-etiolation required these transcription factors. The double mutant had a reduced response to FLS, suggesting FLS-induced de-etiolation was not fully mediated by these proteins, but they still had a role as the response was reduced in comparison to WT. HY5 and HYH are major integration points that allow external and internal signals to be integrated into the light signalling pathway (Chen et al., 2013; Cluis et al., 2004; Job & Datta, 2020); therefore, as a partial resistance was displayed in the double mutant this could suggest FLS is targeting a protein or gene upstream of HY5 and HYH in a parallel path.

It has been proposed that HY5 and HYH are able to act as signal integration points between light and hormone signalling networks to modulate growth in response to phytohormones (Cluis et al., 2004). In a *hy5* mutant the elongated hypocotyl, accelerated

root growth and anthocyanin accumulation are, in part, explained by altered hormone signalling. This mutant also displays reduced *IAA7* and *IAA14* gene expression, two negative regulators of auxin signalling, suggesting auxin signalling is elevated in these mutants. This alteration of auxin responsive genes indicates the presence of HY5 binding sites in their promotors (Cluis et al., 2004). Additionally, the control of both light and auxin signalling requires E3-mediated protein degradation. The COP9 signalosome requires the activity of the E3 ubiquitin ligase, COP1, to degrade HY5 and HYH; however, it has also been shown to be required by the SCF-type E3, SCF^{TIR1} to initiate auxin responses and the degradation of SCF^{TIR1} substrates (Schwechheimer et al., 2001). Reduced responses to auxin, jasmonic acid, and cold stress are also shared in mutants with reduced function in the COP9 signalosome and mutants with reduced SCF-type E3 activity, suggesting the COP9 signalosome has a role in a number of SCF mediated processes. Lastly, AXR1 regulates SCF^{TIR1} and the *axr1* mutant displayed a requirement for this protein in COP9 signalosome mediated repression of photomorphogenesis (Schwechheimer et al., 2002). Therefore, this suggests that the light signalling pathway can regulate and is regulated by hormone pathways, in particular auxin signalling.

In a further effort to understand how FLS is inducing de-etiolation, *pifq* seedlings were treated with FLS. PIF (phytochrome interacting factor) proteins are BHLH transcription factors that negatively regulate photomorphogenesis (Leivar and Quail, 2011). The phytochrome family of photoreceptors responds to the R/FR light spectrum (Bae and Choi, 2008) and upon exposure to RL phytochromes translocate to the nucleus and promote the turnover of PIFs through ubiquitination and subsequent proteasome-mediated degradation. This leads to a de-etiolated phenotype in the dark characterized by inhibition of hypocotyl elongation, cotyledon opening and expression of light-inducible genes (Huq and Quail, 2002; Shin et al., 2009; Stephenson et al., 2009; Leivar et al., 2009); a phenotype similar to FLS treatment. Using the quadruple *pifq* mutant, it was shown FLS effects in the dark were independent of the presence of PIF proteins and, therefore, that the effect on Pchlide was not via this signaling pathway. However, transcriptomic analysis revealed significant crossover of differentially expressed genes (DEGs) in both FLS treated and *pifq* seedlings. It is established in microarray analysis and RNAseq studies that the *pifq* mutant in the dark has a gene expression pattern similar to that of a red-light grown

WT (Shin et al., 2009; Dong et al., 2014). When comparing the genes induced in *pifq* mutants to that induced by FLS treatment it demonstrated a large proportion of both up- and down-regulated DEGs were shared between data sets; in particular genes involved in plastid translation and photosystem assembly. This can be explained as it is likely both FLS induced DEGs and *pifq* DEGs are a result of downstream changes in HY5 regulated genes. However, as indicated previously, *hy5/hyh* mutants are only partially resistant and FLS is additive in a *pifq* mutant; therefore, FLS must be acting in a pathway upstream of these key light signaling regulators.

3.3.3 Reversal of FLS induced de-etiolation is auxin specific

It is not only mutations in negative regulators of light-signalling that cause de-etiolation in the dark. Mutations in hormone biosynthesis and/or signalling mediate de-etiolation. While perception of light is well understood, downstream transduction and how light mediates certain phenotypic changes is not clear, however, almost every plant hormone has been implicated.

When a young shoot reaches the soil surface and is exposed to light there is a reduction in the bioactive GA, GA_1 (Ait-Ali et al., 1999) which causes a reduction in shoot elongation. In pea, the reduction in GA_1 occurs as the *LE* (encoding $PsGA_{3ox1}$) gene that controls the conversion of GA_{20} to GA_1 is downregulated, while $PsGA_{2ox2}$, which codes for a GA 2-oxidase that deactivates GA_1 is upregulated. These changes precede a reduction in GA_1 levels and occur within 1 hour of light exposure (Reid et al., 2002). These changes in GA levels are closely mirrored in *Arabidopsis* as transfer of seedlings from dark to WL induce variations in transcript levels that are akin to GA synthesis and de-activation, also to an accumulation of DELLA proteins (Achard et al., 2007; Alabadí et al., 2008; Cheminant et al., 2011; de Lucas et al., 2008; Feng et al., 2008). These studies revealed the role of GAs in hypocotyl growth in the dark; however, it was not known if this represented repression of photomorphogenesis or a light independent mechanism to control cell expansion. To differentiate between these hypotheses, cotyledon opening and apical hook formation was more closely examined when seedlings were grown on a GA-biosynthesis inhibitor paclobutrazol (PAC). WT seedlings displayed an etiolated morphology when grown in the

dark; however, seedlings grown on PAC displayed a de-etiolated phenotype which could be rescued by co-application of GA. Light-regulated gene expression was also higher in PAC-treated seedlings. Furthermore, GA-deficient mutant *ga1-3* displayed a partial de-etiolation suggesting GA acts to promote hypocotyl elongation and repress expression of light-regulated genes (Alabadí et al., 2004).

It has also been long established that brassinosteroids (BR) play a negative-regulatory role in de-etiolation, mainly based on the de-etiolated phenotype of a number of dark-grown BR mutants such as *det2* (Li et al., 1996; Fujioka et al., 1997)*, dwf4* (Azpiroz et al., 1998; Choe et al., 1998)*, cpd* (Miklós Szekeres et al., 1996)*, bri1* (Clouse et al., 1996) and *bin2* (Li et al., 2001). In addition, treatment of dark-grown seedlings with brassinazole (Brz), a BR biosynthesis inhibitor, also induces some de-etiolated characteristics (Nagata et al., 2000). This phenotype can be restored to a normal etiolated phenotype after application of BRs. Microarray analysis has shown that BRs are able to down-regulate PIF3 (Goda et al., 2002). This is a key transcription factor in the light-signalling pathway which suggests that BRs may act as regulators of the light signalling path rather than or in addition to functioning as downstream targets.

The addition of GA and EBR to dark-grown FLS treated seedlings did not illicit any rescue suggesting FLS is not altering these hormone pathways. However, addition of exogenous auxins IAA, 1-NAA and 2,4-D displayed reversal of the FLS dependent de-etiolation. Auxin and light signaling are closely related; light is able to control auxin levels, transport and distinct responses in cell types (Halliday & Fankhauser, 2003; Halliday et al., 2009). It is suggested HY5 acts as a negative regulator of the auxin signaling pathway due to a study describing a decrease in genes that negatively regulate auxin: IAA7 and IAA14, in *hy5* mutants (Cluis et al., 2004). Auxin is also responsible for cell elongation and the shade avoidance response. Active phyB (Pfr) has been shown to reduce IAA levels through activation of genes that induce synthesis of indole glucosinolates and repression of auxin biosynthesis genes such as TAA1 (Ciolfi et al., 2013; Song et al., 2020; Tao et al., 2008). In contrast, when phyB is photo-converted to the inactive Pr form in low R:FR ratio light conditions, a rapid elevation in auxin-regulated transcript levels are observed. This links hormone and light signaling closely.

A number of dominant *aux/iaa* mutants, *shy2/iaa3, axr2/iaa7* and *axr3/iaa17*, also display de-etiolated phenotypes in the dark (Leyser et al., 1996; Nagpal et al., 2000; Tian et al., 2003a). In these mutants a mutation has been introduced in the DII degron, essentially stabilizing these proteins and reducing their auxin-induced turnover. The mutations that are able to cause de-etiolation in the dark are a result of stabilization of Aux/IAA proteins in the presence of auxin. This stabilization then represses ARF proteins and, thus, reduces the expression of auxin-regulated genes, including Aux/IAAs (Tian et al., 2002a). This dynamic negative-feedback pathway balances Aux/IAA and ARFs in cells to allow a tissue-specific auxin response. As it is unlikely FLS induces a mutation in Aux/IAA proteins to stabilize them, its action could be to block the TIR1 receptor that targets the Aux/IAA proteins for degradation, stopping degradation of these repressors, ultimately leading to photomorphogenesis. Through the co-application of exogenous auxins and FLS it could be suggested that the degradation of Aux/IAA proteins may be activated, and de-etiolation could be reversed.

Application of the ethylene precursor, 1-aminocyclopropane-1-carboxylic acid (ACC), displayed slight reversal of FLS-induced de-etiolation and was partially additive with exogenous IAA. Ethylene regulation of de-etiolation is closely linked to auxin due to the functional overlap of both their biosynthetic and response pathways (Swarup et al., 2002). The enzyme ACC synthase catalyses the conversion of S-adenosyl-l-methionine (SAM) to ACC and auxin is able to induce the transcription of ACC synthase genes to increase ethylene biosynthesis (Abel et al., 1995; Tsuchisaka & Theologis, 2004). Ethylene is also able to induce expression of *ASA1* and *ASB1* that catalyse the first step in tryptophan biosynthesis, which is the precursor of auxin (Ljung et al., 2005; Stepanova et al., 2005). Ethylene has an essential role in the maintenance of the apical hook in etiolated seedlings as ethylene-treated seedlings and ethylene-overproducing mutants display an exaggerated hook curvature phenotype in the dark. In comparison, ethylene insensitive mutants display a hookless phenotype (Guzman & Ecker, 1990). Similarly, IAA-treated seedlings or IAA-overproducing mutants alter hook formation suggesting auxin may be involved here too (Swarup et al., 2002). Furthermore, it has been shown that *Arabidopsis NPH4* gene, which encodes auxin regulated transcriptional activator ARF7, is

involved in apical-hook formation and can be repressed by application of exogenous ethylene.

The well documented relationship between auxin and ethylene begins to explain the partial rescue of de-etiolation by ACC; but the perceived alteration in ethylene responses is unlikely to be the primary target of FLS as it is only occurring at high concentrations and is more likely to be a secondary effect of FLS toxicity. Additionally, Pchlide levels were not reduced following ACC treatment alone, suggesting FLS-induced de-etiolation is independent of ethylene. In the next chapter the aim will be to uncouple the role of auxin in FLS action and explore the potential treatments to alleviate FLS toxicity field conditions.

Chapter 4: The role of auxin in FLS action

4.1 Introduction

Plant growth and development is largely governed by light quality, quantity, direction and duration and, as plants are sessile organisms, they are required to have a high degree of developmental plasticity to maximise chances of survival and reproduction. Seedlings undergo drastic developmental change, named de-etiolation, when moved from dark conditions to light conditions; but, in chapter 3 it was discovered that FLS induced this developmental change in the absence of light. FLS-mediated de-etiolation in the dark was only partially regulated by key light signalling genes, HY5, HYH and PIFs, potentially suggesting another primary pathway is targeted by this chemical that converges with light signalling pathways. The role of phytohormones, specifically auxins, in reversing FLS-induced de-etiolation was clear suggesting a potential role of auxin in FLS action in *Arabidopsis.*

Auxins have been implicated in seedling de-etiolation and many molecular studies have been carried out suggesting light is able to modulate auxin-signalling pathways. In *Arabidopsis* light triggers auxin synthesis in young leaves and etiolated seedlings are largely lacking auxin (Bhalerao et al., 2002). Auxin is then dispersed throughout the seedlings to create auxin gradients and local auxin concentrations in various seedling tissues that leads to discrete responses. In the shoot auxin induces cell expansion (Barbez et al., 2017; Du et al., 2020), whereas, in the root auxin induces lateral root emergence and primary root elongation (Velasquez et al., 2016; Barbez et al., 2017). Light signals can control both the movement of auxin and response to auxin within cells allowing development to be tuned to the light environment and for shoot and root development to be coordinated.

Auxin regulated genes from the *GH3, SAUR* and *Aux/IAA* families, which are upregulated within minutes of auxin application, localise to the nucleus and are upregulated by shade conditions (Hagen and Guilfoyle, 2002; Iglesias et al., 2018). Additionally, *AXR2, AXR3* and *SHY2* cause de-etiolation in dark-grown seedlings indicating these proteins could be light-regulated (Colón-Carmona et al., 2000). This suggestion is supported by work showing the *SHY2* gene is regulated by light (Tian et al., 2003). These dominant mutations stabilize the

proteins by introducing a mutation in their TIR1-binding domain. Furthermore, a number of Aux/IAA proteins can interact with, and are phosphorylated by phyA and phyB *in vitro* (Coló n-Carmona et al., 2000; Xu et al., 2018; Yang et al., 2018). Together these results imply that phosphorylation of Aux/IAA proteins by phytochromes may be the molecular mechanism that underpins the integration of light and auxin signalling. A link between light and auxin signalling also comes from the HY5 gene, which encodes a BZIP transcription factor that acts a positive regulator of photomorphogenesis (Oyama et al., 1997). The *hy5* mutant exhibits a similar light-insensitive hypocotyl elongation phenotype to that seen for an auxin insensitive mutant (Zobel, 1974) and the basic region of HY5 is identical to the soybean transcription factor STF1A which is able to bind to the same motif on the soybean *GH3* promotor that confers auxin inducibility (Liu et al., 1994). This confirms HY5 regulates expression of auxin-induced genes.

In this chapter the role of the phytohormone, auxin, in FLS action will be discussed. Previous studies looking into the effects of FLS on Arabidopsis and described in Chapter 3 showed a profound effect on root development and application of FLS to dark-grown seedlings induced a de-etiolated phenotype. This suggests that a potential mode of action of FLS is to alter auxin biosynthesis, transport and/or perception. The role of auxin in ameliorating some phytotoxic effects of FLS will also be considered with the aim to extrapolate the results to crop species.

4.2 Results

4.2.1 Exogenous IAA displays a more robust rescue of FLS in the dark

Previously, it was observed that applications of exogenous auxins at low micromolar concentrations were able to significantly decrease FLS-induced de-etiolation. To determine the threshold of this rescue, IAA from 1-1000 nM was applied exogenously to seedlings in the presence and absence of 50 μM FLS. The fresh weight of 50 μM FLS-treated seedlings was generally lower than control; however, at 1 μM (1000 nM) IAA fresh weight was significantly increased by 48% and comparable to control levels (figure 4.1). Similarly, 50 μM FLS-treated seedlings had significantly shorter hypocotyls; however, there was a slight but significant increase in hypocotyl length in the presence of 10-500 nM IAA. Pchlide levels were also sensitive to an increase in IAA; the addition of 10 nM IAA alongside 50 μM FLS significantly reduced Pchlide accumulation by 18%, relative to 50μM FLS treatment alone. However, Pchlide levels were only similar to control at 1μM IAA which elicited a 72% decrease in Pchlide accumulation. Likewise, cotyledon opening was significantly reduced from 10nM IAA, but did not reach control levels until 500nM IAA. IAA treatment had little to no effect on seedlings grown in the absence of FLS (figure 4.1) Although IAA at these concentrations was not enough to fully reverse FLS-induced de-etiolation, the effect of sub-μM concentrations of IAA are clear.

In order to ascertain if auxins were able to have the same effect in the light, exogenous IAA was applied alongside FLS at the same concentrations used previously. Following 7 days growth in the light, 1 and 5 μM IAA was not able to significantly improve the growth of FLS-treated seedlings (figure 4.2A). Treatment with IAA appeared to increase both fresh weight and total chlorophyll of seedlings treated with 200 μM FLS, but this increase was not significant. In contrast, seedlings not treated with FLS displayed a reduction in growth following IAA application. It is known that excess auxin results in phytotoxicity, therefore, reduced concentrations of auxins were applied to light-grown seedlings and it was shown that >100 nM IAA was sufficient to increase root length in FLS-treated individuals by 55%. This was not mirrored in fresh weight or total chlorophyll levels for which IAA did not have any effect.

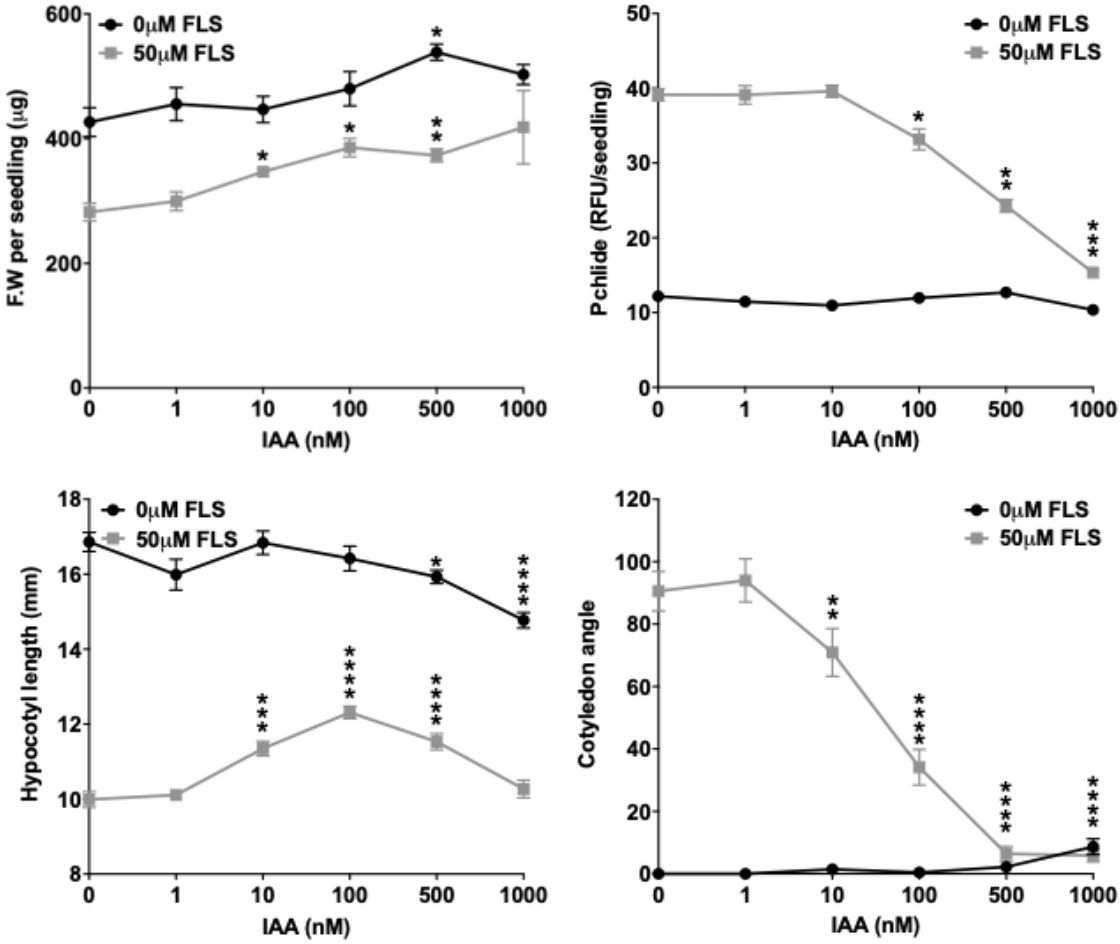

Figure 4.1. IAA is able to rescue FLS induced a de-etiolation at sub-µM concentrations. Col-0 seedlings grown for 5 days in the dark on ½ MS 0.8% agar media with addition of FLS and IAA at indicated concentrations (µM). Vehicle control conditions included addition of 0.1% (v/v) DMSO and 0.1% (v/v) ethanol to media. Hypocotyl length and cotyledon angle measured on ImageJ software. Fresh weight and Pchlide data points represent the mean ± SEM of four biological replicates, hypocotyl and cotyledon data points represent the mean ± SEM of 27-45 individuals per condition. Asterisks indicate * $p<0.05$, ** $p<0.01$, *** $p<0.001$ between black line (-FLS treatment) and grey line (+FLS treatment) by Tukey's post-hoc multiple-comparison test.

Conversely, in control seedlings treated with no FLS, the addition of exogenous IAA reduced growth (figure 4.2B), further suggesting FLS impacts normal auxin signaling in Arabidopsis. Although there was not a complete rescue of FLS toxicity by IAA, the increase in root length and auxin resistance provides some evidence of a role for IAA in FLS phytotoxicity in the light.

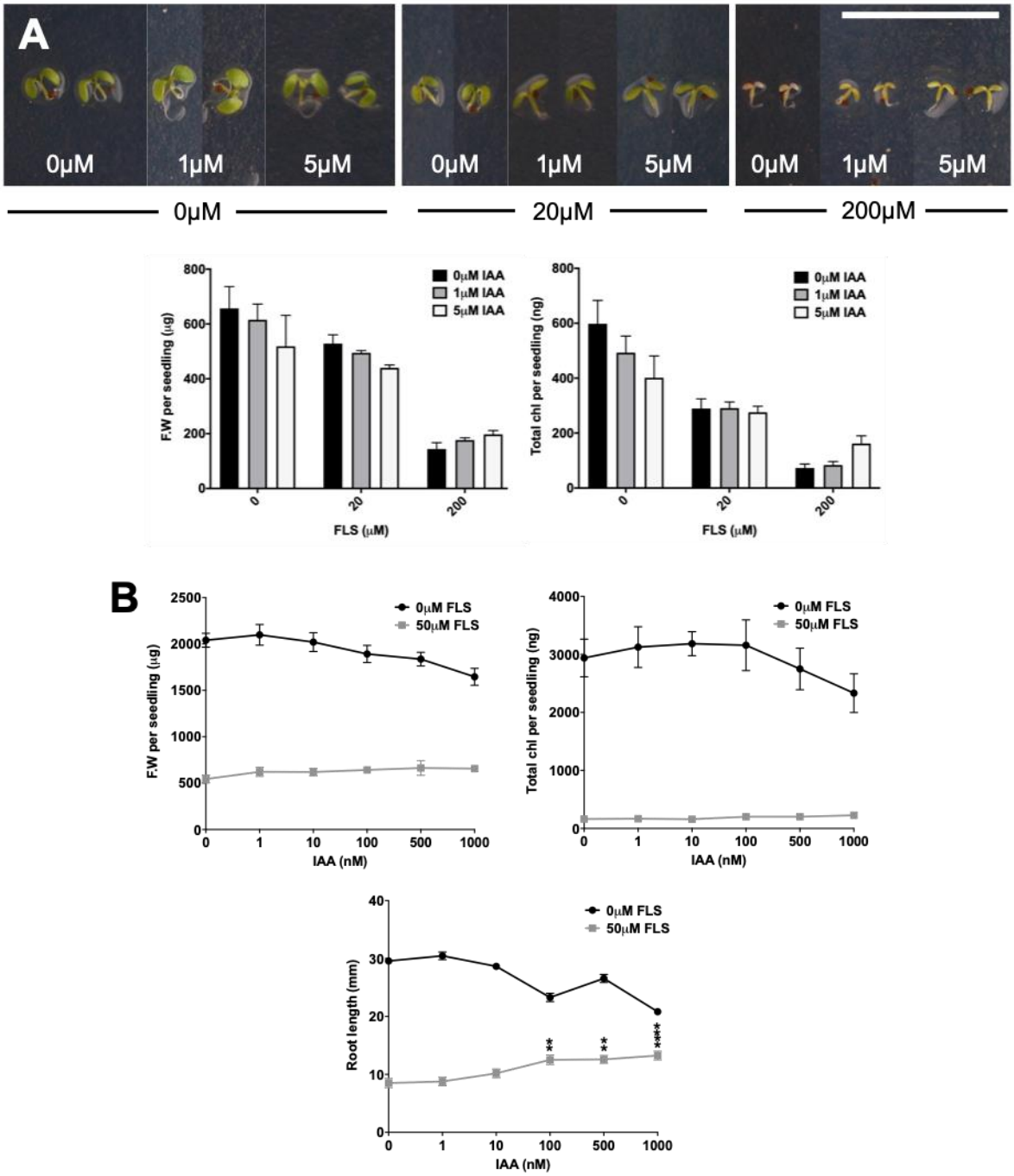

Figure 4.2. Exogenous IAA partially rescues toxicity of high concentration FLS in the light. Col-0 seedlings grown for 7 days in the light on ½ MS 0.8% agar media with (A) FLS at 0, 20 and 200 µM +/- 1 or 5 µM IAA (B) 0 or 50µM FLS alongside increasing concentrations of IAA from 1 nM-1 µM. Data points represent the mean ± SEM of three biological replicates. Asterisks indicate * $p<0.05$, ** $p<0.01$, *** $p<0.001$ between no IAA treatment and IAA treated samples by Tukey's post-hoc multiple-comparison test.

4.2.2 IAA rescue of FLS-induced de-etiolation is not due to a delay in development

It is known that changes in hormone levels, specifically GA deficiency in the *ga1-3* mutant, causes a delay in developmental timing and the de-etiolated phenotype in the dark of a *ga1-3* seedling takes longer to manifest (Alabadí et al., 2004). To determine IAA treatment was truly rescuing FLS-induced de-etiolation and not simply causing a developmental delay, an IAA rescue time course was carried out in which seedlings were harvested from 2-8 days growth in the dark. This allowed a more dynamic understanding of both FLS action and IAA rescue in the dark.

A striking result was demonstrated when measuring Pchlide and cotyledon opening. At day 2 there was no significant difference between conditions; however, from day 4 FLS-treated seedlings without IAA displayed a >3-fold increase in Pchlide accumulation that subsequently plateaued. In all other conditions Pchlide remained at a background level. It is clear that treating seedlings with IAA alongside FLS stops the excessive Pchlide accumulation seen with FLS treatment alone; additionally, IAA + FLS treatment did not show any indication that Pchlide would increase even if the experiment was continued suggesting IAA rescue of FLS-induced Pchlide accumulation is not solely due to a delay in development. Cotyledon opening also followed a similar pattern, although IAA treatment induced low levels of cotyledon opening compared to untreated seedlings (figure 4.3). From this data it can be seen that FLS induces its effects after around 4 days growth in the dark and co-treatment with IAA is able to maintain a rescue over a prolonged period.

In contrast, little rescue of fresh weight and hypocotyl was seen. Seedling fresh weight was significantly higher in the absence of IAA at day 2, regardless of FLS treatment. However, at day 4, seedlings not treated with FLS increased fresh weight compared to seedlings treated with FLS. At day 6, all seedlings began to display a plateau in fresh weight, possibly due to a reduction in energy availability; however, FLS treatment continued to result in significantly lower fresh weight and IAA treatment in the absence of FLS had the highest fresh weight. At the latest time point of 8 days, FLS treated seedlings were significantly different compared to control, regardless of IAA presence (figure 4.3). A

similar pattern was seen when measuring hypocotyl length; at the earlier time points IAA treatment caused a shorter hypocotyl length, independent of FLS treatment, and FLS treatment alone displayed an inhibition of hypocotyl elongation from day 4. At the later time points, FLS-treated seedlings displayed shorter hypocotyls compared to controls, although there was a slight, but not significant, increase in hypocotyl length when FLS and IAA were used simultaneously (figure 4.3). These results demonstrate a similar pattern to IAA rescue at 5 days, only minimal differences in fresh weight and hypocotyl length were observed with IAA treatment.

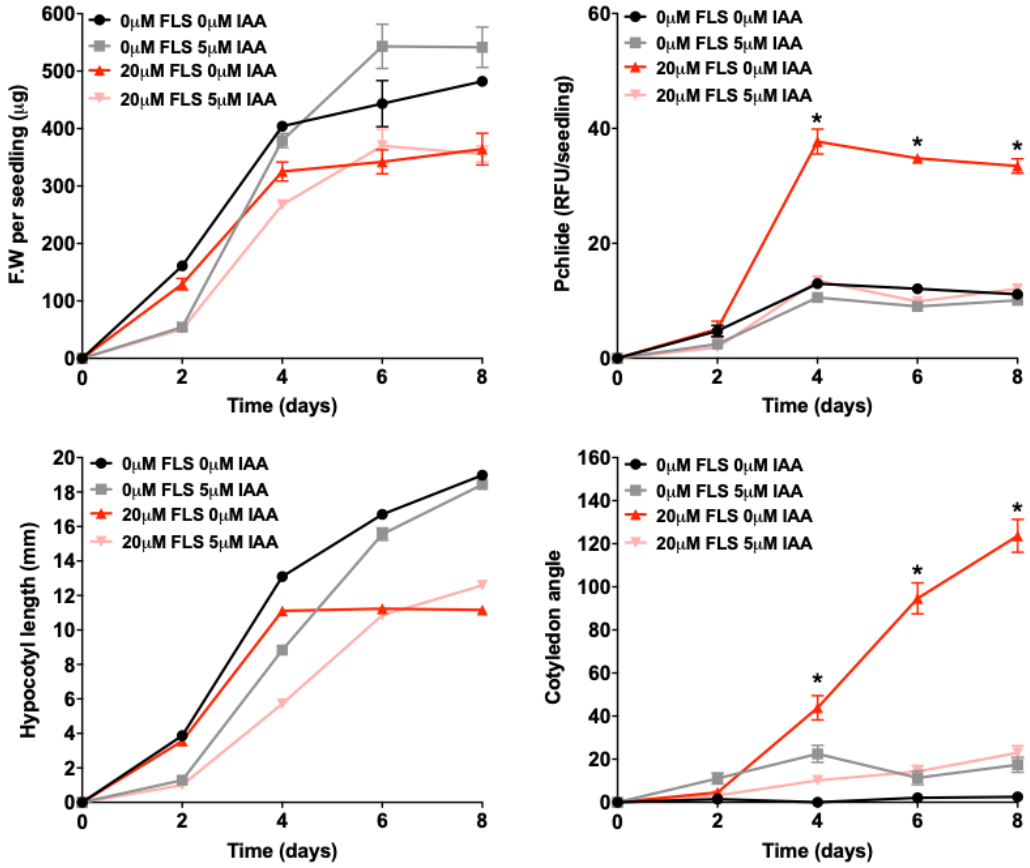

Figure 4.3. IAA rescue of FLS de-etiolation is not due to a delay in development. Col-0 seedlings grown for 5 days in the dark on ½ MS 0.8% agar media with addition of FLS and IAA at indicated concentrations (μM). Vehicle control conditions included addition of 0.1% DMSO and 0.1% ethanol to media. Hypocotyl length and cotyledon angle measured on ImageJ software. Fresh weight and Pchlide data points represent the mean ± SEM of three biological replicates, hypocotyl length and cotyledon angle data points represent the mean ± SEM of 37-81 individuals per condition. Asterisks indicate significant difference ($p<0.05$) between untreated (black line) and IAA treated seedlings by Tukey's post-hoc multiple-comparison test.

4.2.3 Auxin dependent gene expression is variable in light and dark

To further understand how FLS is altering auxin responses in *Arabidopsis*, expression of a number of auxin biosynthesis genes and auxin-responsive genes were studied in both light and dark-grown seedlings. Total RNA was extracted from 7-day old light-light and 5-day old dark-grown seedlings treated with and without 50µM FLS treatment and gene expression was analysed using quantitative RT-PCR (qPCR). IAA genes that encode Aux/IAA repressor proteins were selected as they display a significant increase in expression following auxin exposure (Hagen and Guilfoyle, 2002), while the biosynthesis genes were selected as they each represent a key point in the pathway to synthesise IAA (figure 4.4A).

In the dark 4 out of 5 of the auxin biosynthesis genes tested had increased expression in FLS-treated samples, with a 5-fold increase in expression of ASA1 (figure 4.4B). In contrast, only *TAA1* displayed reduced expression following FLS treatment in the light (figure 4.4C). These qPCR expression results were further validated when plotted against log2fold change scores retrieved from transcriptome analysis producing an R^2 value of 0.66 (figure 4.4D). In the light, all 5 *IAA* genes tested had significantly reduced expression when seedlings were grown in the presence of FLS relative to seedlings grown without FLS (figure 4.4B). *IAA3* expression appeared to be the most affected in the light with expression in these samples being 10 times lower than untreated controls. Following growth in the dark, FLS treatment decreased expression of all *IAA* genes with the exception of *IAA2* (figure 4.4C). Comparison to gene expression in the RNAseq transcriptome analysis (see section 3.2.9) confirmed similar expression levels using in both methods (figure 4.4D).

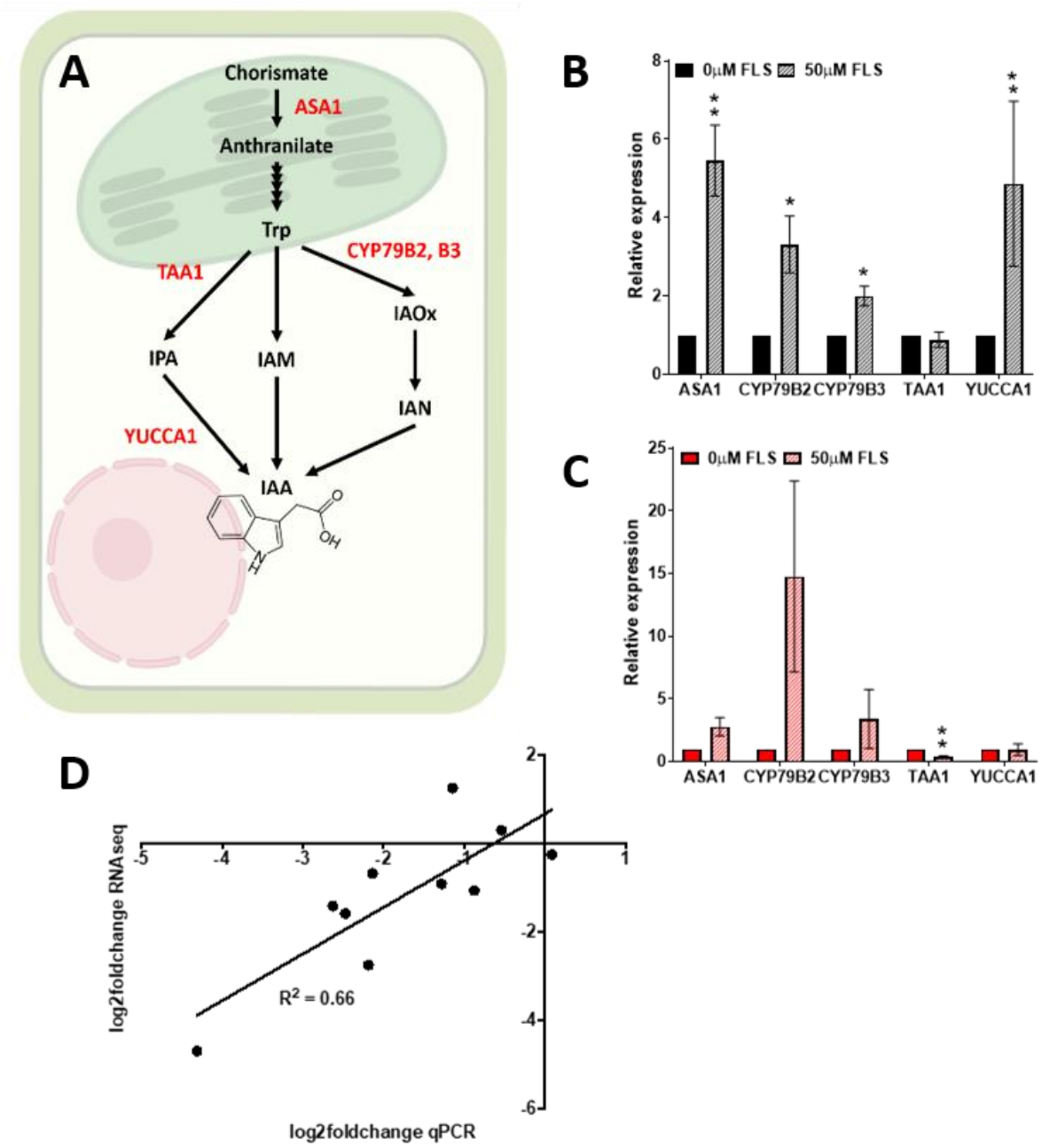

Figure 4.4. Auxin biosynthesis genes are not downregulated in response to FLS. Expression of auxin biosynthesis genes. (A) Simplified schematic of the auxin biosynthesis pathway. Red indicates where the enzyme product of each gene acts, (B) dark- and (C) light-grown samples measured by quantitative RT-PCR, (D) qPCR gene expression was correlated against expression levels of the same genes following transcriptome analysis by RNAseq. RNA was collected from seedlings grown on ½ MS 0.8% agar media ± 50µM FLS for 5 days in the dark (black bars) or 7 days in the light (red bars). Gene expression in whole seedlings was measured by qPCR relative to seedlings grown on 0.1% DMSO and normalised to *YELLOW LEAF SPECIFIC (YLS8)*. Data represents mean ±S.E of three biological replicates. * $p<0.05$, ** $p<0.01$ in a one-way ANOVA test.

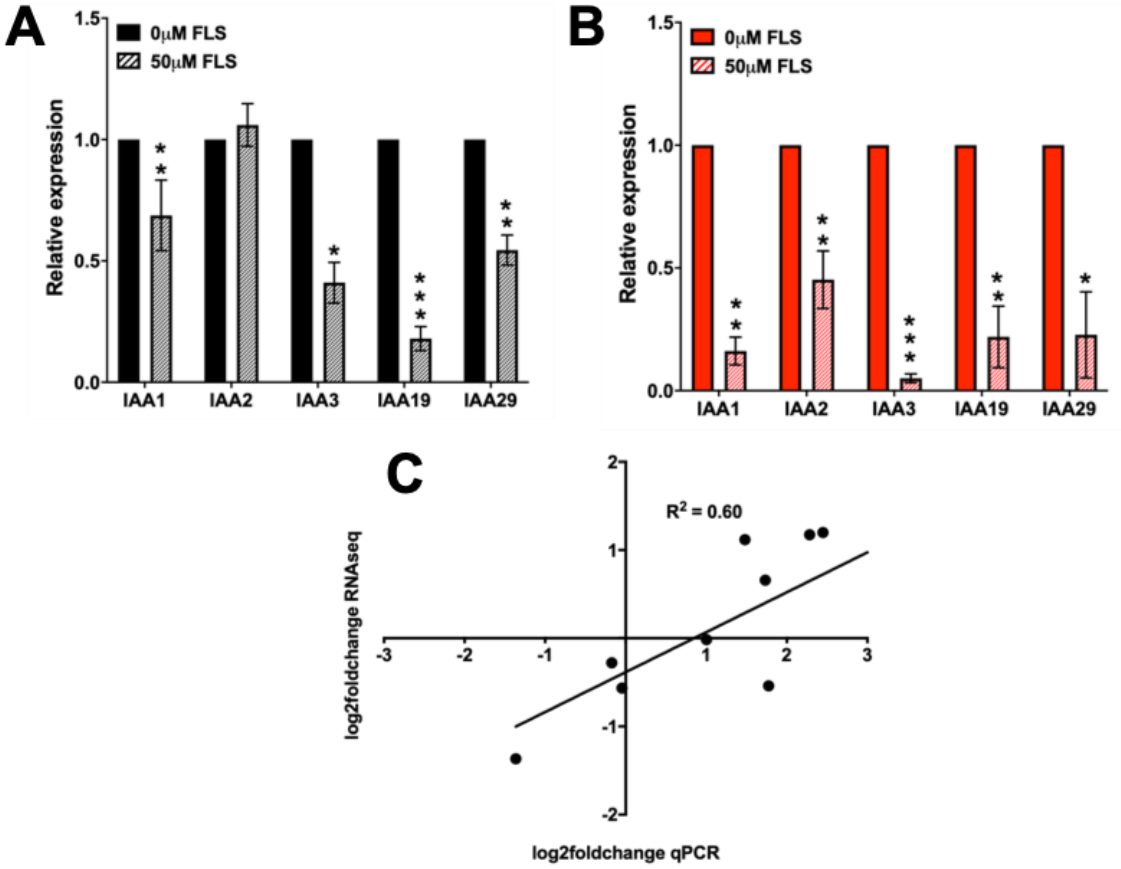

Figure 4.5. Auxin signalling genes are downregulated following FLS exposure. qPCR measuring expression of Aux/IAA genes. RNA collected from seedlings grown on ½ MS 0.8% agar media ± 50µM FLS for 5 days in the dark (A) or 7 days in the light (B). (C) qPCR gene expression was correlated against expression levels of the same genes following transcriptome analysis by RNAseq. Gene expression in whole seedlings was measured by qPCR relative to seedlings grown on 0.1% DMSO and normalised to *YELLOW LEAF SPECIFIC (YLS8)*. Data represents mean ±S.E of three biological replicates. * $p<0.05$, ** $p<0.01$, *** $p<0.001$ in one-way ANOVA test.

Looking further into expression data from the transcriptomic analyses we also see a trend in which auxin responsive gene classes - Aux/IAA, SAUR, GH3s and ARFs have lower expression following FLS treatment in both light and dark (table 4.1; appendix table S8). *Aux/IAA* gene expression was most affected by FLS treatment with 9/28 and 15/27 genes being significantly different following FLS treatment in the dark and light, respectively.

Table 4.1. Summary table of auxin responsive genes from RNAseq analysis. Genes with an adjusted P-value of < 0.05 following Benjamini–Hochberg correction for multiple testing were classed as significantly differentially expressed.

	Dark		Light	
Auxin responsive gene class	**Total genes identified**	**Genes differentially expressed**	**Total genes identified**	**Genes differentially expressed**
Aux/IAAs	28	9	27	15
SAURs	67	6	67	22
GH3s	10	3	10	3
ARFs	16	2	15	5

Interestingly, the most affected gene in this class was *IAA3*. Following FLS treatment in the light, *IAA3* expression was significantly reduced 4.7-fold compared to control seedlings; this strong reduction was not seen in dark-grown samples in which FLS only resulted in a 0.92-fold reduction *in IAA3* expression. This is in contrast to the qPCR results that displayed a significant downregulation of *IAA3* by FLS in the dark. Here we show a clear reduction in auxin-responsive gene expression caused by FLS in the absence of a reduction in auxin biosynthetic gene expression. The results indicate that FLS perturbs auxin signalling and that the proposed inhibition of auxin responses is not due to a reduction in auxin biosynthesis gene expression.

4.2.4 Auxin distribution and quantity is altered following long-term FLS exposure

It is not only auxin quantity that has an effect on plant growth, auxin localisation within the seedling impacts physiology. For example, the polar auxin transport inhibitor N-1-Naphthylphthalamic Acid (NPA) does not decrease auxin levels endogenously, it acts to reduce the transport of auxin to sites of root initiation and elongation and leaf primordia (Scanlon, 2003). In an attempt to discover how FLS is affecting auxin within the plant, auxin levels were visualised using *DR5::VENUS, DII::VENUS* and *IAA2::GFP* reporters.

The *DR5::VENUS* reporter is an output of the auxin response pathway as the *DR5* promotor consists of an auxin response element that initiates the transcription and translation of VENUS, a fast maturing YFP, to give a visual output of auxin signalling (Ulmasov et al., 1997; Heisler et al., 2005). Following 7 days growth in the light, 20 μM FLS had a clear effect on DR5::VENUS expression (figure 4.6A). Relative quantification of fluorescence 200 μm from the root tip showed a 94% decrease in the number of nuclei expressing VENUS. This could be, in part, explained by FLS reducing cell number in the root; however, there was no significant difference in cell numbers 200 micrometres from the root tip between control and FLS-treated dark- or light-grown seedlings - seedlings had, on average 13 cells 200 μm from the root tip. Therefore, this results suggests that FLS is reducing auxin levels or signalling within the root tip leading to phytotoxicity; therefore, a 1 μM IAA treatment was given to seedlings before imaging to determine if this could eliminate any change in auxin levels. Due to the activity of the *DR5::VENUS* reporter being affected by rates of transcription and translation a 3 h treatment was given as it has been described previously that there is a time delay of around 1.5–2 h between changes in auxin abundance and subsequent DR5 reporter activity (Brunoud et al., 2012). Interestingly, a similar pattern was observed, even following auxin feeding. Activity increased by 75% in control seedlings following feeding; however, the reduction in fluorescence by FLS was exacerbated following a short 3-hour 1 μM IAA treatment in which no nuclei expressed VENUS over designated threshold levels (figure 4.6A). Considering auxin feeding was able to increase reporter activity in control seedlings, but not in FLS-treated seedlings, it could be suggested FLS is acting to inhibit auxin signalling.

In contrast, when seedlings were grown for 5 days in the dark, with no IAA treatment, FLS did not alter *DR5::VENUS* fluorescence at all; however, following the 3 h IAA treatment a 1467% increase in fluorescence was seen after FLS treatment indicating a strong synergistic induction of auxin signalling by IAA and FLS (figure 4.6A).

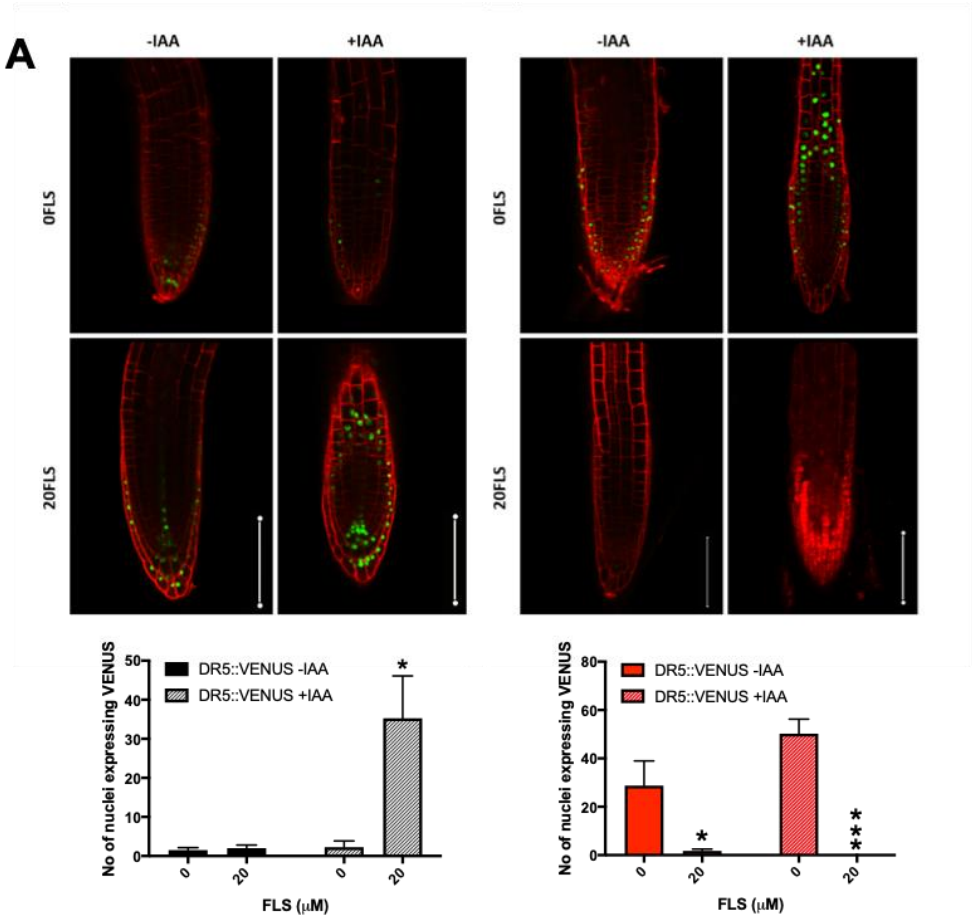
A
-IAA
+IAA
-IAA
+IAA
0FLS
20FLS
0FLS
20FLS
No of nuclei expressing VENUS
DR5::VENUS -IAA
DR5::VENUS +IAA
FLS (μM)
No of nuclei expressing VENUS
DR5::VENUS -IAA
DR5::VENUS +IAA
FLS (μM)

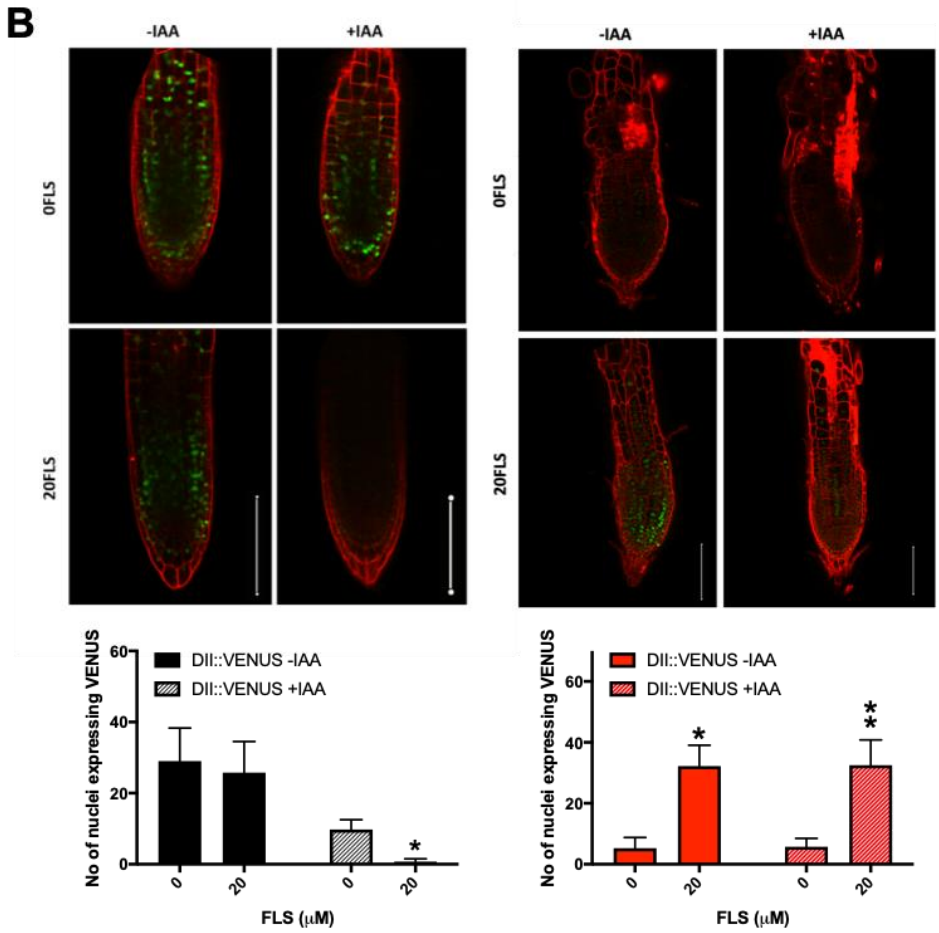
B
-IAA
+IAA
-IAA
+IAA
0FLS
20FLS
0FLS
20FLS
No of nuclei expressing VENUS
DII::VENUS -IAA
DII::VENUS +IAA
FLS (μM)
No of nuclei expressing VENUS
DII::VENUS -IAA
DII::VENUS +IAA
FLS (μM)

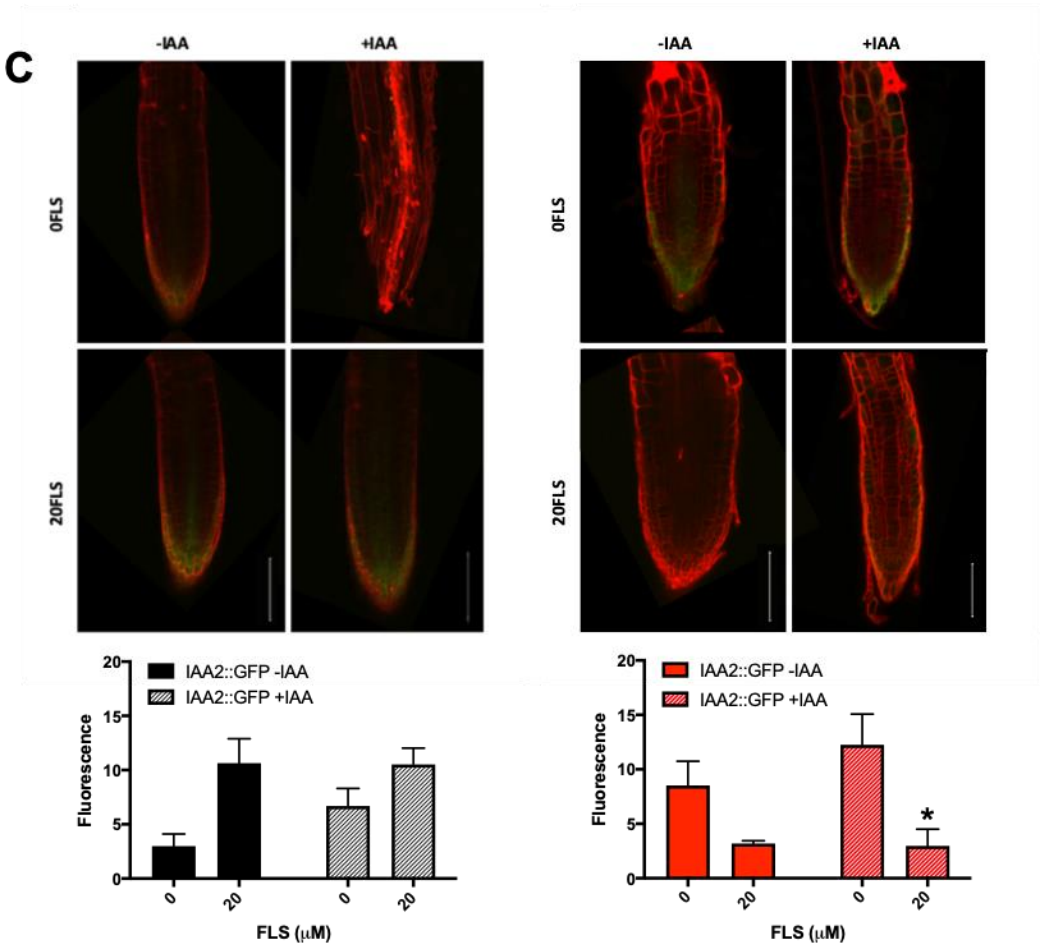

Figure 4.6. The effect of FLS treatment on auxin signalling is different in light and dark at the root tip. Seedlings expressing DR5::VENUS (A), DII::VENUS (B) and IAA2::GFP (C) seedlings were grown for 5 days in the dark (black bars) or 7 days in WL (red bars) on ½ MS 0.8% agar media ±20µM FLS. Prior to staining seedlings were transferred onto a plate containing 1µM IAA for 3h, or received a 3 h mock treatment. Graphs represent mean number of nuclei with fluorescence (DR5/DII) or total fluorescence (GFP) in an area 200 µm from the root tip ±SEM (n=4), * $p<0.05$ ** $p<0.01$ *** $p<0.001$ in one-way ANOVA. Propidium iodide staining shown in red and reporter in green. Scale bar represents 100µm.

In an effort to further confirm FLS effects on auxin, the *IAA2::GFP* reporter was also utilised. The *IAA2* gene is highly inducible by auxin; therefore, GFP activity will be increased in the presence of auxin. When using this reporter, the number of nuclei with GFP activity could not be determined, only relative fluorescence within 200 µm of the root tip. In light-grown seedlings, without a 3 h auxin treatment, GFP fluorescence was 62% lower in FLS-treated seedlings; however, this result was not statistically significant ($p=0.054$) due to variation in the control (figure 4.6C).

This difference became significant after a 3 h auxin treatment when a 76% decrease in GFP fluorescence was seen in FLS-treated seedlings. In contrast to the VENUS reporters, dark-grown, *IAA2::GFP* expressing seedlings were able to display higher fluorescence in FLS-treated seedlings even with no auxin treatment and following auxin treatment there was no significant difference between control and FLS-treated seedlings due to high variability among individuals (figure 4.6C). Nevertheless, reporter activity remained higher in FLS-treated seedlings, indicating FLS caused an increase in auxin signalling in the dark.

Changes in auxin distribution and quantity can also be measured through the use of *DII::VENUS* reporter. *DII::VENUS* was engineered through fusing VENUS to domain II of the Aux/IAA protein, IAA28, and expressing it under a constitutive promoter (Brunoud et al., 2012). Domain II is the auxin-interaction domain found in Aux/IAA proteins and DII::VENUS is rapidly degraded by auxin; therefore, DII::VENUS fluorescence is able to indicate the absence of auxin or auxin perception and is the inverse of the *DR5::VENUS* reporter that is induced by auxin. Following growth in light, seedling root tips displayed a very high DII::VENUS fluorescence when treated with 20µM FLS; a 514% increase in fluorescence was recorded when quantifying the number of nuclei with fluorescence in populations with and without IAA treatment (figure 4.6B). The increase in fluorescence of this reporter inversely correlates with *the DR5::VENUS* expression pattern suggesting a FLS-dependent decrease in auxin signalling at the root tip in the light. In dark-grown seedlings, opposing patterns were also seen; with no IAA treatment FLS had a minimal effect on DII::VENUS expression. However, following IAA treatment, FLS treated seedlings displayed 92% lower fluorescence suggesting an increase in auxin-mediated degradation of Aux/IAA proteins. IAA treatment was also able to reduce DII::VENUS fluorescence by 66% in the absence of FLS.

The use of different reporter genes allows a deeper understanding of the role of auxin in FLS action; in all reporters it has been shown FLS decreases auxin signalling in the light and this is not rescued by the addition of exogenous IAA. In contrast, in the dark, FLS has a minimal effect on auxin signalling at the root, except in the presence of IAA. These observations were universal suggesting FLS effects are not reporter specific.

4.2.5 Auxin signaling at the root tip is decreased rapidly upon FLS exposure

Previously, the effect of FLS on auxin signaling was observed under long term FLS exposure. This showed, particularly in the light, that FLS treatment at >20 µM results in severe phenotypic and gene expression changes (section 3.2.1 and 3.2.9) raising the question of whether the changes in auxin signaling bought about by FLS are a secondary effect. To further understand the dynamics and relationship between FLS and auxin signaling we used the sensitive DII::VENUS reporter in a time course assay to determine if FLS was able to induce the same changes seen previously but within a significantly shorter time frame. DII::VENUS expressing seedlings were grown in the light for 5 days in the absence of FLS before transfer to FLS containing plates for the indicated time periods; control seedlings were moved to plates containing 0.1% DMSO to replicate potential mechanical insults that would affect expression.

Three time course assays were performed, continually decreasing FLS exposure time (figure 4.7A-C). At every time point tested, FLS-treated individuals had significantly more nuclei expressing the DII::VENUS construct at the root tip. Throughout all time course assays the mock-treated individuals (black line) maintained DII::VENUS fluorescence at a steady, low state, with around 15 nuclei showing DII::VENUS fluorescence. FLS exposure significantly increased fluorescence to around 50 nuclei (figure 4.7) resulting in a 162% increase after only 15 minutes of FLS exposure (the shortest time period in which a measurement could be taken) and ending in a 144% increase after 48 hours of exposure. The maintenance of DII::VENUS expression by FLS in three separate assays demonstrates the ability of FLS to interact with the auxin signalling pathway. Additionally, the ability of FLS to induce this expression so quickly indicates the potential of this compound to be directly interfering in auxin signaling.

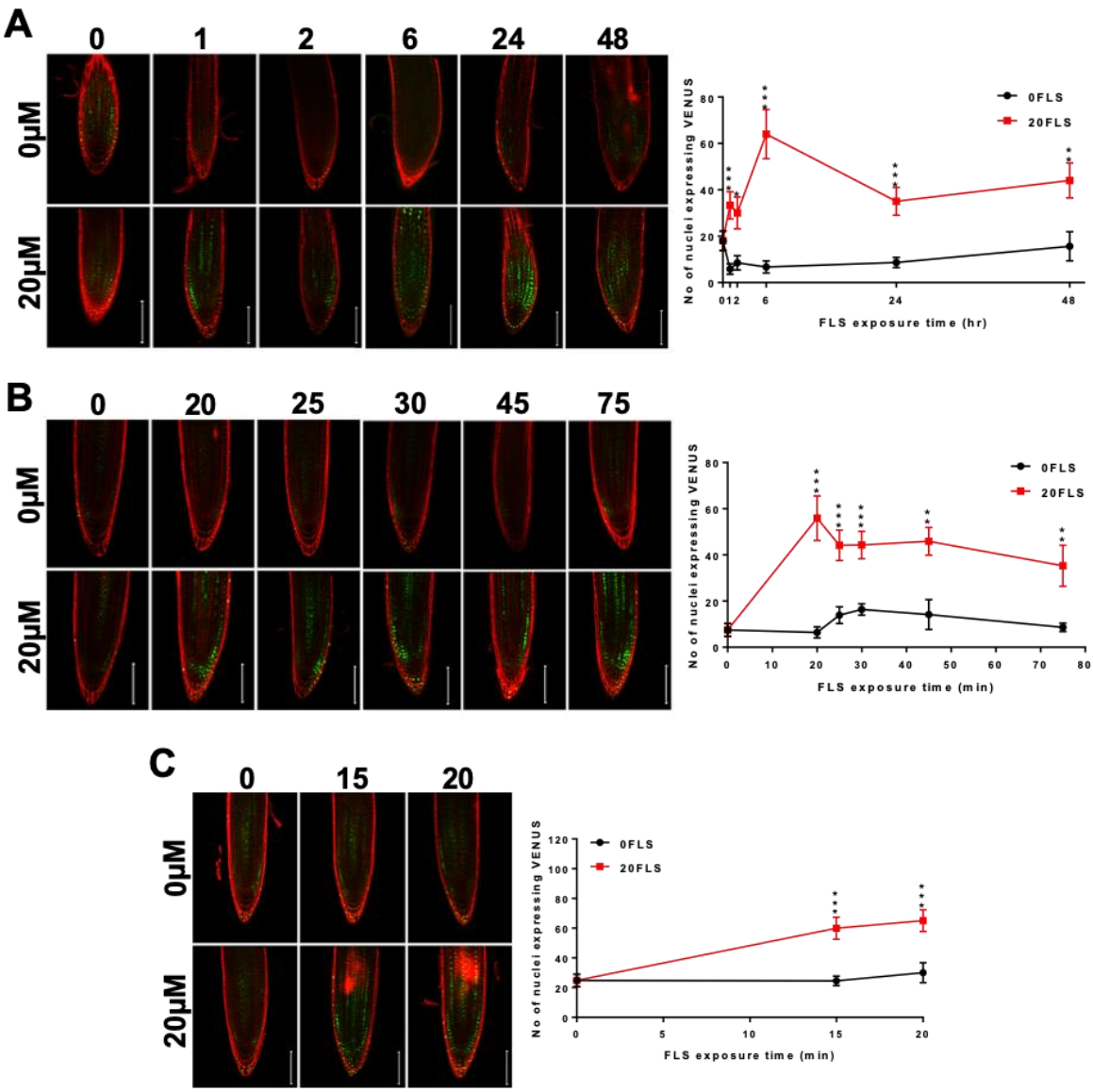

Figure 4.7. The DII::VENUS reporter is stabilised rapidly at the root tip upon FLS exposure. DII::VENUS seedlings were grown for 5 days in WL and exposed to 20 µM fluensulfone (FLS) or mock treatments for the indicated time on ½ MS 0.8% agar plates. Treatments from 0-48 hours (A), 0-60 min (B) and 0-20 min (C). Graphs represent average number of nuclei with fluorescence in an area 200 µm from the root tip ±SEM (n=7-13), * $p<0.05$ ** $p<0.01$ *** $p<0.001$ in one-way ANOVA. Propidium iodide staining displayed in red and DII::VENUS in green. Scale bar represents 100 µm.

4.2.6 TIR1 antagonist, auxinole, phenocopies FLS

Auxin dependent gene expression can be downregulated by acting at a number of points, namely: auxin biosynthesis, auxin transport and auxin signalling. To understand how FLS is altering auxin dependent gene expression phenotypic comparisons were made with established auxin biosynthesis, transport and signaling inhibitors in two light conditions. Kynurenine and yucasin represent auxin biosynthesis inhibitors targeting TAA1 (He et al., 2011) and YUCCA1 (Nishimura et al., 2014); NPA (Depta et al., 1983) is an auxin efflux inhibitor and auxinole is a TIR1 antagonist (Hayashi et al., 2012).

As FLS induces a robust de-etiolated phenotype in the dark, all compounds were added to plant growth media at 20 μM for comparison. Following 5 days growth in the dark, it was evident that the majority did not induce de-etiolation. At 20 μM, in the dark, FLS was able to decrease fresh weight by 34%, hypocotyl length by 30% while increasing Pchlide accumulation by 154% and allowing cotyledons to open. The biosynthetic inhibitors kynurenine and yucasin only displayed a 23% decrease in fresh weight and a 9% increase in hypocotyl length, respectively with no significant effect on Pchlide accumulation or cotyledon opening, while NPA only caused a marginal 9% decrease in hypocotyl length. In contrast, auxinole phenocopied FLS in all aspects; fresh weight was decreased by 20%, hypocotyl length by 9%, but more interestingly, 20 μM auxinole was also able to increase Pchlide by 105% and induced cotyledon opening (figure 4.8A). FLS remained to be more potent at inducing de-etiolation at the same concentrations; but, the specificity of Pchlide accumulation to the TIR1 antagonist auxinole suggests a potential conserved mode of action with FLS. Phenotypic comparisons to FLS were also made following growth in the light. FLS decreased fresh weight, total chlorophyll and root length by 60%, 82% and 56%, respectively. While all other inhibitors were able to reduce root length significantly, only auxinole and kynurenine reduced fresh weight and total chlorophyll was not affected with any treatment (figure 4.8B). The lack of similarity in phenotype in the light, particularly between FLS and auxinole, could be the result of more dominant light-induced pathways masking the effects of these compounds. Nevertheless, the clear de-etiolation by auxinole coupled with the inability of other compounds to phenocopy FLS in the dark suggests the potential of a conserved target, namely the TIR1 receptor.

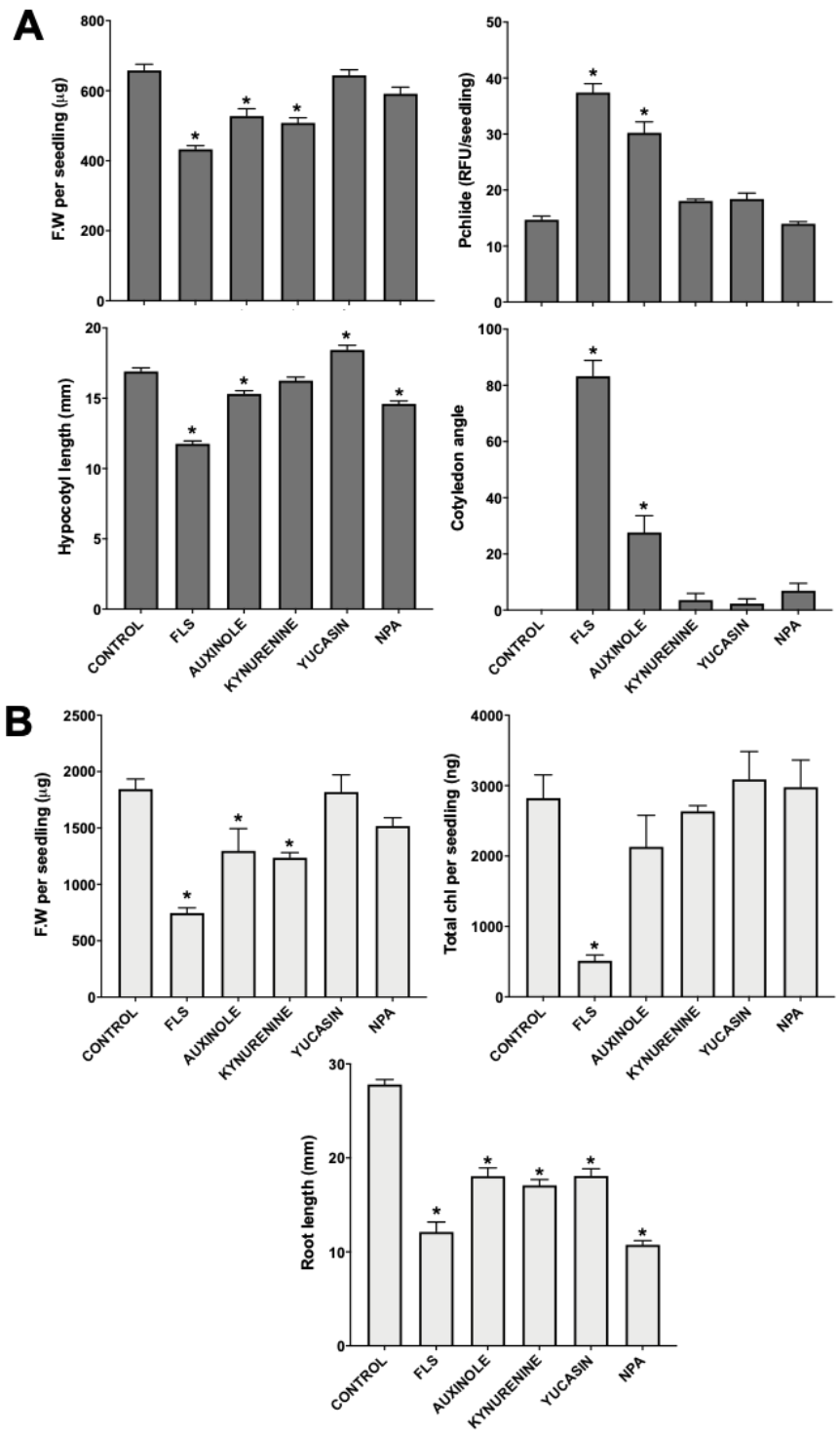

Figure 4.8. Comparing phenotypes of FLS-treated seedlings and seedlings treated with auxin inhibitors. Col-0 seedlings grown for 5 days in the dark (A) or 7 days light (B) on ½ MS 0.8% agar media with addition of inhibitors to a concentration of 20 µM. Vehicle control conditions included addition of 0.1% DMSO to media. Fresh weight, Pchlide and total chlorophyll data points represent the mean ± SEM of three biological replicates; hypocotyl, cotyledon and root length data points represent the mean ± SEM of 32-47 individuals per condition. Asterisks denote P<0.05 in control seedlings compared to FLS treated seedlings by Tukey's post-hoc multiple-comparison test. NPA = Naphthylphthalamic acid.

To probe the hypothesis that FLS could be acting as an auxin antagonist further, in depth comparisons were carried out with auxinole, but also including another proposed auxin receptor inhibitor, the partial antagonist p-chlorophenoxyisobutyric acid (PCIB) (Oono et al., 2003).. Following 5 days growth in the dark, it was clear that PCIB did not induce a de-etiolated phenotype comparable to FLS or auxinole. PCIB at even 200 µM could not induce significant cotyledon opening of seedlings; however, auxinole was able to stimulate cotyledon opening albeit not to the extent of FLS. PCIB also failed to cause the accumulation of Pchlide and levels were maintained at all concentrations; but, auxinole mirrored FLS almost exactly by inducing Pchlide accumulation by 239% at the highest concentration compared to an increase in Pchlide on FLS of 153% (figure 4.9A). Previously, it was shown that transferring FLS-treated seedlings from dark to light conditions resulted in the perturbation of chlorophyll production, likely due to singlet oxygen toxicity from high levels of accumulate Pchlide. Again, auxinole and FLS-treated populations demonstrated a dose dependent decrease in both fresh weight and total chlorophyll levels (figure 4.9B); whereas, PCIB treated seedlings were able to grow significantly more, accumulating more fresh weight and total chlorophyll.

Interestingly, a different relationship was seen between these three compounds when seedlings were grown in the light. All three inhibitors displayed a clear dose dependent decrease in fresh weight, total chlorophyll and root length, with PCIB demonstrating a more similar phenotype to FLS (figure 4.9C). One feature noted was the severe agravitropism of auxinole-treated seedlings, a phenotype not observed following FLS exposure and only mildly in PCIB treated seedlings.

Dynamics of auxin signalling in DII::VENUS expressing seedlings were also compared. In a similar pattern to dark-grown seedlings, it was evident that a short exposure of 20 µM FLS and auxinole was sufficient to inhibit DII::VENUS degradation to a similar extent (figure 4.10A&B). In contrast, PCIB treatment appeared to show only a weak effect, but that was not significant (figure 4.10C).

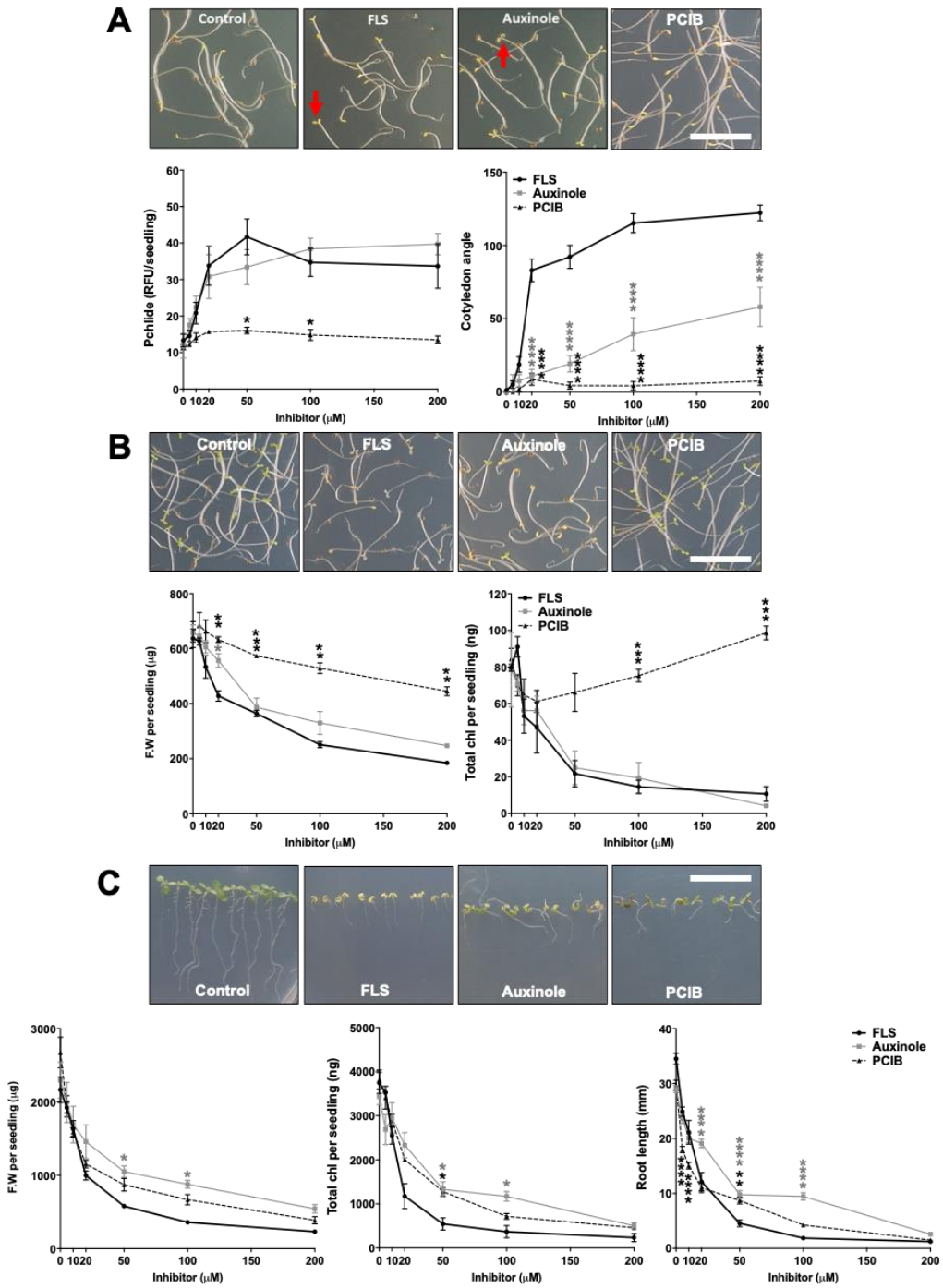

Figure 4.9. Comparing phenotypes of FLS-treated seedlings and seedlings treated with established auxin antagonists, auxinole and PCIB. Col-0 seedlings grown for 5 days in the dark (A), 5 days in dark + 24 h light (B) and 7 days light (C) on ½ MS 0.8% agar media with addition of inhibitors to indicated concentrations. Vehicle control conditions included addition of 0.1% DMSO to media. Fresh weight, Pchlide and total chlorophyll data points represent the mean ± SEM of three biological replicates, cotyledon data and root length data points represent the mean ± SEM of 13-44 individuals per condition. Images are representative seedlings at exposed to 50µM of the indicated chemical in each condition. Red arrows denote de-etiolated seedlings and scale bar represents 1cm. Asterisks indicate * $p<0.05$, ** $p<0.01$, *** $p<0.001$ between FLS treatment and grey lines by Tukey's post-hoc multiple-comparison test.

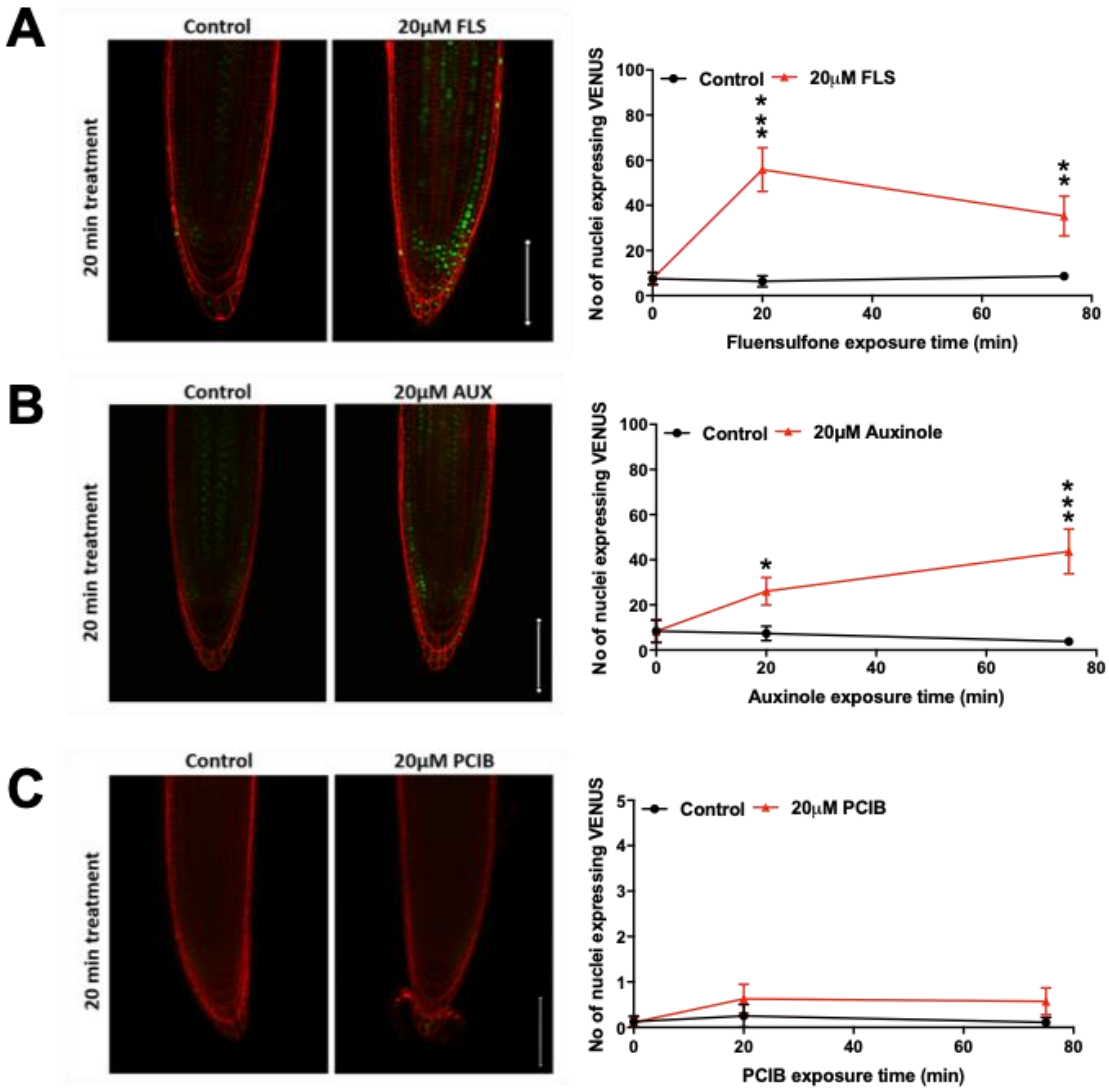

Figure 4.10. DII::VENUS stabilisation in seedlings treated with FLS and known auxin antagonists. DII::VENUS seedlings were grown for 5 days in WL and exposed to 20µM (A) FLS, (B) Auxinole, (C) PCIB or mock treatments for the indicated time on ½ MS 0.8% agar plates. Graph represents mean number of nuclei with fluorescence in an area 200 µm from the root tip ±SEM (n=7-13), * $p<0.05$ ** $p<0.01$ *** $p<0.001$ in one-way ANOVA. Propidium iodide staining displayed in red and DII::VENUS in green. Scale bar represents 100 µm.

4.2.7 Auxin receptor mutants display de-etiolated phenotypes in the dark

The similarities between auxinole and FLS treatment compared to that of other auxin inhibitors raises the hypothesis FLS could also be acting as an auxin receptor antagonist. To begin answering this question, a number of *TIR/AFB* mutants were treated with FLS and grown in the dark to determine if these mutants displayed any resistance. A selection of single (*tir1*), double (*tir1, afb2-3*) and triple (*tir1, afb2-3, afb4-8; tir1, afb2-3, afb5-5*) mutants (M Ruegger et al., 1998; Walsh et al., 2006; Parry et al., 2009) were studied as it is known there are functional redundancies between *TIR1, AFB2* and *AFB3* and also between *AFB4* and *AFB5* (Dharmasiri et al., 2005; Prigge et al., 2016).

FLS was able to induce Pchlide accumulation in all mutants and also induce cotyledon opening. The *tir1-1, afb2-3, afb5-5* triple mutant did display partial resistance to FLS-induced cotyledon opening; however, these mutant seedlings had a lower rate of germination compared to other lines, which may have affected the phenotype. It was interesting to note the effect of TIR1/AFB mutations in the absence of FLS also; the double and two triple mutants displayed significantly elevated levels of Pchlide compared to WT, this was coupled with a subtle, but significant, increase in cotyledon opening in the *tir1-1, afb2-3* double mutant (figure 4.11) further cementing an association between light and auxin signalling pathways in *Arabidopsis.*

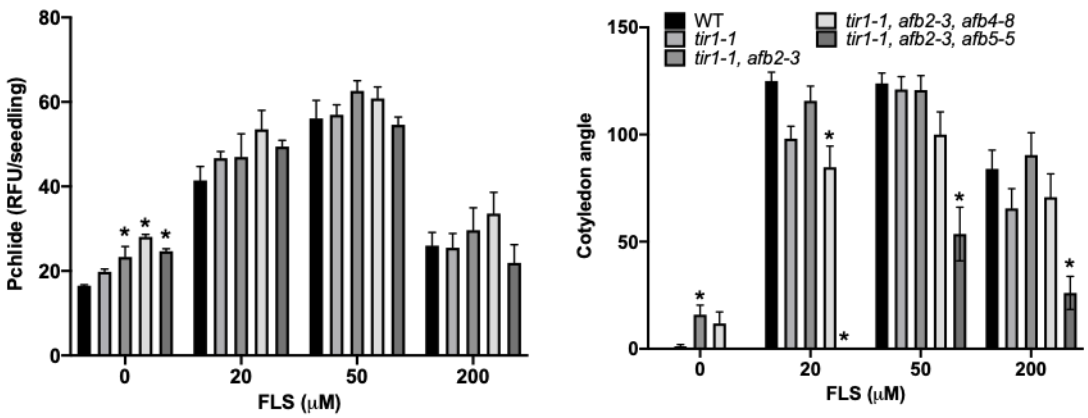

Figure 4.11. Auxin receptor mutants are partially de-etiolated. *tir1/afb* mutants were grown for 5 days in darkness on indicted concentrations of FLS. Cotyledon angle was measured using ImageJ software. Pchlide data points represent the mean ± SEM of three biological replicates, cotyledon angle represents mean ± SEM of 8-30 individuals per condition. Asterisks denote P<0.05 in WT seedlings compared to mutant seedlings by Tukey's post-hoc multiple-comparison test.

4.2.8 Co-treatment with auxins protect seedlings and permits chlorophyll accumulation

Auxin-specific reversal of FLS-induced de-etiolation was established previously with application of exogenous auxins, IAA, 1-NAA and 2,4-D reducing Pchlide accumulation. This result suggested the possibility of using auxins as a potential method to ameliorate FLS phytotoxicity. To explore this further, a greening assay was conducted in seedlings that were treated +/- FLS +/- IAA. As shown previously 20 µM FLS significantly reduced fresh weight and total chlorophyll accumulation from 4 hours post-transfer to light, compared to control seedlings (figure 4.12A). However, addition of IAA at 100 nM and 1 µM was able to allow accumulation of both fresh weight and total chlorophyll over time. The application of IAA at both concentrations displayed a similar rate of chlorophyll accumulation from 0-8 hours in the light; however, at the end of the sampling period, co-treated seedlings were only able to accumulate around 50% of the chlorophyll measured in control seedlings (figure 4.12A). Addition of IAA to seedlings in the absence of FLS had minimal effects; fresh weight and total chlorophyll accumulation was not compromised in the 24-hour period.

In contrast to IAA, application of 2,4-D did not elicit the same rescue. 2 hours post transfer to light of 20 µM FLS-treated seedlings, 10 nM 2,4-D treatment further inhibited fresh weight accumulation, with 5 nM 2,4-D seedlings also demonstrating a reduction in fresh weight. This reduction in fresh weight was sustained throughout the 24-hour assay, resulting in a 43% reduction in the co-treated populations (figure 4.12B). Similar to IAA, 2,4-D application in the absence of FLS did not significantly affect fresh weight. 2,4-D was also not able to permit chlorophyll accumulation in FLS treated seedlings in contrast to IAA. All seedlings exposed to 20 µM FLS, regardless of 2,4-D concentration, were unable to accumulate chlorophyll from 2-24 hours. Control seedlings with and without 2,4-D displayed a large increase in total chlorophyll levels over time; resulting in a 22-fold increase in chlorophyll compared to FLS treated samples at 24 hours (figure 4.12B). Higher concentrations of 2,4-D were tested (up to 50 nM) but 2,4-D herbicidal effects were amplified in this set-up and caused severe and rapid seedling death upon transfer to light (data not shown).

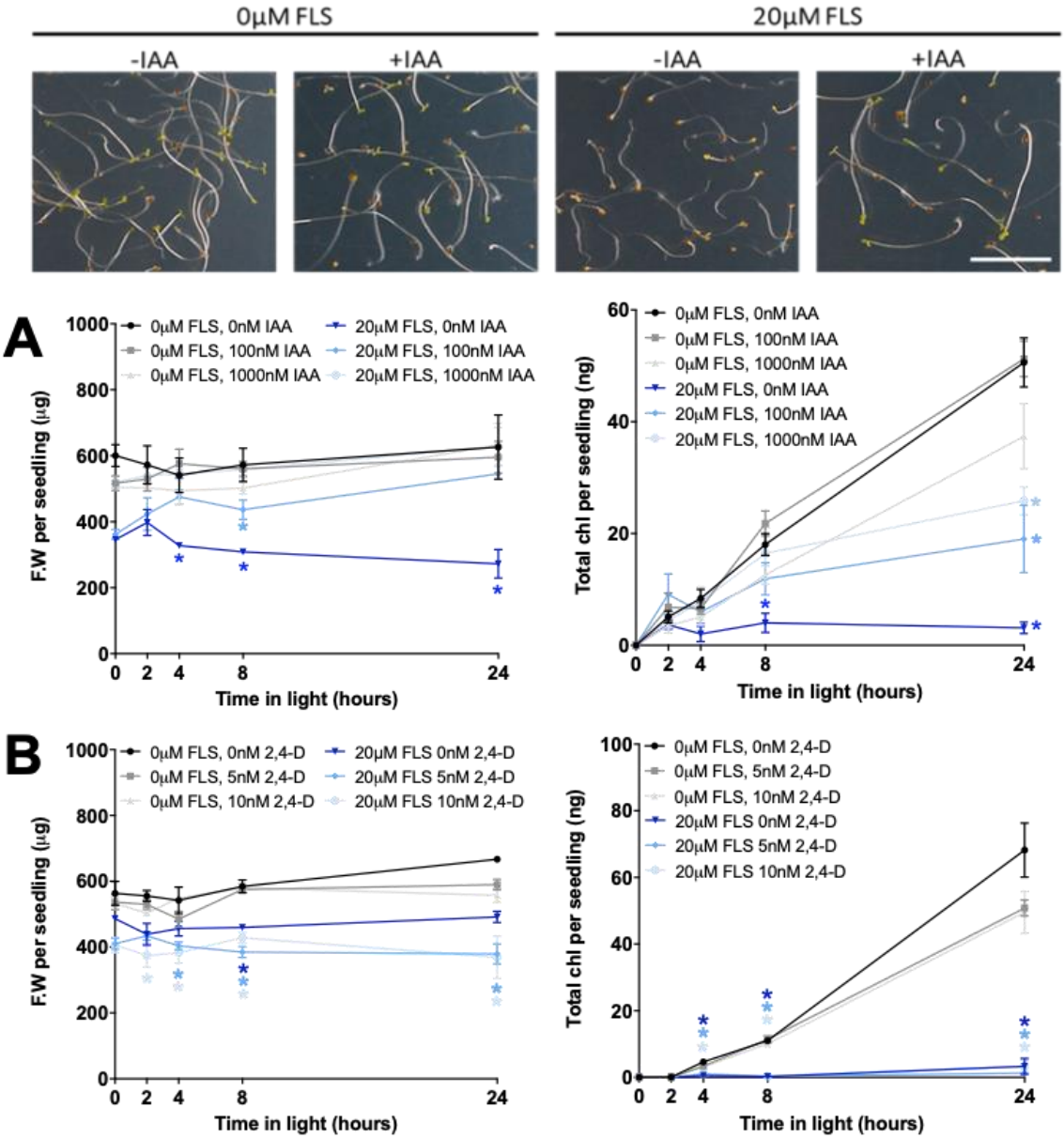

Figure 4.12. IAA treatment reverses the FLS-induced block of chlorophyll production. Col-0 seedlings grown for 5 days on ½ MS 0.8% agar media with addition of FLS and (A) IAA or (B) 2,4-D to indicated concentrations, plates were then moved into WL for the indicated number of hours (0-24h). Data points represent the mean ± SEM of three biological replicates. Asterisks indicate * $p<0.05$, ** $p<0.01$, *** $p<0.001$ between control seedlings (black line) compared to 20 µM FLS treated seedlings by Tukey's post-hoc multiple-comparison test.

4.2.9 Pre-treatment with auxins protect seedlings from FLS-induced protochlorophyllide accumulation

Encouraged by the rescue of chlorophyll accumulation by IAA in both the dark, and in greening assays, auxins were applied as a 'pre-treatment' to FLS to determine if a short exposure to these compounds could ameliorate the effects of FLS. Seedlings were grown in the dark for 2 days +/- 1 µM IAA then transferred to plates containing IAA, FLS or both for a further 3 days in the dark. Focusing on fresh weight and cotyledon opening, there was no significant change with any combination of treatment; although pre-treatment did lead to a marginal increase in cotyledon opening. Pchlide accumulation showed an interesting dynamic; seedlings co-treated with IAA were able to inhibit FLS-dependent Pchlide accumulation as described previously (black bars). Interestingly when seedlings were given 1 µM for 2 days prior to their exposure to FLS (grey bars) Pchlide accumulation was reduced by 24%, on average compared with FLS-treated or FLS and IAA co-treated seedlings (figure 4.13A). When pre-treating with IAA, hypocotyl length was also reduced in seedlings that were subsequently grown in the presence of IAA. However, in seedlings grown in the presence of 20 µM FLS after the IAA pre-treatment, hypocotyl length was not affected (figure 4.13A), indicating FLS could be blocking IAA inhibition of hypocotyl elongation.

The same experimental set-up was repeated and the seedlings were then transferred to WL for a further 24-hours after the 5-day period in the dark. Similarly to dark-grown seedlings, fresh weight was not affected by the IAA pre-treatment. However, chlorophyll accumulation was significantly increased after IAA pre-treatment in control and FLS-treated seedlings (figure 4.13B). Following no IAA pre-treatment (black bars), subsequent growth on FLS +/- IAA resulted in, on average, an 81% reduction in total chlorophyll compared to control. But, when seedlings were exposed to 1 µM IAA for two days prior to FLS, seedlings accumulated an average of 221% more chlorophyll after 24 hours in the light returning chlorophyll to near control levels (figure 4.13B).

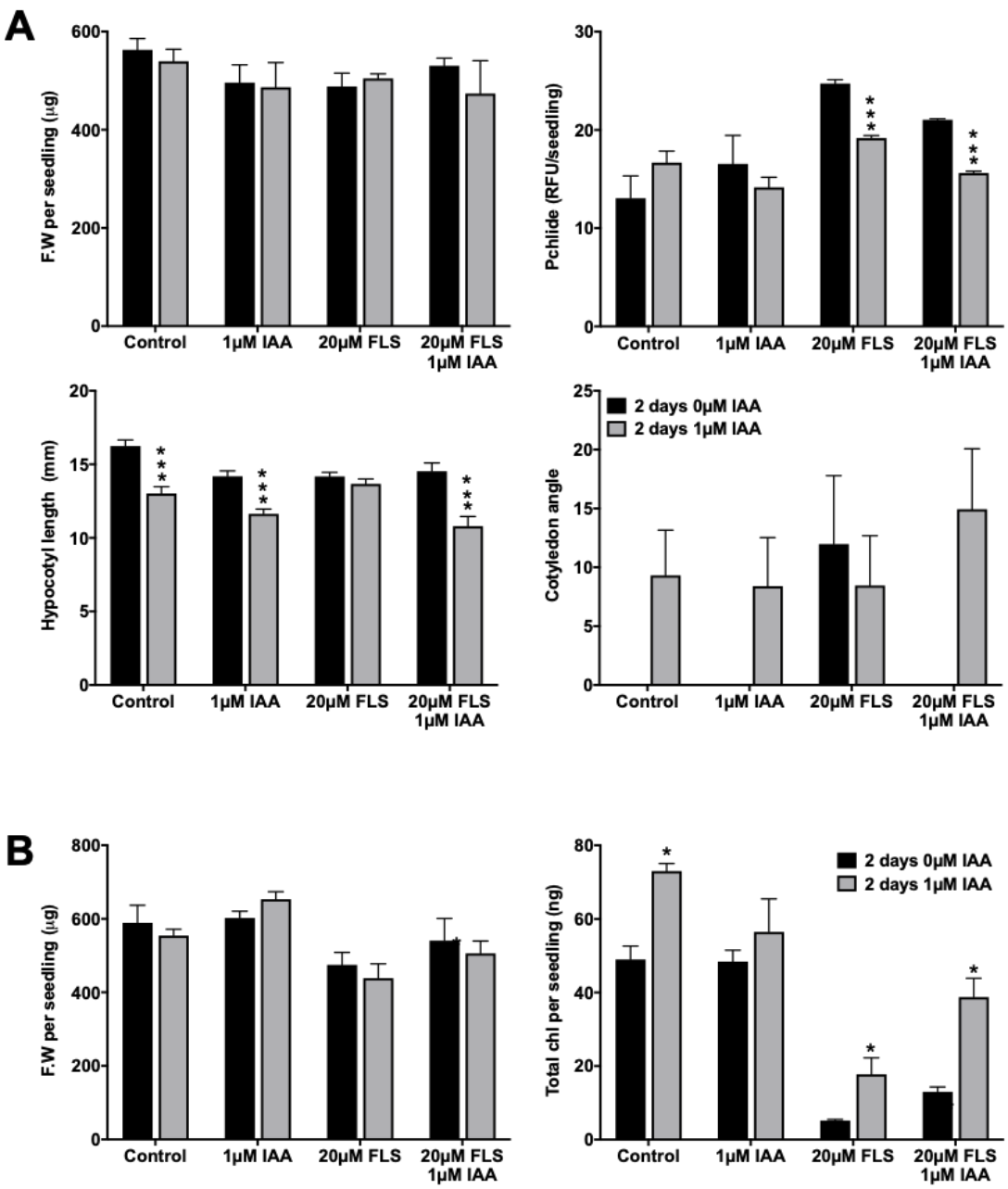

Figure 4.13. Pre-treatment of seedlings with IAA reduces Pchlide accumulation and allows chlorophyll biosynthesis. Col-0 seedlings were grown for 2 days on ½ MS 0.8% agar media with no IAA (black bars) or 1µM IAA (grey bars). Following this, seedlings were transferred to plates with addition of FLS and IAA to indicated concentrations for a further 3 days in the dark (A) and an additional 24-hours continuous WL (B). Data points represent mean ± SEM of three biological replicates, hypocotyl length and cotyledon angle represent mean ± SEM of 18-23 individuals per condition. Asterisks indicate * $p<0.05$, ** $p<0.01$, *** $p<0.001$ between black bars (-IAA pre-treatment) and grey bars (+IAA pre-treatment) by t-test.

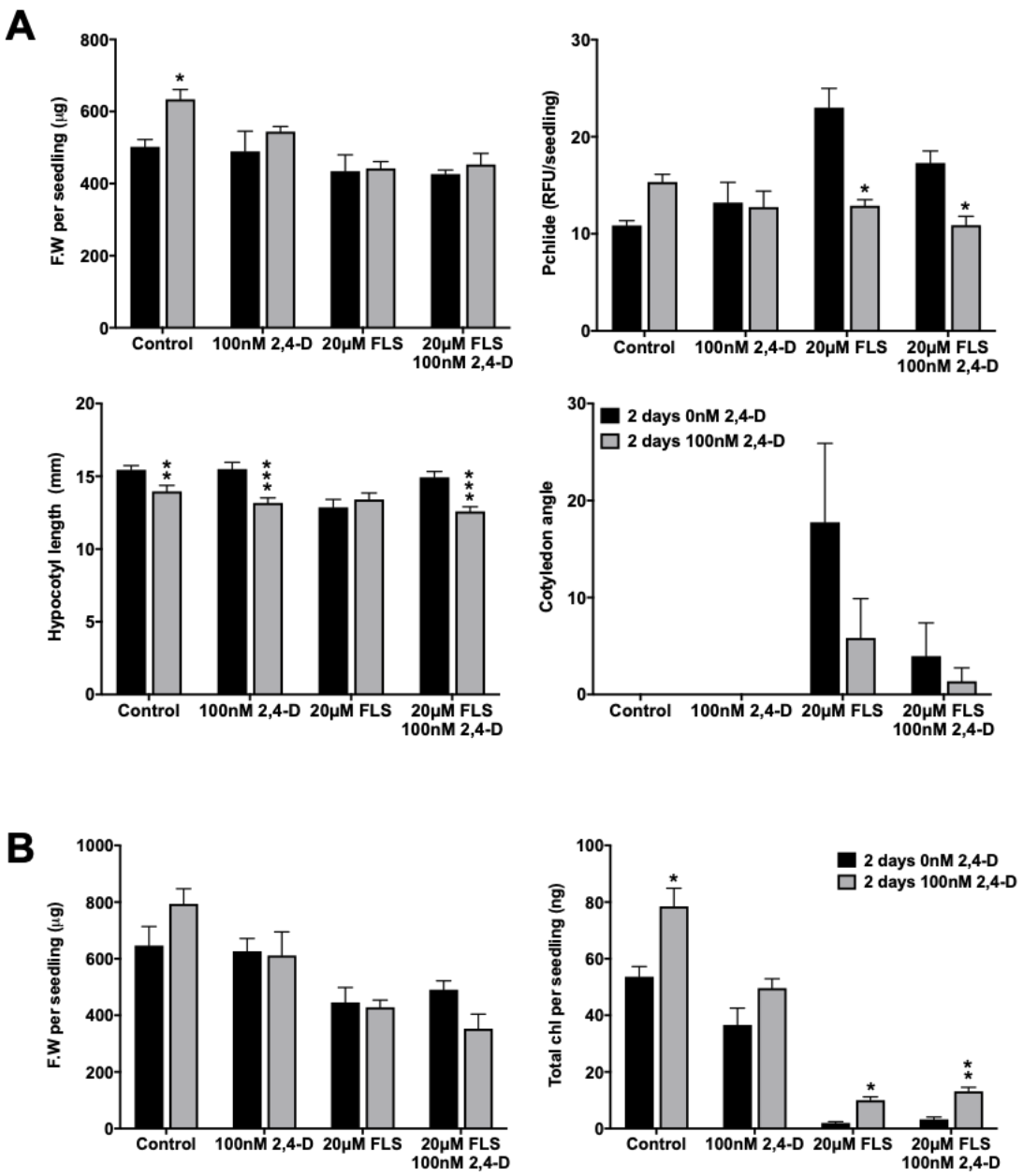

Figure 4.14. Pre-treatment of seedlings with 2,4-D reduces Pchlide accumulation and allows chlorophyll biosynthesis. Col-0 seedlings were grown for 2 days on ½ MS 0.8% agar media with no 2,4-D (black bars) or 100nM 2,4-D (grey bars). Following this, seedlings were transferred to plates with addition of FLS and 2,4-D to indicated concentrations for a further 3 days in the dark (A) and an additional 24-hours continuous WL (B). Data points represents mean ± SEM of three biological replicates, hypocotyl length and cotyledon angle represent mean ± SEM of 18-23 individuals per condition. Asterisks indicate * $p<0.05$, ** $p<0.01$, *** $p<0.001$ between black bars (-2,4-D pre-treatment) and grey bars (+2,4-D pre-treatment) by t-test.

These assays were also completed using 100 nM 2,4-D to compare if natural and synthetic auxin compounds could be used as a treatment. Dark-grown seedlings displayed a very similar pattern of rescue to IAA; fresh wright was largely unaffected apart from an increase in seedlings pre-treated with 100 nM 2,4-D and subsequently grown on normal media (figure 4.14A). In the absence of a 2,4-D pre-treatment (black bars) there was a FLS-dependent increase in Pchlide accumulation that was partially reduced in the presence of 2,4-D, while 2,4D pre-treatment (grey bars) was successful in reducing Pchlide accumulation back to control levels (figure 4.14A). A similar pattern was observed when looking at cotyledon angle, although the variability among individuals was high. Similar to IAA, 2,4-D pre-treatment caused a reduction in hypocotyl length in all subsequent growth conditions except for 20 µM FLS without additional 2,4-D, further supporting the idea that FLS could be blocking the action of auxins. 2,4-D pre-treatment also demonstrated similar outcomes to IAA in the greening assay. There was no discernible effect on fresh weight; however, 2,4-D pre-treatment is sufficient to increase chlorophyll accumulation in FLS-treated seedlings following 24-hours in the light (figure 4.14B). Although chlorophyll levels were not increased to control levels, they were significantly increased compared to seedlings that had not been pre-treated with 2,4-D.

4.2.10 Seed treatment of FLS is phytotoxic to seedlings and reversible by auxin treatment

It has been established FLS induces a de-etiolated phenotype in the dark, perturbs subsequent chlorophyll accumulation when transferred to light and reduces overall growth in the light. In previous assays FLS has been spiked into the media and present throughout the growth period; however, it's efficacy as a seed treatment has not been established. WT *Arabidopsis* seeds were imbibed in water and increasing concentrations of FLS for 24 hours before being grown in 3 light conditions to determine FLS effects. Following 5 days growth in the dark, FLS >20 µM were able to significantly reduce fresh weight by 20% and treatments above 200 µM FLS increased Pchlide accumulation of seedlings by 32%, on average. These significant changes were not coupled with significant difference in morphology (figure 4.15A).

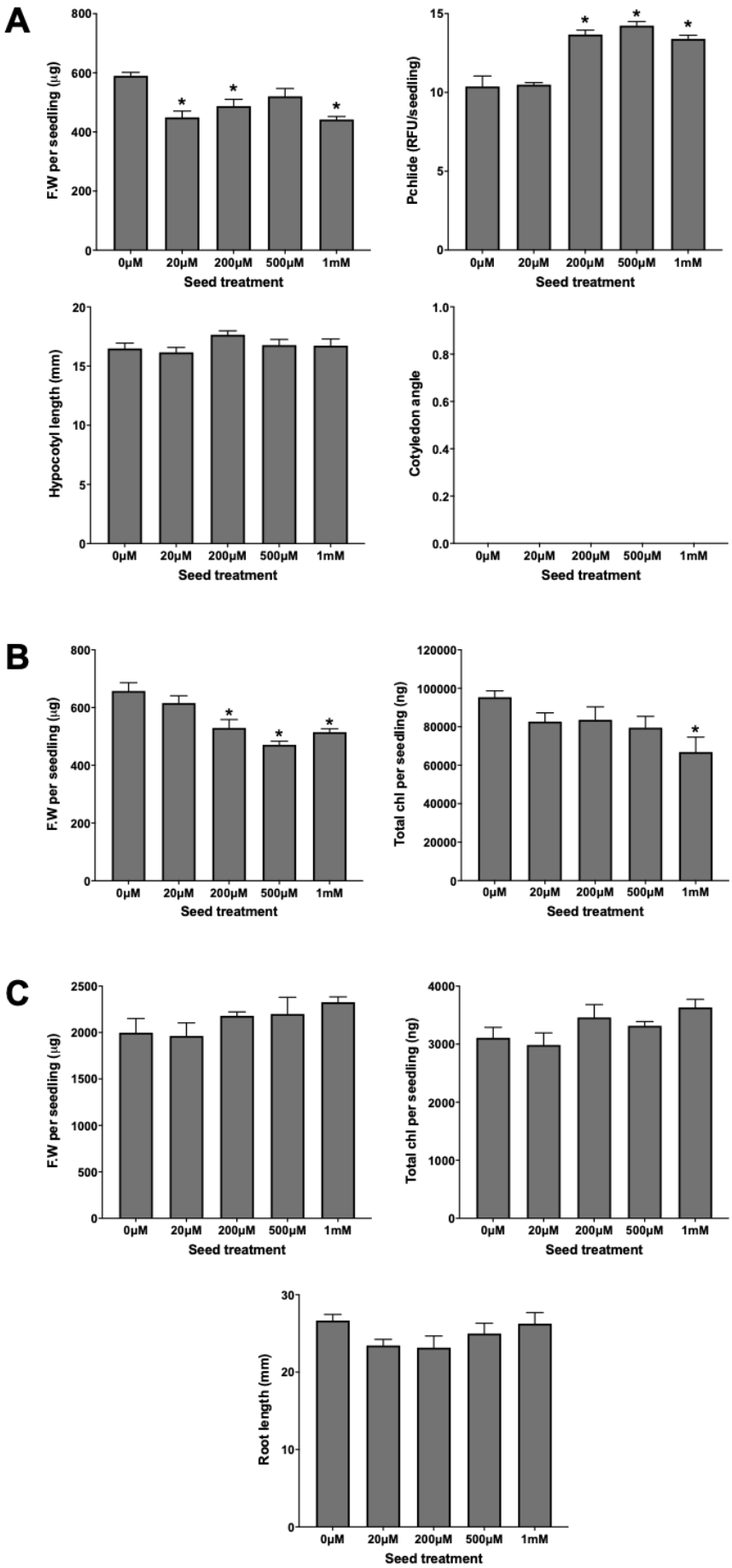
A
F.W per seedling (µg)
Pchlide (RFU/seedling)
Hypocotyl length (mm)
Cotyledon angle
B
F.W per seedling (µg)
Total chl per seedling (ng)
C
F.W per seedling (µg)
Total chl per seedling (ng)
Root length (mm)
0µM
20µM
200µM
500µM
1mM
Seed treatment

Figure 4.15. 24 h seed treatment with FLS is sufficient to induce Pchlide accumulation. Col-0 seed were imbibed for 24-hours in sterile water with indicated amounts of FLS and subsequently grown on ½ MS 0.8% agar media in 3 light conditions: (A) 5 days dark, (B) 5 days dark followed by 24 h light, (C) 7 days continuous light. Data points represent mean ± SEM three biological replicates. Hypocotyl length, cotyledon angle and root length represent mean ± SEM of 17-22 individuals per condition. Asterisks denote P<0.05 in control seedlings compared to FLS treated seedlings by Tukey's post-hoc multiple-comparison test.

In a greening assay >200 µM FLS decreased fresh weight, while only 1 mM was sufficient to reduce subsequent chlorophyll accumulation (figure 4.15B) and after 7 days growth in the light FLS seed treatment had no detrimental effects on growth (figure 4.15C).

As demonstrated previously, the auxins IAA and 2,4-D were able to alleviate a number of FLS-induced phenotypes when applied as a 'pre-treatment' before the seedlings were exposed to FLS. To understand more about this relationship and to explore the potential of using auxins as a seed treatment, seeds were imbibed +/- FLS +/- IAA and subsequently grown on media – FLS (figure 4.16) or +20 µM FLS (figure 4.17) in 3 light conditions. Interestingly, treating seeds with 200 µM IAA inhibited FLS-dependent Pchlide accumulation and reduced Pchlide levels by 40% compared to seeds imbibed in FLS alone (figure 4.16A). A similar pattern was observed for measurements of cotyledon angle; FLS seed treatment alone increased cotyledon opening, while IAA treatment was able to reduce this, but not significantly due to high variability of this response. Seed treatment of IAA only had marginal and not significant effects on seedlings in greening and continuous light assays. IAA seed treatment (grey bars) slightly increased total chlorophyll levels in both assays compared to FLS seed treatment alone (black bars) (figure 4.16B&C). These results were replicated almost exactly in similar assays that treated seeds +/- FLS, +/- IAA, but subsequently grew the seedlings on plates containing 20 µM FLS (figure 4.17). Again, FLS-induced Pchlide accumulation was successfully reversed even in the presence of FLS in the media. This was also true for cotyledon opening in which IAA seed treatment (grey bars) significantly reduced cotyledon opening compared to FLS seed treatment (black bars) (figure 4.17A). In the same manner as the previous study, IAA seed treatment appeared to increase total chlorophyll in both greening and continuous light assays but the differences were not significant (figure 4.17B&C).

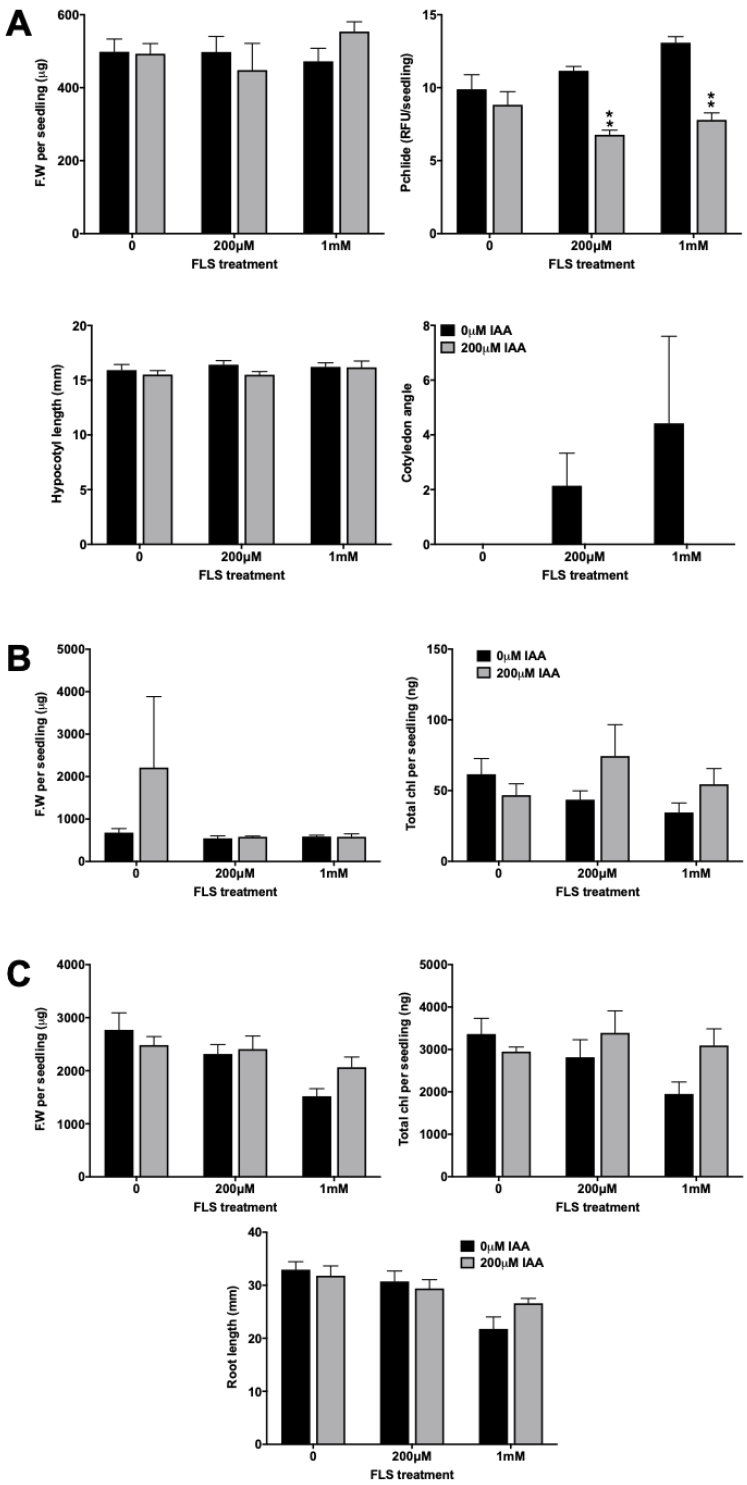

Figure 4.16. 24 h seed treatment with IAA is able offset the effect of an FLS seed treatment. Col-0 seed were imbibed for 24-hours in sterile water with indicated amounts of IAA and/or FLS and subsequently grown on ½ MS 0.8% agar media excluding FLS in 3 light conditions: (A) 5 days dark, (B) 5 days dark followed by 24 h light, (C) 7 days continuous light. Data points represent three biological replicates. Hypocotyl length, cotyledon angle and root length represent mean ± SEM of 15-22 individuals per condition. Asterisks indicate * $p<0.05$, ** $p<0.01$, *** $p<0.001$ between black bars (FLS) and grey bars (FLS+IAA) by t-test.

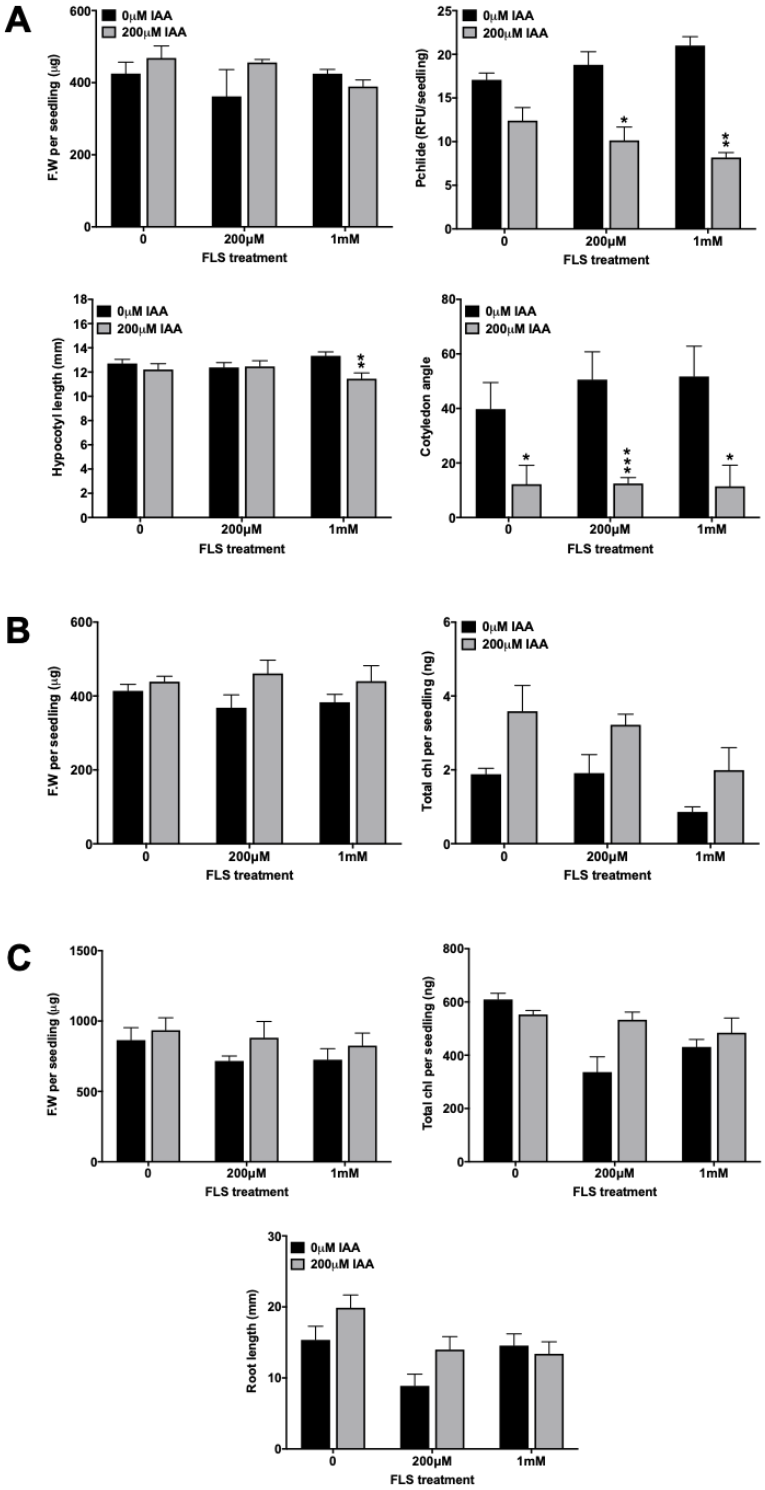

Figure 4.17. IAA seed treatment is sufficient to reduce FLS-induced de-etiolation for seedlings grown in the presence of FLS. Col-0 seed were imbibed for 24-hours in sterile water with indicated amounts of IAA and/or FLS and subsequently grown on ½ MS 0.8% agar media with 20µM FLS in 3 light conditions: (A) 5 days dark, (B) 5 days dark followed by 24 h light, (C) 7 days continuous light. Data points represent mean ± SEM of three biological replicates. Hypocotyl length, cotyledon angle and root length represent mean ± SEM of 13-24 individuals per condition. Asterisks indicate * $p<0.05$, ** $p<0.01$, *** $p<0.001$ between black bars (FLS) and grey bars (FLS+IAA) by t-test.

4.3 Discussion

4.3.1 FLS and auxin present a dichotomous relationship dependent on light conditions

Due to the identification of a number of differentially expressed auxin regulated genes following transcriptomic analysis, a de-etiolated phenotype rescued by exogenous auxins, the reduced response to FLS in the *hy5 hyh* mutant and the understanding that light and auxin signalling pathways are integrated, the role of auxin in FLS mediated de-etiolation was explored using a number of techniques. It was established previously that application of auxins at low micromolar concentrations was sufficient to reverse the effects of FLS in the dark and further work demonstrated this rescue is able to occur even at nanomolar concentrations. The rescue of FLS-induced de-etiolation was not due to a delay in development which is evident in the *ga1-3* mutant. This mutant displays a de-etiolated phenotype that takes longer to emerge due to delayed developmental timing (Alabadí et al., 2004). The maintenance and sensitivity of rescue in FLS+IAA-treated seedlings suggest this effect is not secondary to a general toxicity in the dark. Interestingly, there was a disparity in rescue when treating seeds in the light. IAA dependent rescue of FLS toxicity was minimal, but can be seen after 24 h light after transfer from dark – a physiologically relevant situation, indicating the potential of light signalling interaction in FLS and auxin action.

Further evidence for a role of FLS in the alteration of auxin and light signalling comes from gene expression data demonstrating FLS induced auxin biosynthesis genes in dark-grown seedlings but not light-grown seedlings, while a decrease in IAA gene expression was seen in both conditions. ASA1 is a gene that encodes the alpha subunit of anthranilate synthase, an enzyme that catalyses the first reaction in the tryptophan (Trp) biosynthesis path. CYP79B2 and CYP79B3 encode enzymes that convert Trp to indole-3-acetaldoxime, a precursor of both indole glucosinolates (GSs) and IAA, while TAA1 and YUCCA1 act in the IPyA pathway to convert Trp to IAA in the main Trp-dependent IAA biosynthesis path (Zhao, 2010).

YUCCAs act downstream of TAA1 and are regulated by a number of factors, including PIFs (Müller-Moulé et al., 2016) and are also transcriptionally regulated through a negative feedback mechanism dependent on endogenous auxin levels (Suzuki et al., 2015). In the presence of excess auxin, *YUCCA* expression is downregulated, however in the presence of an auxin biosynthetic inhibitor, *YUCCA* expression is upregulated. Therefore, the upregulation witnessed upon FLS treatment may suggest low endogenous auxin levels in the dark or reduced auxin signalling. In both light- and dark-grown seedlings we also saw significant down regulation in a number of *IAA* genes. To activate transcription of auxin response genes, auxin binds the TIR1/AFB receptor which tags Aux/IAA proteins for degradation. This allows ARF proteins to bind to auxin responsive elements within promoters of target genes, such as *IAAs, SAURs* and *GH3*s (Mockaitis and Estelle, 2008). Downregulation in a number of these auxin responsive genes demonstrated in qPCR and transcriptomic analyses suggests FLS may be either directly or indirectly in the pathway to cause a reduced auxin response. De-etiolation in the dark, characterised by inhibition of hypocotyl elongation, cotyledon opening, expression of light-regulated genes and Pchlide accumulation, coupled with severe effects on primary root elongation and auxin resistance in the light points to FLS targeting a process that connects auxin and light signalling.

Early evidence demonstrated that photoreceptor signalling pathways are able to differentially control cell expansion in hypocotyls and cotyledons through the modification of auxin signalling (Colón-Carmona et al., 2000; Tian et al., 2003). Gain of function mutant, *shy2-2*, which encodes the IAA3 protein, causes a decreased interaction between IAA3 and SCFTIR1 (Tian et al., 2003), resulting in high steady state levels of IAA3 and decreased expression of auxin-responsive genes (Tian et al., 2002). Interestingly, these mutants also display a de-etiolated phenotype when grown in the dark, suggesting the accumulation of IAA3 is affecting light responses (Kim et al., 1998). In the absence of sucrose in the media, light is able to induce expression of IAA3 and this is not seen in the *shy2-2* mutant due to negative autoregulation (Tian et al., 2002). Consistent with the idea that this mutant activates light responses, a number of light-inducible genes such as *LHCB* (*CAB*) are upregulated in the *shy2-2* mutant (Kim et al., 1998). Auxin has been shown to downregulate some light-induced genes (Gil et al., 2001); therefore, the increased

expression of *LHCB* genes in the *shy2-2* mutant could be a result of reduced auxin responses. Furthermore, the *shy2-2* mutant displays comparable levels of light-induced genes to WT when grown in the light which is also true for FLS-treated seedlings.

Studies have also highlighted a molecular convergence of light and auxin signalling to regulate plant development. Mutations in genes encoding phyA and phyB rapidly induce expression of auxin regulated genes, revealing phytochromes as potent repressors of auxin signalling (Devlin et al., 2003). Later, it was shown that photoreceptors, CRY1 and active forms of phyB and phyA can directly interact with various Aux/IAA proteins in response to blue and RL, respectively. Direct physical interactions between the photoreceptors and Aux/IAAs proteins resulted in Aux/IAA protein stabilisation and even prevented interactions of Aux/IAAs proteins with TIR1/AFB receptors (Xu et al., 2018; Yang et al., 2018). It was suggested the photoreceptors outcompete the auxin receptors for Aux/IAA protein binding and subsequent stabilisation allows the interaction between Aux/IAAs and ARF transcription factors, leading to inhibition of ARF-induced gene expression and shorter hypocotyls. CRY1 inhibition of hypocotyl elongation was also demonstrated to be mediated in two ways: the first, by the N-terminal domain of the CRY1 protein stabilising Aux/IAA proteins, while the C-terminal domain interacts with COP1 to stabilise HY5 (He et al., 2015; Yang et al., 2000).

As discussed previously, HY5 and HYH bZip transcription factors are positive regulators of photomorphogenesis (Holm et al., 2002) and their accumulation is rapidly induced by light, following COP1 deactivation (Osterlund et al., 2000; Sibout et al., 2006). HY5 and HYH are also proposed to act as signal integration points between light and hormone signalling networks. Consistent with this suggestion, both *AXR2/IAA7* and *SRL/IAA14* gene expression is repressed in *hy5* and *hyh* mutants (Cluis et al., 2004; Sibout et al., 2006) suggesting HY5 and HYH are negative regulators of the auxin signalling pathway.

The relationship between light and auxin signalling has also been raised when interpreting the effect of FLS and IAA treatment on seedlings. In *Arabidopsis* a number of mutants have been identified that are resistant to the effects of exogenous auxins, named *AXR* mutants. Two of these *AXR* genes encode Aux/IAA repressor proteins IAA7

(*AXR2*) and 17 (*AXR3*) (Leyser et al. 1996; Nagpal et al., 2000) and *AXR1* encodes a ubiquitin-activating E1 enzyme essential in light and auxin signalling (Leyser et al., 1993) and interestingly, both *axr2* and *axr3* mutants show a de-etiolated phenotype in the dark (Nagpal et al., 2000), similar to FLS. Resistance to exogenous auxins was also observed in FLS-treated seedlings in the light. In control seedlings, exogenous application of IAA reduced fresh weight, total chlorophyll and root length of seedlings characteristic of excess auxin treatment; however, FLS treated seedlings did not display the same phenotypes, in fact, root length was significantly increased upon exogenous IAA application. This same relationship was also displayed in the confocal imaging experiments in which application of exogenous IAA did not affect FLS-dependent transcription of the DR5::VENUS reporter or the stabilisation of the DII::VENUS protein. The gain-of-function mutation in *axr2* acts in a similar way to *shy2-2,* stabilising IAA7 and reducing auxin signalling (Timpte et al., 1994); additionally, the *axr1* mutant displays reduced Aux/IAA protein degradation due to mutations within the E1 ubiquitin-activating enzyme that functions to tag Aux/IAA proteins for degradation (Leyser et al., 1993). This suggests the auxin resistance observed in FLS treated samples could be explained by the stabilisation of Aux/IAA proteins. However; the 3 h IAA treatment was sufficient to increase DR5::VENUS transcription and degrade DII::VENUS in dark-grown FLS-treated seedlings, suggesting activation of auxin signalling. This specific effect is only seen in dark-grown seedlings, much like the ability of exogenous auxin to rescue responses to FLS. Thus, there is a dichotomous relationship of auxin and light signalling, exacerbated by FLS.

4.3.2 The role of FLS as an auxin receptor antagonist

Arabidopsis mutants with stabilised Aux/IAA repressor proteins can phenocopy the effects of FLS in multiple aspects including de-etiolation and gene expression profile; however, Aux/IAA stabilisation could be affected in multiple ways. As mentioned previously, the AXR1 protein is required for the function of a ubiquitin-activating E1 enzyme to repress photomorphogenesis in the dark (Leyser et al., 1993). If FLS was affecting transcription of the *AXR1* gene, protein stability of key light and auxin signalling molecules may be maintained in the dark, causing subsequent photomorphogenic growth, characteristic of stabilised HY5, HYH and Aux/IAA repressor proteins. FLS could

also directly be affecting the function of the SCF^{TIR1} complex which acts to degrade the Aux/IAA proteins that negatively regulate auxin signalling, acting as an auxin receptor antagonist. Aux/IAA repressor protein bind TIR1/AFB receptors in an auxin-dependent manner to induce their degradation and initiate ARF-mediated transcription of auxin regulated genes. Stabilised Aux/IAA proteins bind to ARFs and repress auxin signalling; therefore, if there was an inhibition of Aux/IAA protein degradation, these proteins would accumulate and auxin-dependent genes would not be expressed even when auxin biosynthesis was not perturbed.

The potent auxin receptor antagonist, auxinole (α-[2,4-dimethylphenylethyl-2-oxo]-IAA), was designed following *in silico* virtual screening for TIR1/AFB receptor antagonist activity. This molecule competitively inhibits a number of auxin responses in *Arabidopsis* and molecular docking analysis demonstrates the compound's phenyl ring is able to form a strong interaction with Phe82 of the TIR1 receptor, a key residue essential for Aux/IAA protein docking (Hayashi et al., 2012). In the TIR1-IAA-Aux/IAA complex, auxin binds to TIR1 and the tryptophan and second proline residues in the WPPV motif in domain II of the Aux/IAA proteins form a hydrophobic interaction with the aromatic ring of IAA. This increases the binding affinity of Aux/IAA, allowing IAA to act as a 'molecular glue' (Tan et al., 2007) . Phe82 of TIR1 has a role in binding both IAA and Aux/IAA proteins (Hao et al., 2010); therefore, auxinole was designed to block binding of the WPPV motif to Phe82 of TIR1. The IAA moiety of auxinole is positioned in TIR1 in the same coordination as IAA; however, the phenyl ring in auxinole forms a hydrophobic interaction with Phe82 to prevent the access and subsequent docking of Aux/IAA proteins. Auxinole also has two additional methyl groups on its phenyl ring that limits its rotation and enhances antagonistic activity (Hayashi et al., 2012). Additionally, pull-down assays indicate auxinole is able to reduce IAA-dependent binding of the IAA7 degron peptide leading to stabilisation of these Aux/IAA repressor proteins *in vivo*.

Exposure to FLS for as little as 15 minutes caused rapid DII::VENUS stabilisation and comparisons to various auxin inhibitors initially suggested FLS was not acting to rescue auxin biosynthesis or transport. Interestingly, a similarity was observed between the effects of FLS and auxinole; both compounds caused de-etiolation that subsequently

reduced chlorophyll production in the light and reduced plant growth in the light. Further studies with the partial auxin receptor agonist, p-Chlorophenoxy isobutylic acid (PCIB) (Oono et al., 2003), indicate the similarity between FLS and auxinole effects, including the dynamics of signalling in the root tip. PCIB was not able to mirror DII::VENUS stabilisation or de-etiolation, only reduce growth in the light; although it has been shown PCIB cannot fully antagonise all auxin-dependent responses (Hayashi et al., 2008), potentially explaining the disparity.

Further evidence for a role of FLS as an auxin antagonist comes from studies on the TIR1/AFB family of auxin receptors. TIR1 and 5 AFB proteins make up a small family of auxin receptors (Dharmasiri et al., 2005) that link auxin perception to Aux/IAA protein degradation. Treating a number of single, double and triple *tir1/afb* mutants with FLS resulted in only a partial resistance in the triple mutant lines; however, these genes have overlapping functions and act in a partially redundant fashion to mediate auxin responses (Dharmasiri et al., 2005). Interestingly, in the absence of FLS, the double and triple *tir1/afb* mutants displayed increased Pchlide and partial cotyledon opening suggesting a role of TIR1/AFB proteins in the maintenance of an etiolated phenotype.

In the case of FLS, light signalling is clearly induced in the dark. This suggests positive regulators of photomorphogenesis, such as HY5 and HYH, are stabilised. This then, in turn, is assumed to reduce auxin signalling, characterised by reduction in *IAA* gene expression and inhibition of hypocotyl elongation. The mechanism by which FLS is directly acting is yet unknown. However, given the fact Aux/IAA protein stabilisation via auxin receptor antagonist treatment or mutations in auxin receptors leads to similar phenotypes, it can be suggested that FLS may also be acting to inhibit receptor activity and stabilise Aux/IAA proteins.

4.3.3 Auxins may have a role in protecting against FLS phytotoxicity in the field

Auxin rescue of FLS-induced de-etiolation initiated further studies to explore the potential role of auxin as a treatment to reverse FLS phytotoxicity in the field. FLS phytotoxicity is not observed in the majority of applications to crop species (Morris et al., 2015; Noe et al., 2015; Oka, 2014; Oka et al., 2009; 2012). However, foliar application of elevated levels of FLS, above what is used commercially, resulted in reduced growth in tomato and eggplant (Giannakou et al., 2019; Morris et al., 2016). In *Arabidopsis* it was determined phytotoxicity came from the chloro-thiazole-sulfone scaffold (personal communication, ADAMA) and it was suggested the reduced shoot and root growth was down to a disruption in phytohormone signaling (personal communication, ADAMA).

Any potential treatments to alleviate yield loss in the field is useful information to enhance FLS commercial use; therefore, the role of exogenous auxins was investigated. Exogenous application of IAA, but not 2,4-D, allowed FLS-treated seedlings to accumulate chlorophyll following a period of growth in the dark, while both auxins were successful in ameliorating FLS effects even when applied before FLS exposure, suggesting auxins could function as a protective treatment.

The use of auxin analogues as herbicides is long standing, with 2,4-D being the most commonly and widely used compound in this group (Costa and Aschner, 2014; Quareshy et al., 2018). Its primary function is to promote the uncontrolled growth of dicots, but not monocots, allowing this compound to be successfully used for weed control in crop fields. Its relative specificity for dicots, moderate acute toxicity in humans and low development of resistance (Busi et al., 2018) has led to a sustained role in agriculture. The use of the natural auxin, IAA, is less common; however, its use as a fertilizer has been studied in cereal crops. The effects of auxin (IAA) and its precursor L-tryptophan were studied when added to nitrogen-enriched compost (NEC). It was found that enrichment of 50% NEC with L-tryptophan and IAA improved yield and nutrient uptake of cereal crops, although L-tryptophan was more effective than pure IAA (Ahmad et al., 2008).

FLS seed treatment was sufficient to bring about a reduction in growth and even a small reduction in growth could scale up in the field to result in significant yield losses. Treating seeds with IAA was able to overcome this growth reduction by FLS and was even able to increase seedling growth in the presence of FLS, demonstrating IAA may have a role in protection against FLS.

Seed treatments are commonly used within agriculture and refer to the application of certain agents to seeds prior to sowing for the control of pests that attack seeds, seedlings or plants. Primarily, seed treatments are to minimize the effects of early season insects and seed-borne disease in a sustainable manner. The more environmentally friendly options such as crop rotation, sanitation and ploughing are not effective enough to support necessary crop yield for the growing agricultural sector, while chemical control methods bear their own disadvantages including cost, non-target organism toxicity and health hazards (Sharma et al. , 2015). Seed treatment, be it basic dressing or coating and pelleting, could provide a good practice in order to balance effective pest management while ensuring cost effectiveness and reduced effects on ecosystems. Plant disease prevention through the use of fungicidal seed treatment on small grain cereal crops has been extremely successful (Mathre et al., 2001). Seed treatments to control nematode infestation are also currently on the market including Syngenta's 'Cruiser Maxx Potato Extreme' to control the soybean cyst nematode and Bayer Crop Science's VOTiVO™ (*Bacillus firmus*) to reduce nematode impact (Crop Protection Monthly, 2014). Seed treatments are available for a number of different chemical classes demonstrating the possibility of using FLS as a nematicidal seed treatment, in conjunction with auxin derived compounds to reduce potential phytotoxicity. Although appropriate concentrations are required to promote growth and prevent auxin acting as a herbicide.

Chapter 5: A forward genetics approach to identify targets that facilitate FLS susceptibility

5.1 Introduction

Molecular genetic analysis requires an organism that is well-characterised and easily manipulated. As discussed previously, *Arabidopsis* is well-suited to manipulation and continues to be a useful model organism to conduct genetic screens, allowing identification of genes and characterisation of defined mutants. Due to the fact that a high number of *Arabidopsis* mutants have been identified and characterised, using this organism for mode of action studies allows identification of a phenocopy for FLS treatment that could indicate a possible FLS target. It also lends particularly well for mode of action studies on agricultural products due to the fact the results may be directly applicable to crop species or identify a potential target in crop species for further study. Studies utilising existing *Arabidopsis* mutants have provided insight into the molecular mode of action for herbicides, such as Dicamba (Gleason et al., 2011) and Flufenacet, (Lechelt-Kunze et al., 2003) allowing development of herbicide resistance in crop plants.

Forward genetic screens in *Arabidopsis* also allow for mode of action studies through studying gene function through the identification of a desired phenotype (Page and Grossniklaus, 2002; Bolle et al., 2011). This is achieved following mutagenesis of a large number of WT seeds, either with a chemical mutagen or irradiation. Chemical treatments such as ethyl methane sulfonate (EMS) introduces many mutations in each plant and it is suggested that it is possible to find a mutation in any gene through screening fewer than 5000 plants from the M1 generation (Greene et al., 2003). In most cases the M1 seed is grown to maturity and the seeds (M2) are screened for the desired phenotype, allowing recessive mutations to be recovered. Dominant mutations in the M1 generation have also been reported (McConnell et al., 2001), but this is rare. The use of forward genetic screens in *Arabidopsis* has been fundamental in identifying genes involved in photomorphogenesis through screening for mutants that show defects in seedling development. The *long hypocotyl (hy)* (Chory et al., 1989; Koornneef et al., 1980)*, det* and *cop* (Chory et al., 1989; Deng et al., 1991) mutants discussed previously were all identified through this method.

Forward genetic screens for gene targets of chemicals using EMS have also been carried out to successfully to identify genes that underpin resistance of the herbicides chlorsulfuron and imidazolinone (Jander et al., 2003). M2 generation plants were grown on concentrations of herbicides that induced 100% lethality and lines that were able to survive were selected, grown to maturity and seed from these plants were screened in the next generation to confirm resistance. All resistant mutants were backcrossed to WT and F1 plants were all resistant, indicating mutations were dominant. All mutations in the chlorosulfuron-resistant lines had the same nucleotide change in the *CSR1* gene and three nucleotide changes in the *CSR1* gene were present in imidazolinone-resistant lines (Jander et al., 2003). Forward genetic screens have also been carried out that identified reduced sensitivity to sulfanilamide compounds used as antimicrobial chemotherapeutics. Seedlings were grown in the presence of 3µM sulfanilamide and lines with reduced sensitivity and enhanced sensitivity were selected. Mutations were mapped to genes with no functional annotation, however, it was the first demonstration of such phenotypes for either gene (Schreiber et al., 2012). This suggests *Arabidopsis* is a viable organism to use in mode of action studies on both clinical drugs and agricultural products.

In this chapter EMS mutagenesis to identify FLS resistance will be discussed with particular focus on isolation and characterisation of potentially-resistant lines selected from the M2 generation. A forward genetic screen using EMS has previously been carried out on *C. elegans* using 1mM FLS for 24h as a selection protocol for resistance. Two strains were selected that were able to develop to an adult stage and propagate, however, development and propagation were poor. One strain retained a higher pumping rate on FLS compared to WT, however, this strain still died when left for 48h on 1mM FLS (Kearn, 2015). This suggests there was only low-level resistance and neither strain has mutations in the major target of FLS. Furthermore, at 1mM it is certainly possible that FLS interacts with multiple targets, hence multiple mutations would be required for high-level resistance. In this chapter the aim was to use a selection protocol that will only require a single mutation to acquire high-level FLS resistant *Arabidopsis* lines. From this the mutation may be mapped to a single gene and the mode of action of FLS can be ascertained.

5.2 Results

5.2.1 Determination of mutagenesis and screening protocol

In order to optimise the conditions for the screen, the FLS concentration to be used and mutagen effectiveness were assessed. Due to the large numbers of seeds planning to be screened, the candidate concentration of FLS to use was required to be high enough to determine a discernible difference between seedlings that displayed resistance or not, but low enough to allow the possibility of resistance and recovery of resistant seedlings. The screening conditions used were either under continuous WL or a dark to light greening assay and based on data shown in chapter 3, 50 µM was suggested to be a suitable concentration. This concentration gave a clear visual difference between control and FLS-treated seedlings and all phenotypic measurements recorded were significantly lower when treated with 50 µM FLS.

To confirm 50 µM FLS was an appropriate concentration to use in the screen, a penetrance test was carried out in which WT seedlings were grown for 7 days in continuous WL on media ±50 µM FLS. Seeds were sown individually on 9cm plates, the same manner planned for the screen. After 7 days growth, none of the 2,050 WT seeds on 50 µM FLS displayed a phenotype comparable to the untreated WT seeds, suggesting 50 µM FLS was sufficient to minimise the possibility of a false positive (figure 5.1A). No quantitative recordings were taken on these seedlings as selection of potential resistant mutants in the screen would, initially, be carried out visually and later confirmed quantitatively.

As the protocol for EMS mutagenesis is very variable in terms of EMS concentrations and exposure time, an initial small-scale mutagenesis was carried out using 4 concentrations of EMS. Around 1500 WT *Arabidopsis* seeds (M_1 seed) per condition were treated with 0.25, 0.5, 0.75 or 1% (w/v) EMS for 4 hours and continually agitated to ensure all seeds were exposed. These seeds were grown to maturity in pools of ~10 and allowed to self-fertilise. The resulting M_2 seeds were used to determine mutagen effectiveness in preparation for a large-scale mutagenesis. Germination, bleaching and growth were recorded to compare the effects of increasing EMS concentration. Germination of M_2

seed was decreased to a large extent in the 0.5 and 0.75% conditions, whereas 0.25% and 1% had a rate similar to untreated seed (figure 5.1B,C). This could suggest 0.5% EMS was the concentration causing more mutations; however, when growing the initial M_1 seed to maturity it was noted that seeds treated with 0.75% or 1% EMS had extremely low viability and the plants that were able to grow to maturity were mostly sterile. Therefore, the M_2 seed that was able to be collected following 0.75% or 1% EMS were likely more viable than seed from plants treated with 0.25% and 0.5% EMS. A similar pattern was evident when recording the number of individuals that were bleached or had reduced growth with 0.5% displaying the highest rates consistently (figure 5.1B, C). In conclusion, the mutagen was able to induce an effect at all concentrations tested and in subsequent large-scale mutagenesis 0.75% EMS was used.

5.2.2 Isolation of FLS resistant mutants

Following treatment of seeds with 0.75% EMS, 608 pools of M_1 plants, averaging ~8 plants per pool were harvested, giving seed from an estimated ~4800 M_1 generation plants for screening. M_1 plants were allowed to self to permit recessive homozygous mutations in the M_2 generation. M_2 seeds from these 608 pools were screened in two conditions: continuous WL and a greening assay. An average of around 500 seeds were sown per pool/per plate/per screening condition, giving an estimate of ~608,000 M_2 seeds screened from the ~4800 M_1 individuals. From these 608,000 seeds screened, 94 potential resistant lines were selected, recovered and grown to maturity to assess if resistance has been retained in this generation (figure 5.2 for method of screening).

Eighty-seven of the 94 individuals were selected from the continuous light screens on their ability to grow significantly better on 50 µM FLS compared to the majority of the population and a WT population grown on the same plate. Individuals were primarily selected for increased aerial tissue growth, primary root elongation and greening. The other 7 individuals were selected from greening assays conducted on 50 µM FLS. These individuals were selected on their ability to produce chlorophyll after transfer to WL. This screen seemed to be more stringent, only leading to a small number of individuals being selected by this method.

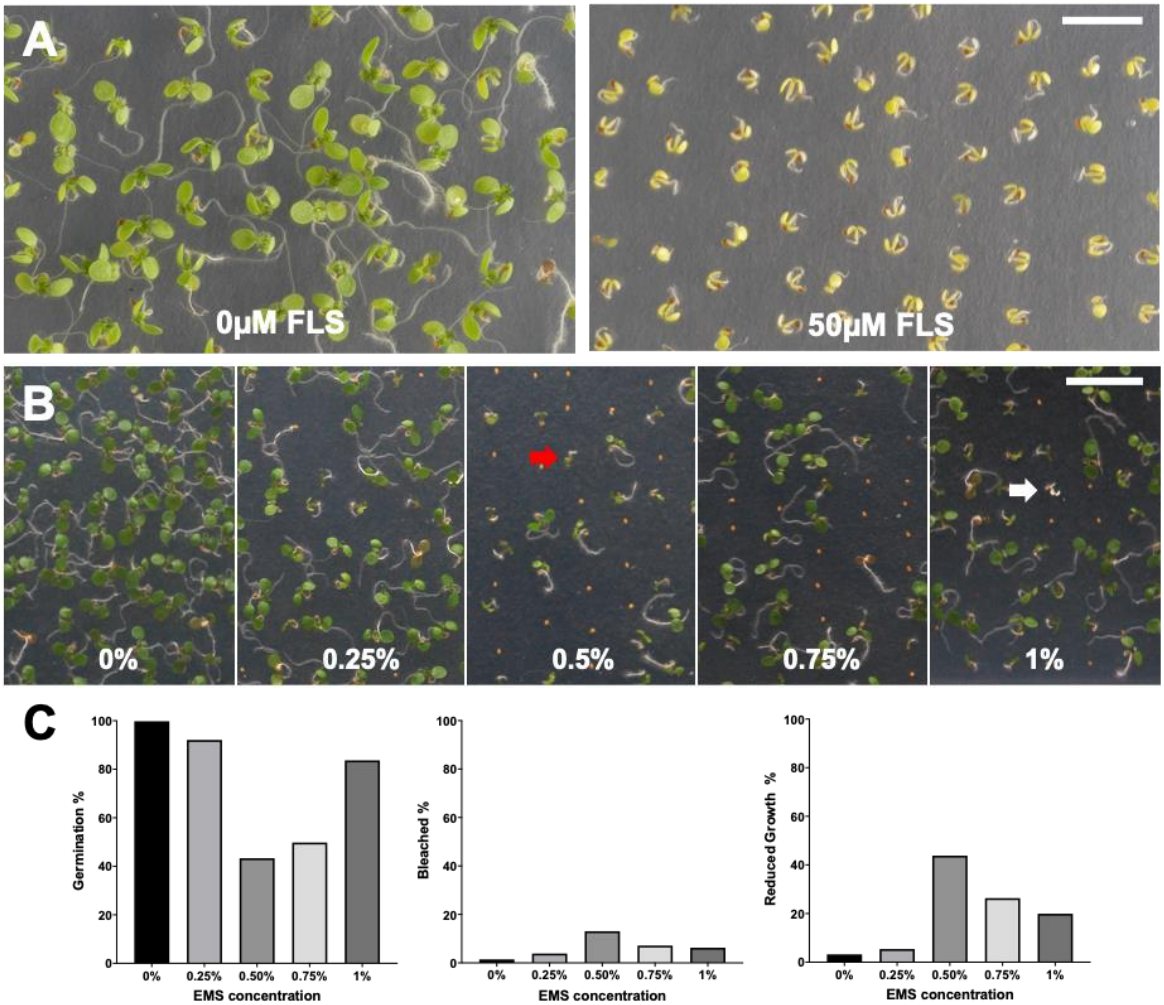

Figure 5.1. EMS mutagenesis of *Arabidopsis* seedlings. (A) Preliminary screen to test for penetrance of the FLS concentration used in the mutagenesis screen. WT (Col-0) seedlings grown for 7 days in continuous light on media with addition and omission of 50µM FLS for comparison. A total of 2050 WT individuals were tested over two time periods. (B) M2 progeny, from ~1500 WT (Col-0) mutated M1 parental lines per condition, were harvested and grown on media for 7 days in continuous light to determine mutagen effectiveness. 900 individuals per condition. Red arrow represents seedling with reduced growth and white arrow indicates a bleached seedling. (C) Visual abnormalities including germination, bleaching and reduced growth (defined by cotyledon breadth <2mm) were recorded. Scale bars represent 1cm.

The names of each mutant represent the % EMS used, the pool number (#) and the number of separate individuals selected from the same pool (x). However, for ease of reference in further work, each individual is referred to by a single number, denoting the timeline in which they were screened and selected (appendix table S9). Each potentially resistant line was rescued from FLS and grown to maturity on soil.

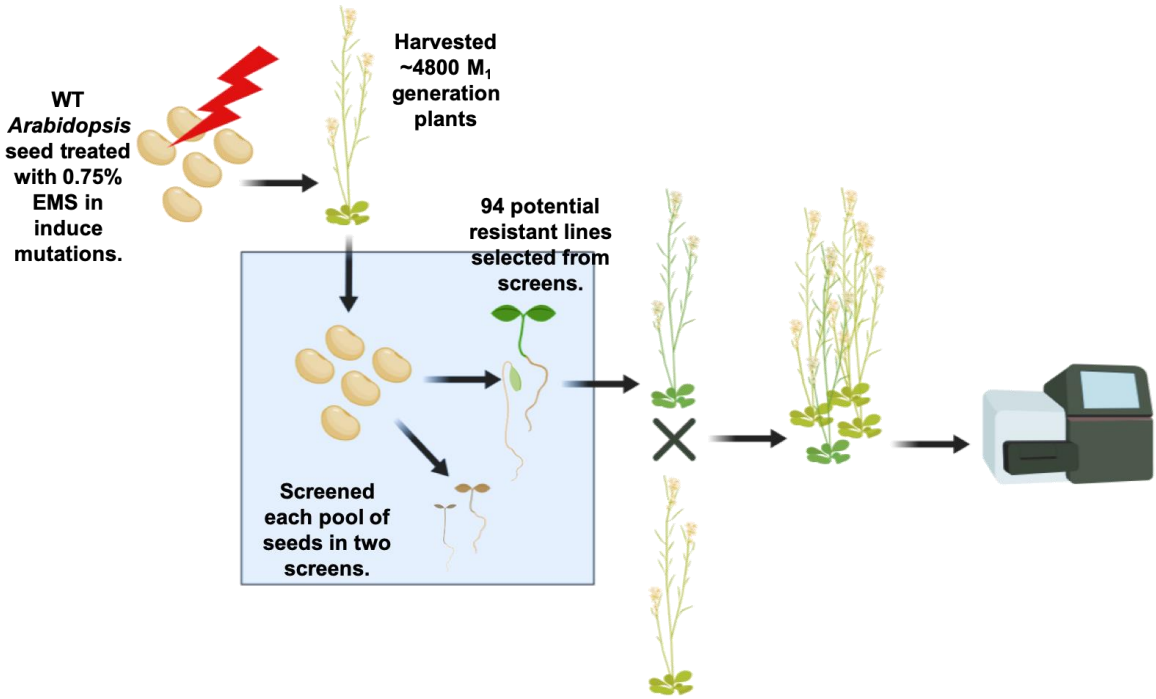

Figure 5.2. Schematic of forward genetic screen. WT *Arabidopsis* seed was treated with EMS and allowed to grow and self-fertilise to form an M_2 seed that was screened on FLS. All M_1 pool were represented in the screen. Resistant lines were selected, back-crossed and segregated for sequencing and SNP mapping.

They were then allowed to self-fertilise to produce M_3 seed. This generation of seeds from each of the 94 lines was then subjected to a re-screening protocol +/- 50 µM FLS, alongside WT. Fresh weight, total chlorophyll and primary root length were quantified to identify the most resistant lines (figure 5.3, appendix figure S1). In some cases, lines appeared to have lost resistance to FLS. However, a number of lines were able to display improved growth and this was particularly evident when measuring primary root length (figure 5.3; table 5.1). Focussing on primary root elongation, as this was a prominent selection characteristic, a number of patterns were observed in mutants. Either they displayed WT levels of growth, which was the case for the majority of lines, decreased growth +/- FLS (table 5.1), or increased growth. Increased growth could be further subdivided into separate categories: increased growth with and without FLS or increased growth only with or without FLS. From these analyses, six mutants determined to demonstrate the highest level of resistance were selected for further analysis.

Table 5.1. Significant changes in root length of mutant lines compared to WT following a re-screen on 50 µM FLS. Numbers refer to mutants in appendix figure S1.

	No. of lines
No Change	34
Increase +/- FLS	10
Increase – FLS only	16
Increase + FLS only	12
Decrease +/- FLS	5
Decrease – FLS only	9
Decrease + FLS only	2
Decrease – FLS, Increase + FLS	3

Five mutants, #22, 61, 69, 93 and 94, all displayed significantly increased primary root length on 50 µM FLS compared to WT in the absence of improved growth on 0 µM FLS (figure 5.3A, C-F). In addition, mutant #51 displayed increase root length in both the absence and presence of FLS, compared to WT (figure 5.3B), potentially suggesting a mutation that allow increased primary root elongation and may provide a good comparison to other lines.

5.2.3 Secondary screening of selected resistant lines

The 6 lines taken forward were subjected to a more in-depth study of their resistance. Each line was assayed in 3 growth conditions: 7 d WL, a greening assay transferring from dark to light, and 5 d dark. Looking at each line, in continuous light #22 was able to significantly increase fresh weight, total chlorophyll and primary root length on 50 µM FLS compared to WT by 40%, 67% and 96%, respectively. In the dark, #22 increased fresh weight by 66% and decreased FLS-induced Pchlide accumulation by 51% but did not affect morphology. Additionally, in the greening assay, an increase in fresh weight and total chlorophyll was measured; 22% and 474%, respectively (figure 5.4). In line #51, increased growth was also observed; however, this was only in fresh weight or root and hypocotyl length and occurred both in the presence and the absence of FLS. Chl and Pchlide levels remained unchanged in #51 (figure 5.5). This indicates line #51 could be carrying a mutation to enhance cell elongation and does not confer true FLS resistance. Lines #61, #69, #93 and #94 displayed intermediate levels of FLS resistance (figures 5.6-9) summarized in table 5.2.

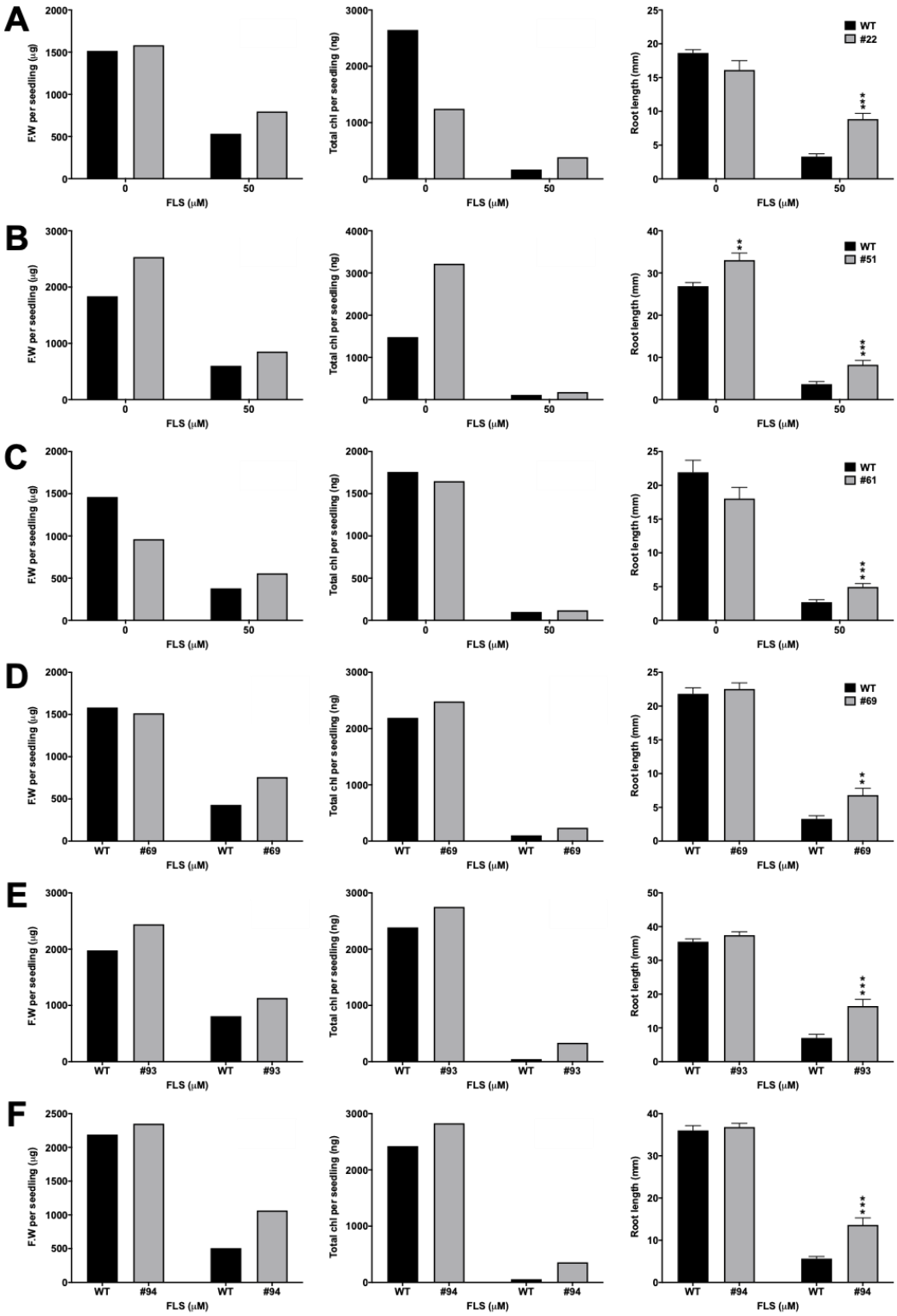

Figure 5.3. Re-screen of 6 lines that show the highest level of FLS-resistance. WT seedlings were grown in WL alongside each line for 7 days light on ½ MS 0.8% agar media with addition of FLS to 50 µM. Vehicle control condition included addition of 0.1% (v/v) DMSO to media. Fresh weight and total chlorophyll data points represent the mean of one biological replicate, root length data points represent the mean ± SEM of 7-30 individuals per condition. Asterisks indicate * $p<0.05$, ** $p<0.01$, *** $p<0.001$ between WT seedlings and resistant lines by t-test.

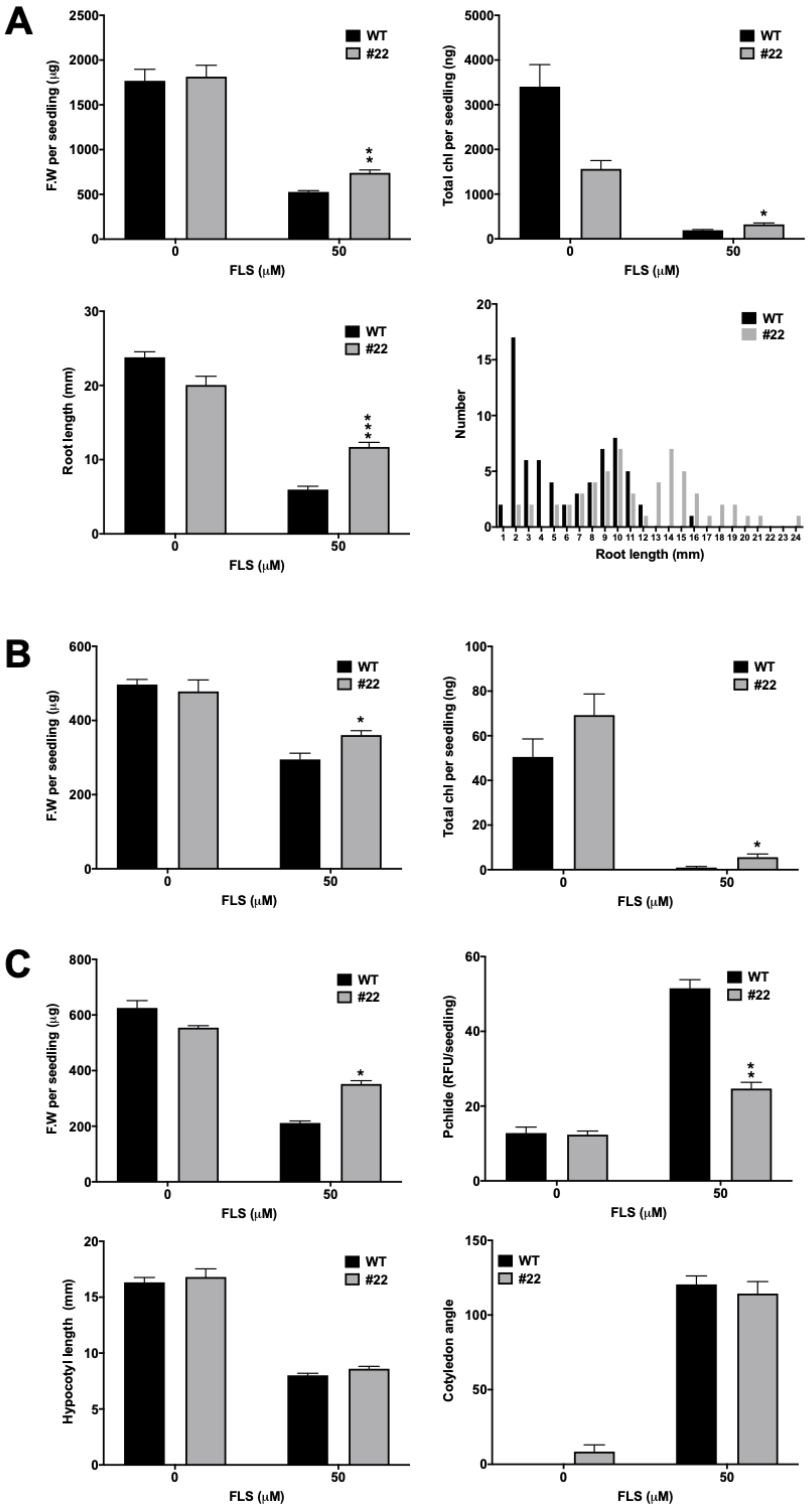

Figure 5.4. Performance of FLS-resistant line #22 in 3 growth conditions. WT seedlings were grown alongside line #22 for 7 days light (A), 5 days in dark + 24 h light (B) and 5 days in the dark (C) on ½ MS 0.8% agar media with addition of FLS to 50 µM. Vehicle control condition included addition of 0.1% DMSO to media. Fresh weight, Pchlide and total chlorophyll data points represent the mean ± SEM of three biological replicates, cotyledon data and root length data points represent the mean ± SEM of 16-60 individuals per condition. Asterisks indicate * $p<0.05$, ** $p<0.01$, *** $p<0.001$ between WT seedlings and resistant lines by t-test.

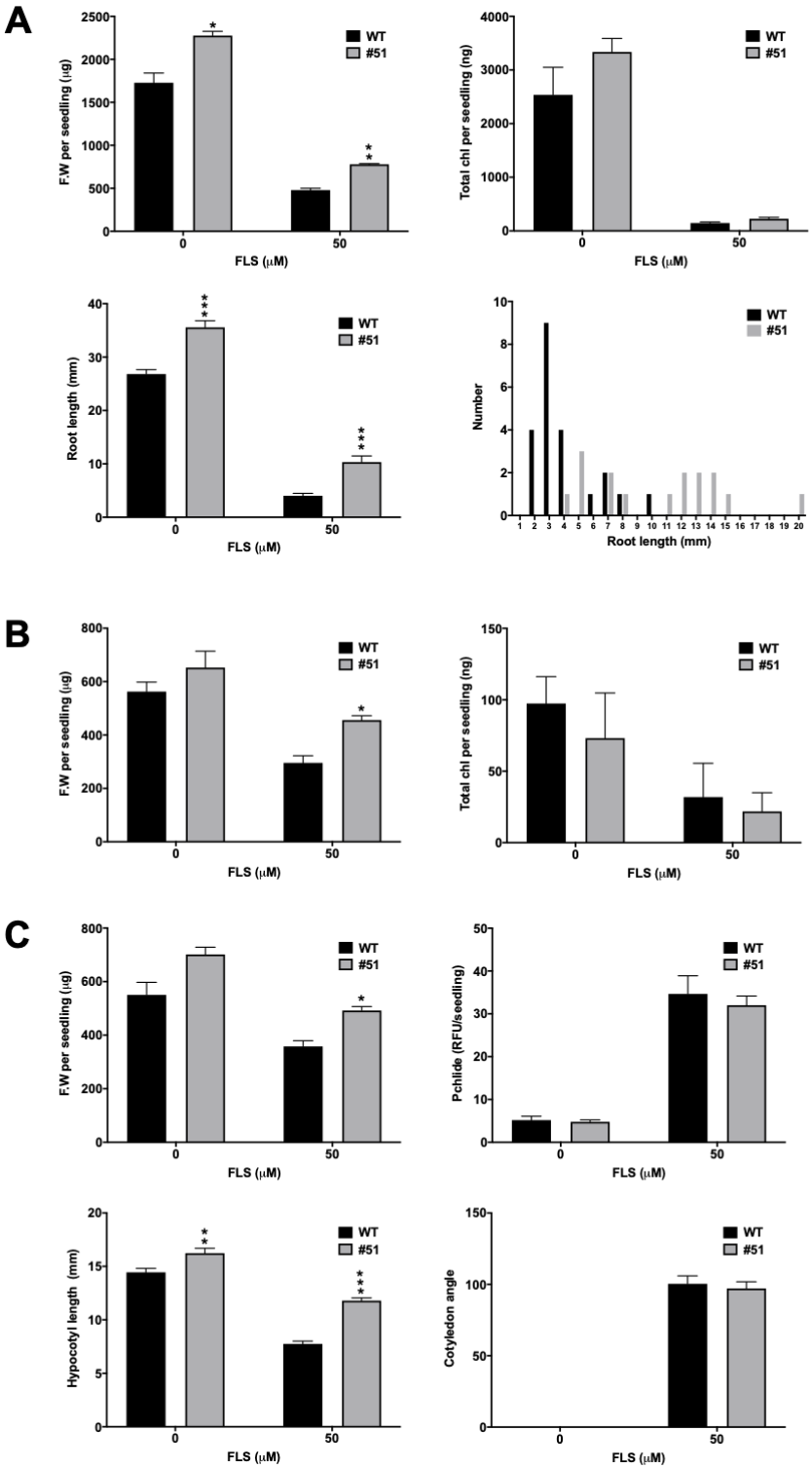

Figure 5.5. Performance of FLS-resistant line #51 in 3 growth conditions. WT seedlings were grown alongside line #51 for 7 days light (A), 5 days in dark + 24 h light (B) and 5 days in the dark (C) on ½ MS 0.8% agar media with addition of FLS to 50 µM. Vehicle control condition included addition of 0.1% DMSO to media. Fresh weight, Pchlide and total chlorophyll data points represent the mean ± SEM of three biological replicates, cotyledon data and root length data points represent the mean ± SEM of 16-22 individuals per condition. Asterisks indicate * $p<0.05$, ** $p<0.01$, *** $p<0.001$ between WT seedlings and resistant lines by t-test.

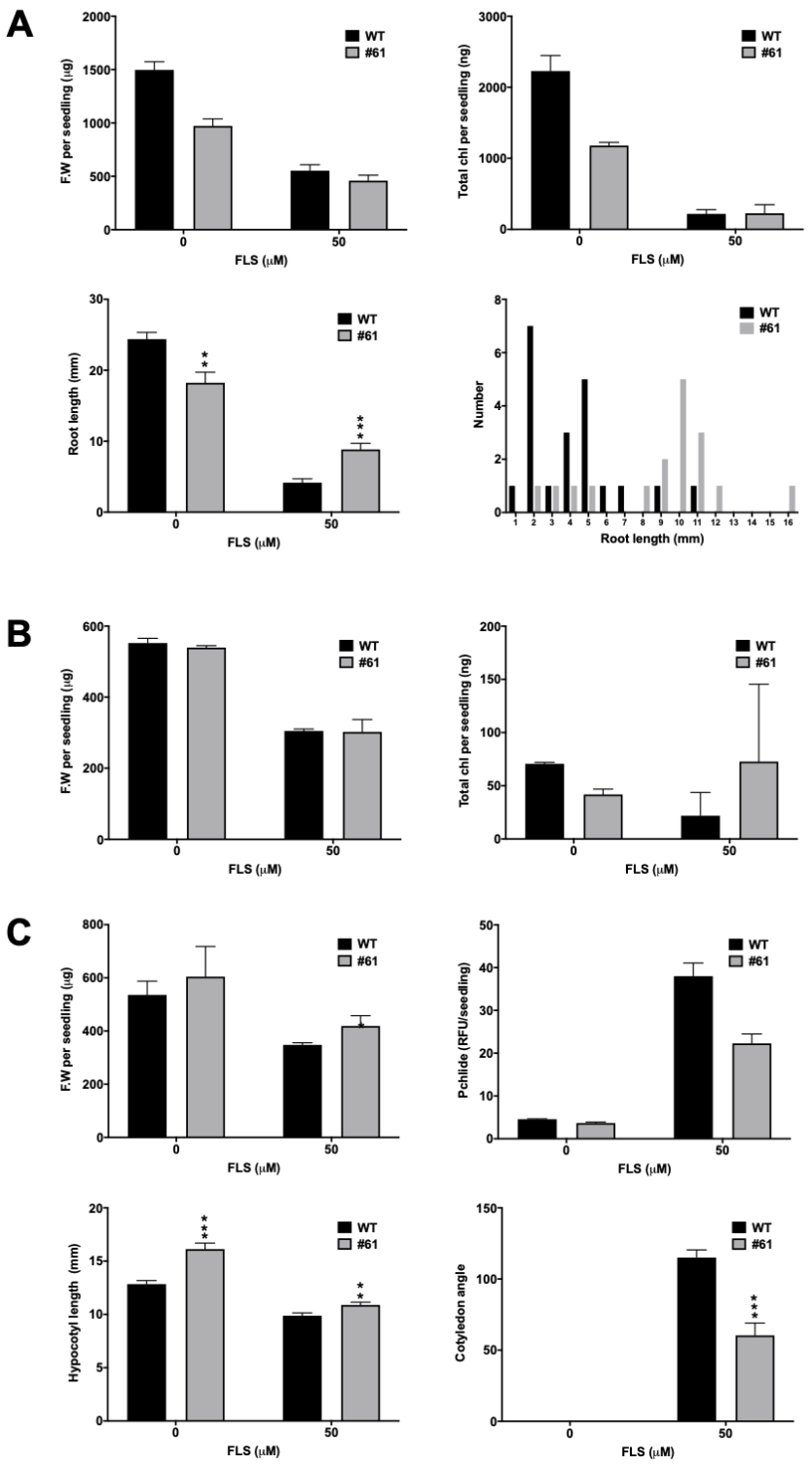

Figure 5.6. Performance of FLS-resistant line #61 in 3 growth conditions. WT seedlings were grown alongside line #61 for 7 days light (A), 5 days in dark + 24 h light (B) and 5 days in the dark (C) on ½ MS 0.8% agar media with addition of FLS to 50 µM. Vehicle control condition included addition of 0.1% DMSO to media. Fresh weight, Pchlide and total chlorophyll data points represent the mean ± SEM of three biological replicates, cotyledon data and root length data points represent the mean ± SEM of 14-21 individuals per condition. Asterisks indicate * $p<0.05$, ** $p<0.01$, *** $p<0.001$ between WT seedlings and resistant lines by t-test.

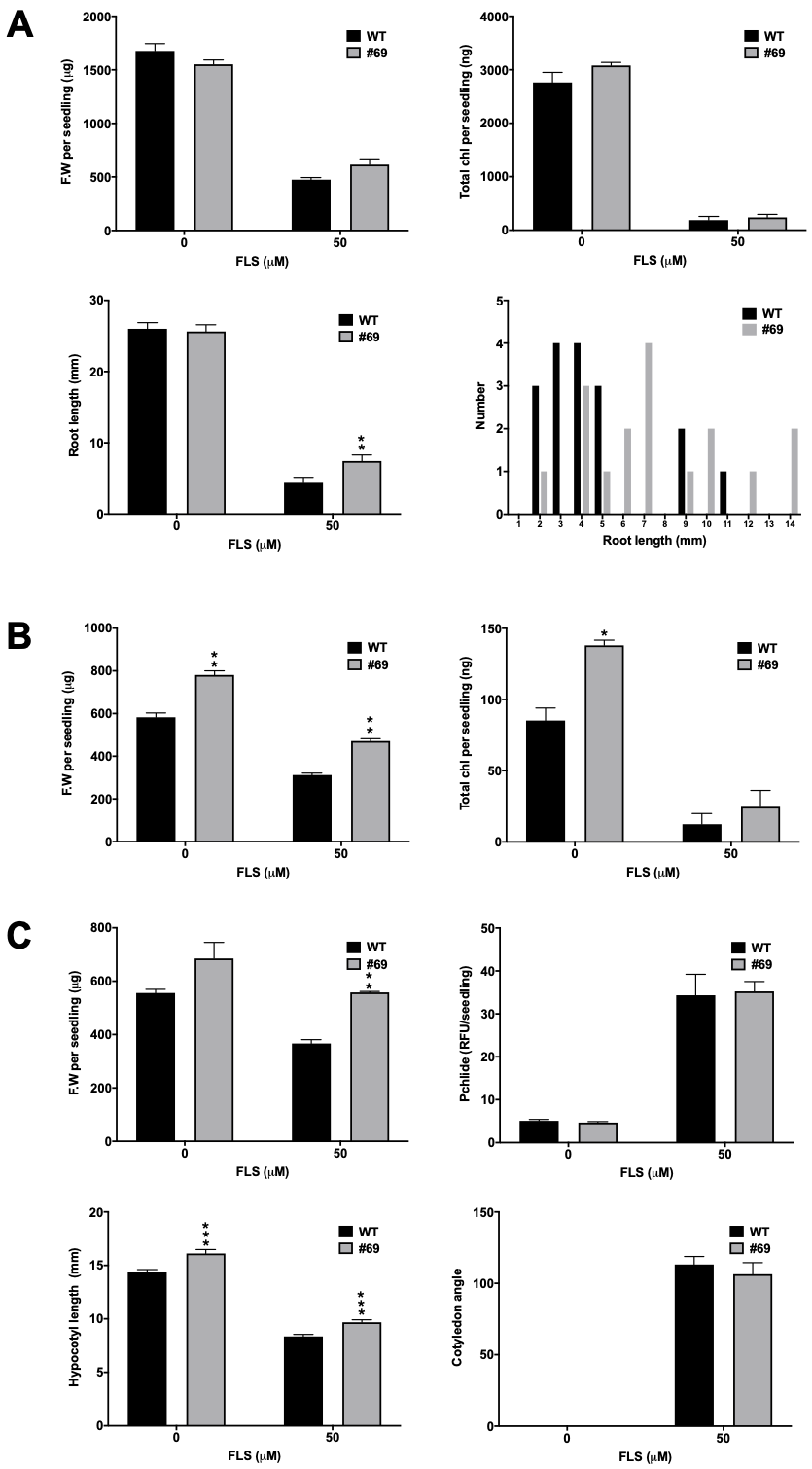

Figure 5.7. Performance of FLS-resistant line #69 in 3 growth conditions. WT seedlings were grown alongside line #69 for 7 days light (A), 5 days in dark + 24 h light (B) and 5 days in the dark (C) on ½ MS 0.8% agar media with addition of FLS to 50 µM. Vehicle control condition included addition of 0.1% DMSO to media. Fresh weight, Pchlide and total chlorophyll data points represent the mean ± SEM of three biological replicates, cotyledon data and root length data points represent the mean ± SEM of 17-22 individuals per condition. Asterisks indicate * $p<0.05$, ** $p<0.01$, *** $p<0.001$ between WT seedlings and resistant lines by t-test.

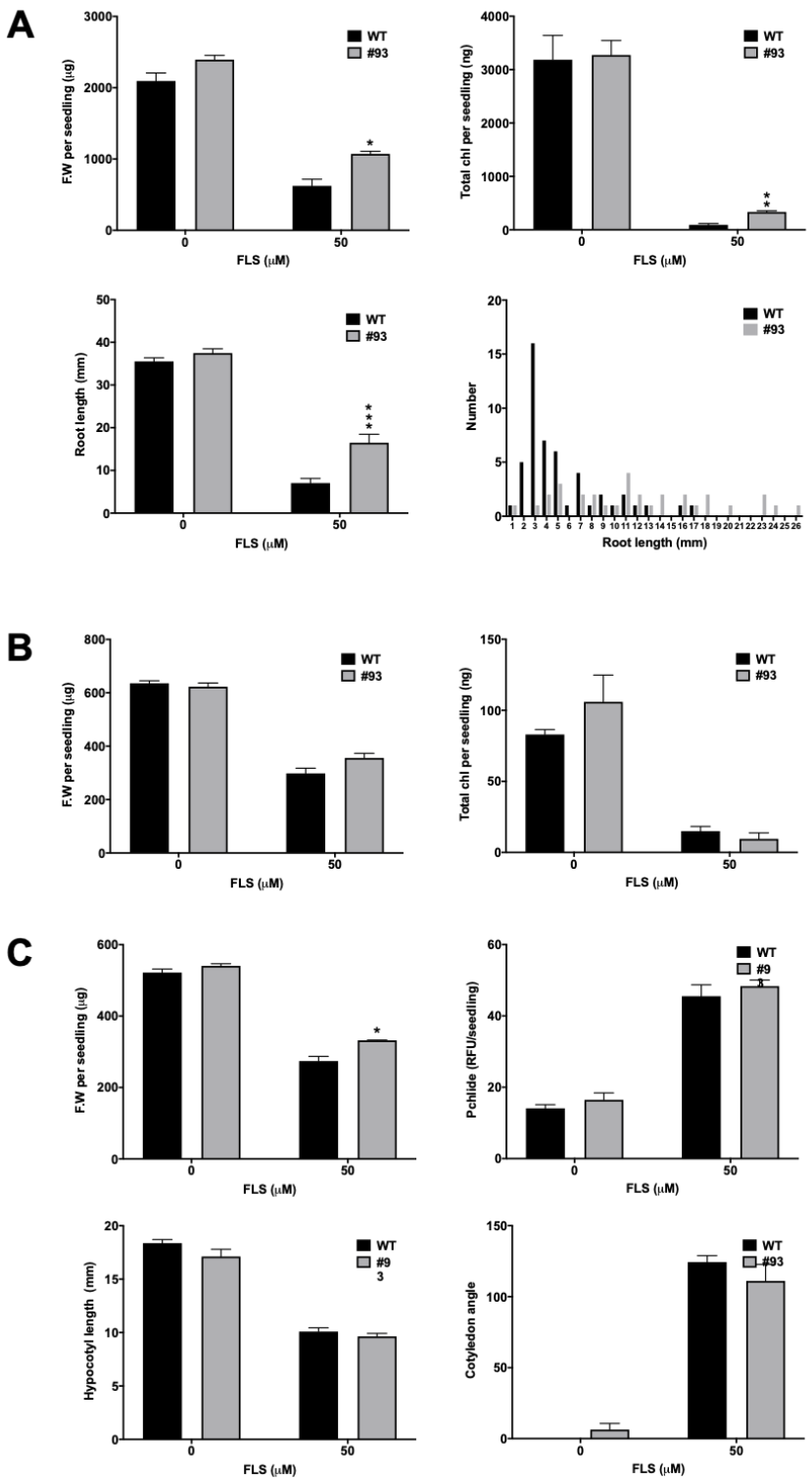

Figure 5.8. Performance of FLS-resistant line #93 in 3 growth conditions. WT seedlings were grown alongside line #93 for 7 days light (A), 5 days in dark + 24 h light (B) and 5 days in the dark (C) on ½ MS 0.8% agar media with addition of FLS to 50 µM. Vehicle control condition included addition of 0.1% DMSO to media. Fresh weight, Pchlide and total chlorophyll data points represent the mean ± SEM of three biological replicates, cotyledon data and root length data points represent the mean ± SEM of 10-23 individuals per condition. Asterisks indicate * $p<0.05$, ** $p<0.01$, *** $p<0.001$ between WT seedlings and resistant lines by t-test.

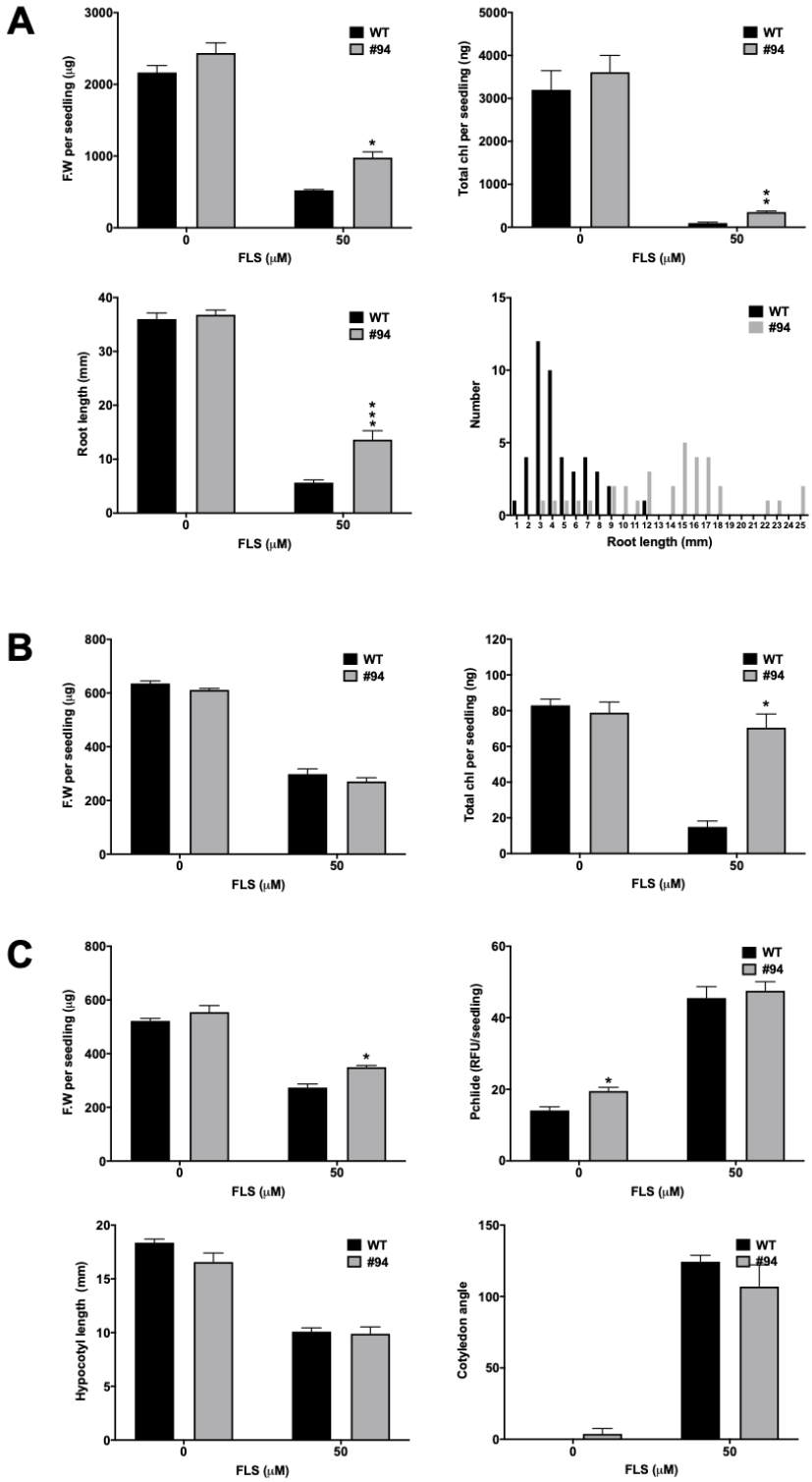

Figure 5.9. Performance of FLS-resistant line #94 in 3 growth conditions. WT seedlings were grown alongside line #94 for 7 days light (A), 5 days in dark + 24 h light (B) and 5 days in the dark (C) on ½ MS 0.8% agar media with addition of FLS to 50 µM. Vehicle control condition included addition of 0.1% DMSO to media. Fresh weight, Pchlide and total chlorophyll data points represent the mean ± SEM of three biological replicates, cotyledon data and root length data points represent the mean ± SEM of 7-23 individuals per condition. Asterisks indicate * $p<0.05$, ** $p<0.01$, *** $p<0.001$ between WT seedlings and resistant lines by t-test.

Table 5.2. Secondary screening of six FLS-resistant mutants. Col-0 row arrows represent the effects of 50 µM FLS on WT seedlings. Arrows associated with mutants represent significant differences between mutant and Col-0 lines on 50 µM FLS (e.g. green arrow displays significantly increased root length on FLS compared to WT). Dashes represent no change to WT on FLS.

	7 days light			5 days dark, 24hr light		5 days dark			
	Fresh weight	Total chlorophyll	Root length	Fresh weight	Total chlorophyll	Fresh weight	Pchlide	Hypocotyl length	Cotyledon angle
Col-0	↓	↓	↓	↓	↓	↓	↑	↓	↑
#22	↑	↑	↑	↑	↑	↑	↓	–	–
#51	↑	–	↑	↑	–	↑	–	↑	–
#61	–	–	↑	–	–	–	–	↑	↓
#69	–	–	↑	↑	–	↑	–	↑	–
#93	↑	↑	↑	–	–	↑	–	–	–
#94	↑	↑	↑	–	↑	↑	–	–	–

	Emergence	Bolting	Flowering
Col-0	4 ± 0	28 ± 0.2	30 ± 0.2
#22	16 ± 0.3	46 ± 0	48 ± 0
#51	4 ± 0	31 ± 2.6	33 ± 3.1
#61	12 ± 1.7	42 ± 10.5	44 ± 10
#69	4 ± 0	32 ± 2	34 ± 2
#93	4 ± 0	28 ± 1.1	30 ± 1.1
#94	6 ± 1.7	28 ± 1.2	30 ± 1.2

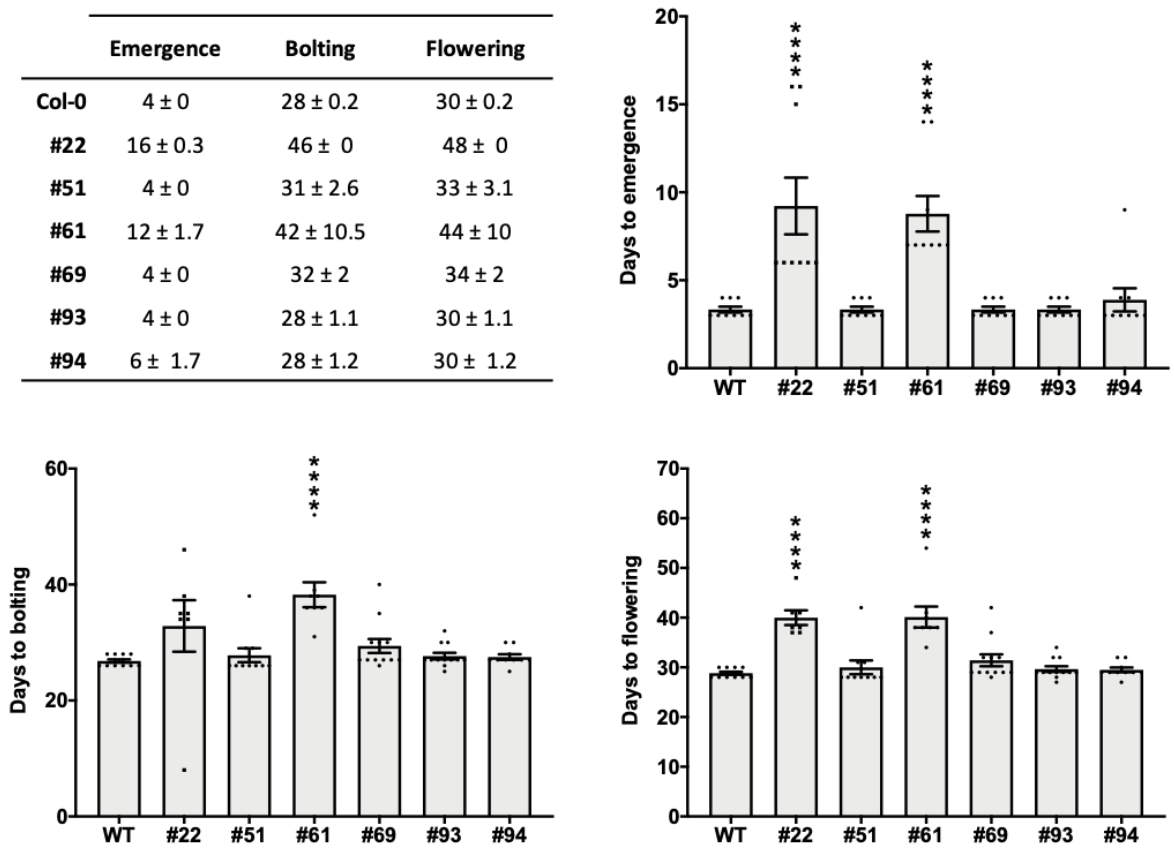

Figure 5.10. Developmental characterization of FLS- resistant lines. 7-12 individuals for WT and each FLS-resistant mutant were grown in soil and monitored daily for seedling emergence, bolting and formation of the first flower. Data points represent the mean ± SEM of 7-12 individuals per line. Asterisks indicate **** $p<0.0001$ between WT seedlings and resistant lines by Dunnett's post-hoc multiple-comparison test.

5.2.4 Characterizing the development of FLS-resistant lines

The next step in the screening protocol was to back-cross the most resistant lines with WT to achieve a segregating population for sequencing. It was noted that seed yield and growth of mutants was severely perturbed, which ultimately lead to unsuccessful backcrossing in all lines except #51 from which a small number of seeds were harvested.

To inform on the role of the mutations within these lines, the development of seedlings and young plants was recorded. Days to germination, bolting and flowering were logged in multiples individuals to build a profile of development (figure 5.11). Lines #22 and #61 displayed significantly increased time to germinate, taking 3-4 times as long as WT for seedlings to emerge from soil. Line #61 also displayed delayed bolting time, while both #22 and #61 took significantly longer to flower. Other lines, #51, #69, #93 and #94 had comparable timelines to WT (figure 5.11).

Once each line had flowered, multiple flower buds were removed from different inflorescences to assess reproductive organ formation (figure 5.11). Interestingly, line #22 displayed a significant increase in both stamen and pistil length, 21% and 29%, respectively. Although both reproductive parts were increased, the pistil displayed more elongation, causing a reduction in stamen:pistil ratio by 18%. This was not coupled with a change in stamen number (figure 5.11). Lines #61 and #69 demonstrated a decrease in stamen lengths by 13% and 11%, respectively; however, no other lines had significantly different pistil lengths to WT. However; marginal alterations in stamen and pistil lengths did affect lines #51 and #69 and they exhibited a 13% and 6% decrease in stamen:pistil ratio, respectively. Stamen number was also reduced in these mutants, with both lines, on average, having 4 stamens per flower, compared to the standard 6 in WT (figure 5.11).

Once siliques had formed on each plant, their final length was recorded. Unsurprisingly, all lines that displayed aberrant silique or stamen growth had significantly shorter siliques than WT, with line #22 displaying the largest reduction of 67% (figure 5.12). However, lines #93 and #94 also demonstrated reduction in silique length in the absence of stamen or pistil changes suggesting a subtler phenotype.

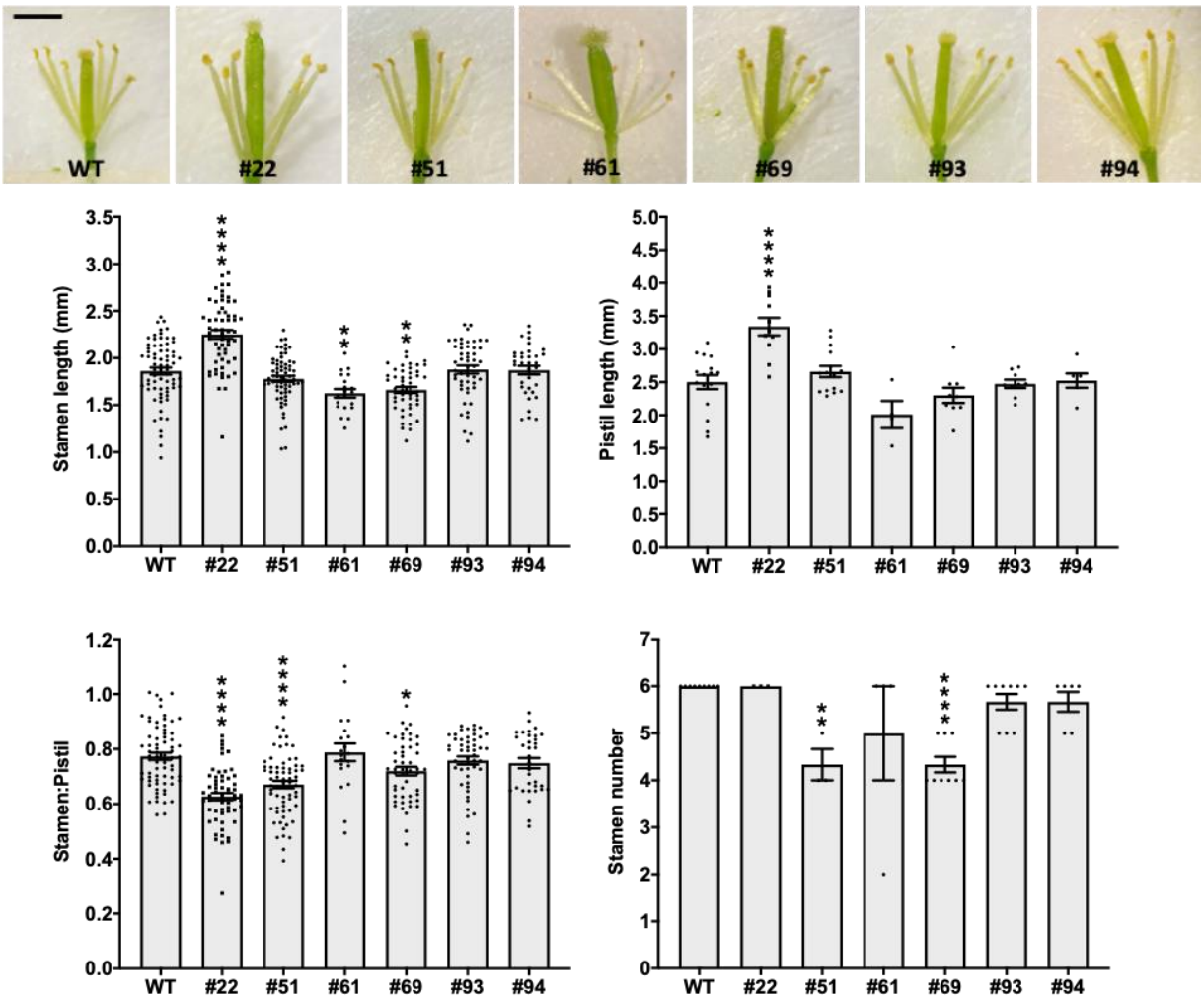

Figure 5.11. Reproductive organ measurements in FLS-resistant lines. Data points represent the mean ± SEM of 20-71 stamens and 4-16 pistils from varying inflorescences were measured from mutants. To determine relationship between stamen and pistils length, values were plotted as a ratio. Asterisks indicate * $p<0.05$, ** $p<0.01$, *** $p<0.001$, **** $p<0.0001$ between WT seedlings and resistant lines by Dunnett's post-hoc multiple-comparison test. Scale bar represents 1 cm.

Finally, these plants were allowed to self-fertilise so seed yield and size could be recorded in each mutant line. Seed yields were variable between plants, however, lines #22 and #61 exhibited a severe reduction of 93% and 94%, respectively, resulting in almost no recovery of seeds from these individuals. Lines #51 and #69 also displayed a reduction in yield, although this wasn't significant; whereas, #93 and #94 yielded similar to WT (figure 5.13). All of these yield changes were not coupled with changes in seed size, excluding line #69 that had an 11% increase in size (figure 5.13).

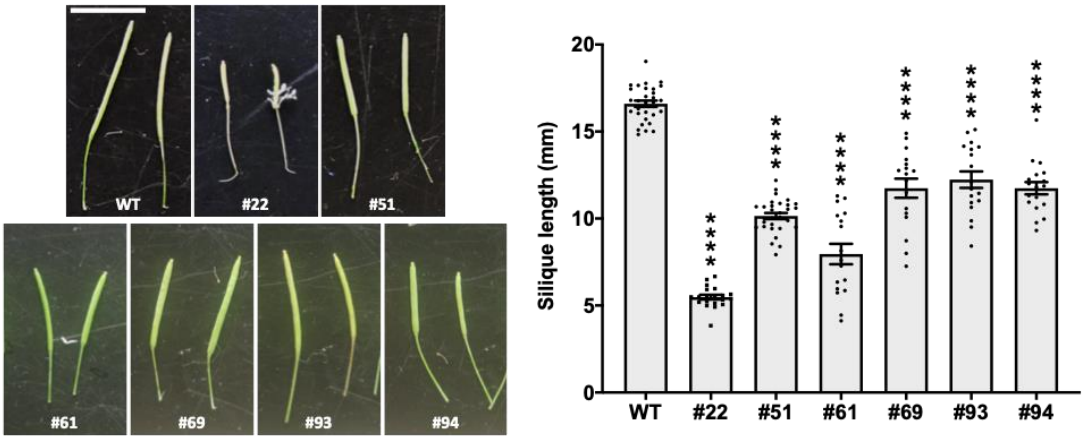

Figure 5.12. Silique development in FLS-resistant lines. Data points represent the mean ± SEM of 17-31 siliques per line. Asterisks indicate **** p<0.0001 between WT seedlings and resistant lines by Dunnett's post-hoc multiple-comparison test.

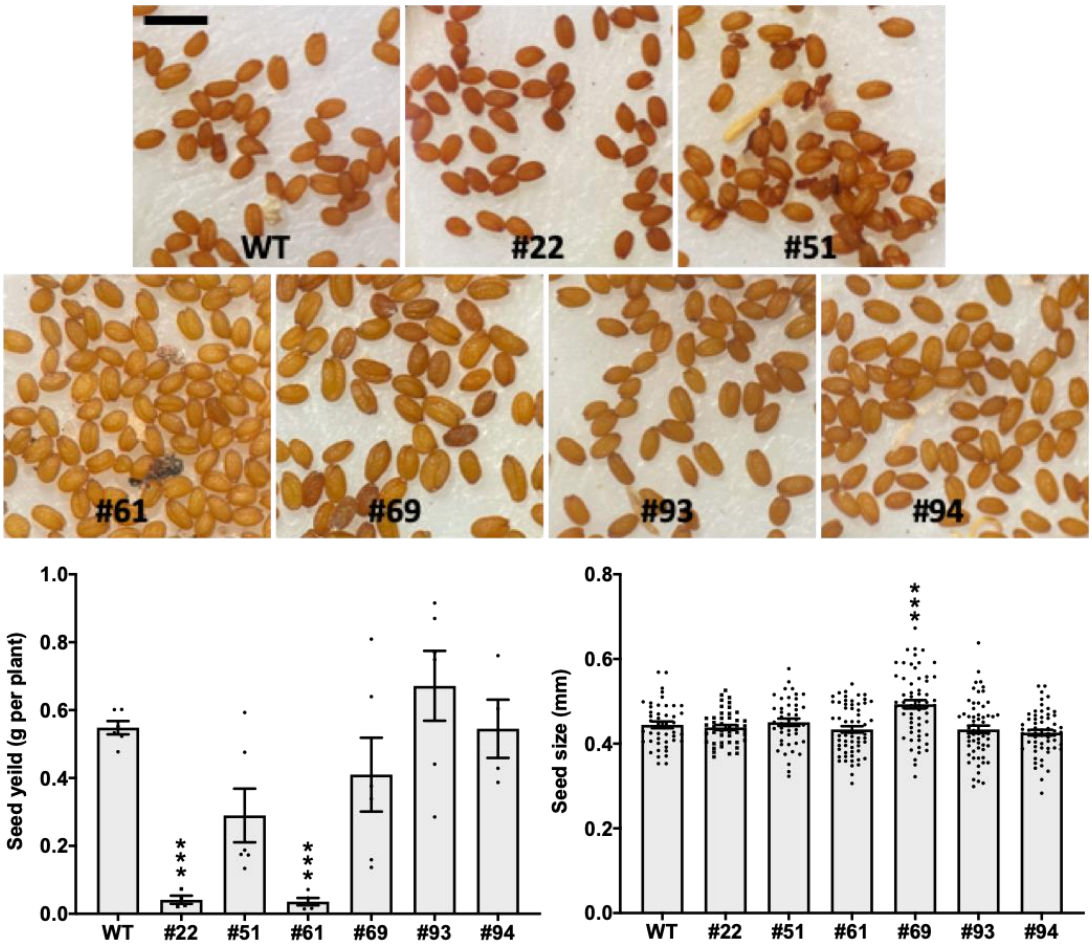

Figure 5.13. Seed yield and seed size in FLS-resistant lines. Seed yield data points represent the mean ± SEM of 4-7 mature plants per line, seed size data points represent the mean ± SEM of 45-60 individual seeds per line. Asterisks indicate *** p<0.001 between WT seedlings and resistant lines by Dunnett's post-hoc multiple-comparison test. Scale bar represents 0.5 cm.

5.3 Discussion

Although the genetic basis of these resistant mutations has not been discovered yet, in depth studies into the development of each line has given a further understanding into the potential roles of FLS to inform on its mode of action. Lines resistant to FLS primarily displayed improved growth, specifically in the presence of FLS except for line #51, which demonstrated improved growth regardless of FLS application. Line #51 had increased root length and hypocotyl elongation compared to the other mutants, ultimately leading to increased fresh weight; although, this was in the absence of changes in Pchlide and chlorophyll levels suggesting that the mutation(s) within this line leads to increased cell elongation. Although line #51 displays features of increased growth on FLS, this effect is global, occurring even in normal growth conditions, suggesting this mutation is not specifically FLS-resistant.

Auxin is the dominant phytohormone in the regulation of elongation responses, responding to changes in light and gravity; however, the developmental context and interactions with other hormones play a large role in auxin mediated cell elongation (Del Bianco and Kepinski, 2011). Auxin and brassinosteroid demonstrate synergistic interactions in promoting hypocotyl elongation and have highly overlapping transcriptional responses (Goda et al., 2004); while normal auxin responses require gibberellin (Chapman et al., 2012). Auxin response factors 6 (ARF6) and 8 (ARF8) are closely related and were previously shown to redundantly regulate hypocotyl elongation in *Arabidopsis* (Nagpal et al., 2005), with double mutants displaying significantly shorter hypocotyls that WT or single mutants. The majority of ARF6 target genes are also targets of BZR1 and/or PIF4 indicating the interdependency on hormone and light signalling pathways (Oh et al., 2014).

The precise mechanism of cell elongation by auxin is via the 'acid growth theory', first proposed in the 1970s (Hager et al., 1971; Cleland, 1976). This theory proposes that auxin causes the activation of plasma membrane localized H^+-ATPases, that in turn lead to acidification of the apoplast and thus trigger cell-wall loosening enzymes to enhance cell elongation (Hager, 2003). This hypothesis applies to both shoots and roots (Barbez et al.,

2017), in which at low concentrations auxin signalling promotes the apoplastic acidification, but at high auxin concentrations apoplastic alkalization occurs to reduce elongation (Barbez et al., 2017). This demonstrates a complex, concentration and tissue dependent role of auxin in cell elongation.

Similar patterns between resistant lines were observed, with lines #22 and #61 displaying a number of related features including delayed development, reduced silique length and severely affected seed yield. Lines #93 and #94 were also consistently similar in all responses. Analogous phenotypes in independently selected lines #22 and #61 suggest the possibility that they are allelic mutations, although sequencing will be needed to confirm this. In comparison, lines #93 and #94 were selected from the same pool initially; each pool contained seed from multiple M1 plants so the similarities can be explained by these lines both originating from the same parent plant.

Line #22 showed the highest level of resistance to FLS in multiple conditions while presenting an interesting phenotype at the reproductive stage. Compared to WT, line #22 had longer stamen filaments and pistils, resulting in a reduced stamen:pistil ratio, and thus unsuccessful self-pollination. Pistils are the female part of the plant, while stamens are male and their function is to produce pollen grains ready for release at flower opening. In *Arabidopsis*, 6 stamen primordia develop and sequentially mature through an early phase of stamen formation, and a late phase consisting of anther dehiscence, pollen grain maturation, and filament elongation (Smyth et al., 1990). Stamen development should be coordinated with pistil growth to allow self-pollination; however, alterations leading to uncoordinated development can result in sterility.

Auxin not only controls cell elongation, it is also required for meristem initiation and stamen development. Reduction in auxin biosynthesis in *yuc4* and *yuc1/yuc4* mutants (Ståldal et al., 2012), and inhibition of auxin transport by NPA or *pin* mutations (Bennett et al., 1995; Okada et al., 1991) all display a reduced number of stamens and reduced number of floral organs. In addition, late stage stamen development, particularly filament elongation is severely affected by mutations in *ARF3* (Sessions et al., 1997), *ARF5* (Przemeck et al., 1996), *ARF6* and *ARF8* (Nagpal et al., 2005), all of which display

significantly shorter stamen filaments compared to WT. Late stage anther dehiscence, pollen maturation and filament elongation is also regulated by the auxin receptor TIR1/AFB family and in triple and quadruple mutants anther dehiscence and pollen maturation were recorded earlier and filament elongation was inhibited (Cecchetti et al., 2008). Interestingly, pistil length were also recorded to be 25% shorter than WT in these mutants (Cecchetti et al., 2008). Auxin signalling is also involved in seed development including embryo, endosperm and seed coat development in both dicots and monocots (Cao et al., 2020). A number of auxin biosynthesis, transport and signalling genes have been implicated, namely *TIR1/AFB* and *ARF* genes (Dharmasiri et al., 2005; Goetz et al., 2006).

It is clear auxin plays a major role in tightly regulating a number of developmental processes and differences observed in the FLS-resistant lines can be explained in relation to mutations in auxin signalling pathways. In a number of the resistant lines stamen filament elongation is uncoordinated to pistil development and stamen number is reduced. This leads to reduced self-pollination and subsequent reduced seed yield. In the highly resistant line #22, stamen and pistil length are increased, while in lines #61 and #69 stamen length is reduced. Resistance to FLS, on this basis, suggests in line #22 there could be mutations within auxin signalling to stabilise ARF proteins, or conversely, increase the degradation of Aux/IAA repressor proteins that de-activate ARFs. Theoretically, as ARFs are positive regulators of elongation, these mutations would lead to increased transcription of ARF-induced genes leading to longer stamens and filaments. In addition, this would explain a level of FLS resistance. As discussed previously, FLS is hypothesised to be acting as an auxin receptor antagonist to stabilise Aux/IAA proteins, therefore, mutations to stabilise ARFs could cause resistance.

Through the study of stamen and pistil development it was revealed that reproductive growth was altered in resistant lines. Attempts to backcross the mutants failed prior to these observations, but this information could inform on better practise to achieve coordinated development of WT and resistant lines for successful backcrossing in the future in order to achieve segregating populations for sequencing and identification of the causative mutations.

Although the genetic basis of these resistant mutations has not been discovered yet, in depth studies into the development of each line has given a further understanding into the potential roles of FLS to inform on its mode of action. Lines resistant to FLS primarily displayed improved growth, specifically in the presence of FLS; however, line #51 demonstrated improved growth regardless of FLS application. Line #51 had increased root length and hypocotyl elongation compared to mutants, ultimately leading to increased fresh weight; although, this was in the absence of changes in Pchlide and chlorophyll levels indicating mutations within this line lead to increased cell elongation. Although line #51 displays feature of increased growth on FLS, this effect is global, occurring even in normal growth conditions, suggesting this mutation is not truly FLS-resistant.

Chapter 6: General Discussion

6.1 FLS acts to stabilize Aux/IAA proteins in *Arabidopsis*

The primary aim of this project was to elucidate the mode of action of FLS. Through various molecular, genetic and phenotypic studies it is suggested FLS primary mode of action in *Arabidopsis* is to stabilise Aux/IAA repressor proteins by acting as an auxin receptor antagonist (figure 6.1). FLS-induced phenotypes include the development of a de-etiolated phenotype in the dark that is rescued by application of exogenous auxins, but not other hormones tested, coupled with changes in endogenous auxin levels and auxin regulated gene expression preferentially over other hormones. Additionally, it is shown FLS can act rapidly to stabilise the DII::VENUS reporter and can be phenocopied by the known auxin receptor antagonist, auxinole.

Auxin acts as a molecular glue, increasing binding affinity of Aux/IAA repressor proteins to the F-box proteins of the TIR1/AFB family. Aux/IAA proteins bind via their DII domain and are then ubiquitinated and subsequently degraded by the 26s proteasome. Auxin response factor proteins (ARFs) are then de-repressed and auxin-inducible genes are transcribed, including *Aux/IAA* genes. This results in a sophisticated negative feedback loop in response to auxin levels, allowing normal growth and development of the root system in the light and maintenance of the etiolated phenotype in the dark (figure 6.1 left). Upon application of exogenous FLS, it is suggested that FLS is able to bind TIR1/AFB receptors; however, Aux/IAA proteins are not able to form a TIR1/AFB-FLS-Aux/IAA complex due to incompatible binding. This results in the stabilisation of Aux/IAA proteins and subsequent downstream effects seen following FLS treatment (figure 6.1 right).

Initial evidence of FLS acting as an auxin-like compound came from severe inhibition of primary root elongation when applied exogenously, while displaying a transient increase in growth following short-term, low concentration exposure. It is known that auxin signalling is tightly regulated in plants, with signalling outcomes finely tuned by subcellular, cellular and tissue locations and that at optimum concentrations auxin acts as a growth promotor (Enders and Strader, 2015). However, when in excess, auxin and auxin-related molecules negatively affect growth, inhibiting primary root elongation and promoting uncontrolled growth (Thimann, 1939).

Further evidence for FLS role as an auxin receptor antagonist comes from the de-etiolated phenotype induced by application of FLS, coupled with the rescue of this phenotype by auxins IAA, 1-NAA and 2,4-D and the observation of an auxin resistant phenotype in the light. As discussed previously, a number of mutations/alterations in the core light signalling pathway can induce de-etiolation in the absence of light; however, de-etiolation in the presence of FLS was specifically reversed by exogenous application of auxins. The gain-of-function mutants *axr2, axr3* (Nagpal et al., 2000; Timpte et al., 1994; Yang et al., 2004). and *shy2-2* (Kim et al., 1998a; Tian et al., 2003a) display the same phenotype as FLS-treated seedlings. These particular mutants have a single amino acid mutation within the DII domain of Aux/IAA proteins IAA7, IAA17 and IAA3 causing their stabilisation which leads to de-etiolation. Mutations in this key domain alters the Aux/IAA degradation rates in response to auxin meaning exogenous auxin application could not reverse their phenotypes. However, as we suggest FLS is competing with endogenous IAA to bind TIR1/AFB receptors, the application of exogenous auxins in the dark could reduce the number of FLS molecules bound to TIR1/AFB.

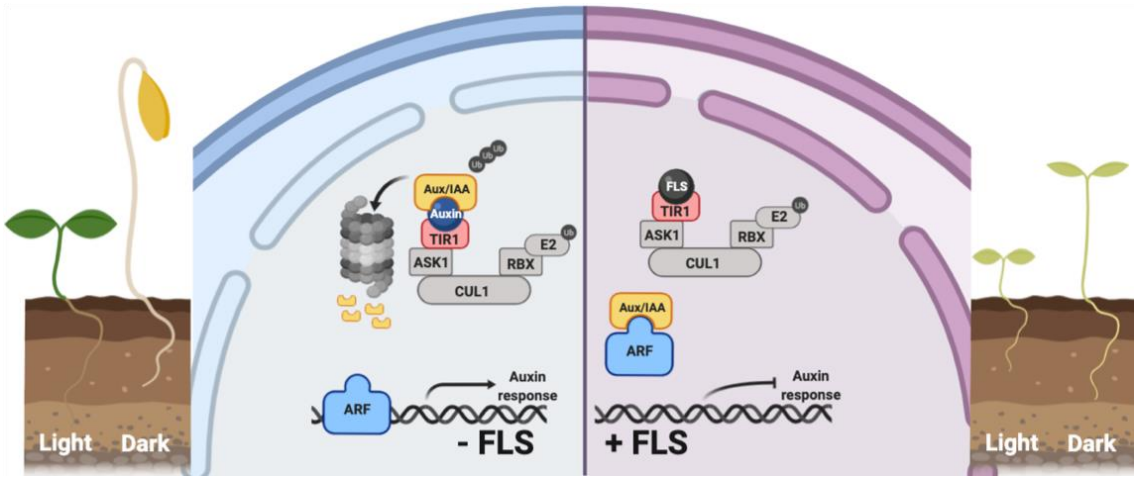

Figure 6.1. Model for FLS action on auxin signalling. (Left) Schematic depiction and simplified diagram of the auxin signalling pathway in *Arabidopsis* grown without FLS treatment. Auxin (IAA – navy) binds to its receptor TIR1 (red) and this allows the binding of Aux/IAA proteins (yellow) in domain II. Aux/IAA proteins are targeted for degradation via the 26s proteasome. The removal of Aux/IAA proteins allows ARF transcription factors (blue) to bind to promoters of auxin responsive genes (including *IAA* genes) to induce auxin signalling. (Right) Schematic depiction of the auxin signalling pathway in *Arabidopsis* grown in the presence of FLS. FLS (black) could potentially bind to the TIR1 receptor in place of auxin and prevent TIR1 from binding Aux/IAA repressor proteins. This causes repression of ARF proteins and downstream responses are not activated. FLS could also be acting to directly stabilize Aux/IAA proteins to achieve a similar outcome.

Exogenous auxin rescue of FLS-induced phenotypes is specific to dark-grown seedlings suggesting the mode of action is distinct depending on the light conditions. However, dark-grown seedlings are largely devoid of auxin and light triggers its synthesis (Bhalerao et al., 2002). This was further confirmed by endogenous hormone quantification. Therefore, in the dark, the addition of exogenous auxins alongside FLS increases the population of auxin-bound TIR1/AFBs to non-toxic levels. On the other hand, in the light the seedling has a high level of endogenous auxin competing with the exogenous FLS bound to TIR1/AFB so the application of more auxin in this scenario would not be effective in reducing the response to FLS.

Key similarities between known auxin receptor antagonists, auxin signalling pathway inhibitors and FLS further support the hypothesis. Auxinole was designed as a potent auxin antagonist, acting to bind to TIR1 in place of auxin and block the key Phe82 residue, essential for Aux/IAA protein docking (Hayashi et al., 2012). Two compounds: furyl acrylate ester of a thiadiazole heterocycle and 4-thiazolidinone appended with a derivatized acetic acid, were identified as inhibitors of auxin transcriptional activity via a chemical genetic screen for compounds able to silence auxin-activated transcription (Armstrong et al., 2004). All 3 compounds demonstrated stabilisation of Aux/IAA proteins and auxinole was confirmed to have antagonist activity in pull-down assays. Phenotypically, FLS and auxinole share a number of characteristics, including but not limited to de-etiolation and rapid DII::VENUS reporter stabilisation; while FLS treatment demonstrated significant gene expression overlap with the inhibitors of auxin transcriptional activity. This evidence further suggests FLS role as an auxin receptor antagonist.

6.2 Application of *Arabidopsis* mode of action to plant parasitic nematode species

The initial reasoning for studying FLS mode of action (MOA) in *Arabidopsis* was to inform on the MOA in plant parasitic nematode (PPN) species for which FLS is targeted. Initial studies deemed its mode of action to be distinct from anticholinesterases and macrocyclic lactones (Kearn et al., 2014), while more recent work has suggested its role

as a metabolic inhibitor (Feist et al., 2020). A precise molecular target within PPNs would be valuable as more nematicides with the same efficacy and specificity could be developed.

The hypothesis that FLS is acting as an auxin receptor antagonist *in planta* is solely based on data presented here. However, information gained through studies in *Arabidopsis* can help to explain a number of observations seen in nematodes and suggest a common target pathway. Auxin is synthesised from the amino acid, tryptophan and within this biosynthetic pathway also leads to the production of 5-hydroxytryptamine (5-HT/serotonin). In seedlings, 5-HT is able to display functional overlap with auxin and is able to antagonise the effect of auxins (Pelagio-Flores et al., 2011). Within PPNs, tryptophan-derived 5-HT has an essential role in the activation of stylet thrusting and this movement is crucial for successful root invasion of *G. pallida* juveniles (Crisford et al., 2018). It has been shown that a number of 5-HT antagonists such as reserpine, methiothepin and octopamine potently inhibit *G. pallida* infectivity by inhibiting stylet thrusting (Kearn, 2015; Crisford et al., 2018), highlighting a promising route to target PPNs.

Interestingly, FLS was suggested to interact with the serotonergic signalling pathway within PPNs. Initial observations demonstrated that FLS is able to stimulate stylet thrusting at >500 μM, similarly to 5-HT. Additionally, FLS was able to block the induction of stylet thrusting by 5-HT suggesting a potential role as an antagonist in this pathway (Kearn, 2015). Furthermore, pre-incubation with both methiothepin and octopamine was able to reduce FLS-stimulated stylet thrusting (Kearn, 2015) signifying FLS could, at least in part, be targeting PPNs via the serotonergic signalling pathway and acting as a partial agonist to a 5-HT receptor. It was proposed that application of FLS to PPNs reduced the number of receptors available for 5-HT occupancy, thus bringing about inhibition of stylet thrusting in the presence of 5-HT, but stimulation in the absence. This hypothesis is similar to what has been suggested for FLS action on the *Arabidopsis* auxin signalling pathway and begins to make robust connections between mode of action in different organisms.

6.3 The role of auxin in ameliorating FLS effects

The practical application of this work could be vital in ameliorating potential side effects of FLS on crop plants in the field. Although dicots seem to be more susceptible to phytotoxicity, these species tend to be high value and any reduction to yield has major financial consequences for farmers. It is important to understand the dynamics of FLS treatment on plants to improve application rate, concentration and potential effects on other organisms. It has been demonstrated that FLS is able to affect seedling growth before, during and after germination; but, seedlings are able to recover from exposure to concentrations below 20 μM. The highest concentration any organism is likely to be exposed to in the field is <30 μM immediately after FLS application (Kearn, 2015) suggesting any phytotoxicity to seedlings would be minimal. However, seed germination and the early stages of seedling growth are the most sensitive to both biotic and abiotic stresses and can affect subsequent growth and yield; therefore, having a potential treatment to reduce FLS-induced stress on crop species could increase long-term yield.

The role of auxin in FLS action has been discussed in depth previously and while mode of action is valuable to investigate, the impact of this in the field presents new methods to ameliorate FLS toxicity. The auxins IAA, 1-NAA and 2,4-D are able to significantly reduce FLS-induced de-etiolation of dark-grown seedlings and allow subsequent development of the seedling in the light. This effect was also seen if auxins were used as a pre-treatment before FLS exposure or even as a seed treatment, suggesting the potential use of auxins as a pre-plant treatment to prevent negative effects of FLS on germinating/young seedlings in the soil.

As discussed previously, 2,4-D based products are some of the most widely used herbicides on the market and have been used for over 70 years. 2,4-D was first commercialised for use in the 1940s, and has revolutionised weed control. It is a synthetic auxin herbicide that stimulates uncontrolled growth when applied in doses in excess of what is required for normal endogenous auxin signalling within dicots (Quareshy et al., 2018). Its effect on dicots has been described in three phases: stimulation, inhibition and decay (Grossmann, 2010). Stimulation begins within minutes of application and it

characterised by ethylene and ABA hyperaccumulation and metabolic activation of ATPases and ion channels. The inhibition phase includes production of ROS, stomatal closure and physiological defence responses that ultimately lead to the decay phase. This occurs around 3 days post-application and is distinguished by destruction of chloroplasts, membranes and vascular systems, leading to plant death (Grossmann, 2010).

It is understandable that the idea of using exogenous auxins, such as 2,4-D, to ameliorate the effects of FLS is concerning due to their primary uses as herbicides; however, application of L-tryptophan and IAA to nitrogen-based fertiliser has been shown to increase biomass and yield in cereal crops (Ahmad et al., 2008; Ahmad et al., 2008; Zaman et al., 2015). This presents the possibility of using auxins, or auxin pre-cursors, in the field without the potential of herbicidal action. Furthermore, evidence has demonstrated auxin does not have to be present throughout FLS application to still ameliorate effects, although this does enhance its ability to alleviate these effects, and that even auxin seed treatment is sufficient to relieve some side effects of FLS.

The possibility of using auxins as a seed treatment may be a more attractive option in the field as this treatment does not require re-application meaning the potential of auxin-based toxicity is reduced. But, theoretically, this would be adequate enough to attenuate FLS phytotoxicity to allow germination and initial seedling growth vital for plant establishment and considerable yield.

Seed priming is commonly used as a tool to advance the seed metabolic processes and improve germination rate. There are a number of methods including hydropriming, halopriming, osmopriming, thermopriming, solid matrix priming and biopriming (Ashraf and Foolad, 2005). All methods essentially imbibe seeds pre-planting to improve uniformity of germination and to increase final yield. Many studies have shown priming seed with plant hormones can increase seed germination under stress conditions; for example, treating wheat seed with IAA or 1-NAA alleviated the adverse effects of high salinity (Balki & Padole, 1982; Gulnaz et al., 1999). Auxin priming of sorgum, faba bean and cotton seed is also able to increase final yield under non-stress conditions (Thakre and Ghate, 1984; Harb, 1992). This confirms that the use of auxins in a seed priming

treatment is commercially viable, although appropriate ratios would have to be tested in the presence of FLS at field relevant concentrations to maximise yield and prevent herbicidal action.

6.4 Auxin and light signaling pathways are closely linked to regulate photomorphogenic growth

Not only have these results informed on the mode of action of FLS, they have also substantiated a relationship between light and auxin signalling. The association of light and auxin signalling is established but not fully understood; in seedlings, light brings about photomorphogenic growth, allowing a sessile organism to change its development in response to the environment. Auxin is an essential regulator of growth in plants with functions in organogenesis, tropic responses, cell division and expansion (Woodward and Bartel, 2005) and light is able to trigger vast changes within the complex auxin signalling pathways. In data presented here there is a clear relationship between auxin levels and light; endogenous hormone quantification displayed a 70% decrease in IAA levels when seedlings were grown in the dark and confocal imaging using 3 reporter lines consistently displayed lowers levels of auxin signalling at the root tip in dark grown seedlings. This is consistent with the idea that etiolated seedlings are largely devoid of IAA (Bhalerao et al., 2002).

In *Arabidopsis* seedlings, photomorphogenesis is closely tied to endogenous auxin levels. Auxin biosynthesis mutants *sav3/taa1* are deficient in endogenous auxin and are seen to have exaggerated photomorphogenic phenotypes, including short hypocotyls and more expanded cotyledons (Tao et al., 2008). Conversely, *yucca* and *red1* mutants with high endogenous auxin lead to reduced photomorphogenic growth characterised by hypocotyl elongation and reduced cotyledon expansion (Hoecker et al., 2004; Kim et al., 2007). Phytochromes have a large role in coordinating light and auxin signalling to alter development; active phyB (Pfr) is able to reduce IAA levels by activation of SUR2 and repression of TAA1, while reduced phyB Pfr under low R:FR ratio light elicits the opposite response and increase IAA levels (Tao et al., 2008). Both phyA and phyB are strong repressors of auxin-related gene transcription as removal of these photoreceptors

initiates a rapid elevation in transcription of *Aux/IAAs, SAURs* and *GH3s* (Devlin et al., 2003). Phytochromes have also been suggested to directly control auxin signalling via Aux/IAA repressor proteins. When translocated to the nucleus in response to light, PHYA and PHYB are able to interact with *Arabidopsis* SHY2/IAA3, AXR3/IAA17, IAA1, IAA9 and pea IAA4 (Colón-Carmona et al., 2000; Tian et al., 2003; Yang et al., 2018; Xu et al., 2018) to phosphorylate and stabilise these proteins. Other key mediators in controlling auxin signalling are the bZip transcription factors, HY5 and HYH, and BHLH transcription factors, PIFs. HY5 and HYH transcription factors promote photomorphogenesis (Holm et al., 2002) while also repressing auxin signalling (Cluis et al., 2004). Conversely, it has been shown PIF4 and PIF5 are positive regulators of auxin biosynthesis and induce auxin regulated gene expression, particularly in shade conditions (Franklin et al., 2011; Hornitschek et al., 2012; Nozue et al., 2011).

While here we have confirmed auxin levels are reduced in dark-grown seedlings, another noteworthy observation was made that in the dark mutations within TIR1/AFB receptors promote partial de-etiolation in *Arabidopsis*. Auxins are perceived by a co-receptor complex consisting of TIR1/AFB and Aux/IAA proteins, leading to degradation of Aux/IAAs and activation of ARF dependent transcription (Dharmasiri et al., 2005). The TIR1/AFB protein family consists of 6 members: TIR1 and 5 AFBs which display functional redundancies between each other, specifically *TIR1, AFB2/3* and *AFB4/5* (Dharmasiri et al., 2005; Prigge et al., 2020). This could explain why partial de-etiolation was only seen in double and triple mutants. It is known TIR1 is a primary receptor and is essential in root elongation, while AFB5 has a larger role in hypocotyl and inflorescence development (Prigge et al., 2020). Furthermore, levels of TIR1/AFB proteins are not equal spatially or temporally and levels are dynamic in response to a constantly changing environment (Vidal et al., 2010; Wang et al., 2016). It has been established that a number of auxin resistant mutations, resulting in Aux/IAA protein stabilisation (IAA3, IAA7 and IAA17), confer partial de-etiolation in the dark (Kim et al., 1998b; Leyser et al., 1996; Nagpal et al., 2000); however, mutations within the TIR1/AFB receptors have not been thoroughly investigated in regards to their role in photomorphogenesis. However, it would seem a practical assumption that reduced presence of TIR1/AFB receptors within seedlings would ultimately lead to the stabilisation of Aux/IAA proteins and subsequent de-etiolation.

6.5 Conclusions and future research directions

The data presented here support a model for FLS MOA as an auxin receptor antagonist. Evidence for this comes from phenotypic, molecular and genetic analysis; however, TIR1/AFB-Aux/IAA pairs have various affinities for each other and for different auxins. This results in a range of Aux/IAA half-lives and outputs depending on cell-type and development stage making the explanation of some observations challenging. Therefore, although we present a number of instances in which FLS acts as an auxin receptor antagonist, further work needs to be done to understand its specificity and effectiveness as a potential tool in dissecting the auxin signalling path further.

In the immediate future, TIR1 pull-down assays in the presence of IAA and/or FLS should be completed to determine if FLS is able to reduce IAA binding to TIR1. Established TIR1 receptor antagonist, auxinole, has been shown to reduce efficacy of IAA binding to TIR1 (Hayashi et al., 2012)indicating a suitable comparison for FLS. This would certainly be able to determine if FLS was physically able to bind TIR1 to block IAA and Aux/IAA protein docking. Additionally, quantifying Aux/IAA protein levels in the presence of FLS would support its ability to stabilize these proteins. In addition, the FLS-resistant lines isolated from the forward genetic screen should be sequenced and SNPs mapped. Knock-out lines based on each SNP can be generated and screened for FLS resistance. This could result in the identification of a number of FLS targets, whether that be uptake carrier proteins, influx/efflux transporters to move it around the plant or a molecular target within a specific signaling pathway.

In conclusion, this project has generated valuable knowledge about the effect of FLS on plants and how best to ameliorate these effects within the field. It has also demonstrated a strong role of auxin in FLS action in plants and the suggestion of a serotonergic mode of action in nematodes, which can be followed up to generate more effective and selective nematicides to reduce crop loss. Finally, this project has also established and corroborated a strong link between auxin and light signalling to coordinate plant development, and potentially discovered a new tool to dissect the complex auxin signalling pathways within plants.

Appendix : Supplementary data

S1. Phytohormone extraction and quantification

The Proteomics & Mass Spectrometry Facility at the Danforth Plant Science Centre is kindly acknowledged for its contribution in performing phytohormone extraction and mass spectrometry of samples. This material is based upon work supported by the National Science Foundation under Grant No. DBI-1427621 for acquisition of the QTRAP LC-MS/MS.

S1.1 Materials

Analytical reference standards for the analytes indole-3-acetic acid (IAA; Sigma-Aldrich St. Louis, MO), N-(3-indolylacetyl)-DL-aspartic acid (IAA-Asp; Sigma-Aldrich, St. Louis, MO), (+/-)-jasmonic acid (JA; Tokyo Chemical Industry Company, Tokyo, Japan), salicylic acid (SA; Acros Organics, Geel, Belgium), (+/-)-abscisic acid (ABA; Sigma-Aldrich, St. Louis, MO), N-jasmonyl-L-isoleucine (JA-Ile; Toronto Research Chemicals, Toronto, ON), 12-oxo-phytodienoic acid (OPDA; Cayman Chemical, Kalamazoo, MI), *cis*-zeatin (*c*Z; Santa Cruz Biotechnology, Santa Cruz, CA), *trans*-zeatin (*t*Z; Caisson Labs, Smithfield, UT), DL-dihydrozeatin (DHZ; Research Products International, Mount Prospect, IL), *trans*-zeatin riboside (*t*ZR; Gold Biotechnology, St. Louis, MO) as well as the internal standards - d_5-JA (Tokyo Chemical Industry Company, Tokyo, Japan), d_5-IAA (CDN Isotopes, Pointe-Claire, QC), d_5-dinor-OPDA (Cayman Chemical, Kalamazoo, MI), d_6-SA(CDN Isotopes, Pointe-Claire, QC), d_6-ABA (ICON Isotopes, Dexter, MI), d_5-*trans*- zeatin (OlChemIm, Olomouc, Czech Republic), d_5-*trans*-zeatin riboside (OlChemIm, Olomouc, Czech Republic), $^{13}C_6{}^{15}N$ JA-Ile (New England Peptide, Gardner, MA), and $^{13}C_4{}^{15}N$ IAA-Asp (New England Peptide, Gardner, MA). LC-MS grade methanol (MeOH) and acetonitrile (ACN) were sourced from J.T. Baker (Avantor Performance Materials, Radnor, PA) and LC-MS grade water was purchased from Honeywell Research Chemicals (Mexico City, Mexico). Stock solutions were prepared in 50% methanol and stored at -80° C. Standard solutions were prepared fresh in 30% methanol.

S1.2 Phytohormone extraction

Phytohormones *c*/*t*Z, DHZ, *t*ZR, SA, ABA, IAA, IAA-Asp, JA, JA-Ile and OPDA were extracted at a tissue concentration of 100 mg/mL in ice cold 1:1 MeOH: ACN. Around 100 mg of tissue sample were weighed and 10 µL of mixed stable-isotope labelled standards (1.25

µM for d_5-*t*Z, d_5-*t*ZR, d_4-SA, d_6-ABA, d_5-JA, d5- IAA and $^{13}C_6{}^{15}N$-IAA-Asp, 12.5 µM for $^{13}C_6{}^{15}N$-JA-Ile and d5-dinor-OPDA) were added into each sample prior to extraction. The samples were homogenized with a TissueLyzer-II (Qiagen) for 5 minutes at 15 Hz and then centrifuged at 16,000 x g for 5 minutes at 4° C. The supernatants were transferred to new 2 mL tubes and the pellets were re-extracted with 600 µL 1:1 ice cold MeOH: ACN. These extracts were combined and dried in a vacuum centrifuge. The samples were then reconstituted in 100 µL 30% methanol, centrifuged to remove particulates, and then passed through a 0.8 µm polyethersulfone spin filter (Sartorius, Stonehouse, UK) prior to dispensing into HPLC vials or well plates for LC-MS/MS analysis.

S1.3 LC-MS/MS Analysis

Phytohormones *c*/*t*Z, DHZ, *t*ZR, SA, ABA, IAA, IAA-Asp, JA, JA-Ile and OPDA were quantified using a targeted multiple reaction monitoring (MRM)/isotope dilution-based LC-MS/MS method. A Shimadzu Prominence-XR UFLC (UPLC) system connected to a SCIEX hybrid triple quadrupole-linear ion trap MS equipped with Turbo V^{TM} electrospray ionization (ESI) source (SCIEX, Framingham, MA) were used for the quantitative analysis. Three microliters of the reconstituted samples were loaded onto a 4.6 x 50 mm 1.8 µm ZORBAX Eclipse XDB-C_{18} column (Agilent Technologies, Santa Clara, CA, USA) and the phytohormones were eluted within 12.0 minutes, in a binary gradient of 0.1% acetic acid in water (mobile phase A) and 0.1% acetic acid in 3:1 ACN:MeOH (mobile phase B). The initial condition of the gradient was 10% B from 0 to 2.0 minutes, ramped to 50% B at 4.0 minutes, further ramped to 65% at 8.5 minutes, and then quickly raised to 95% B at 9.0 minutes and kept at 95% B until 12.0 minutes. The flow rate was also changed during the gradient, starting at 0.6 mL/min from 0 to 3.5 minutes, and then dropped to 0.3 mL/min at 4.0 minutes and kept at 0.3 mL/min until 12 minutes. Source parameters were set as follows: curtain gas 25 psi; source gas1 40 psi; source gas2 50 psi; collisionally activated dissociation (CAD) gas set to ‘medium’; interface heater temperature 500° C; ionspray voltage set to ±4500 V. Individual analyte and internal standard ions were monitored using previously optimized MRM settings programmed into a polarity switching method (cytokinins and auxins detected in positive ion mode, others detected in negative ion mode). Analyst 1.6.2 software (SCIEX, Framingham, MA) was used for data acquisition;

MultiQuant 3.0.2 software (SCIEX, Framingham, MA) was used for data analysis. The detected phytohormones were quantified based upon comparison of the analyte-to-internal standard integrated area ratios with a standard curve constructed using those same analytes, internal standards and internal standard concentrations (1.25 µM d_5-dinor-OPDA and $^{13}C_6{}^{15}N$-JA-Ile; others 0.125 µM). The analytical method was calibrated over the linear range of 4.8 fmol to 30 pmol loaded on the column.

Table S1. Gene ontology enrichment analysis of biological processes. This table represents the most highly enriched biological processes from 1263 significantly downregulated genes following FLS treatment in the dark.

GO biological process	Genes in reference genome	Genes in sample	Expected genes	Fold Enrichment	P-value	False Discovery Rate
tricyclic triterpenoid metabolic process	4	4	0.18	22.18	2.10E-04	1.43E-02
cell-cell junction assembly	5	4	0.23	17.74	3.65E-04	2.18E-02
response to symbiont	14	5	0.63	7.92	1.04E-03	4.95E-02
water transport	29	10	1.31	7.65	4.36E-06	5.15E-04
cellulose catabolic process	25	7	1.13	6.21	3.56E-04	2.17E-02
wax biosynthetic process	22	6	0.99	6.05	1.06E-03	4.93E-02
cuticle development	34	8	1.53	5.22	3.74E-04	2.19E-02
amino acid transmembrane transport	53	12	2.39	5.02	1.91E-05	1.74E-03
gravitropism	79	16	3.56	4.49	2.90E-06	3.65E-04
auxin polar transport	78	12	3.52	3.41	4.83E-04	2.62E-02
hyperosmotic response	73	11	3.29	3.34	9.55E-04	4.82E-02
response to water deprivation	339	47	15.28	3.07	1.70E-10	1.44E-07
hemicellulose metabolic process	101	14	4.55	3.07	4.40E-04	2.45E-02
auxin-activated signaling pathway	164	19	7.39	2.57	3.76E-04	2.16E-02
protein autophosphorylation	217	25	9.78	2.56	7.52E-05	5.85E-03
lipid transport	207	23	9.33	2.46	2.07E-04	1.42E-02
cell wall organization	517	57	23.31	2.45	8.12E-09	3.00E-06
pectin metabolic process	175	19	7.89	2.41	9.60E-04	4.77E-02
response to cold	414	44	18.67	2.36	1.06E-06	1.56E-04
root morphogenesis	247	26	11.14	2.33	2.21E-04	1.45E-02
anatomical structure formation involved in morphogenesis	192	20	8.66	2.31	9.96E-04	4.91E-02
drug catabolic process	248	25	11.18	2.24	4.28E-04	2.43E-02
unidimensional cell growth	273	27	12.31	2.19	4.57E-04	2.50E-02
response to abscisic acid	572	55	25.79	2.13	7.27E-07	1.23E-04

Table S2. Gene ontology enrichment analysis of cellular component. This table represents the most highly enriched cellular component classes from 1263 significantly downregulated genes following FLS treatment in the dark.

GO biological process	Genes in reference genome	Genes in sample	Expected genes	Fold Enrichment	P-value	False Discovery Rate
Casparian strip	11	6	0.5	12.1	0.0000523	0.00129
ER body	10	5	0.45	11.09	0.00031	0.00578
cell surface	15	6	0.68	8.87	0.000198	0.0039
lysosome	56	11	2.52	4.36	0.000129	0.00268
plant-type vacuole membrane	119	18	5.37	3.35	0.0000258	0.000686
late endosome	79	11	3.56	3.09	0.00169	0.0265
plasmodesma	1006	108	45.36	2.38	3.45E-15	9.18E-13
cytoplasmic vesicle part	214	22	9.65	2.28	0.00095	0.016
trans-Golgi network	312	30	14.07	2.13	0.00024	0.00464
anchored component of membrane	315	29	14.2	2.04	0.00068	0.0117
apoplast	452	40	20.38	1.96	0.000124	0.00264
intrinsic component of plasma membrane	337	29	15.19	1.91	0.00168	0.0266
endoplasmic reticulum	999	83	45.04	1.84	3.83E-07	0.0000151
integral component of membrane	4075	266	183.73	1.45	1.04E-09	5.84E-08

Table S3. Gene ontology enrichment analysis of biological processes. This table represents the top 50 most highly enriched biological processes from 3679 significantly upregulated genes following FLS treatment in the light.

GO biological process	Genes in reference genome	Genes in sample	Expected genes	Fold Enrichment	P-value	False Discovery Rate
pyridoxine biosynthetic process	8	7	1.05	6.65	0.000785	0.0155
pyridoxal phosphate biosynthetic process	7	6	0.92	6.52	0.00204	0.0332
leucine catabolic process	7	6	0.92	6.52	0.00204	0.033
photosystem II stabilization	7	6	0.92	6.52	0.00204	0.0329
plastoquinone biosynthetic process	7	6	0.92	6.52	0.00204	0.0328
photoinhibition	14	12	1.84	6.52	0.000012	0.000374
cytochrome b6f complex assembly	7	6	0.92	6.52	0.00204	0.0327
cellular response to light intensity	10	8	1.32	6.08	0.000492	0.0104
detection of external biotic stimulus	10	8	1.32	6.08	0.000492	0.0104
regulation of response to oxidative stress	9	7	1.18	5.91	0.00126	0.0227
photosynthetic acclimation	9	7	1.18	5.91	0.00126	0.0225
vitamin E biosynthetic process	9	7	1.18	5.91	0.00126	0.0225
chlorophyll catabolic process	12	9	1.58	5.7	0.000304	0.00683
positive regulation of RNA polymerase II transcriptional preinitiation complex assembly	8	6	1.05	5.7	0.00322	0.0481
proteasomal ubiquitin-independent protein catabolic process	22	16	2.89	5.53	1.92E-06	0.0000701
photosystem II repair	15	10	1.97	5.07	0.000278	0.00638
defense response to bacterium, incompatible interaction	40	26	5.26	4.94	6.97E-09	4.63E-07
plastid translation	14	9	1.84	4.89	0.00068	0.0135
photosystem II assembly	22	14	2.89	4.84	2.51E-05	0.000726
xanthophyll metabolic process	14	8	1.84	4.34	0.00235	0.0367
response to superoxide	14	8	1.84	4.34	0.00235	0.0365
response to molecule of fungal origin	16	9	2.1	4.28	0.00137	0.0242
systemic acquired resistance, salicylic acid mediated signaling pathway	16	9	2.1	4.28	0.00137	0.0242
endoplasmic reticulum unfolded protein response	18	10	2.37	4.22	0.000803	0.0157
protein stabilization	15	8	1.97	4.05	0.00323	0.0481
plant-type hypersensitive response	67	34	8.81	3.86	4.59E-09	3.31E-07
response to molecule of bacterial origin	34	17	4.47	3.8	3.71E-05	0.00105
response to ozone	32	16	4.21	3.8	6.24E-05	0.00169
regulation of chlorophyll metabolic process	24	12	3.16	3.8	0.000509	0.0106
thylakoid membrane organization	47	23	6.18	3.72	2.23E-06	0.0000792
negative regulation of programmed cell death	23	11	3.03	3.64	0.00115	0.0211
protein-chromophore linkage	23	11	3.03	3.64	0.00115	0.021
cellular oxidant detoxification	21	10	2.76	3.62	0.00196	0.0321
defense response to fungus, incompatible interaction	45	21	5.92	3.55	1.07E-05	0.00034
protein targeting to chloroplast	39	18	5.13	3.51	5.02E-05	0.0014
protein quality control for misfolded or incompletely synthesized proteins	22	10	2.89	3.46	0.00255	0.0391
regulation of systemic acquired resistance	22	10	2.89	3.46	0.00255	0.039
response to absence of light	40	18	5.26	3.42	6.49E-05	0.00174
glycerol ether metabolic process	29	13	3.82	3.41	0.000675	0.0135
ATP hydrolysis coupled proton transport	26	11	3.42	3.22	0.00247	0.0379
photosynthetic electron transport chain	45	19	5.92	3.21	8.08E-05	0.00213
cellular response to decreased oxygen levels	31	13	4.08	3.19	0.0011	0.0204
response to hypoxia	67	28	8.81	3.18	2.18E-06	0.0000781
response to hydrogen peroxide	79	33	10.39	3.18	2.84E-07	0.0000135
cellular response to heat	65	27	8.55	3.16	3.6E-06	0.000121
regulation of photomorphogenesis	29	12	3.82	3.15	0.00185	0.0309
carotenoid biosynthetic process	34	14	4.47	3.13	0.000827	0.0161
neurotransmitter metabolic process	34	14	4.47	3.13	0.000827	0.016
response to chitin	137	56	18.02	3.11	4.8E-11	4.3E-09
regulation of dephosphorylation	27	11	3.55	3.1	0.00311	0.0468

Table S4. Gene ontology enrichment analysis of cellular component. This table represents the most highly enriched cellular component classes from 3679 significantly upregulated genes following FLS treatment in the light.

GO biological process	Genes in reference genome	Genes in sample	Expected genes	Fold Enrichment	P-value	False Discovery Rate
chloroplastic endopeptidase Clp complex	8	7	1.05	6.65	0.000785	0.00949
ESCRT I complex	8	6	1.05	5.7	0.00322	0.0314
proteasome core complex, alpha-subunit complex	10	7	1.32	5.32	0.00192	0.0204
autophagosome membrane	12	7	1.58	4.43	0.00404	0.0377
proteasome regulatory particle, base subcomplex	19	11	2.5	4.4	0.00034	0.00453
chloroplast photosystem II	19	11	2.5	4.4	0.00034	0.00447
stromule	35	19	4.6	4.13	0.00000536	0.0000851
chloroplast thylakoid lumen	81	40	10.66	3.75	3.86E-10	8.22E-09
photosystem II oxygen evolving complex	23	11	3.03	3.64	0.00115	0.0134
plastoglobule	79	36	10.39	3.46	1.46E-08	2.73E-07
chloroplast inner membrane	80	34	10.52	3.23	1.36E-07	2.38E-06
peroxisomal membrane	43	15	5.66	2.65	0.00287	0.0288
intrinsic component of mitochondrial membrane	46	15	6.05	2.48	0.0041	0.0379
mitochondrial matrix	165	42	21.71	1.93	0.00029	0.00391
plant-type vacuole membrane	119	29	15.65	1.85	0.00439	0.0399
apoplast	452	95	59.46	1.6	0.0000658	0.00096
plasma membrane	3843	713	505.56	1.41	1.03E-18	3.77E-17
cytosol	2245	404	295.34	1.37	4.24E-09	8.06E-08
plasmodesma	1006	175	132.34	1.32	0.000716	0.00886
integral component of membrane	4075	688	536.08	1.28	1.36E-10	3.08E-09

Table S5. Gene ontology enrichment analysis of biological processes. This table represents the most highly enriched biological processes from 4141 significantly downregulated genes following FLS treatment in the light.

GO biological process	Genes in reference genome	Genes in sample	Expected genes	Fold Enrichment	P-value	False Discovery Rate
phragmoplast assembly	6	6	0.89	6.74	0.00213	0.0335
AMP salvage	7	6	1.04	5.78	0.00352	0.0488
cellular response to iron ion starvation	7	6	1.04	5.78	0.00352	0.0487
guard mother cell differentiation	10	8	1.48	5.39	0.00101	0.0193
anthocyanin-containing compound biosynthetic process	17	12	2.52	4.76	0.00013	0.00342
procambium histogenesis	10	7	1.48	4.72	0.00355	0.049
auxin efflux	13	9	1.93	4.67	0.00101	0.0193
microtubule-based movement	70	48	10.38	4.62	4.63E-14	8.55E-12
nuclear DNA replication	12	8	1.78	4.49	0.00228	0.0352
DNA replication initiation	23	15	3.41	4.4	3.72E-05	0.00113
very long-chain fatty acid biosynthetic process	17	11	2.52	4.36	0.000426	0.00918
microtubule nucleation	14	9	2.08	4.33	0.00147	0.0255
cutin biosynthetic process	18	11	2.67	4.12	0.000606	0.0124
DNA unwinding involved in DNA replication	17	10	2.52	3.97	0.00133	0.0236
cell wall pectin metabolic process	48	28	7.12	3.93	1.06E-07	6.75E-06
asymmetric cell division	21	12	3.11	3.85	0.000541	0.0112
flavonol metabolic process	16	9	2.37	3.79	0.00288	0.0416
negative regulation of DNA-dependent DNA replication	16	9	2.37	3.79	0.00288	0.0413
phloem transport	18	10	2.67	3.75	0.00183	0.0302
mitotic spindle organization	22	12	3.26	3.68	0.000739	0.0146
male meiotic nuclear division	24	13	3.56	3.65	0.000472	0.0101
positive gravitropism	32	17	4.75	3.58	7.98E-05	0.00221
DNA-dependent DNA replication maintenance of fidelity	19	10	2.82	3.55	0.00247	0.0375
ribosomal large subunit assembly	42	22	6.23	3.53	8.91E-06	0.000323
transmembrane receptor protein tyrosine kinase signaling pathway	119	60	17.65	3.4	9.24E-13	1.44E-10
wax biosynthetic process	22	11	3.26	3.37	0.00207	0.0329
negative regulation of mitotic cell cycle phase transition	24	12	3.56	3.37	0.00132	0.0236
plant-type cell wall modification involved in multidimensional cell growth	27	13	4	3.25	0.0011	0.0208
cytoplasmic translation	59	28	8.75	3.2	2.52E-06	0.000103
ribosomal small subunit assembly	34	16	5.04	3.17	0.000372	0.00841
regulation of DNA endoreduplication	24	11	3.56	3.09	0.0035	0.0488
purine ribonucleoside metabolic process	33	15	4.89	3.06	0.000744	0.0146
maturation of LSU-rRNA	29	13	4.3	3.02	0.00181	0.0301
spindle assembly	38	17	5.64	3.02	0.000391	0.00868
regulation of meristem growth	45	20	6.67	3	0.000133	0.00348
mitotic cell cycle checkpoint	32	14	4.75	2.95	0.00147	0.0255
positive regulation of cell proliferation	61	26	9.05	2.87	3.08E-05	0.000968
plant-type cell wall loosening	38	16	5.64	2.84	0.00153	0.0264
leaf vascular tissue pattern formation	31	13	4.6	2.83	0.00288	0.0417
mitotic sister chromatid segregation	36	15	5.34	2.81	0.00235	0.036
response to zinc ion	41	17	6.08	2.8	0.0011	0.0208
cuticle development	34	14	5.04	2.78	0.00361	0.0496
negative regulation of chromosome organization	40	16	5.93	2.7	0.0019	0.0312
cytoplasmic microtubule organization	43	17	6.38	2.67	0.00142	0.025
response to nematode	74	29	10.98	2.64	4.09E-05	0.00123
regulation of mitotic nuclear division	73	28	10.83	2.59	6.97E-05	0.00199
anatomical structure arrangement	60	23	8.9	2.58	0.000387	0.00864
positive regulation of cell cycle	84	32	12.46	2.57	2.11E-05	0.000693
glucosinolate biosynthetic process	53	20	7.86	2.54	0.00121	0.0219
serine family amino acid biosynthetic process	51	19	7.56	2.51	0.00181	0.0301

Table S6. Gene ontology enrichment analysis of cellular component. This table represents the most highly enriched cellular component classes from 4141 significantly downregulated genes following FLS treatment in the light.

GO biological process	Genes in reference genome	Genes in sample	Expected genes	Fold Enrichment	P-value	False Discovery Rate
MCM complex	6	6	0.89	6.74	0.00213	0.0208
chaperonin-containing T-complex	11	10	1.63	6.13	0.000116	0.00152
tubulin complex	13	10	1.93	5.19	0.000293	0.00359
nuclear pore inner ring	8	6	1.19	5.06	0.00549	0.046
kinesin complex	65	47	9.64	4.88	2.08E-14	5.82E-13
DNA polymerase complex	10	7	1.48	4.72	0.00355	0.0331
condensed nuclear chromosome, centromeric region	10	7	1.48	4.72	0.00355	0.0328
cell surface	15	10	2.22	4.49	0.000656	0.00734
cytosolic large ribosomal subunit	147	93	21.8	4.27	4.93E-24	4.37E-22
cytosolic small ribosomal subunit	108	68	16.02	4.25	6.9E-18	2.53E-16
gamma-tubulin complex	13	8	1.93	4.15	0.00328	0.0314
preprophase band	17	9	2.52	3.57	0.00391	0.0356
spindle microtubule	17	9	2.52	3.57	0.00391	0.0353
nuclear replisome	20	10	2.97	3.37	0.00328	0.0309
kinetochore	27	13	4	3.25	0.0011	0.0116
centrosome	46	21	6.82	3.08	0.0000678	0.000913
cyclin-dependent protein kinase holoenzyme complex	51	23	7.56	3.04	0.0000361	0.000534
nucleosome	45	20	6.67	3	0.000133	0.00171
cortical microtubule cytoskeleton	26	11	3.86	2.85	0.00562	0.0467
cytoplasmic microtubule	26	11	3.86	2.85	0.00562	0.0464
phragmoplast	75	29	11.12	2.61	0.0000463	0.000657
plasmodesma	1006	336	149.21	2.25	1.03E-34	1.56E-32
trans-Golgi network	312	97	46.27	2.1	1.81E-09	4.48E-08
nucleolus	453	138	67.19	2.05	2.24E-12	6.1E-11
plant-type cell wall	387	116	57.4	2.02	2.92E-10	7.4E-09
anchored component of plasma membrane	171	44	25.36	1.73	0.00203	0.02
apoplast	452	109	67.04	1.63	0.0000107	0.000171
endosome	420	101	62.29	1.62	0.00003	0.00045
vacuolar membrane	637	140	94.48	1.48	0.0000457	0.000657

Table S7. Hormone quantification of FLS-treated samples. Endogenous phytohormones were quantified through liquid chromatography mass spectrometry analysis (LC/MS) from plant tissue treated +/- 50 µM FLS for 7 days continuous light or 5 days dark. DD=Dark-grown, LL=Light-grown, 0/50 represents FLS treatment and 1-3 represents biological replicates. NF=Not found.

		Result (pmole/g frozen sample)										
Sample weight (mg)	Sample Name	IAA	t-ZR	JA-Ile	OPDA	JA	ABA	IAA-Asp	c-Zeatin	t-Zeatin	SA	DHZ
78.70	DD01	9.0	<1.3	3.9	72.7	36.1	29.9	4.2	<1.3	NF	48.7	<1.3
155.60	DD02	9.4	<1.3	2.4	46.1	21.5	36.8	6.6	<1.3	NF	33.9	<1.3
122.80	DD03	8.1	<1.3	<1.3	62.2	27.8	27.9	4.7	<1.3	NF	52.2	<1.3
130.60	DD501	9.0	<1.3	1.9	101.3	18.8	18.0	6.1	<1.3	NF	131.0	<1.3
151.90	DD502	5.1	<1.3	1.6	57.0	12.5	7.5	5.3	<1.3	NF	81.2	<1.3
111.70	DD503	8.7	<1.3	<1.3	60.5	11.5	14.9	6.3	1.8	NF	33.7	<1.3
133.00	LL01	29.2	<1.3	<1.3	5857.0	9.8	15.8	3.6	1.4	NF	401.0	<1.3
135.50	LL02	30.3	<1.3	<1.3	7130.0	11.1	21.2	2.5	1.7	NF	365.0	<1.3
125.90	LL03	28.8	<1.3	<1.3	4522.0	11.2	14.6	5.1	<1.3	NF	323.0	<1.3
129.80	LL501	13.9	<1.3	<1.3	3947.0	101.7	9.4	4.9	<1.3	NF	850.0	2.2
132.00	LL502	10.4	<1.3	3.0	2401.0	106.0	11.2	3.7	<1.3	NF	658.0	1.8
110.40	LL503	16.3	<1.3	<1.3	3138.0	154.3	13.1	4.0	<1.3	NF	1106.0	1.7

Table S8. Expression of auxin-related genes in transcriptomic analysis. Transcript level changes of auxin-related genes to FLS treatment from light and dark grown seedlings samples. Black text denotes no significant gene expressions changes, blue text denotes significantly down regulated and red denotes significantly upregulated transcript levels in response to FLS treatment.

Gene ID	Gene name	Dark-grown log2fold change	Light-grown log2fold change
AT3G62980	TIR1	0.511828	0.028369
AT4G03190	AFB1	0.212804	-2.68938
AT3G26810	AFB2	-0.50928	-0.44835
AT1G12820	AFB3	-0.38092	-0.1419
AT4G24390	AFB4	-0.43962	-0.65522
AT5G49980	AFB5	-0.42265	-0.23451
AT1G10940	ASK1	0.243026	0.271633
AT4G02570	CUL1	-0.10404	0.408041
AT5G20570	RBX1	0.140893	0.648234
AT1G59750	ARF1	-0.41806	-0.48012
AT5G62000	ARF2	-0.31987	-0.3031
AT2G33860	ARF3	0.063378	-0.71391
AT5G60450	ARF4	0.21221	-1.06634
AT1G19850	ARF5	-0.09563	-1.8758
AT1G30330	ARF6	-0.46664	-0.7482
AT5G20730	ARF7	-0.34466	0.416405
AT5G37020	ARF8	0.079879	-0.63084
AT4G23980	ARF9	-0.45656	-0.2807
AT2G28350	ARF10	-0.73661	-0.68989
AT2G46530	ARF11	-1.2192	-0.73548
AT1G34310	ARF12	NA	NA
AT1G34170	ARF13	NA	NA
AT1G35540	ARF14	NA	NA
AT1G35520	ARF15	NA	NA
AT4G30080	ARF16	-0.36485	0.027795
AT1G77850	ARF17	-0.26569	0.498916
AT3G61830	ARF18	-0.46382	-2.50043
AT1G19220	ARF19	-0.07955	-0.55503
AT1G35240	ARF20	0.365997	NA
AT1G34410	ARF21	NA	NA
AT1G34390	ARF22	NA	NA
AT1G43950	ARF23	NA	NA
AT4G14560	IAA1	0.291956	-1.41828
AT3G23030	IAA2	-0.25487	1.252087
AT1G04240	IAA3	-0.9182	-4.70498
AT5G43700	IAA4	-0.64823	-0.92668
AT1G15580	IAA5	-6.33028	NA
AT1G52830	IAA6	-2.9711	NA
AT3G23050	IAA7	0.050384	-0.19281
AT2G22670	IAA8	-0.14194	-1.5999
AT5G65670	IAA9	-0.12806	-0.89871
AT1G04100	IAA10	0.437983	1.247466
AT4G28640	IAA11	0.408701	-0.42732
AT1G04550	IAA12	-0.26944	-0.33068
AT2G33310	IAA13	-0.76563	-0.97611
AT4G14550	IAA14	-1.01272	-1.0122
AT1G80390	IAA15	NA	0.445437
AT3G04730	IAA16	0.152404	0.419049
AT1G04250	IAA17	-1.51334	-3.91179
AT1G51950	IAA18	0.322414	1.020637
AT3G15540	IAA19	-1.58828	-1.58828
AT2G46990	IAA20	-0.04815	-0.13225
AT5G20730	IAA21	-0.07955	-0.55503
AT1G19220	IAA22	0.354655	0.05572
AT5G20730	IAA23	-0.43928	-0.43506
AT1G19850	IAA24	1.210189	1.367828
AT5G20730	IAA25	0.136456	-1.80617
AT3G16500	IAA26	-0.27995	-0.30861
AT4G29080	IAA27	1.081168	1.30429
AT5G25890	IAA28	0.872053	-0.78805
AT4G32280	IAA29	-1.06843	-1.06843
AT2G14960	GH3.1	-6.87261	-6.82486
AT4G37390	GH3.2	-0.26739	-0.99372
AT2G23170	GH3.3	0.398947	-1.67979
AT1G59500	GH3.4	NA	NA
AT4G27260	GH3.5	-0.40974	-0.57409
AT5G54510	GH3.6	-0.52779	0.18801
AT2G47750	GH3.9	-0.43188	-1.73428
AT2G46370	GH3.11	-0.16044	-0.10966
AT5G13320	GH3.12	-1.5148	4.374463
AT5G13370	GH3.15	1.142902	2.339219
AT1G28130	GH3.17	-1.64297	-0.326

Gene ID	Gene name	Dark-grown log2fold change	Light-grown log2fold change
AT4G34770	SAUR1	-0.07428	-1.53442
AT4G34780	SAUR2	3.974112	NA
AT4G34790	SAUR3	-2.02602	4.120157
AT4G34800	SAUR4	-1.13142	-1.7519
AT4G34810	SAUR5	-1.16976	0.383243
AT2G21210	SAUR6	-0.61658	0.357434
AT2G21200	SAUR7	-1.28374	0.257507
AT2G16580	SAUR8	-0.99469	-7.70678
AT4G36110	SAUR9	-0.97113	-1.03929
AT2G18010	SAUR10	-1.23494	-4.27056
AT5G66260	SAUR11	-3.27918	2.023093
AT2G21220	SAUR12	-0.84084	-2.22381
AT4G38825	SAUR13	-0.49846	-3.78152
AT4G38840	SAUR14	0.00225	-1.36372
AT4G38850	SAUR15	-1.92136	-0.94305
AT4G38860	SAUR16	-0.85558	-0.56036
AT4G09530	SAUR17	-2.99412	NA
AT3G51200	SAUR18	NA	NA
AT5G18010	SAUR19	-1.22152	-5.04962
AT5G18020	SAUR20	-2.02689	-4.03923
AT5G18030	SAUR21	-0.98188	-1.91686
AT5G18050	SAUR22	-0.89628	-5.59923
AT5G18060	SAUR23	-0.95905	-6.15078
AT5G18080	SAUR24	-1.41466	-6.35151
AT4G13790	SAUR25	-0.203	NA
AT3G03850	SAUR26	-1.62325	-5.21865
AT3G03840	SAUR27	-1.89327	-3.88551
AT3G03830	SAUR28	-1.47903	NA
AT3G03820	SAUR29	-0.73186	-6.61969
AT5G53590	SAUR30	-1.49195	-1.27046
AT4G00880	SAUR31	-0.6142	-3.95582
AT2G46690	SAUR32	-0.71139	-0.87116
AT3G61900	SAUR33	-1.82166	0.855766
AT4G22620	SAUR34	0.368361	4.775335
AT4G12410	SAUR35	1.674592	-2.78058
AT2G45210	SAUR36	-0.16907	2.771311
AT4G31320	SAUR37	NA	-7.3807
AT2G24400	SAUR38	-0.19496	-3.78152
AT3G43120	SAUR39	NA	NA
AT1G79130	SAUR40	NA	NA
AT1G16510	SAUR41	0.913837	2.046026
AT2G28085	SAUR42	-4.29156	NA
AT5G42410	SAUR43	NA	-2.88109
AT5G03310	SAUR44	0.714631	-3.3887
AT2G36210	SAUR45	-4.65548	0.582377
AT2G37030	SAUR46	-1.676	NA
AT3G20220	SAUR47	NA	NA
AT3G09870	SAUR48	NA	NA
AT4G34750	SAUR49	0.902686	0.348381
AT4G34760	SAUR50	-0.77097	-1.5382
AT1G75580	SAUR51	0.080112	-0.64207
AT1G75590	SAUR52	2.190461	-7.02226
AT1G19840	SAUR53	0.200981	-8.03848
AT1G19830	SAUR54	-6.12475	-5.65054
AT5G50760	SAUR55	-0.99958	0.279573
AT1G76190	SAUR56	NA	-0.97067
AT3G53250	SAUR57	-2.49964	-0.81529
AT1G43040	SAUR58	NA	-3.74959
AT3G60690	SAUR59	0.641569	2.390061
AT1G20470	SAUR60	-3.5295	-1.1713
AT1G29420	SAUR61	0.027056	-3.3887
AT1G29430	SAUR62	-1.28782	-1.97937
AT1G29440	SAUR63	-1.94058	-7.4835
AT1G29450	SAUR64	-1.49752	-6.32958
AT1G29460	SAUR65	-1.23536	-7.04784
AT1G29500	SAUR66	-1.27705	-1.64091
AT1G29510	SAUR67	-2.42646	-6.89142
AT1G29490	SAUR68	-2.48974	NA
AT5G10990	SAUR69	NA	-2.62202
AT5G20810	SAUR70	-0.84768	0.059941
AT1G56150	SAUR71	2.786446	-1.63394
AT3G12830	SAUR72	0.260569	1.22264
AT3G03847	SAUR73	NA	NA
AT3G12955	SAUR74	-1.20971	-0.62675
AT5G27780	SAUR75	NA	NA
AT5G20820	SAUR76	0.258225	-1.76959
AT1G17345	SAUR77	1.286004	-1.58783
AT1G72430	SAUR78	-0.54921	1.325409
AT2G35290	SAUR79	0.183441	2.665684

Table 9. Details of 94 potentially resistant lines selected from screening on 50 μM FLS. The names of each mutant represent % EMS treatment, # indicates pool number and (x) denotes separate individuals selected from the same pool.

Mutant pool	EMS% pool #	M_2 harvested	Date screened	M_3 harvested	Selected from LL or DD
1	1% #1 (1)	7.3.17	26.7.17	5.10.17	LL
2	1% #1 (2)	7.3.17	26.7.17	5.10.17	LL
3	0.75% #2	7.3.17	31.7.17	16.11.17	LL
4	1% #3 (1)	7.3.17	30.8.17	27.11.18	LL
5	1% #3 (2)	7.3.17	30.8.17	27.11.18	LL
6	1% #3	7.3.17	30.8.17	23.1.18	LL
7	0.75% #6 (1)	7.3.17	7.10.17	1.3.18	LL
8	0.75% #6 (2)	7.3.17	7.10.17	1.3.18	LL
9	0.5% #1	21.8.17	9.12.17	13.4.18	LL
10	0.5% #4	21.6.17	8.3.18	11.7.18	LL
11	0.5% #20 (1)	19.6.17	23.3.16	11.7.18	LL
12	0.5% #20 (2)	19.6.17	23.3.17	11.7.18	LL
13	0.5%#15 (1)	21.6.17	23.3.18	30.7.18	LL
14	0.75% #19	20.4.18	20.7.18	31.10.18	DD
15	0.75% #13	20.4.18	20.7.18	31.10.18	DD
16	0.25% #2	20.4.18	2.7.18	31.10.18	LL
17	0.25% #13 (1)	20.4.18	16.7.17	21.11.18	LL
18	0.25% #13 (2)	20.4.18	16.7.18	21.11.18	LL
19	0.75% #3 (2)	20.4.18	19.7.18	31.10.18	LL
20	0.75% #14 (1)	20.4.18	20.7.18	31.10.18	LL
21	0.75% #14 (2)	20.4.18	20.7.18	31.10.18	LL
22	0.75% #15 (2)	20.4.18	20.7.18	21.11.18	LL
23	0.75% #15 (1)	20.4.18	20.7.18	21.11.18	LL
24	0.75% #22 (1)	24.4.18	25.7.18	21.11.18	LL
25	0.75% #22 (2)	24.4.18	25.7.18	21.11.18	LL
26	0.75% #22 (3)	24.4.18	25.7.18	21.11.18	LL
27	0.75% #26	24.4.18	25.7.18	21.11.18	LL
28	0.5% #4 (1)	27.6.17	2.7.18	5.11.18	LL
29	0.5% #4 (2)	27.6.17	2.7.18	5.11.18	LL
30	0.5% #4 (3)	27.6.17	2.7.18	5.11.18	LL
31	0.5% #4 (4)	27.6.17	2.7.18	5.11.18	LL
32	0.5% #26 (3)	22.2.17	15.6.17	5.11.18	LL
33	0.5% #30	22.2.17	15.6.17	5.11.18	LL
34	0.5% #33	22.2.17	15.6.17	5.11.18	LL
35	0.5% #34	22.2.17	15.6.17	5.11.18	LL
36	0.75% #31 (1)	24.4.18	26.7.18	21.11.18	LL
37	0.75% #31 (2)	24.4.18	26.7.18	21.11.18	LL
38	0.75% #33 (1)	24.4.18	26.7.18	21.11.18	LL
39	0.75% #33 (3)	24.4.18	26.7.18	21.11.18	LL
40	0.75% #51 (1)	24.4.18	31.7.18	21.11.18	LL
41	0.75% #51 (2)	24.4.18	31.7.18	21.11.18	LL
42	0.75% #51 (3)	24.4.18	31.7.18	21.11.18	LL
43	0.75% #51 (4)	24.4.18	31.7.18	21.11.18	LL
44	0.75% #60	24.4.18	3.8.18	21.11.18	LL
45	0.75% #198 (1)	15.5.18	10.8.18	21.11.18	DD
46	0.75% #198 (2)	15.5.18	10.8.18	21.11.18	DD
47	0.75% #198 (3)	15.5.18	10.8.18	21.11.18	DD
48	0.75% #198 (6)	15.5.18	10.8.18	21.11.18	DD
49	0.75% #124 (1)	8.5.18	21.8.18	5.12.18	LL
50	0.75% #124 (2)	8.5.18	21.8.18	5.12.18	LL
51	0.75% #124 (3)	8.5.18	21.8.18	5.12.18	LL
52	0.75% #125 (1)	8.5.18	21.8.18	5.12.18	LL
53	0.75% #125 (2)	8.5.18	21.8.18	5.12.18	LL
54	0.75% #125 (3)	8.5.18	21.8.18	5.12.18	LL
55	0.75% #125 (4)	8.5.18	21.8.18	5.12.18	LL
56	0.75% #125 (5)	8.5.18	21.8.18	5.12.18	LL
57	0.75% #125 (6)	8.5.18	21.8.18	5.12.18	LL
58	0.75% #125 (7)	8.5.18	21.8.18	5.12.18	LL
59	0.75% #127 (1)	8.5.18	21.8.18	5.12.18	LL
60	0.75% #127 (2)	8.5.18	21.8.18	5.12.18	LL
61	0.75% #134	8.5.18	21.8.18	5.12.18	LL
62	0.75% #135 (1)	8.5.18	20.8.18	5.12.18	LL
63	0.75% #135 (2)	8.5.18	20.8.18	5.12.18	LL
64	0.75% #135 (3)	8.5.18	20.8.18	5.12.18	LL
65	0.75% #135 (4)	8.5.18	20.8.18	5.12.18	LL
66	0.75% #145 (1)	11.5.18	17.8.18	5.12.18	LL
67	0.75% #145 (2)	11.5.18	17.8.18	5.12.18	LL
68	0.75% #145 (3)	11.5.18	17.8.18	5.12.18	LL
69	0.75% #152 (1)	11.5.18	17.8.18	5.12.18	LL
70	0.75% #152 (2)	11.5.18	17.8.18	5.12.18	LL
71	0.75% #152 (3)	11.5.18	17.8.18	5.12.18	LL
72	0.75% #152 (4)	11.5.18	17.8.18	5.12.18	LL
73	0.75% #152 (5)	11.5.18	17.8.18	5.12.18	LL
74	0.75% #152 (6)	11.5.18	17.8.18	5.12.18	LL
75	0.75% #4 (1)	2.7.19	15.7.19	24.10.19	LL
76	0.75% #4 (2)	2.7.19	15.7.19	24.10.19	LL
77	0.75% #5 (1)	2.7.19	15.7.19	24.10.19	LL
78	0.75% #5 (2)	2.7.19	15.7.19	24.10.19	LL
79	0.75% #5 (3)	2.7.19	15.7.19	24.10.19	LL
80	0.75% #5 (4)	2.7.19	15.7.19	24.10.19	LL
81	0.75% #10	2.7.19	15.7.19	4.11.19	LL
82	0.75% #18 (1)	2.7.19	18.7.19	24.10.19	LL
83	0.75% #18 (2)	2.7.19	18.7.19	4.11.19	LL
84	0.75% #43 (1)	3.7.19	26.7.19	24.10.19	LL
85	0.75% #43 (2)	3.7.19	26.7.19	24.10.19	LL
86	0.75% #43 (3)	3.7.19	26.7.19	24.10.19	LL
87	0.75% #43 (4)	3.7.19	26.7.19	24.10.19	LL
88	0.75% #43 (5)	3.7.19	26.7.19	24.10.19	LL
89	0.75% #64	3.7.19	21.7.19	24.10.19	LL
90	0.75% #69	4.7.19	31.7.19	24.10.19	LL
91	0.75% #78	4.7.19	16.8.19	24.10.19	DD
92	0.75% #100	4.7.19	12.9.19	18.12.19	LL
93	0.75% #115 (1)	8.7.19	12.9.19	18.12.19	LL
94	0.75% #115 (2)	8.7.19	12.9.19	18.12.19	LL

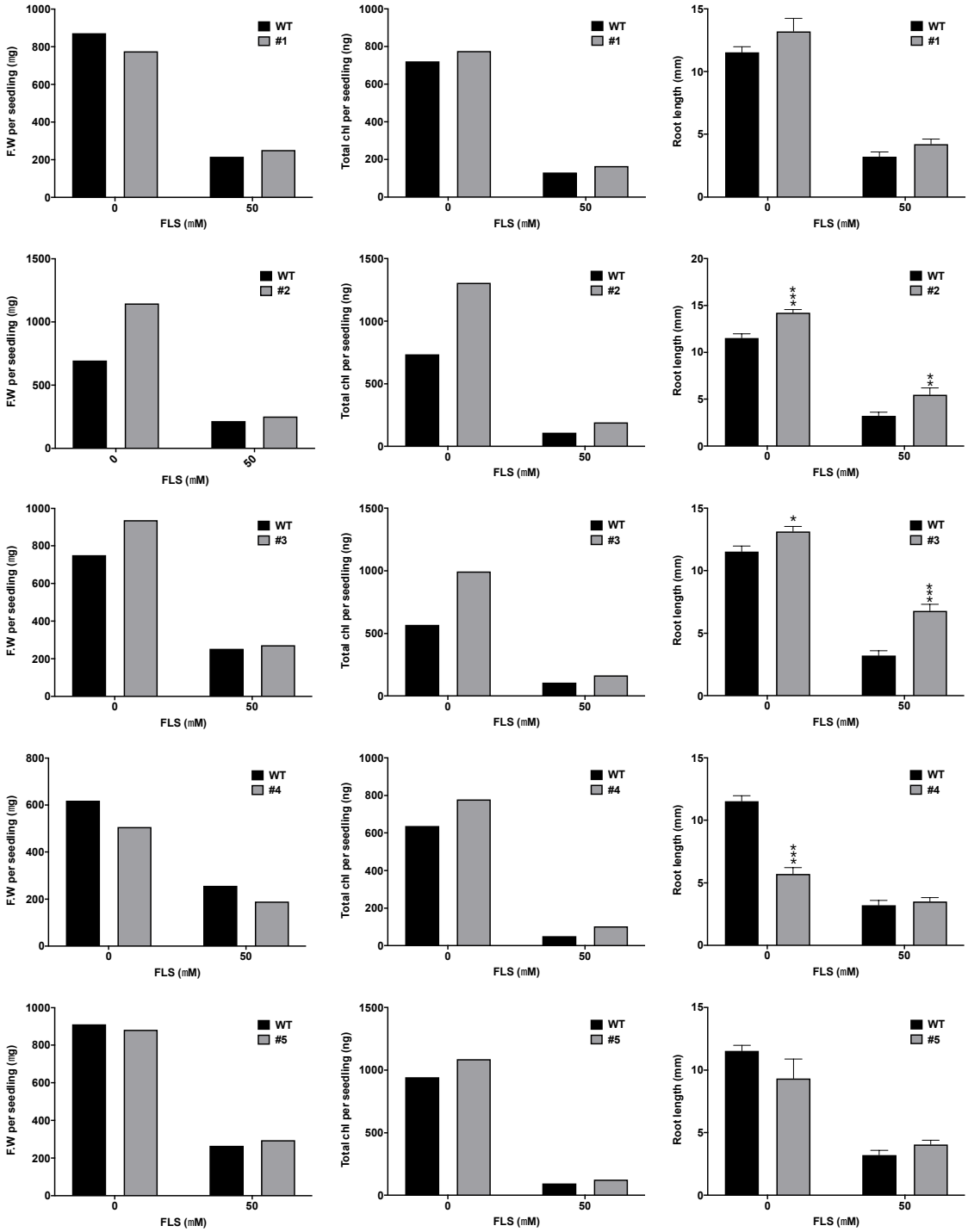
F.W per seedling (mg)
Total chl per seedling (ng)
Root length (mm)
FLS (mM)
WT
#1
#2
#3
#4
#5
0
50
*
**
***

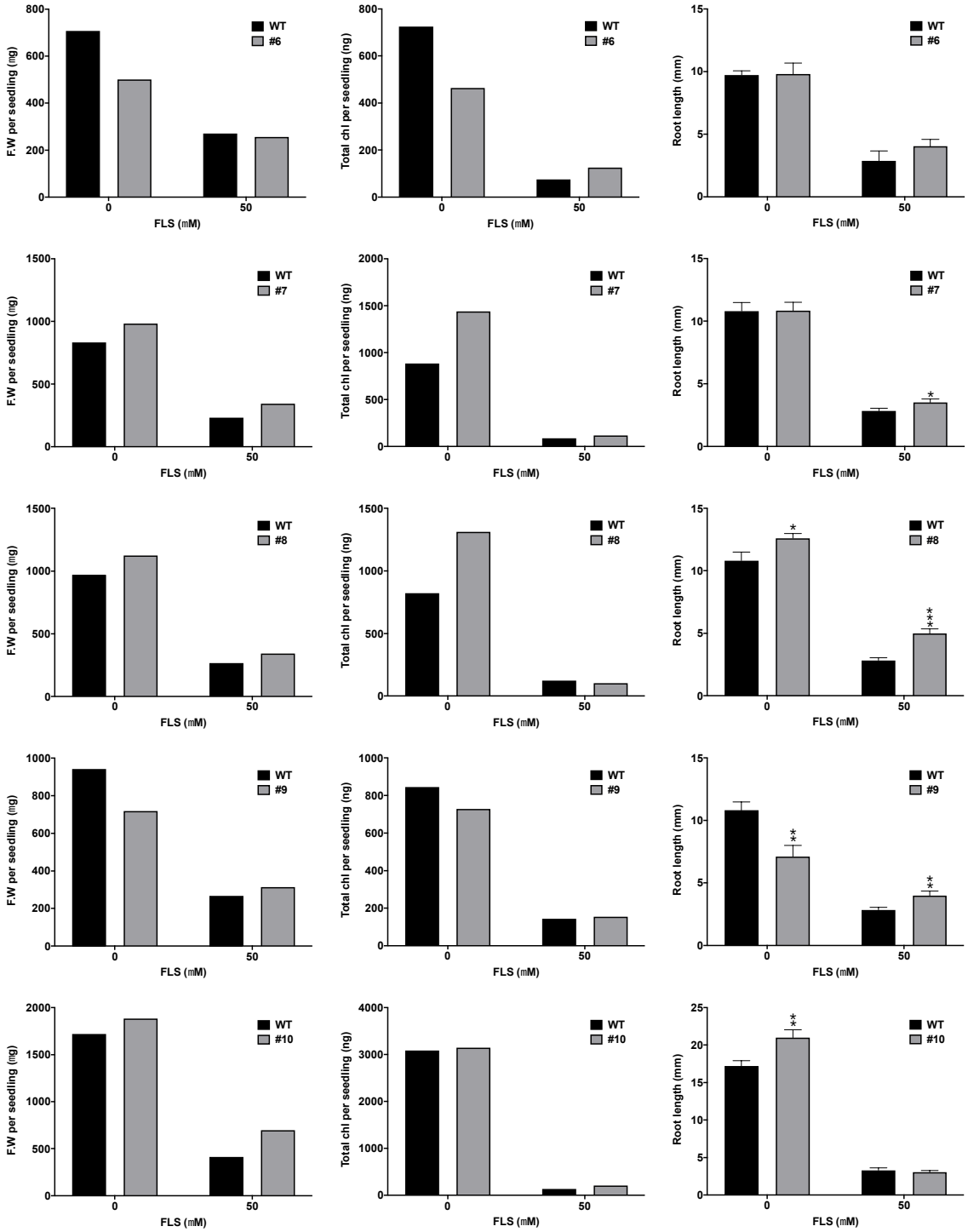
F.W per seedling (mg)
Total chl per seedling (ng)
Root length (mm)
FLS (mM)
WT
#6
#7
#8
#9
#10
0
50
*
**
***

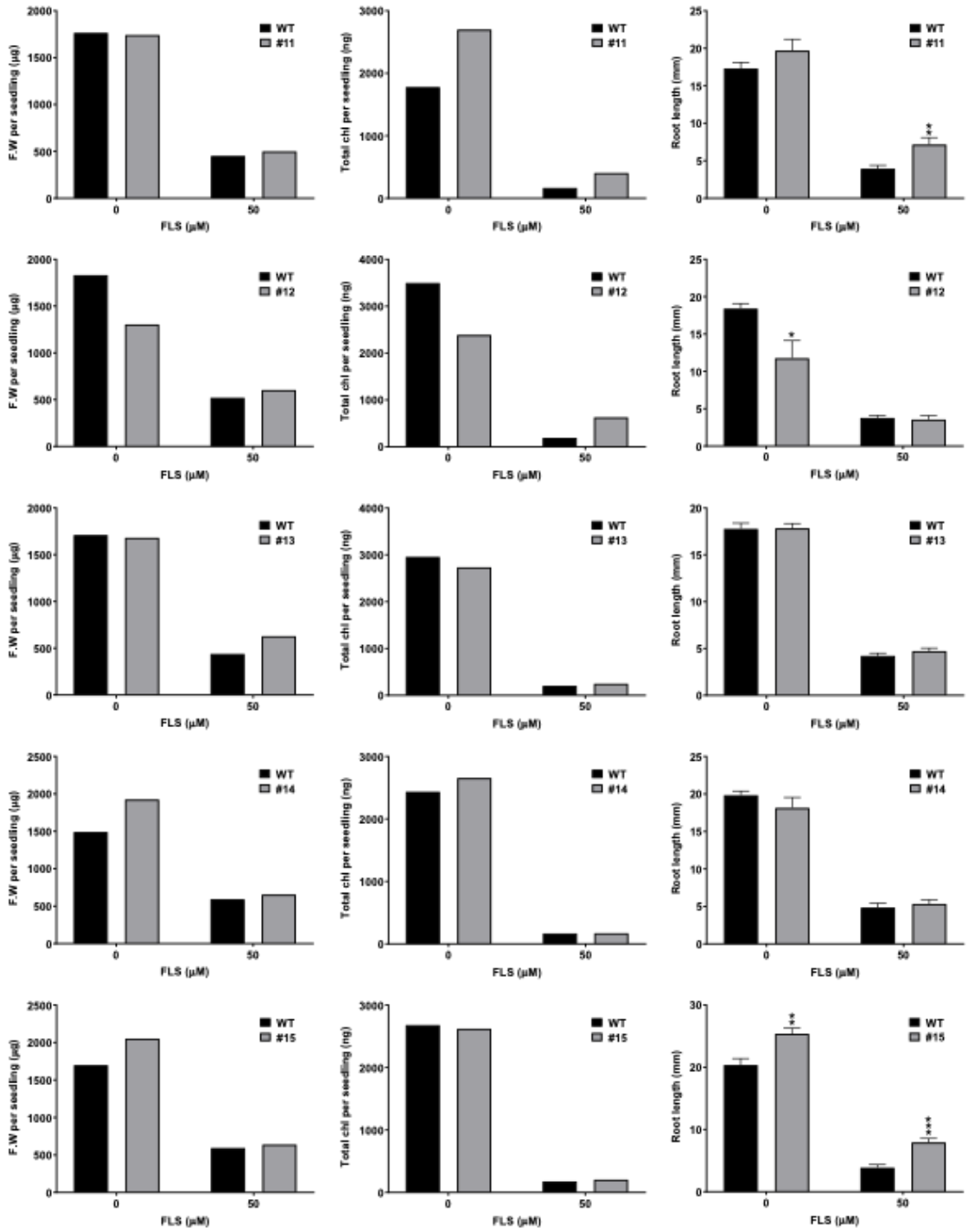
F.W per seedling (µg)
Total chl per seedling (ng)
Root length (mm)
FLS (µM)
WT
#11
#12
#13
#14
#15
0
50
*
**
***

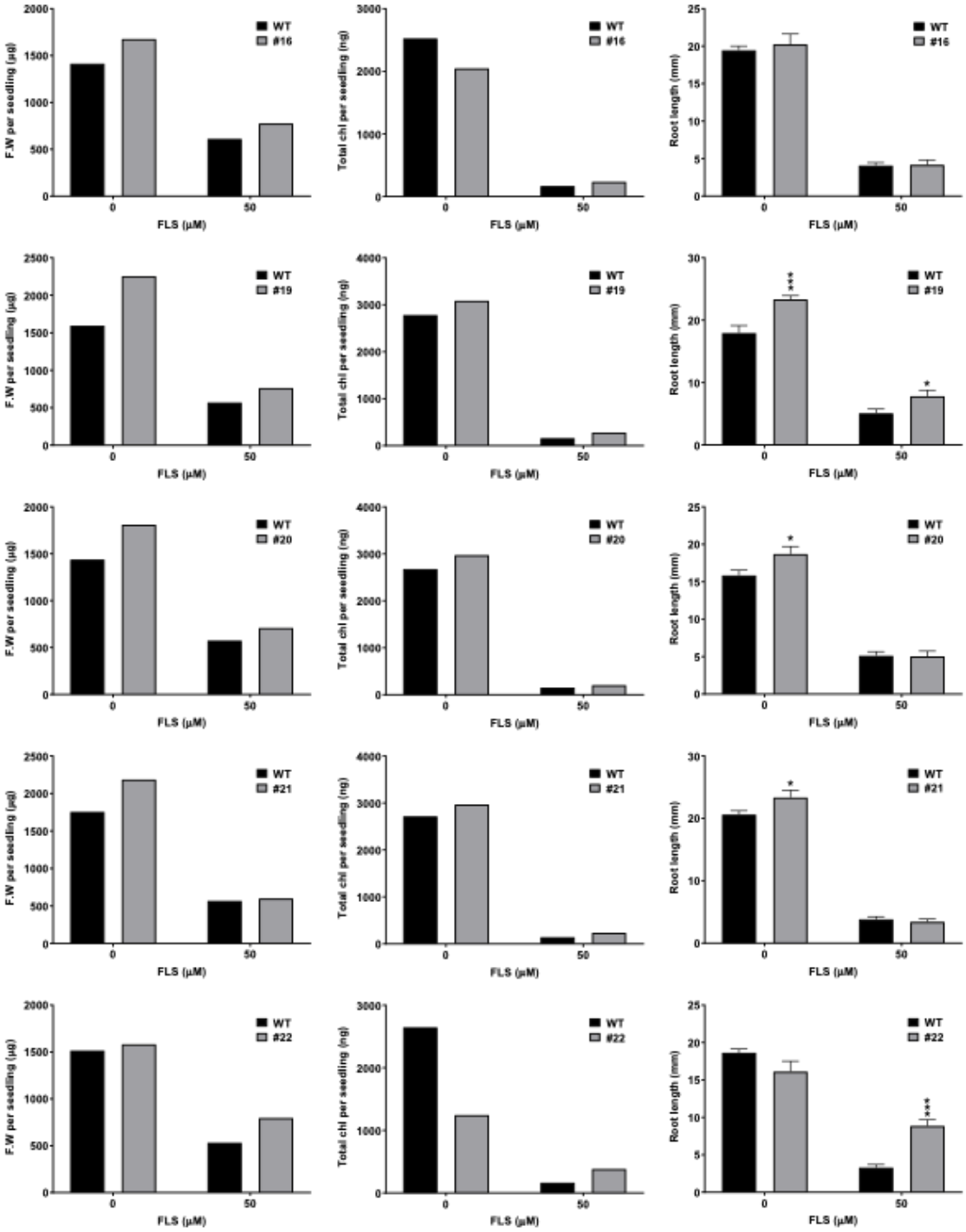
F.W per seedling (µg)
Total chl per seedling (ng)
Root length (mm)
FLS (µM)
0
50
WT
#16
#19
#20
#21
#22
***
*

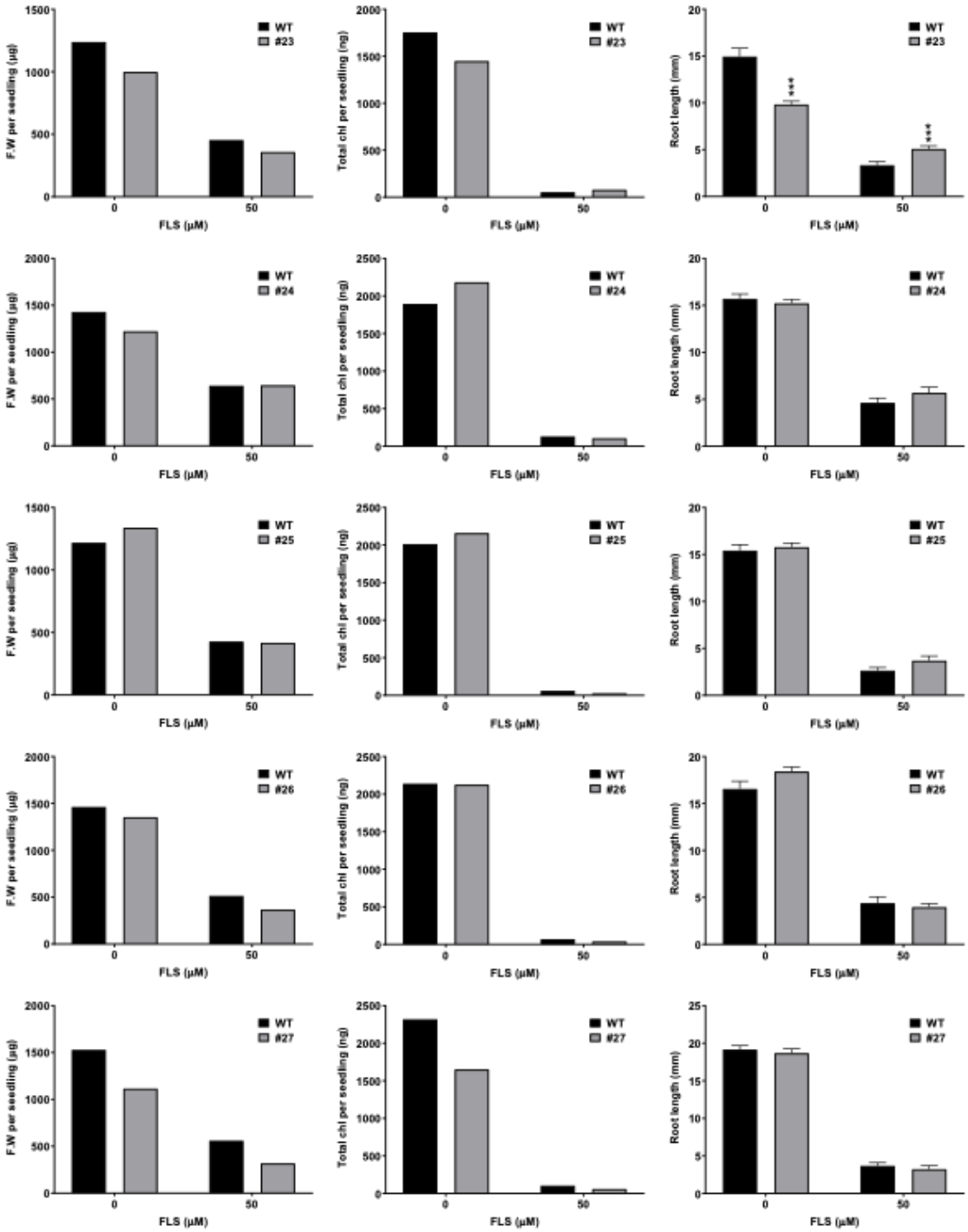
F.W per seedling (µg)
Total chl per seedling (ng)
Root length (mm)
FLS (µM)
WT
#23
#24
#25
#26
#27
***

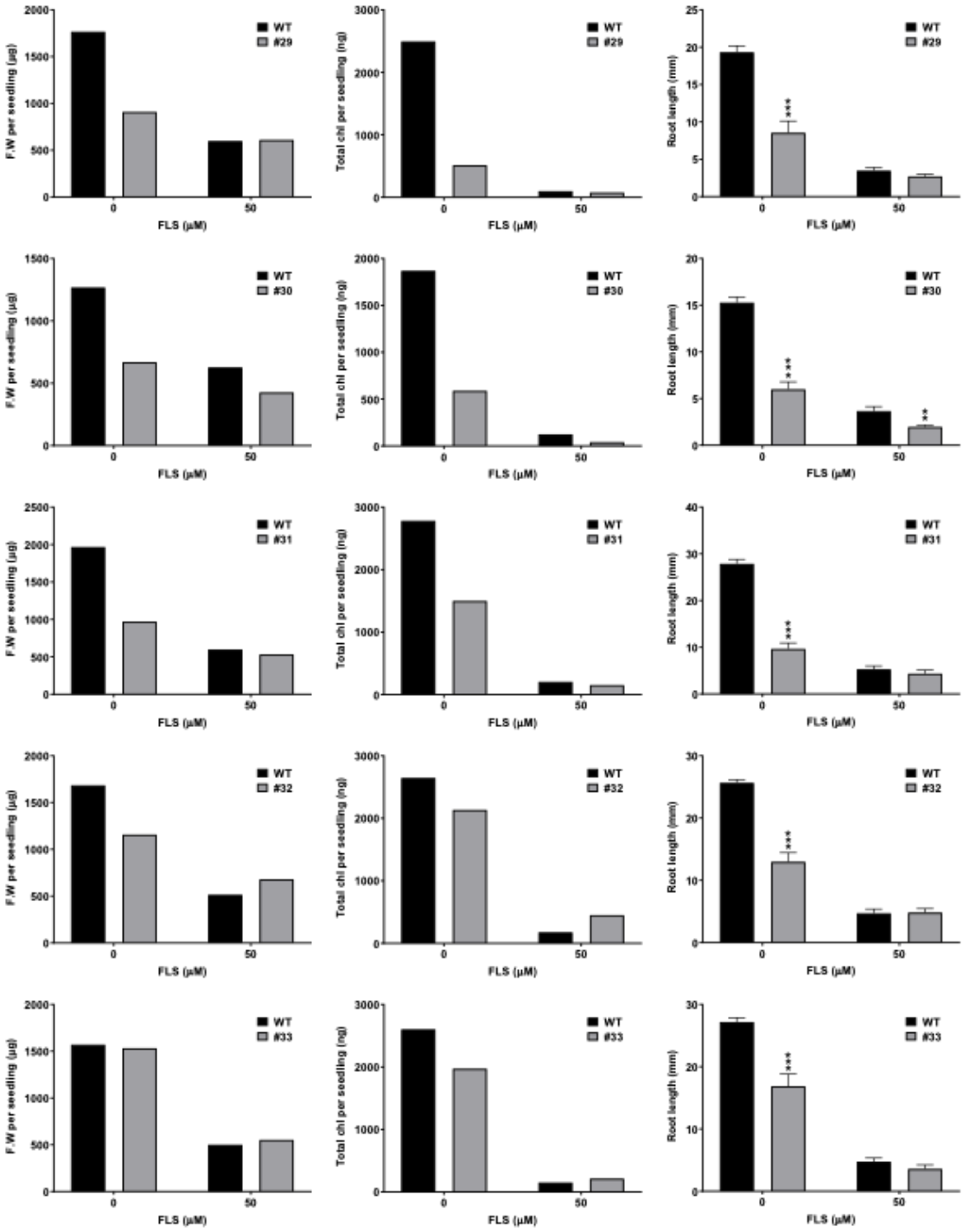
F.W per seedling (µg)
Total chl per seedling (ng)
Root length (mm)
FLS (µM)
WT
#29
#30
#31
#32
#33
0
50
***
**

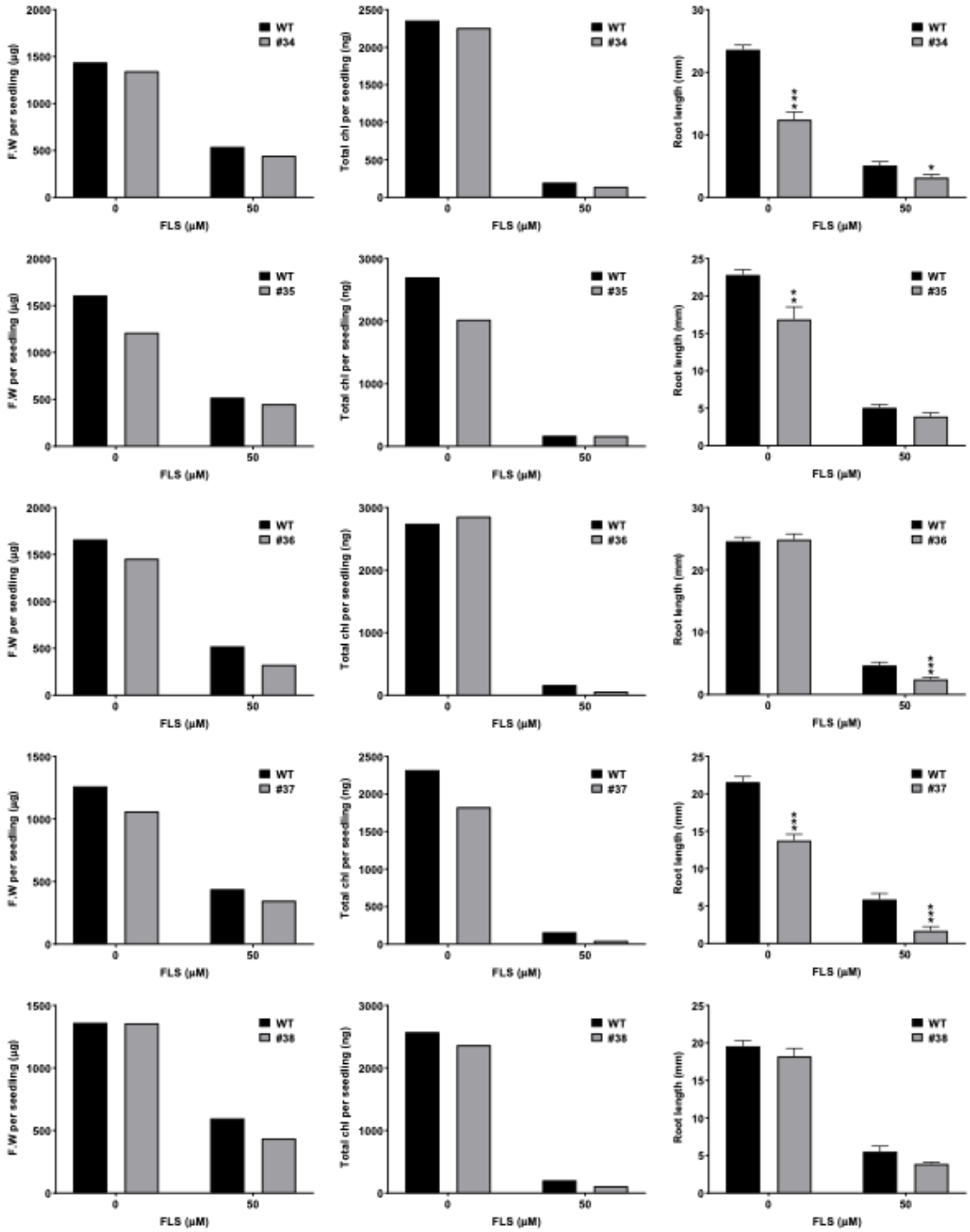
F.W per seedling (µg)
Total chl per seedling (ng)
Root length (mm)
FLS (µM)
WT
#34
#35
#36
#37
#38
0
50
***
**
*

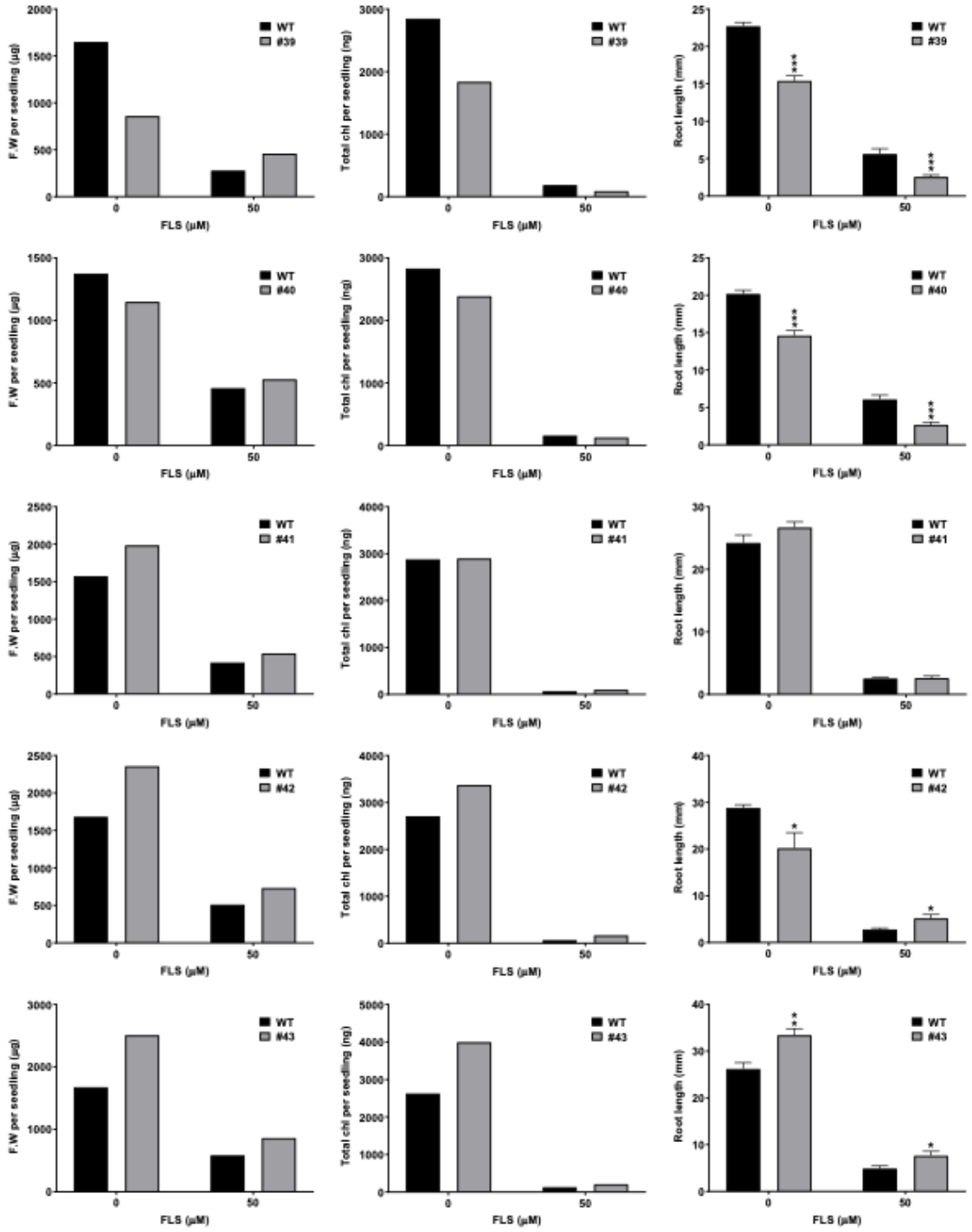
F.W per seedling (µg)
Total chl per seedling (ng)
Root length (mm)
FLS (µM)
WT
#39
#40
#41
#42
#43

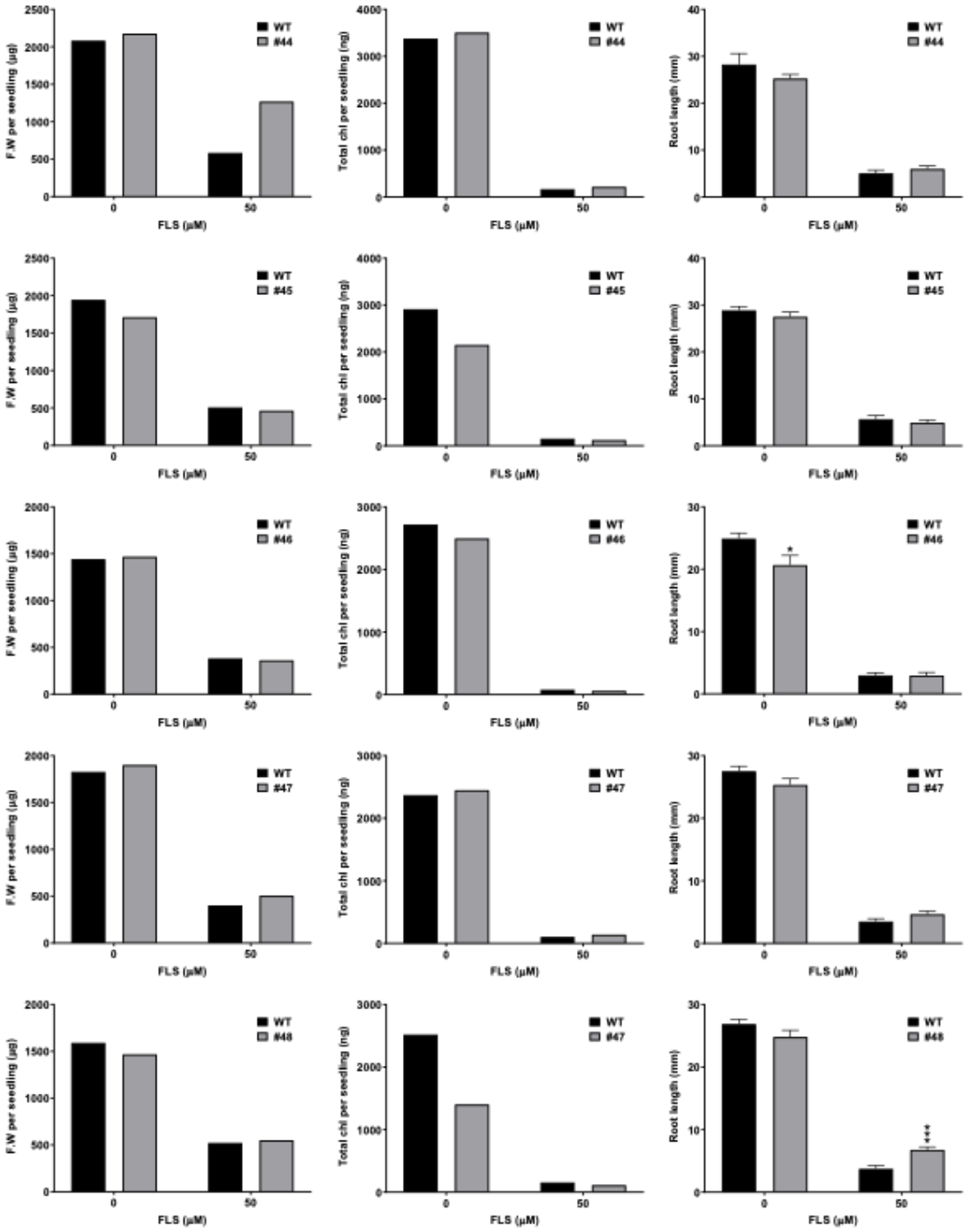
F.W per seedling (µg)
Total chl per seedling (ng)
Root length (mm)
FLS (µM)
0
50
WT
#44
#45
#46
#47
#48
*
***

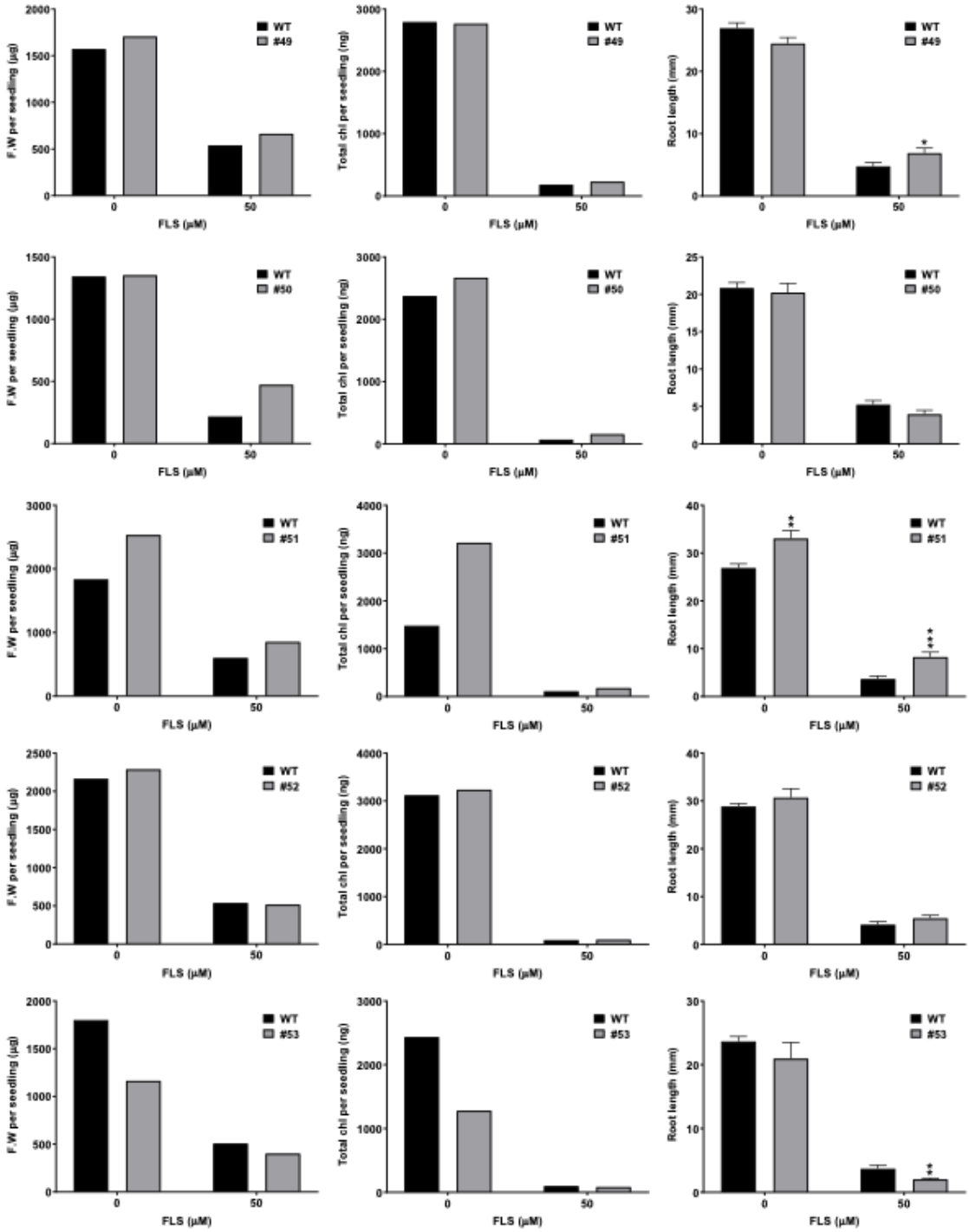
F.W per seedling (µg)
Total chl per seedling (ng)
Root length (mm)
FLS (µM)
WT
#49
#50
#51
#52
#53
0
50
*
**
***

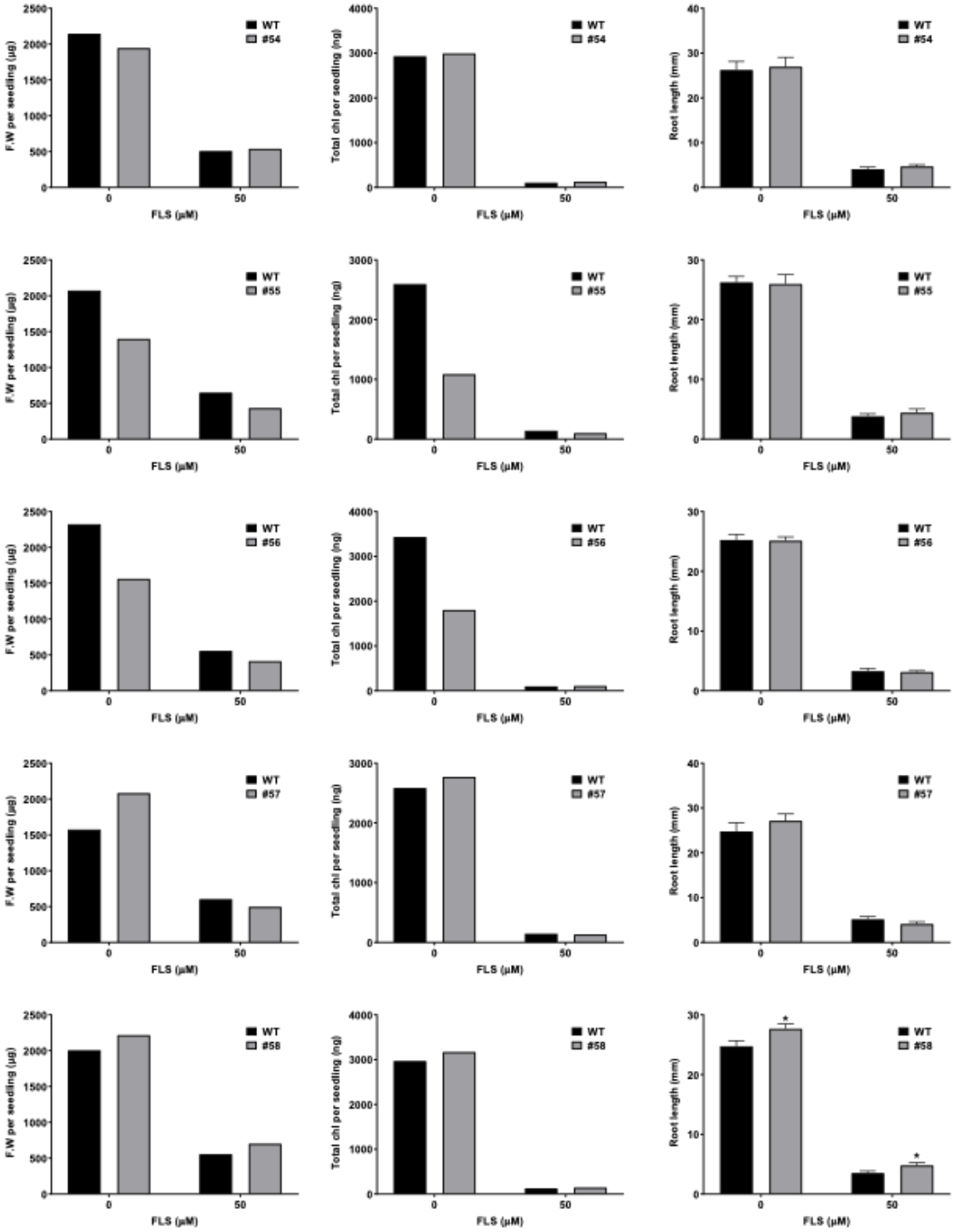
F.W per seedling (µg)
Total chl per seedling (ng)
Root length (mm)
FLS (µM)
0
50
WT
#54
#55
#56
#57
#58
*

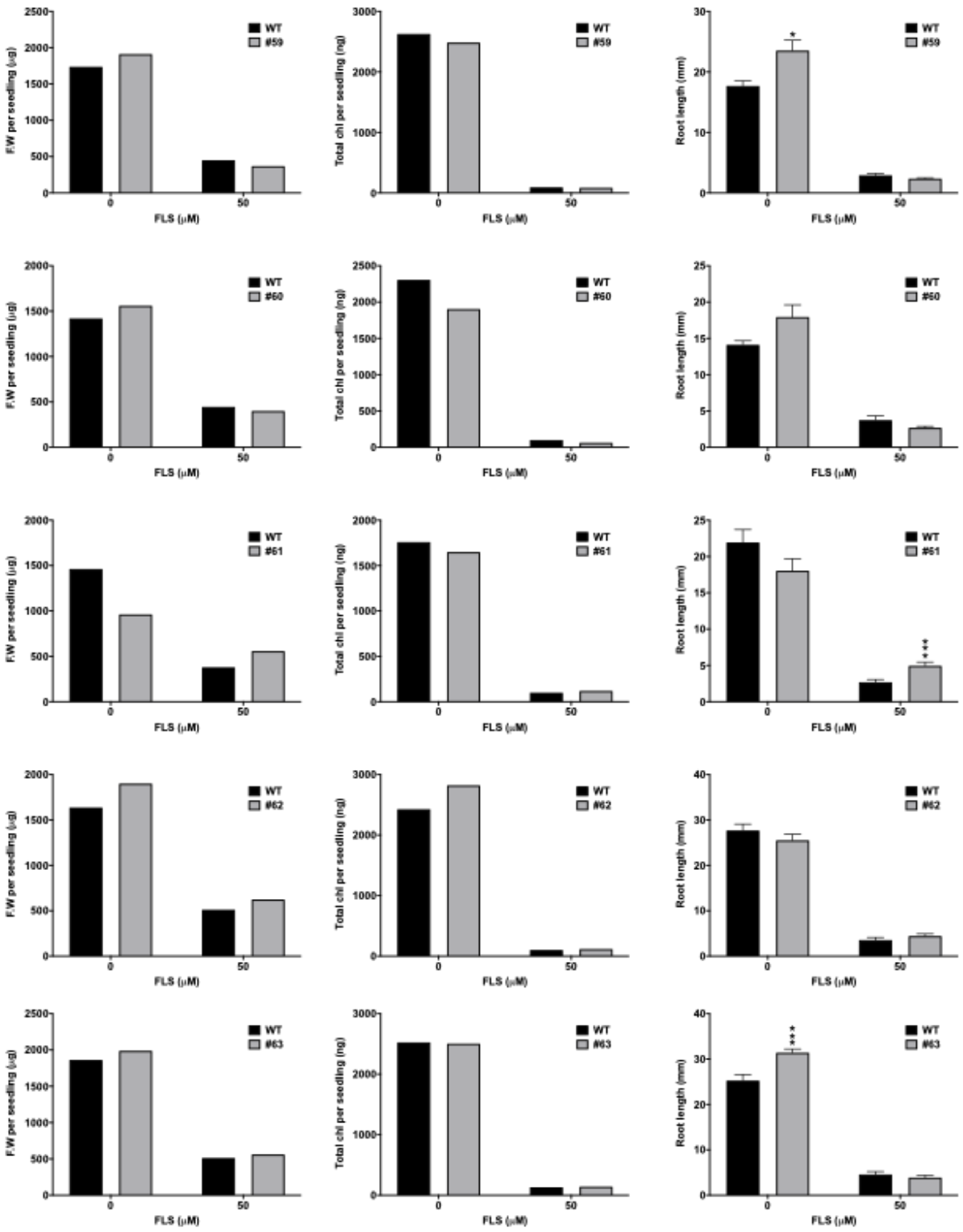
F.W per seedling (µg)
Total chl per seedling (ng)
Root length (mm)
FLS (µM)
WT
#59
#60
#61
#62
#63
0
50
*
***

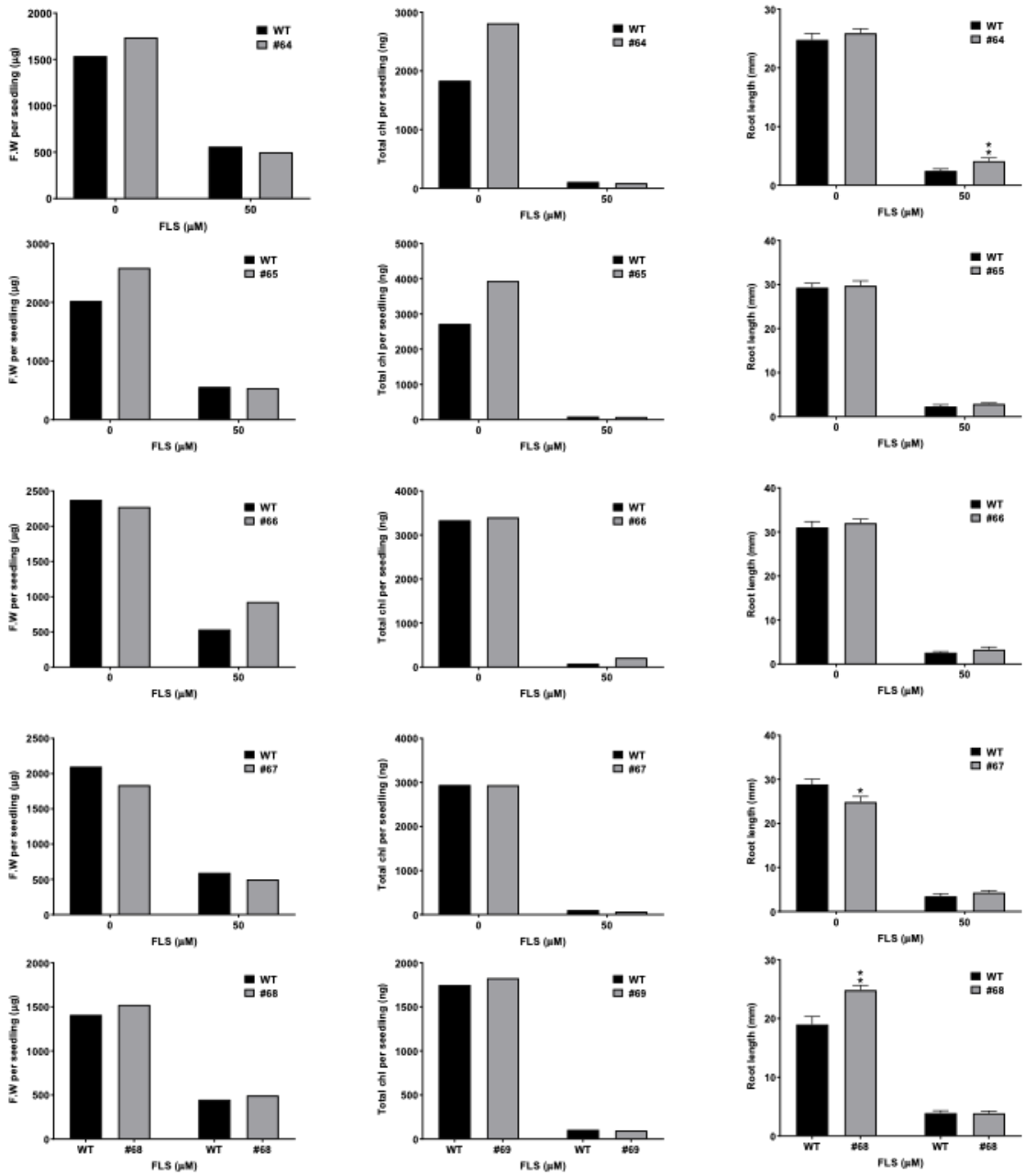
F.W per seedling (µg)
Total chl per seedling (ng)
Root length (mm)
FLS (µM)
WT
#64
#65
#66
#67
#68
#69
0
50
*
**

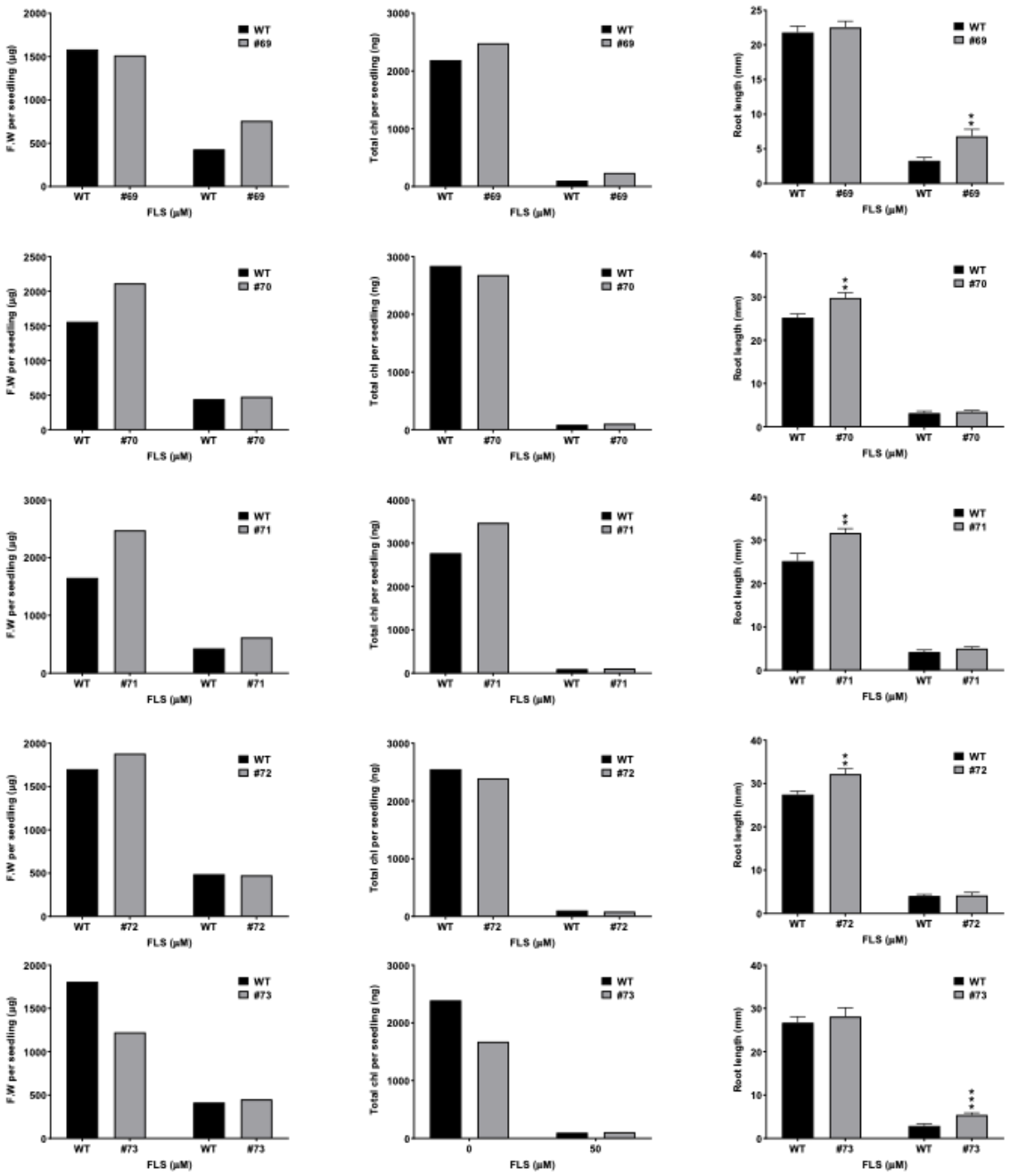
F.W per seedling (µg)
Total chl per seedling (ng)
Root length (mm)
FLS (µM)
WT
#69
#70
#71
#72
#73
0
50

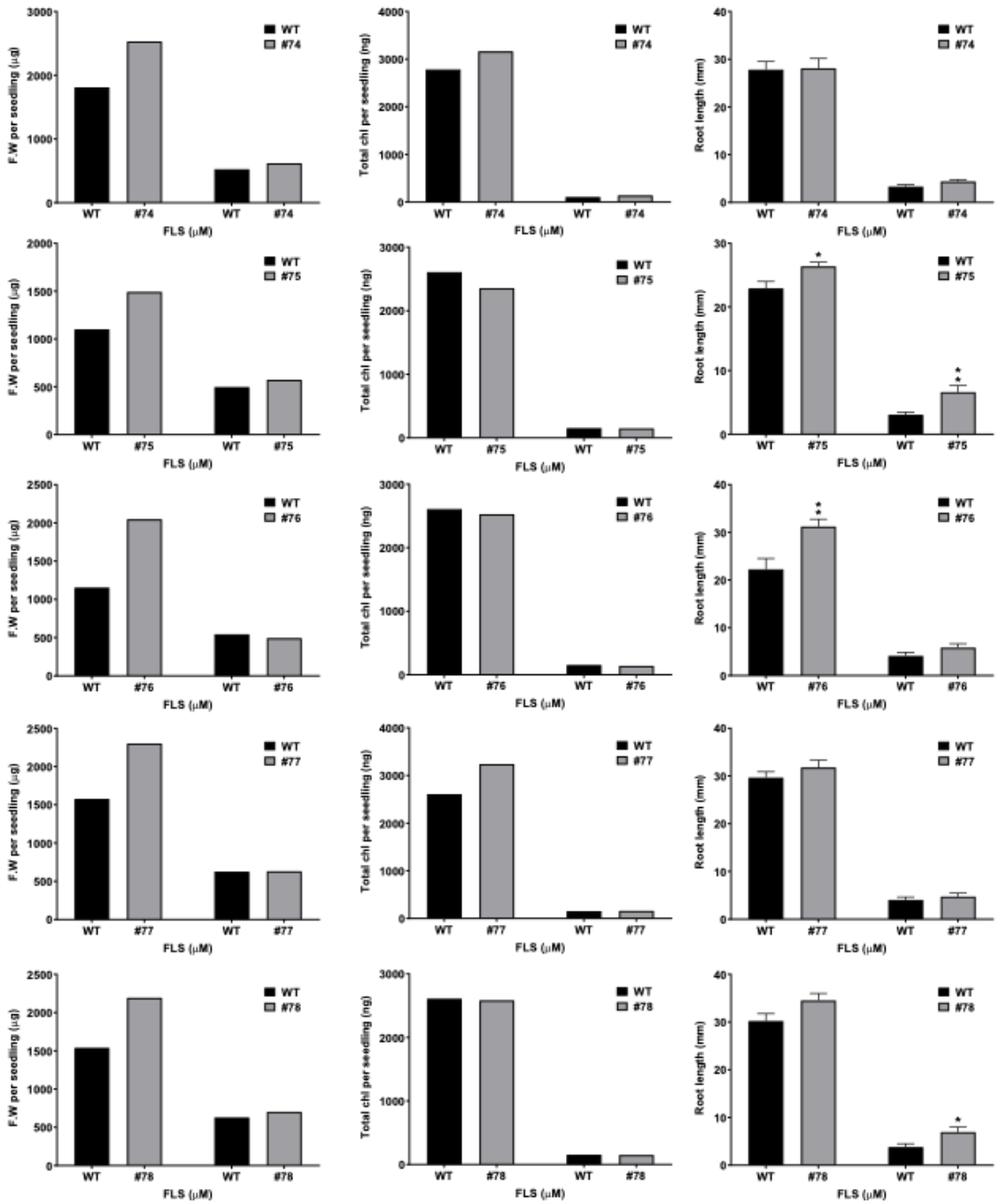
F.W per seedling (µg)
Total chl per seedling (ng)
Root length (mm)
WT
#74
#75
#76
#77
#78
FLS (µM)

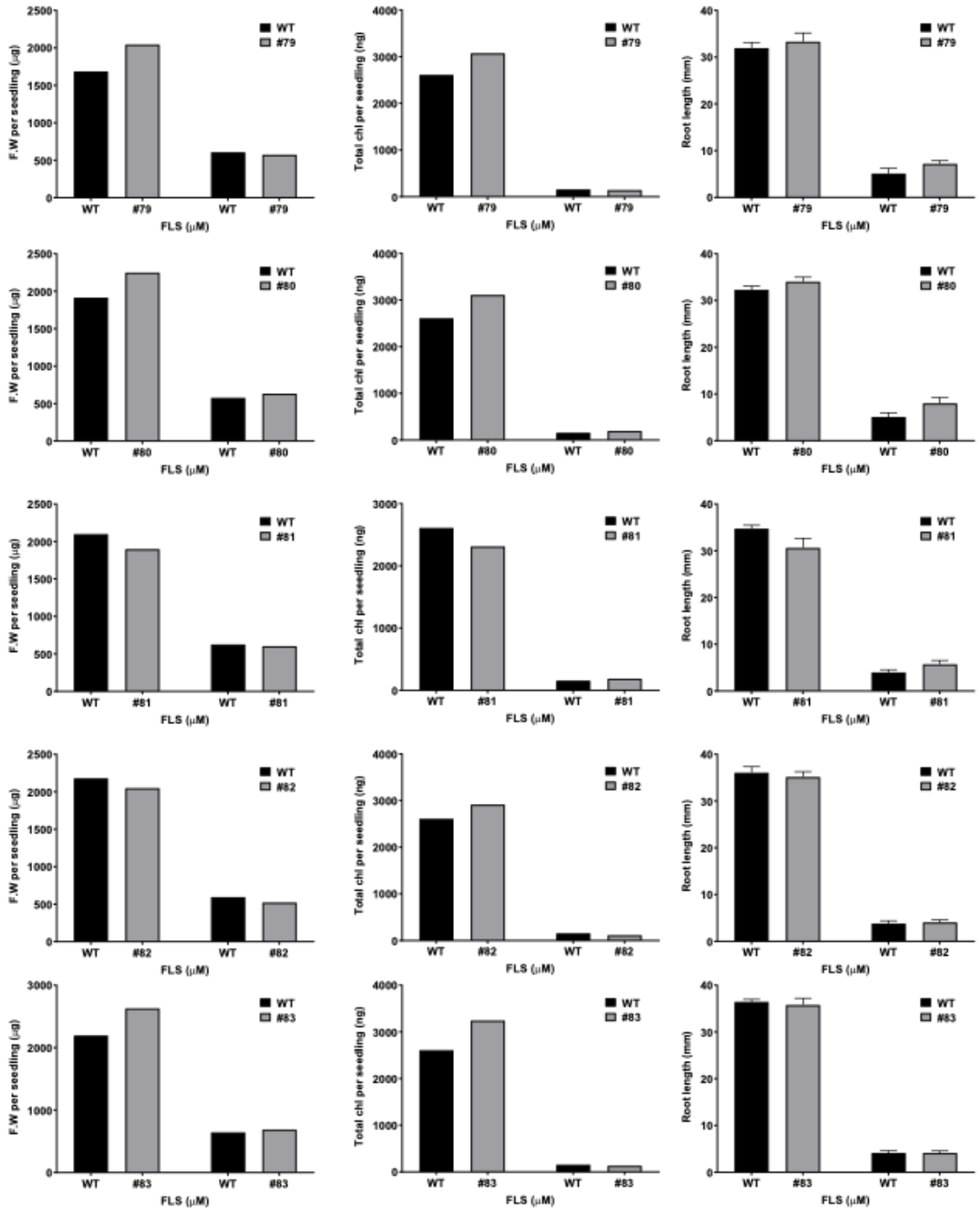
F.W per seedling (µg)
Total chl per seedling (ng)
Root length (mm)
FLS (µM)
WT
#79
#80
#81
#82
#83

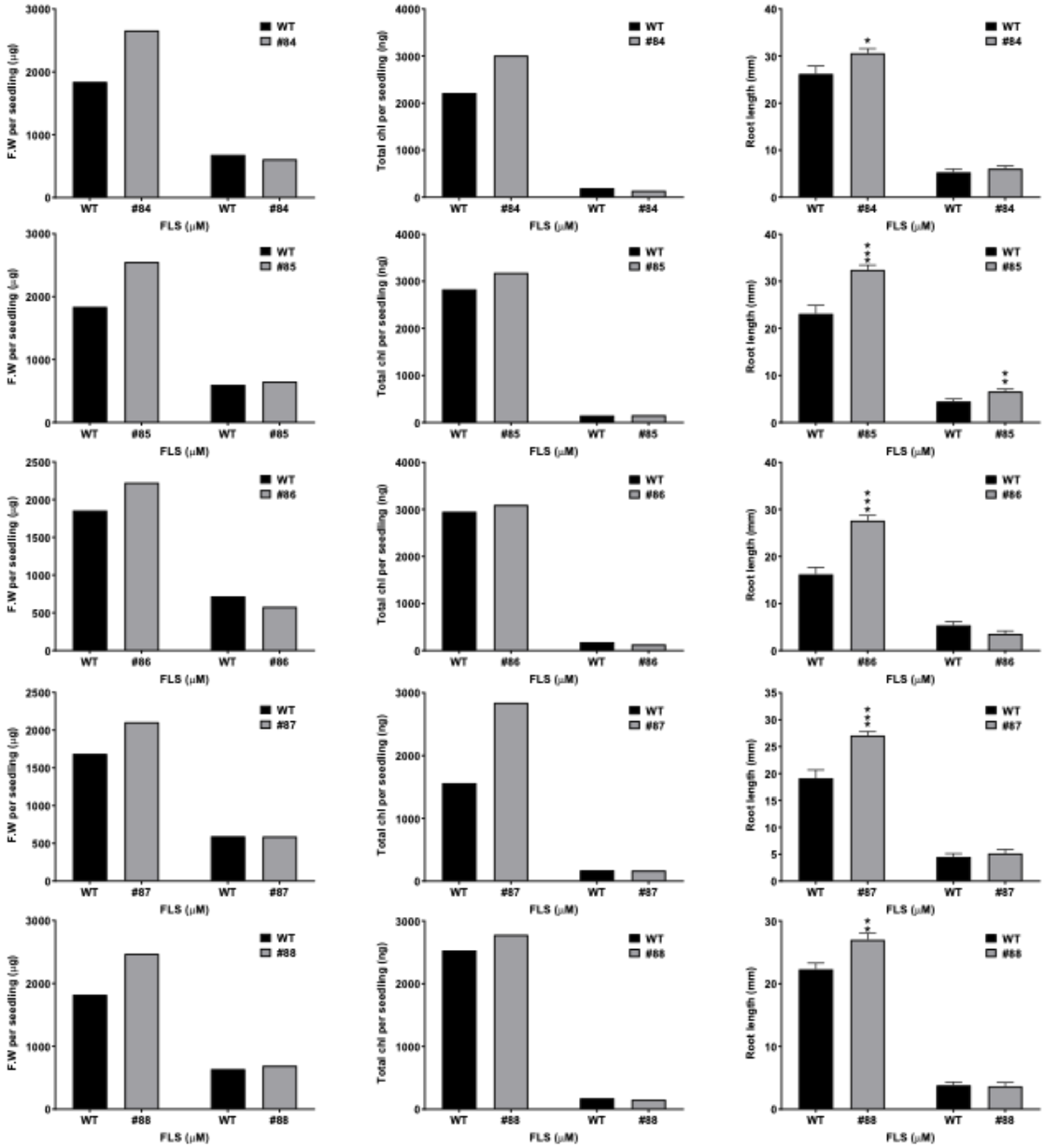
F.W per seedling (µg)
Total chl per seedling (ng)
Root length (mm)
WT
#84
#85
#86
#87
#88
FLS (µM)

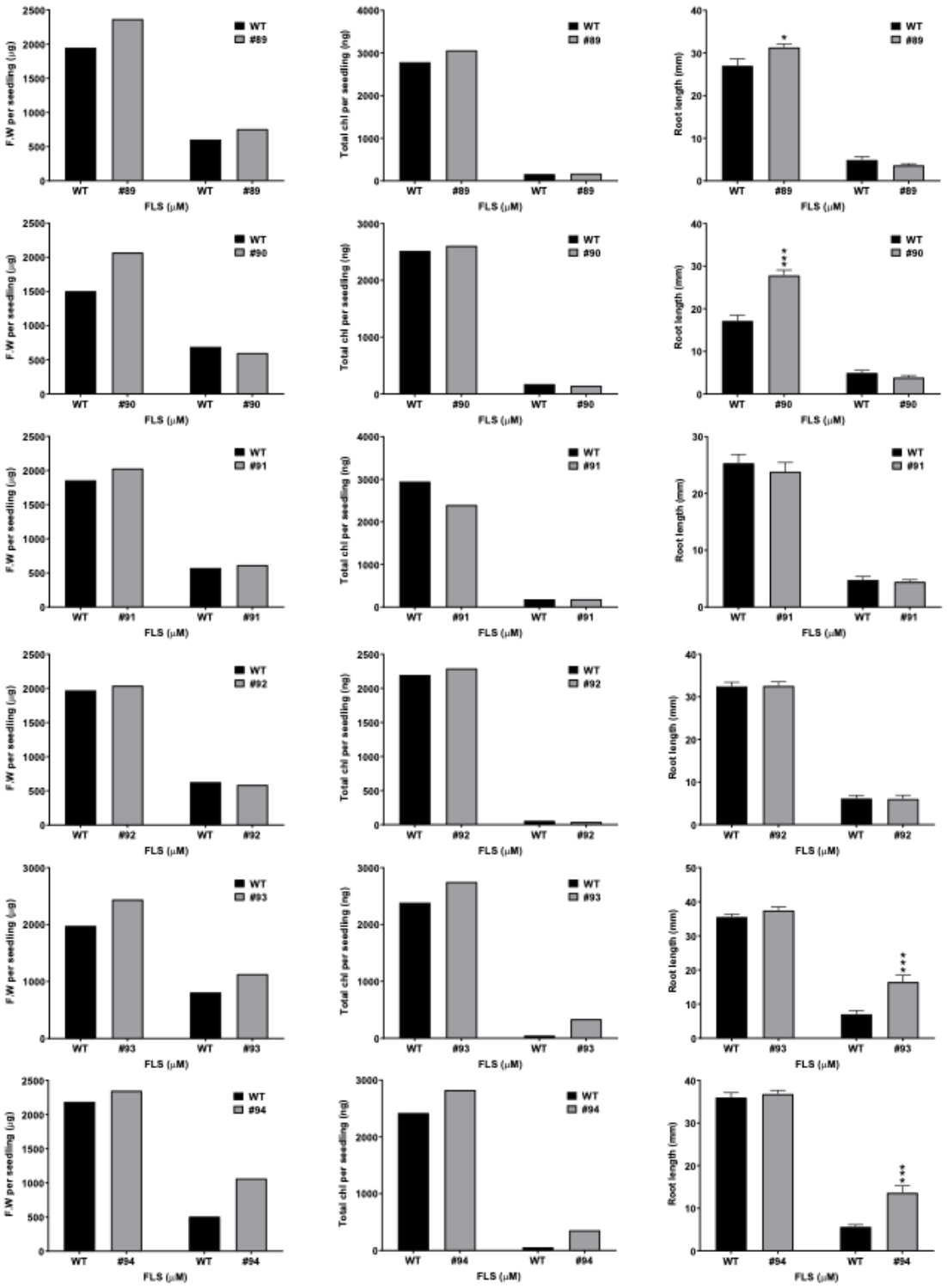

Figure S1. Re-screen of 91 potentially FLS-resistant lines. WT seedlings were grown in WL alongside each line for 7 days light on ½ MS 0.8% agar media with addition of FLS to 50 µM. Vehicle control condition included addition of 0.1% (v/v) DMSO to media. Fresh weight and total chlorophyll data points represent the mean of one biological replicate, root length data points represent the mean ± SEM of 4-41 individuals per condition. Asterisks indicate * $p<0.05$, ** $p<0.01$, *** $p<0.001$ between WT seedlings and resistant lines by t-test.

List of references

Abas, L., Benjamins, R., Malenica, N., Paciorek, T.T., Wiřniewska, J., Moulinier-Anzola, J.C., Sieberer, T., Friml, J. and Luschnig, C. 2006. Intracellular trafficking and proteolysis of the Arabidopsis auxin-efflux facilitator PIN2 are involved in root gravitropism. *Nature Cell Biology*. **8**, pp.249–256.

Abdeen, A., Schnell, J. and Miki, B. 2010. Transcriptome analysis reveals absence of unintended effects in drought-tolerant transgenic plants overexpressing the transcription factor ABF3. *BMC Genomics*. **11**, pp.1–21.

Abel, S., Nguyen, M D, Chow, W. and Theologis, A. 1995. ACS4, a primary indoleacetic acid-responsive gene encoding 1-aminocyclopropane-1-carboxylate synthase in Arabidopsis thaliana. Structural characterization, expression in Escherichia coli, and expression characteristics in response to auxin [corrected]. *The Journal of biological chemistry*. **270**, pp.19093–9.

Abel, S., Nguyen, Minh D and Theologis, A. 1995. The PS-IAA4/5-like Family of Early Auxin-inducible mRNAs in Arabidopsis thaliana. *Journal of Molecular Biology*. **251**, pp.533–549.

Abel, S. and Theologis, A. 1996. Early genes and auxin action. *Plant Physiology*. **111**, pp.9–17.

Achard, P., Liao, L., Jiang, C., Desnos, T., Bartlett, J., Fu, X. and Harberd, N.P. 2007. DELLAs Contribute to Plant Photomorphogenesis. *Plant physiology*. **143**, pp.1163–1172.

Ahmad, M. and Cashmore, A.R. 1993. HY4 gene of A. thaliana encodes a protein with characteristics of a blue-light photoreceptor. *Nature*. **366**, pp.162–166.

Ahmad, M., Lin, C. and Cashmore, A.R. 1995. Mutations throughout an Arabidopsis blue-light photoreceptor impair blue-light-responsive anthocyanin accumulation and inhibition of hypocotyl elongation. *The Plant Journal*. **8**, pp.653–8.

Ahmad, R., Arshad, M., Zahir, Z.A., Naveed, M., Khalid, M. and Asghar, A.H.N. 2008. Integrating N-enriched compost with biologically active substances for improving growth and yield of cereals. *Pakistan Journal of Botany*. **40**, pp.283–293.

Ahmad, R., Khalid, A., Arshad, M., Zahir, Z.A. and Mahmood, T. 2008. Effect of compost enriched with N and L-tryptophan on soil and maize Effect of compost enriched with

N and L-tryptophan on soil and maize. *Agron. Sustain. Dev*. **28**, pp.299–305.

Ait-Ali, T., Frances, S., Weller, J.L., Reid, J.B., Kendrick, R.E. and Kamiya, Y. 1999. Regulation of gibberellin 20-oxidase and gibberellin 3beta-hydroxylase transcript accumulation during De-etiolation of pea seedlings. *Plant physiology*. **121**, pp.783–91.

Alabadí, D., Gallego-Bartolomé, J., Orlando, L., García-Cárcel, L., Rubio, V., Martínez, C., Frigerio, M., Iglesias-Pedraz, J.M., Espinosa, A., Deng, X.W. and Blázquez, M.A. 2008. Gibberellins modulate light signaling pathways to prevent Arabidopsis seedling de-etiolation in darkness. *Plant Journal*. **53**, pp.324–335.

Alabadí, D., Gil, J., Blázquez, M.A. and García-Martínez, J.L. 2004. Gibberellins Repress Photomorphogenesis in Darkness. *Plant physiology*. **134**, pp.1050–1057.

Alfonso, A., Grundahl, K., Duerr, J.S., Han, H.P. and Rand, J.B. 1993. The Caenorhabditis elegans unc-17 gene: a putative vesicular acetylcholine transporter. *Science*. **261**.

de Almeida Engler, J., De Vleesschauwer, V., Burssens, S., Celenza, J.L., Inzé, D., Van Montagu, M., Engler, G., Gheysen, G. and Gheysen, G. 1999. Molecular markers and cell cycle inhibitors show the importance of cell cycle progression in nematode-induced galls and syncytia. *The Plant cell*. **11**, pp.793–808.

Andrews, S. 2010. Babraham Bioinformatics - FastQC A Quality Control tool for High Throughput Sequence Data. [Accessed 2 January 2021]. .

Ang, L.H. and Deng, X.W. 1994. Regulatory hierarchy of photomorphogenic loci: allele-specific and light-dependent interaction between the HY5 and COP1 loci. *The Plant cell*. **6**, pp.613–28.

Archacki, R., Buszewicz, D., Sarnowski, T.J., Sarnowska, E., Rolicka, A.T., Tohge, T., Fernie, A.R., Jikumaru, Y., Kotlinski, M., Iwanicka-Nowicka, R., Kalisiak, K., Patryn, J., Halibart-Puzio, J., Kamiya, Y., Davis, S.J., Koblowska, M.K. and Jerzmanowski, A. 2013. BRAHMA ATPase of the SWI/SNF Chromatin Remodeling Complex Acts as a Positive Regulator of Gibberellin-Mediated Responses in Arabidopsis M. A. Blazquez, ed. *PLoS ONE*. **8**, p.e58588.

Armstrong, J.I., Yuan, S., Dale, J.M., Tanner, V.N. and Theologis, A. 2004. Identification of inhibitors of auxin transcriptional activation by means of chemical genetics in Arabidopsis. *Proceedings of the National Academy of Sciences of the United States of America*. **101**, pp.14978–14983.

von Arnim, A.G. and Deng, X.-W. 1994. Light inactivation of arabidopsis photomorphogenic repressor COP1 involves a cell-specific regulation of its nucleocytoplasmic partitioning. *Cell*. **79**, pp.1035–1045.

Ashburner, M., Ball, C.A., Blake, J.A., Botstein, D., Butler, H., Cherry, J.M., Davis, A.P., Dolinski, K., Dwight, S.S., Eppig, J.T., Harris, M.A., Hill, D.P., Issel-Tarver, L., Kasarskis, A., Lewis, S., Matese, J.C., Richardson, J.E., Ringwald, M., Rubin, G.M. and Sherlock, G. 2000. Gene ontology: Tool for the unification of biology. *Nature Genetics*. **25**, pp.25–29.

Ashraf, M. and Foolad, M.R. 2005. Pre-sowing seed treatment - A shotgun approach to improve germination, plant growth and crop yield under saline and non-saline conditions. *Advances in Agronomy*. **88**, pp.223–271.

Atkinson, H.J. and Ballantyne, A.J. 1977a. Changes in the adenine nucleotide content of cysts of Globodera rostochiensis associated with the hatching of juveniles. *Annals of Applied Biology*. **87**, pp.167–174.

Atkinson, H.J. and Ballantyne, A.J. 1977b. Changes in the oxygen consumption of cysts of Globodera rostochiensis associated with the hatching of juveniles. *Annals of Applied Biology*. **87**, pp.159–166.

Atkinson, H.J. and Ballantyne, A.J. 1979. Evidence for the involvement of calcium in the hatching of Globodera rostochiensis. *Annals of Applied Biology*. **93**, pp.191–198.

Aubertot, J.N., West, J.S., Bousset-Vaslin, L., Salam, M.U., Barbetti, M.J. and Diggle, A.J. 2006. Improved resistance management for durable disease control: A case study of phoma stem canker of oilseed rape (Brassica napus). *European Journal of Plant Pathology*. **114**, pp.91–106.

Azpiroz, R., Wu, Y., Locascio, J.C. and Feldmann, K.A. 1998. An Arabidopsis Brassinosteroid-Dependent Mutant Is Blocked in Cell Elongation. *The Plant Cell*. **10**, pp.219–230.

Badescu, G.O. and Napier, R.M. 2006. Receptors for auxin: will it all end in TIRs? *Trends in Plant Science*. **11**, pp.217–223.

Bae, G. and Choi, G. 2008. Decoding of light signals by plant phytochromes and their interacting proteins. *Annual Review of Plant Biology*. **59**, pp.281–311.

Balki A.S. and Padole V.R. 1982. Effect of Pre-soaking Seed Treatments with Plant Hormones on Wheat under Conditions, of Soil Salinity. *Journal of the Indian Society*

of Soil Science. **30**, pp.361–365.

Barbez, E., Dünser, K., Gaidora, A., Lendl, T. and Busch, W. 2017. Auxin steers root cell expansion via apoplastic pH regulation in Arabidopsis thaliana. *Proceedings of the National Academy of Sciences of the United States of America*. **114**, pp.E4884–E4893.

Barrero, J.M., Rodríguez, P.L., Quesada, V., Alabadí, D., Blázquez, M.A., Boutin, J.P., Marion-Poll, A., Ponce, M.R. and Micol, J.L. 2008. The ABA1 gene and carotenoid biosynthesis are required for late skotomorphogenic growth in Arabidopsis thaliana. *Plant, Cell and Environment*. **31**, pp.227–234.

Bartel, B. 1997. Auxin biosynthesis. *Annual Review of Plant Physiology and Plant Molecular Biology*. **48**, pp.51–66.

Bauer, D., Viczián, A., Kircher, S., Nobis, T., Nitschke, R., Kunkel, T., Panigrahi, K.C.S., Adám, E., Fejes, E., Schäfer, E. and Nagy, F. 2004. Constitutive photomorphogenesis 1 and multiple photoreceptors control degradation of phytochrome interacting factor 3, a transcription factor required for light signaling in Arabidopsis. *The Plant cell*. **16**, pp.1433–45.

Behm, C.A. 1997. The role of trehalose in the physiology of nematodes. *International journal for parasitology*. **27**, pp.215–29.

Bekal, S., Niblack, T.L. and Lambert, K.N. 2003. A Chorismate Mutase from the Soybean Cyst Nematode Heterodera glycines Shows Polymorphisms that Correlate with Virulence. *Molecular Plant-Microbe Interactions*. **16**, pp.439–446.

Benková, E., Michniewicz, M., Sauer, M., Teichmann, T., Seifertová, D., Jürgens, G. and Friml, J. 2003. Local, Efflux-Dependent Auxin Gradients as a Common Module for Plant Organ Formation. *Cell*. **115**, pp.591–602.

Bennett, M., Marchant, A., Green, H.G., May, S.T., Ward, S.P., Millner, P.A., Walker, A.R., Schulz, B. and Feldmann, K.A. 1996. Arabidopsis AUX1 gene: A permease-like regulator of root gravitropism. *Science*. **273**, pp.948–950.

Bennett, S.R.M., Alvarez, J., Bossinger, G. and Smyth, D.R. 1995. Morphogenesis in pinoid mutants of Arabidopsis thaliana. *The Plant Journal*. **8**, pp.505–520.

Bethony, J., Brooker, S., Albonico, M., Geiger, S.M., Loukas, A., Diemert, D. and Hotez, P.J. 2006. Soil-transmitted helminth infections: ascariasis, trichuriasis, and hookworm. *The Lancet*. **367**, pp.1521–1532.

Bhalerao, R., Eklöf, J., Ljung, K., Marchant, A., Bennett, M. and Sandberg, G. 2002. Shoot-

derived auxin is essential for early lateral root emergence in Arabidopsis seedlings. *The Plant Journal*. **29**, pp.325–32.

Bhaskara, G.B., Nguyen, T.T. and Verslues, P.E. 2012. Unique drought resistance functions of the highly ABA-induced clade a protein phosphatase 2Cs. *Plant Physiology*. **160**, pp.379–395.

Del Bianco, M. and Kepinski, S. 2011. Context, specificity, and self-organization in auxin response. *Cold Spring Harbor Perspectives in Biology*. **3**, pp.10–20.

Bilkert, J. and Rao, P. 1985. Sorption and leaching of three non fumigant nematicides in soils. *Journal of Environmental Science and Health Part B-Pesticides Food Contaminants and Agricultural Wastes*. **20**, pp.1–26.

Bird, A.F. 1961. The ultrastructure and histochemistry of a nematode-induced giant cell. *The Journal of biophysical and biochemical cytology*. **11**, pp.701–15.

Bird, A.F. and Bird, J. 1991. *The Structure of Nematodes* [Online]. Academic Press. [Accessed 25 May 2017]. .

Bird, A.F. and Loveys, B.R. 1975. The Incorporation of Photosynthates by Meloidogne javanica. *Journal of nematology*. **7**, pp.111–113.

Bird, D.M. and Opperman, C.H. 1998. Caenorhabditis elegans: A Genetic Guide to Parasitic Nematode Biology. *Journal of nematology*. **30**, pp.299–308.

Bishopp, A., Help, H., El-Showk, S., Weijers, D., Scheres, B., Friml, J., Benková, E., Mähönen, A.P. and Helariutta, Y. 2011. A mutually inhibitory interaction between auxin and cytokinin specifies vascular pattern in roots. *Current Biology*. **21**, pp.917–926.

Blaxter, M., Elsen, S. van den, Holterman, M., Karssen, G. and Mooyman, P. 2011. Nematodes: The Worm and Its Relatives. *PLoS Biology*. **9**, p.e1001050.

Blaxter, M., De Ley, P., Garey, J.R., Liu, L.X., Scheldeman, P., Vierstraete, A., Vanfleteren, J.R., Mackey, L.Y., Dorris, M., Frisse, L.M., Vida, J.T. and Thomas, W.K. 1998. A molecular evolutionary framework for the phylum Nematoda. *Nature*. **392**, pp.71–75.

Bleecker, A.B. and Kende, H. 2000. Ethylene: A Gaseous Signal Molecule in Plants. *Annual Review of Cell and Developmental Biology*. **16**, pp.1–18.

Bleve-Zacheo, T. and Melillo, M.T. 1997. The Biology of Giant Cells *In*: *Cellular and Molecular Aspects of Plant-Nematode Interactions* [Online]. Springer Netherlands,

pp.65–79. [Accessed 26 May 2017]. .

de Boer, J.M., McDermott, J.P., Wang, X., Maier, T., Qui, F., Hussey, R.S., Davis, E.L. and J Baum, T. 2002. The use of DNA microarrays for the developmental expression analysis of cDNAs from the oesophageal gland cell region of Heterodera glycines. *Molecular plant pathology*. **3**, pp.261–70.

Bolle, C., Schneider, A. and Leister, D. 2011. Perspectives on Systematic Analyses of Gene Function in Arabidopsis thaliana: New Tools, Topics and Trends. *Current Genomics*. **12**, pp.1–14.

Brautigam, C.A., Smith, B.S., Ma, Z., Palnitkar, M., Tomchick, D.R., Machius, M. and Deisenhofer, J. 2004. Structure of the photolyase-like domain of cryptochrome 1 from Arabidopsis thaliana. *Proceedings of the National Academy of Sciences of the United States of America*. **101**, pp.12142–7.

Bridge, J. and Starr, J.L. 2007. *Plant nematodes of agricultural importance : a colour handbook*. Taylor & Francis, CRC Press.

Briggs, W.R. and Christie, J.M. 2002. Phototropins 1 and 2: Versatile plant blue-light receptors. *Trends in Plant Science*. **7**, pp.204–210.

Brunoud, G., Wells, D.M., Oliva, M., Larrieu, A., Mirabet, V., Burrow, A.H., Beeckman, T., Kepinski, S., Traas, J., Bennett, M. and Vernoux, T. 2012. A novel sensor to map auxin response and distribution at high spatio-temporal resolution. *Nature*. **482**, pp.103–106.

Busi, R., Goggin, D.E., Heap, I.M., Horak, M.J., Jugulam, M., Masters, R.A., Napier, R.M., Riar, D.S., Satchivi, N.M., Torra, J., Westra, P. and Wright, T.R. 2018. Weed resistance to synthetic auxin herbicides. *Pest Management Science*. **74**, pp.2265–2276.

Cabrera y Poch, H.L., Peto, C.A. and Chory, J. 1993. A mutation in the Arabidopsis DET3 gene uncouples photoregulated leaf development from gene expression and chloroplast biogenesis. *The Plant Journal*. **4**, pp.671–682.

Cai, D., Kleine, M., Kifle, S., Harloff, H.J., Sandal, N.N., Marcker, K.A., Klein-Lankhorst, R.M., Salentijn, E.M., Lange, W., Stiekema, W.J., Wyss, U., Grundler, F.M.W. and Jung, C. 1997. Positional cloning of a gene for nematode resistance in sugar beet. *Science*. **275**, pp.832–4.

Calvo-araya, J.A., Orozco-aceves, M., Agrarias, E.D.C., Nacional, U., Rica, D.C., Rica, C., Regional, I., Estudios, D., Tóxicas, S., Nacional, U., Rica, D.C. and Rica, C. 2016.

Nematicidal Efficacy of Fluensulfone against False Root-knot Nematode (Nacobbus aberrans) in Cucumber Crop under Field Conditions. . **14**, pp.1–8.

Campbell, N.A. and Reece, J.B. 2008. *Biology*. Pearson Benjamin Cummings.

Cao, J., Li, G., Qu, D., Li, X. and Wang, Y. 2020. Into the seed: Auxin controls seed development and grain yield. *International Journal of Molecular Sciences*. **21**.

Carbon, S., Douglass, E., Dunn, N., Good, B., Harris, N.L., Lewis, S.E., Mungall, C.J., Basu, S., Chisholm, R.L., Dodson, R.J., Hartline, E., Fey, P., Thomas, P.D., Albou, L.P., Ebert, D., Kesling, M.J., Mi, H., Muruganujan, A., Huang, X., Poudel, S., Mushayahama, T., Hu, J.C., LaBonte, S.A., Siegele, D.A., Antonazzo, G., Attrill, H., Brown, N.H., Fexova, S., Garapati, P., Jones, T.E.M., Marygold, S.J., Millburn, G.H., Rey, A.J., Trovisco, V., Dos Santos, G., Emmert, D.B., Falls, K., Zhou, P., Goodman, J.L., Strelets, V.B., Thurmond, J., Courtot, M., Osumi, D.S., Parkinson, H., Roncaglia, P., Acencio, M.L., Kuiper, M., Lreid, A., Logie, C., Lovering, R.C., Huntley, R.P., Denny, P., Campbell, N.H., Kramarz, B., Acquaah, V., Ahmad, S.H., Chen, H., Rawson, J.H., Chibucos, M.C., Giglio, M., Nadendla, S., Tauber, R., Duesbury, M.J., Del, N.T., Meldal, B.H.M., Perfetto, L., Porras, P., Orchard, S., Shrivastava, A., Xie, Z., Chang, H.Y., Finn, R.D., Mitchell, A.L., Rawlings, N.D., Richardson, L., Sangrador-Vegas, A., Blake, J.A., Christie, K.R., Dolan, M.E., Drabkin, H.J., Hill, D.P., Ni, L., Sitnikov, D., Harris, M.A., Oliver, S.G., Rutherford, K., Wood, V., Hayles, J., Bahler, J., Lock, A., Bolton, E.R., De Pons, J., Dwinell, M., Hayman, G.T., Laulederkind, S.J.F., Shimoyama, M., Tutaj, M., Wang, S.J., D'Eustachio, P., Matthews, L., Balhoff, J.P., Aleksander, S.A., Binkley, G., Dunn, B.L., Cherry, J.M., Engel, S.R., Gondwe, F., Karra, K., MacPherson, K.A., Miyasato, S.R., Nash, R.S., Ng, P.C., Sheppard, T.K., Shrivatsav Vp, A., Simison, M., Skrzypek, M.S., Weng, S., Wong, E.D., Feuermann, M., Gaudet, P., Bakker, E., Berardini, T.Z., Reiser, L., Subramaniam, S., Huala, E., Arighi, C., Auchincloss, A., Axelsen, K., Argoud, G.P., Bateman, A., Bely, B., Blatter, M.C., Boutet, E., Breuza, L., Bridge, A., Britto, R., Bye-A-Jee, H., Casals-Casas, C., Coudert, E., Estreicher, A., Famiglietti, L., Garmiri, P., Georghiou, G., Gos, A., Gruaz-Gumowski, N., Hatton-Ellis, E., Hinz, U., Hulo, C., Ignatchenko, A., Jungo, F., Keller, G., Laiho, K., Lemercier, P., Lieberherr, D., Lussi, Y., Mac-Dougall, A., Magrane, M., Martin, M.J., Masson, P., Natale, D.A., Hyka, N.N., Pedruzzi, I., Pichler, K., Poux, S., Rivoire, C., Rodriguez-Lopez, M., Sawford, T., Speretta, E., Shypitsyna, A., Stutz, A., Sundaram, S., Tognolli, M., Tyagi, N., Warner,

K., Zaru, R., Wu, C., Chan, J., Cho, J., Gao, S., Grove, C., Harrison, M.C., Howe, K., Lee, R., Mendel, J., Muller, H.M., Raciti, D., Van Auken, K., Berriman, M., Stein, L., Sternberg, P.W., Howe, D., Toro, S. and Westerfield, M. 2019. The Gene Ontology Resource: 20 years and still GOing strong. *Nucleic Acids Research*. **47**, pp.D330–D338.

Casal, J.J. and Sánchez, R.A. 1998. Phytochromes and seed germination. *Seed Science Research*. **8**, pp.317–329.

Castillo, P. 2012. Systematics of Cyst Nematodes (Nematoda: Heteroderinae). *Plant Pathology*. **61**, pp.424–424.

Castro, C.E., McKinney, H.E. and Lux, S. 1991. Plant protection with inorganic ions. *Journal of nematology*. **23**, pp.409–13.

Cayrol, J.C. 1983. BIOLOGICAL CONTROL OF MELOIDOGYNE BY ARTHROBOTRYS-IRREGULARIS. *Revue de Nématologie*. **6**, pp.265–274.

Cecchetti, V., Altamura, M.M., Falasca, G., Costantino, P. and Cardarelli, M. 2008. Auxin regulates Arabidopsis anther dehiscence, pollen maturation, and filament elongation. *Plant Cell*. **20**, pp.1760–1774.

Chan, Z., Grumet, R. and Loescher, W. 2011. Global gene expression analysis of transgenic, mannitol-producing, and salt-tolerant Arabidopsis thaliana indicates widespread changes in abiotic and biotic stress-related genes. *Journal of Experimental Botany*. **62**, pp.4787–4803.

Chapman, E.J., Greenham, K., Castillejo, C., Sartor, R., Bialy, A., Sun, T. and Estelle, M. 2012. Hypocotyl Transcriptome Reveals Auxin Regulation of Growth-Promoting Genes through GA-Dependent and -Independent Pathways M. A. Blazquez, ed. *PLoS ONE*. **7**, p.e36210.

Chattopadhyay, S., Ang, L.H., Puente, P., Deng, X.W. and Wei, N. 1998. Arabidopsis bZIP protein HY5 directly interacts with light-responsive promoters in mediating light control of gene expression. *The Plant cell*. **10**, pp.673–83.

Cheminant, S., Wild, M., Bouvier, F., Pelletier, S., Renou, J.P., Erhardt, M., Hayes, S., Terry, M.J., Genschik, P. and Achard, P. 2011. DELLAs regulate chlorophyll and carotenoid biosynthesis to prevent photooxidative damage during seedling deetiolation in Arabidopsis. *Plant Cell*. **23**, pp.1849–1860.

Chen, D., Xu, G., Tang, W., Jing, Y., Ji, Q., Fei, Z. and Lin, R. 2013. Antagonistic basic helix-loop-Helix/bZIP transcription factors form transcriptional modules that integrate

light and reactive oxygen species signaling in Arabidopsis. *Plant Cell*. **25**, pp.1657–1673.

Chen, H., Zhang, J., Neff, M.M., Hong, S.W., Zhang, H., Deng, X.W. and Xiong, L. 2008. Integration of light and abscisic acid signaling during seed germination and early seedling development. *Proceedings of the National Academy of Sciences of the United States of America*. **105**, pp.4495–4500.

Chen, L. and Hellmann, H. 2013. Plant E3 ligases: Flexible enzymes in a sessile world. *Molecular Plant*. **6**, pp.1388–1404.

Chen, Z., Chen, S. and Dickson, D. 2004. Nematode management and utilization *In*: *Nematology Advances and perspectives*. Wallingford, UK: CABI Publishing, p.1201.

Cheng, C.Y., Krishnakumar, V., Chan, A.P., Thibaud-Nissen, F., Schobel, S. and Town, C.D. 2017. Araport11: a complete reannotation of the Arabidopsis thaliana reference genome. *Plant Journal*. **89**, pp.789–804.

Chini, A., Fonseca, S., Fernández, G., Adie, B., Chico, J.M., Lorenzo, O., García-Casado, G., López-Vidriero, I., Lozano, F.M., Ponce, M.R., Micol, J.L. and Solano, R. 2007. The JAZ family of repressors is the missing link in jasmonate signalling. *Nature*. **448**, pp.666–671.

Chitwood, D. 2003. Nematicides *In*: J. R. Plimmer, D. W. Gammon and N. R. Ragsdale, eds. *Encyclopedia of Agrochemicals*. Wiley.

Chitwood, D.J. and Perry, R.N. 2009. Reproduction, physiology and biochemistry. *In*: R. N. Perry, M. Moens and J. L. Starr, eds. *Root-knot nematodes* [Online]. Wallingford, UK: CABI Publishing, pp.182–200. [Accessed 25 May 2017]. .

Choe, S., Dilkes, B.P., Fujioka, S., Takatsuto, S., Sakurai, A. and Feldmann, K.A. 1998. The DWF4 gene of Arabidopsis encodes a cytochrome P450 that mediates multiple 22alpha-hydroxylation steps in brassinosteroid biosynthesis. *The Plant cell*. **10**, pp.231–243.

Chory, J. 1992. A genetic model for light-regulated seedling Arabidopsis. *Development*. **115**, pp.337–354.

Chory, J., Nagpal, P. and Peto, C.A. 1991. Phenotypic and Genetic Analysis of det2, a New Mutant That Affects Light-Regulated Seedling Development in Arabidopsis. *The Plant cell*. **3**, pp.445–459.

Chory, Joanne, Nagpal, P. and Petob, C.A. 1991. Phenotypic and Genetic Analysis of det2,

a New Mutant That Affects Light-Regulated Seedling Development in Arabidopsis. *The Plant Cell*. **3**, pp.445–459.

Chory, J, Peto, C., Feinbaum, R., Pratt, L. and Ausubel, F. 1989. Arabidopsis thaliana mutant that develops as a light-grown plant in the absence of light. *Cell*. **58**, pp.991–9.

Chory, Joanne, Peto, C., Feinbaum, R., Pratt, L. and Ausubel, F. 1989. Arabidopsis thaliana mutant that develops as a light-grown plant in the absence of light. *Cell*. **58**, pp.991–999.

Chory, J., Peto, C.A., Ashbaugh, M., Saganich, R., Pratt, L. and Ausubel, F. 1989. Different Roles for Phytochrome in Etiolated and Green Plants Deduced from Characterization of Arabidopsis thaliana Mutants. *The Plant Cell*. **1**, pp.867–880.

Chow, B. and McCourt, P. 2006. Plant hormone receptors: perception is everything. *Genes & development*. **20**, pp.1998–2008.

Christie, J.M., Salomon, M., Nozue, K., Wada, M. and Briggs, W.R. 1999. LOV (light, oxygen, or voltage) domains of the blue-light photoreceptor phototropin (nph1): binding sites for the chromophore flavin mononucleotide. *Proceedings of the National Academy of Sciences of the United States of America*. **96**, pp.8779–83.

Ciolfi, A., Sessa, G., Sassi, M., Possenti, M., Salvucci, S., Carabelli, M., Morelli, G. and Ruberti, I. 2013. Dynamics of the shade-avoidance response in Arabidopsis. *Plant Physiology*. **163**, pp.331–353.

Clack, T., Mathews, S. and Sharrock, R.A. 1994. The phytochrome apoprotein family in Arabidopsis is encoded by five genes: the sequences and expression of PHYD and PHYE. *Plant molecular biology*. **25**, pp.413–27.

Clarke, A.J. and Hennessy, J. 1976. The Distribution of Carbohydrates in Cysts of Heterodera Rostochiensis. *Nematologica*. **22**, pp.190–195.

Clarke, A.J. and Hennessy, J. 1983. The role of calcium in the hatching of Globodera rostochiensis. *Revue de Nématologie*. **6**, pp.247–255.

Cleland, R.E. 1976. Kinetics of Hormone-induced H + Excretion . *Plant Physiology*. **58**, pp.210–213.

Clouse, S.D., Langford, M. and Mcmorris, T.C. 1996. A Brassinosteroid-Insensitive Mutant in Arabidopsis thaliana Exhibits Multiple Defects in Growth and Development'. *Plant physiology*. **11**, pp.671–678.

Clouse, S.D. and Sasse, J.M. 1998. Brassinosteroids: Essential Regulators of Plant Growth and Development. *Annual Review of Plant Physiology and Plant Molecular Biology*. **49**, pp.427–451.

Cluis, C.P., Mouchel, C.F. and Hardtke, C.S. 2004. The *Arabidopsis* transcription factor HY5 integrates light and hormone signaling pathways. *The Plant Journal*. **38**, pp.332–347.

Colón-Carmona, A., Chen, D.L., Yeh, K.C. and Abel, S. 2000. Aux/IAA proteins are phosphorylated by phytochrome in vitro. *Plant Physiology*. **124**, pp.1728–1738.

Cooper, A.F. and Van Gundy, S.D. 1971a. Ethanol Production and Utilization by Aphelenchus avenae and Caenorhabditis sp. *Journal of nematology*. **3**, pp.205–14.

Cooper, A.F. and Van Gundy, S.D. 1971b. Senescence, quiescence, and cryptobiosis *In*: B. M. Zuckerman, ed. *Plant parasitic nematodes* [Online]. [Accessed 26 May 2017]. .

Costa, L.G. 2006. Current issues in organophosphate toxicology. *Clinica Chimica Acta*. **366**, pp.1–13.

Costa, L.G. and Aschner, M. 2014. Toxicology of Pesticides *In*: *Reference Module in Biomedical Sciences* [Online]. Elsevier. [Accessed 12 November 2020]. .

Crisford, A., Calahorro, F., Ludlow, E., Marvin, J.M.C., Hibbard, J.K., Lilley, C.J., Kearn, J., Keefe, F., Harmer, R., Urwin, P.E., O'connor, V., Holden, L. and Holden-Dye, L. 2018. Identification and characterisation of serotonin signalling in the potato cyst nematode Globodera pallida reveals new targets for crop protection.

Curtis, R., Jones, J., Davies, K., Sharon, E. and Spiegel, Y 2011. Plant nematode surfaces: Protection of the plant nematode from host defence reposnses *In*: K. G. Davies and Yitzhak Spiegel, eds. *Biological control of plant-parasitic nematodes* [Online]. Springer, Dordrecht, p.311. [Accessed 26 May 2017]. .

Dąbrowska-Bronk, J., Czarny, M., Wiśniewska, A., Fudali, S., Baranowski, Ł., Sobczak, M., Święcicka, M., Matuszkiewicz, M., Brzyżek, G., Wroblewski, T., Dobosz, R., Bartoszewski, G. and Filipecki, M. 2015. Suppression of NGB and NAB/ERabp1 in tomato modifies root responses to potato cyst nematode infestation. *Molecular Plant Pathology*. **16**, pp.334–348.

Dall'Osto, L., Bressan, M. and Bassi, R. 2015. Biogenesis of light harvesting proteins. *Biochimica et Biophysica Acta - Bioenergetics*. **1847**, pp.861–871.

Darwin, C.R. and Darwin, F. 1880. *The power of movement in plants* [Online]. London. [Accessed 1 June 2017]. .

Davies, P.J. 1987. The Plant Hormones: Their Nature, Occurrence, and Functions *In*: *Plant Hormones and their Role in Plant Growth and Development* [Online]. Dordrecht: Springer Netherlands, pp.1–11. [Accessed 1 June 2017]. .

Decker, H. and Sveshnikovam, N.M. 1983. *Plant Nematodes and Their Control: Phytonematology* [Online]. New Delhi, India: Amerind Publishing Co. Pvt. Ltd. [Accessed 25 May 2017]. .

Deng, X W, Caspar, T. and Quail, P.H. 1991. cop1: a regulatory locus involved in light-controlled development and gene expression in Arabidopsis. *Genes & development*. **5**, pp.1172–82.

Deng, Xing Wang, Caspar, T. and Quail, P.H. 1991. cop1: A regulatory locus involved in light-controlled development and gene expression in Arabidopsis. *Genes & Development*. **5**, pp.1172–1182.

Depta, H., Eisele, K. and Hertel, R. 1983. Specific inhibitors of auxin transport: action on tissue segments and in vitro binding to membranes from maize coleoptiles. *Plant science*. **31**.

Devine, K.J. and Jones, P.W. 2003. Investigations into the chemoattraction of the potato cyst nematodes Globodera rostochiensis and G. pallida towards fractionated potato root leachate. *Nematology*. **5**, pp.65–75.

Devlin, P.F., Yanovsky, M.J. and Kay, S.A. 2003. A Genomic Analysis of the Shade Avoidance Response in Arabidopsis. *Plant Physiology*. **133**, pp.1617–1629.

Dewhurst, I. and Tasheva, M. 2013. *Fluensulfone toxicity studies and data*.

Dharmasiri, N., Dharmasiri, S. and Estelle, M. 2005. The F-box protein TIR1 is an auxin receptor. *Nature*. **435**, pp.441–445.

Dharmasiri, N., Dharmasiri, S., Weijers, D., Lechner, E., Yamada, M., Hobbie, L., Ehrismann, J.S., Jürgens, G. and Estelle, M. 2005. Plant development is regulated by a family of auxin receptor F box proteins. *Developmental Cell*. **9**, pp.109–119.

Dharmasiri, S. and Estelle, M. 2002. The role of regulated protein degradation in auxin response. *Plant Molecular Biology*. **49**, pp.401–408.

Dhurvas Chandrasekaran, D. 2015. *High-resolution NMR structure and functional studies of the oligomerization domain of PsIAA4, an auxin-inducible transcriptional repressor from pea (Pisum sativum)*.[Online] Martin Luther University Halle-Wittenberg (MLU), Germany. [Accessed 26 August 2020]. .

Dinesh, D.C., Villalobos, L.I.A.C. and Abel, S. 2016. Structural Biology of Nuclear Auxin Action. *Trends in Plant Science*. **21**, pp.302–316.

Dinneny, J.R., Long, T.A., Wang, J.Y., Jung, J.W., Mace, D., Pointer, S., Barron, C., Brady, S.M., Schiefelbein, J. and Benfey, P.N. 2008. Cell identity mediates the response of Arabidopsis roots to abiotic stress. *Science*. **320**, pp.942–945.

Dombrecht, B., Gang, P.X., Sprague, S.J., Kirkegaard, J.A., Ross, J.J., Reid, J.B., Fitt, G.P., Sewelam, N., Schenk, P.M., Manners, J.M. and Kazana, K. 2007. MYC2 differentially modulates diverse jasmonate-dependent functions in Arabidopsis. *Plant Cell*. **19**, pp.2225–2245.

Dong, J., Tang, D., Gao, Z., Yu, R., Li, K., He, H., Terzaghi, W., Deng, X.W. and Chen, H. 2014. Arabidopsis DE-ETIOLATED1 represses photomorphogenesis by positively regulating phytochrome-interacting factors in the dark. *Plant Cell*. **26**, pp.3630–3645.

Doyle, E.A. and Lambert, K.N. 2002. Cloning and Characterization of an Esophageal-Gland-Specific Pectate Lyase from the Root-Knot Nematode Meloidogyne javanica. *Molecular Plant-Microbe Interactions*. **15**, pp.549–556.

Doyle, E.A. and Lambert, K.N. 2003. Meloidogyne javanica Chorismate Mutase 1 Alters Plant Cell Development. *Molecular Plant-Microbe Interactions*. **16**, pp.123–131.

Dropkin, V.H. and Acedo, J. 1974. An electron microscopic study of glycogen and lipid in female Meloidogyne incognita (root-knot nematode). *The Journal of parasitology*. **60**, pp.1013–21.

Du, M., Spalding, E.P. and Gray, W.M. 2020. Rapid Auxin-Mediated Cell Expansion. *Annual Review of Plant Biology*. **71**, pp.379–402.

Duek, P.D. and Fankhauser, C. 2005. bHLH class transcription factors take centre stage in phytochrome signalling. *Trends in Plant Science*. **10**, pp.51–54.

Duniway, J.M. 2002. Status of Chemical Alternatives to Methyl Bromide for Pre-Plant Fumigation of Soil. *Phytopathology*. **92**, pp.1337–1343.

Eisenhauera, N., Ackermannb, M., Gassc, S., Klierc, M., Migunovad, V., Nitschkee, N., Ruessb, L., Sabaisc, A.C.W., Weissere, W.W. and Scheu, S. 2010. Nematicide impacts on nematodes and feedbacks on plant productivity in a plant diversity gradient. *Acta Oecologica-International Journal of Ecology*. **36**, pp.477–483.

Elizabeth Patton, E., Willems, A.R. and Tyers, M. 1998. Combinatorial control in ubiquitin-dependent proteolysis: Don't Skp the F-box hypothesis. *Trends in Genetics*. **14**,

pp.236–243.

Ellenby, C. 1968. Desiccation Survival in the Plant Parasitic Nematodes, Heterodera rostochiensis Wollenweber and Ditylenchus dipsaci (Kuhn) Filipjev. *Proceedings of the Royal Society of London*. **169**.

Ellenby, C. and Perry, R.N. 1976. The Influence of the Hatching Factor on the Water Uptake of the Second Stage Larva of the Potato Cyst Nematode Heterodera Rostochiensis. *Journal of Experimental Biology*. **64**.

Ellis, J. and Jones, D. 1998. Structure and function of proteins controlling strain-specific pathogen resistance in plants. *Current Opinion in Plant Biology*. **1**, pp.288–293.

Enders, T.A. and Strader, L.C. 2015. Auxin activity: Past, present, and future. *American Journal of Botany*. **102**, pp.180–196.

Esau, K. 1977. *Anatomy of seed plants* 2nd ed. New, York: John Wiley & Sons, Inc.

Evans, R.M. 1988. The steroid and thyroid hormone receptor superfamily. *Science*. **240**, pp.889–895.

Feist, E., Kearn, J., Gaihre, Y., O'Connor, V. and Holden-Dye, L. 2020. The distinct profiles of the inhibitory effects of fluensulfone, abamectin, aldicarb and fluopyram on Globodera pallida hatching. *Pesticide Biochemistry and Physiology*., p.104541.

Feng, S., Martinez, C., Gusmaroli, G., Wang, Y., Zhou, J., Wang, F., Chen, L., Yu, L., Iglesias-Pedraz, J.M., Kircher, S., Schäfer, E., Fu, X., Fan, L.-M. and Deng, X.W. 2008. Coordinated regulation of Arabidopsis thaliana development by light and gibberellins. *Nature*. **451**, pp.475–479.

Forrest, J.M.S. and Perry, R.N. 1980. Hatching of Globodera pallida eggs after brief exposures to potato root diffusate. *Nematologica*. **26**, pp.130–132.

Franklin, K.A., Lee, S.H., Patel, D., Kumar, S.V., Spartz, A.K., Gu, C., Ye, S., Yu, P., Breen, G., Cohen, J.D., Wigge, P.A. and Gray, W.M. 2011. Phytochrome-Interacting Factor 4 (PIF4) regulates auxin biosynthesis at high temperature. *Proceedings of the National Academy of Sciences of the United States of America*. **108**, pp.20231–20235.

Franklin, K.A. and Whitelam, G.C. 2005. Phytochromes and Shade-avoidance Responses in Plants. *Annals of Botany*. **96**, pp.169–175.

Friml, J., Benková, E., Blilou, I., Wisniewska, J., Hamann, T., Ljung, K., Woody, S., Sandberg, G., Scheres, B., Jürgens, G. and Palme, K. 2002. AtPIN4 mediates sink-driven auxin gradients and root patterning in Arabidopsis. *Cell*. **108**, pp.661–673.

Fujioka, S., Li, J., Choi, Y., Seto, H., Takatsuto, S., Noguchi, T., Tsuyoshi Watanabe, A., Kuriyama, H., Yokota, T., Chory, J. and Sakuraia, A. 1997. The Arabidopsis deetiolafed2 Mutant 1s Blocked Early in Brassínosteroid Biosynthesis. *The Plant Cell American Society of Plant Physiologists*. **9**.

Fuller, V.L., Lilley, C.J., Atkinson, H.J. and Urwin, P.E. 2007. Differential gene expression in Arabidopsis following infection by plant-parasitic nematodes Meloidogyne incognita and Heterodera schachtii. *Molecular Plant Pathology*. **8**, pp.595–609.

Fuller, V.L., Lilley, C.J. and Urwin, P.E. 2008. Nematode resistance. *New Phytologist*. **180**, pp.27–44.

Gagne, J.M., Downes, B.P., Shiu, S.H., Durski, A.M. and Vierstra, R.D. 2002. The F-box subunit of the SCF E3 complex is encoded by a diverse superfamily of genes in Arabidopsis. *Proceedings of the National Academy of Sciences of the United States of America*. **99**, pp.11519–11524.

Giannakou, I.O. and Panopoulou, S. 2019. The use of fluensulfone for the control of root-knot nematodes in greenhouse cultivated crops: Efficacy and phytotoxicity effects M. Tejada Moral, ed. *Cogent Food & Agriculture*. **5**, p.1643819.

Gil, P., Dewey, E., Friml, J., Zhao, Y., Snowden, K.C., Putterill, J., Palme, K., Estelle, M. and Chory, J. 2001. BIG: a calossin-like protein required for polar auxin transport in Arabidopsis. *Genes & development*. **15**, pp.1985–97.

Gleason, C., Foley, Rhonda C and Singh, K.B. 2011. Mutant analysis in Arabidopsis provides insight into the molecular mode of action of the auxinic herbicide dicamba. *PLoS ONE*. **6**.

Gleason, C., Foley, Rhonda C. and Singh, K.B. 2011. Mutant Analysis in Arabidopsis Provides Insight into the Molecular Mode of Action of the Auxinic Herbicide Dicamba M. Blazquez, ed. *PLoS ONE*. **6**, p.e17245.

Goda, H., Sawa, S., Asami, T., Fujioka, S., Shimada, Y. and Yoshida, S. 2004. Comprehensive comparison of auxin-regulated and brassinosteroid-regulated genes in Arabidopsis. *Plant physiology*. **134**, pp.1555–73.

Goda, H., Shimada, Y., Asami, T., Fujioka, S. and Yoshida, S. 2002. Microarray Analysis of Brassinosteroid-Regulated Genes in Arabidopsis. *Plant Physiology*. **130**, pp.1319–1334.

Goellner, M., Smant, G., De Boer, J.M., Baum, T.J. and Davis, E.L. 2000. Isolation of Beta-

1,4-Endoglucanase Genes from Globodera tabacum and their Expression During Parasitism. *Journal of nematology*. **32**, pp.154–65.

Goellner, M., Wang, X. and Davis, E.L. 2001. Endo-beta-1,4-glucanase expression in compatible plant-nematode interactions. *The Plant cell*. **13**, pp.2241–55.

Goetz, M., Vivian-Smith, A., Johnson, S.D. and Koltunow, A.M. 2006. AUXIN RESPONSE FACTOR8 is a negative regulator of fruit initiation in Arabidopsis. *Plant Cell*. **18**, pp.1873–1886.

Golinowski, W., Grundler, F.M.W. and Sobczak, M. 1996. Changes in the structure of Arabidopsis thaliana during female development of the plant-parasitic nematode Heterodera schachtii. *Protoplasma*. **194**, pp.103–116.

Golinowski, W. and Magnusson, C. 1991. Tissue response induced by *Heterodera schachtii* (Nematoda) in susceptible and resistant white mustard cultivars. *Canadian Journal of Botany*. **69**, pp.53–62.

Goverse, A., de Almeida Engler, J., Verhees, J., van der Krol, S., Helder, J. and Gheysen, G. 2000. Cell cycle activation by plant parasitic nematodes. *Plant Molecular Biology*. **43**, pp.747–761.

Goverse, A., Overmars, H., Engelbertink, J., Schots, A., Bakker, J. and Helder, J. 1998. Are locally disturbed plant hormone balances r esponsible for feeding cell development by cyst nematodes? *In*: *Proceedings of the 24th International Nematology Symposium*. Dundee, UK, p.41.

Gray, William M, Kepinski, S., Rouse, D., Leyser, O. and Estelle, M. 2001. Auxin regulates SCFTIR1-dependent degradation of AUX/IAA proteins. *Nature*. **414**, pp.271–276.

Gray, William M., Kepinski, S., Rouse, D., Leyser, O. and Estelle, M. 2001. Auxin regulates SCFTIR1-dependent degradation of AUX/IAA proteins. *Nature*. **414**, pp.271–276.

Gray, W.M., Del Pozo, J.C., Walker, L., Hobbie, L., Risseeuw, E., Banks, T., Crosby, W.L., Yang, M., Ma, H. and Estelle, M. 1999. Identification of an SCF ubiquitin-ligase complex required for auxin response in Arabidopsis thaliana. *Genes & Development*. **13**, pp.1678–1691.

Greene, E.A., Codomo, C.A., Taylor, N.E., Henikoff, J.G., Till, B.J., Reynolds, S.H., Enns, L.C., Burtner, C., Johnson, J.E., Odden, A.R., Comai, L. and Henikoff, S. 2003. Spectrum of chemically induced mutations from a large-scale reverse-genetic screen in Arabidopsis. *Genetics*. **164**, pp.731–40.

Griffiths, J., Murase, K., Rieu, I., Zentella, R., Zhang, Z.-L., Powers, S.J., Gong, F., Phillips, A.L., Hedden, P., Sun, T. and Thomas, S.G. 2006. Genetic characterization and functional analysis of the GID1 gibberellin receptors in Arabidopsis. *The Plant cell*. **18**, pp.3399–414.

Grossmann, K. 2010. Auxin herbicides: Current status of mechanism and mode of action. *Pest Management Science*. **66**, pp.113–120.

Grossmann, K. 2003. Mediation of Herbicide Effects by Hormone Interactions. *Journal of Plant Growth Regulation*. **22**, pp.109–122.

Guilfoyle, T.J. and Hagen, G. 2007. Auxin response factors. *Current Opinion in Plant Biology*. **10**, pp.453–460.

Gulnaz, A., Iqbal, J. and Azam, F. 1999. Seed treatment with growth regulators and crop productivity. II. Response of critical growth stages of wheat (Triticum aestivum L.) under salinity stress. *Cereal Research Communications*. **27**, pp.419–426.

Guo, H. and Ecker, J.R. 2003. Plant Responses to Ethylene Gas Are Mediated by SCFEBF1/EBF2-Dependent Proteolysis of EIN3 Transcription Factor. *Cell*. **115**, pp.667–677.

Guo, Y., Ni, J., Denver, R., Wang, X. and Clark, S.E. 2011. Mechanisms of Molecular Mimicry of Plant CLE Peptide Ligands by the Parasitic Nematode Globodera rostochiensis. *Plant Physiology*. **157**, pp.476–484.

Gutierrez, O.A., Wubben, M.J., Howard, M., Roberts, B., Hanlon, E. and Wilkinson, J.R. 2009. The role of phytohormones ethylene and auxin in plant-nematode interactions. *Russian Journal of Plant Physiology*. **56**, pp.1–5.

Guzman, Plinio and Ecker, J.R. 1990. Exploiting the Triple Response of Arabidopsis to Identify Ethylene-Related Mutants. *The Plant Cell*. **2**, p.513.

Guzman, P. and Ecker, J.R. 1990. Exploiting the Triple Response of Arabidopsis To Identify Ethylene-Related Mutants. *The Plant Cell*. **2**, pp.513–523.

Hagen, G. and Guilfoyle, T. 2002. Auxin-responsive gene expression: genes, promoters and regulatory factors. *Plant Molecular Biology*. **49**, pp.373–385.

Hager, A. 2003. Role of the plasma membrane H+-ATPase in auxin-induced elongation growth: Historical and new aspects *In*: *Journal of Plant Research* [Online]. Springer, pp.483–505. [Accessed 14 November 2020]. .

Hager, A., Menzel, H. and Krauss, A. 1971. Versuche und Hypothese zur Primärwirkung

des Auxins beim Streckungswachstum. *Planta*. **100**, pp.47–75.

Halliday, K.J. and Fankhauser, C. 2003. Phytochrome-hormonal signalling networks. *New Phytologist*. **157**, pp.449–463.

Halliday, K.J., Martínez-García, J.F. and Josse, E.-M. 2009. Integration of light and auxin signaling. *Cold Spring Harbor perspectives in biology*. **1**, p.a001586.

Hammes, U.Z., Schachtman, D.P., Berg, R.H., Nielsen, E., Koch, W., Mcintyre, L.M. and Taylor, C.G. 2005. Nematode-Induced Changes of Transporter Gene Expression in Arabidopsis Roots. . **18**, pp.1247–1257.

Hannah, M.A., Wiese, D., Freund, S., Fiehn, O., Heyer, A.G. and Hincha, D.K. 2006. Natural genetic variation of freezing tolerance in arabidopsis. *Plant Physiology*. **142**, pp.98–112.

Hao, G.-F. and Yang, G.-F. 2010. The Role of Phe82 and Phe351 in Auxin-Induced Substrate Perception by TIR1 Ubiquitin Ligase: A Novel Insight from Molecular Dynamics Simulations B. Kobe, ed. *PLoS ONE*. **5**, p.e10742.

Hao, Y., Wang, H., Qiao, S., Leng, L. and Wang, X. 2016. Histone deacetylase HDA6 enhances brassinosteroid signaling by inhibiting the BIN2 kinase. *Proceedings of the National Academy of Sciences*. **113**, pp.10418–10423.

Harb, E.Z. 1992. Effect of soaking seeds in some growth regulators and micronutrients on growth, some chemical constituents and yield of faba bean and cotton plants. *Bulletin of Faculty of Agriculture, Cairo Univ. (Egypt)*.

Harborne, J.B. 1990. Role of secondary metabolites in chemical defence mechanisms in plants. *Ciba Foundation symposium*. **154**, pp.126–34; discussion 135-9.

Hayashi, K.I., Neve, J., Hirose, M., Kuboki, A., Shimada, Y., Kepinski, S. and Nozaki, H. 2012. Rational design of an auxin antagonist of the SCF TIR1 auxin receptor complex. *ACS Chemical Biology*. **7**, pp.590–598.

Hayashi, K.I., Tan, X., Zheng, N., Hatate, T., Kimura, Y., Kepinski, S. and Nozaki, H. 2008. Small-molecule agonists and antagonists of F-box protein-substrate interactions in auxin perception and signaling. *Proceedings of the National Academy of Sciences of the United States of America*. **105**, pp.5632–5637.

Haydock, P.P.J., Woods, S.R., Grove, I.G. and Hare, M.C. 2006. Chemical control of nematodes. *In*: R. N. Perry and M. Moens, eds. *Plant nematology* [Online]. Wallingford: CABI, pp.392–410. [Accessed 5 June 2017]. .

He, S.B., Wang, W.X., Zhang, J.Y., Xu, F., Lian, H.L., Li, L. and Yang, H.Q. 2015. The CNT1 domain of arabidopsis CRY1 alone is sufficient to mediate blue light inhibition of hypocotyl elongation. *Molecular Plant*. **8**, pp.822–825.

He, W., Brumos, J., Li, H., Ji, Y., Ke, M., Gong, X., Zeng, Q., Li, W., Zhang, X., An, F., Wen, X., Li, P., Chu, J., Sun, X., Yan, C., Yan, N., Xie, D.-Y., Raikhel, N., Yang, Z., Stepanova, A.N., Alonso, J.M. and Guo, H. 2011. A Small-Molecule Screen Identifies l-Kynurenine as a Competitive Inhibitor of TAA1/TAR Activity in Ethylene-Directed Auxin Biosynthesis and Root Growth in Arabidopsis. *The Plant Cell*. **23**.

Heisler, M.G., Ohno, C., Das, P., Sieber, P., Reddy, G. V., Long, J.A. and Meyerowitz, E.M. 2005. Patterns of Auxin Transport and Gene Expression during Primordium Development Revealed by Live Imaging of the Arabidopsis Inflorescence Meristem. *Current Biology*. **15**, pp.1899–1911.

Hewezi, T., Howe, P., Maier, T.R., Hussey, R.S., Mitchum, M.G., Davis, E.L. and Baum, T.J. 2008. Cellulose Binding Protein from the Parasitic Nematode Heterodera schachtii Interacts with Arabidopsis Pectin Methylesterase: Cooperative Cell Wall Modification during Parasitism. *The Plant Cell*. **20**, pp.3080–3093.

Heyes, D.J., Levy, C., Sakuma, M., Robertson, D.L. and Scrutton, N.S. 2011. A Twin-track Approach Has Optimized Proton and Hydride Transfer by Dynamically Coupled Tunneling during the Evolution of Protochlorophyllide Oxidoreductase. *Journal of Biological Chemistry*. **286**, pp.11849–11854.

Hillocks, R.J. and Cooper, J.E. 2012. Integrated pest management – can it contribute to sustainable food production in Europe with less reliance on conventional pesticides? *Outlook on Agriculture*. **41**, pp.237–242.

Hoang, N., Bouly, J.-P. and Ahmad, M. 2008. Evidence of a Light-Sensing Role for Folate in Arabidopsis Cryptochrome Blue-Light Receptors. *Molecular Plant*. **1**, pp.68–74.

Hoecker, U., Toledo-Ortiz, G., Bender, J. and Quail, P.H. 2004. The photomorphogenesis-related mutant red1 is defective in CYP83B1, a red light-induced gene encoding a cytochrome P450 required for normal auxin homeostasis. *Planta*. **219**, pp.195–200.

Hoffmann, M.H. 2002. Biogeography of Arabidopsis thaliana (L.) Heynh. (Brassicaceae). *Journal of Biogeography*. **29**, pp.125–134.

Holden-Dye, L. and Walker, R.J. 2011. Neurobiology of plant parasitic nematodes. *Invertebrate Neuroscience*. **11**, pp.9–19.

Holm, M., Ma, L.-G., Qu, L.-J. and Deng, X.-W. 2002. Two interacting bZIP proteins are direct targets of COP1-mediated control of light-dependent gene expression in Arabidopsis. *Genes & development*. **16**, pp.1247–59.

Holovachov, O., van Megen, H., Bongers, T., Bakker, J., Helder, J., van den Elsen, S., Holterman, M., Karssen, G. and Mooyman, P. 2009. A phylogenetic tree of nematodes based on about 1200 full-length small subunit ribosomal DNA sequences. *Nematology*. **11**, pp.927–950.

Holterman, M., van der Wurff, A., van den Elsen, S., van Megen, H., Bongers, T., Holovachov, O., Bakker, J. and Helder, J. 2006. Phylum-Wide Analysis of SSU rDNA Reveals Deep Phylogenetic Relationships among Nematodes and Accelerated Evolution toward Crown Clades. *Molecular Biology and Evolution*. **23**, pp.1792–1800.

Hornitschek, P., Kohnen, M. V., Lorrain, S., Rougemont, J., Ljung, K., López-Vidriero, I., Franco-Zorrilla, J.M., Solano, R., Trevisan, M., Pradervand, S., Xenarios, I. and Fankhauser, C. 2012. Phytochrome interacting factors 4 and 5 control seedling growth in changing light conditions by directly controlling auxin signaling. *Plant Journal*. **71**, pp.699–711.

Hou, Y., Von Arnim, A.G. and Deng, X.W. 1993. A New Class of Arabidopsis Constitutive Photomorphogenic Genes Involved in Regulating Cotyledon Development. *The Plant cell*. **5**, pp.329–339.

Hsieh, H.-L. and Okamoto, H. 2014. Molecular interaction of jasmonate and phytochrome A signalling. *Journal of Experimental Botany*. **65**, pp.2847–2857.

Hua, Z. and Vierstra, R.D. 2011. The cullin-RING ubiquitin-protein ligases. *Annual Review of Plant Biology*. **62**, pp.299–334.

Huala, E., Oeller, P.W., Liscum, E., Han, I.S., Larsen, E. and Briggs, W.R. 1997. Arabidopsis NPH1: A Protein Kinase with a Putative Redox-Sensing Domain. *Science*. **278**, pp.2120–2123.

Huang, J. 1987. *Interactions of nematodes with rhizobia* (J. A. Veech & D. W. Dickson, eds.). Hyattsville, USA: Society of Nematologists.

Huq, E., Al-Sady, B., Hudson, M., Kim, C., Apel, K. and Quail, P.H. 2004. Phytochrome-Interacting Factor 1 Is a Critical bHLH Regulator of Chlorophyll. *Science*. **305**, pp.1937–1941.

Huq, E. and Quail, P.H. 2002. PIF4, a phytochrome-interacting bHLH factor, functions as a

negative regulator of phytochrome B signaling in Arabidopsis. *The EMBO journal*. **21**, pp.2441–50.

Husain, K., Ansari, R.A. and Ferder, L. 2010. Pharmacological agents in the prophylaxis/treatment of organophosphorous pesticide intoxication. *Indian Journal of Experimental Biology*. **48**, pp.642–650.

Hussey, R. and Grundler, F.M.W. 1998. Nematode parasitism of plants. *In*: D. PERRY, R. & WRIGHT, ed. *The physiology and biochemistry of free-living and plant-parasitic nematodes.* Wallingford, UK: CABI Publishing.

Hussey, R.S. 1989. Disease-Inducing Secretions of Plant-Parasitic Nematodes. *Annual Review of Phytopathology*. **27**, pp.123–141.

Hyman, L.H. 1951. *The Invertebrates - volume 3* [Online] (McGraw-Hill, ed.). Lincoln, UK: Anybook Ltd. [Accessed 25 May 2017]. .

Iglesias, M.J., Sellaro, R., Zurbriggen, M.D. and Casal, J.J. 2018. Multiple links between shade avoidance and auxin networks. *Journal of Experimental Botany*. **69**, pp.213–228.

Ishimaru, Y., Hayashi, K., Suzuki, T., Fukaki, H., Prusinska, J., Meester, C., Quareshy, M., Egoshi, S., Matsuura, H., Takahashi, K., Kato, N., Kombrink, E., Napier, R.M., Hayashi, K.I. and Ueda, M. 2018. Jasmonic acid inhibits auxin-induced lateral rooting independently of the CORONATINE INSENSITIVE1 receptor. *Plant Physiology*. **177**, pp.1704–1716.

Jammes, F., Lecomte, P., De Almeida-Engler, J., Dé Rique Bitton, F., Martin-Magniette, M.L., Renou, J.P., Abad, P. and Favery, B. 2005. Genome-wide expression profiling of the host response to root-knot nematode infection in Arabidopsis a. *The Plant Journal*. **44**, pp.447–458.

Jander, G., Baerson, S.R., Hudak, J.A., Gonzalez, K.A., Gruys, K.J. and Last, R.L. 2003. Ethylmethanesulfonate saturation mutagenesis in Arabidopsis to determine frequency of herbicide resistance. *Plant physiology*. **131**, pp.139–46.

Jasmer, D.P., Goverse, A. and Smant, G. 2003. Parasitic nematode interactions with mammals and plants. *Annual Review of Phytopathology*. **41**, pp.245–270.

Jensen, P.E., Gibson, L.C. and Hunter, C.N. 1999. ATPase activity associated with the magnesium-protoporphyrin IX chelatase enzyme of Synechocystis PCC6803: evidence for ATP hydrolysis during Mg2+ insertion, and the MgATP-dependent

interaction of the ChlI and ChlD subunits. *The Biochemical journal*. **339 (Pt 1)**, pp.127–34.

Job, N. and Datta, S. 2020. PIF3-HY5 module regulates *BBX11* to suppress protochlorophyllide levels in dark and promote photomorphogenesis in light. *New Phytologist*., nph.17149.

Johnson, R. and Vigelierchio, D. 1961. Accumulation of plant parasitic nematode larvae around carbon dioxide and oxygen. *Proceedings of the Helminthological Society of Washington*. **28**, pp.171–174.

Jones, J.T., Haegeman, A., Danchin, E.G.J., Gaur, H.S., Helder, J., Jones, M.G.K., Kikuchi, T., Manzanilla-López, R., Palomares-Rius, J.E., Wesemael, W.M.L. and Perry, R.N. 2013. Top 10 plant-parasitic nematodes in molecular plant pathology. *Molecular Plant Pathology*. **14**, pp.946–961.

Jones, M.G. and Payne, H.L. 1978. Early stages of nematode-induced giant-cell formation in roots of Impatiens balsamina. *Journal of nematology*. **10**, pp.70–84.

Jones, M.G.K. 1981. Host cell responses to endoparasitic nematode attack: structure and function of giant cells and syncytia. *Annals of Applied Biology*. **97**, pp.353–372.

Juergensen, K., Scholz-Starke, J., Sauer, N., Hess, P., van Bel, A.J.E. and Grundler, F.M.W. 2003. The Companion Cell-Specific Arabidopsis Disaccharide Carrier AtSUC2 Is Expressed in Nematode-Induced Syncytia. *Plant physiology*. **131**, pp.61–69.

Kanehisa, M. and Goto, S. 2000. KEGG: Kyoto Encyclopedia of Genes and Genomes. *Nucleic Acids Research*. **28**, pp.27–30.

Kasahara, H., Hanada, A., Kuzuyama, T., Takagi, M., Kamiya, Y. and Yamaguchi, S. 2002. Contribution of the mevalonate and methylerythritol phosphate pathways to the biosynthesis of gibberellins in Arabidopsis. *The Journal of biological chemistry*. **277**, pp.45188–94.

Kay, S.A. and Griffiths, W.T. 1983. Light-Induced Breakdown of NADPH-Protochlorophyllide Oxidoreductase In Vitro. *Plant physiology*. **72**, pp.229–36.

Kearn, J. 2015. *Mode of action studies on the nematicide fluensulfone* [Online] (A. thesis presented for the degree of D. of Philosophy, ed.). University of Southampton.

Kearn, J., Lilley, C., Urwin, P., Connor, V.O. and Holden-dye, L. 2017. Progressive metabolic impairment underlies the novel nematicidal action of fluensulfone on the potato cyst nematode Globodera pallida. *Ypest*., pp.1–8.

Kearn, J., Lilley, C., Urwin, P., O ’connor, V. and Holden-Dye, L. 2017. Progressive metabolic impairment underlies the novel nematicidal action of fluensulfone on the potato cyst nematode Globodera pallida. *Pesticide Biochemistry and Physiology*., pp.1–8.

Kearn, J., Ludlow, E., Dillon, J., O’Connor, V. and Holden-Dye, L. 2014. Fluensulfone is a nematicide with a mode of action distinct from anticholinesterases and macrocyclic lactones. *Pesticide Biochemistry and Physiology*. **109**, pp.44–57.

Keating, B.A., Carberry, P.S., Bindraban, P.S., Asseng, S., Meinke, H. and Dixon, J. 2010. Eco-efficient Agriculture: Concepts, Challenges, and Opportunities. *Crop Science*. **50**, S-109.

Kepinski, S. and Leyser, O. 2005. The Arabidopsis F-box protein TIR1 is an auxin receptor. *Nature*. **435**, pp.446–451.

Kim, B.C., Soh, M.S., Hong, S.H., Furuya, M. and Nam, H.G. 1998. Photomorphogenic development of the Arabidopsis shy2-1D mutation and its interaction with phytochromes in darkness. *Plant Journal*. **15**, pp.61–68.

Kim, D., Langmead, B. and Salzberg, S.L. 2015. HISAT: A fast spliced aligner with low memory requirements. *Nature Methods*. **12**, pp.357–360.

Kim, J.I., Sharkhuu, A., Jing, B.J., Li, P., Jae, C.J., Baek, D., Sang, Y.L., Blakeslee, J.J., Murphy, A.S., Bohnert, H.J., Hasegawa, P.M., Yun, D.J. and Bressan, R.A. 2007. yucca6, a dominant mutation in arabidopsis, affects auxin accumulation and auxin-related phenotypes. *Plant Physiology*. **145**, pp.722–735.

Kim, J.S., Lim, J.Y., Shin, H., Kim, B.G., Yoo, S.D., Kim, W.T. and Huh, J.H. 2019. ROS1-dependent DNA demethylation is required for ABA-inducible NIC3 expression. *Plant Physiology*. **179**, pp.1810–1821.

Kinoshita, T., Caño-Delgado, A., Seto, H., Hiranuma, S., Fujioka, S., Yoshida, S. and Chory, J. 2005. Binding of brassinosteroids to the extracellular domain of plant receptor kinase BRI1. *Nature*. **433**, pp.167–171.

Kircher, S., Kozma-Bognar, L., Kim, L., Adam, E., Harter, K., Schafer, E. and Nagy, F. 1999. Light quality-dependent nuclear import of the plant photoreceptors phytochrome A and B. *The Plant cell*. **11**, pp.1445–56.

Kircher, S. and Schopfer, P. 2012. Photosynthetic sucrose acts as cotyledon-derived long-distance signal to control root growth during early seedling development in

Arabidopsis. *Proceedings of the National Academy of Sciences of the United States of America*. **109**, pp.11217–21.

Kolde, C. 2015. CRAN - Package pheatmap. [Accessed 2 January 2021]. .

Koltai, H., Dhandaydham, M., Opperman, C., Thomas, J. and Bird, D. 2001. Overlapping Plant Signal Transduction Pathways Induced by a Parasitic Nematode and a Rhizobial Endosymbiont. *Molecular Plant-Microbe Interactions*. **14**, pp.1168–1177.

Kong, S.G. and Okajima, K. 2016. Diverse photoreceptors and light responses in plants. *Journal of Plant Research*. **129**, pp.111–114.

Koornneef, M., Alonso-Blanco, C. and Vreugdenhil, D. 2004. Naturally Occuring Natural Genetic Variation in Arabidopsis Thaliana. *Annual Review of Plant Biology*. **55**, pp.141–172.

Koornneef, M., van Eden, J., Hanhart, C.J., Stam, P., Braaksma, F.J. and Feenstra, W.J. 1983. Linkage map of Arabidopsis thaliana. *Journal of Heredity*. **74**, pp.265–272.

Koornneef, M., Rolff, E. and Spruit, C.J.P. 1980. Genetic Control of Light-inhibited Hypocotyl Elongation in Arabidopsis thaliana. *Zeitschrift für Pflanzenphysiologie*. **100**, pp.147–160.

Koussevitzky, S., Nott, A., Mockler, T.C., Hong, F., Sachetto-Martins, G., Surpin, M., Lim, J., Mittler, R. and Chory, J. 2007. Signals from Chloroplasts Converge to Regulate Nuclear Gene Expression. *Science*. **316**, pp.715–719.

Kubeš, M. and Napier, R. 2019. Non-canonical auxin signalling: fast and curious. *Journal of Experimental Botany*. **70**, pp.2609–2614.

Kyndt, T., Denil, S., Haegeman, A., Trooskens, G., Bauters, L., Van Criekinge, W., De Meyer, T. and Gheysen, G. 2012. Transcriptional reprogramming by root knot and migratory nematode infection in rice. *New Phytologist*. **196**, pp.887–900.

L-C Wang, K., Li, H. and Ecker, J.R. 2002. Ethylene Biosynthesis and Signaling Networks. *The Plant Cell*., pp.131–151.

Lagarias, J.C. and Rapoport, H. 1980. Chromopeptides from phytochrome. The structure and linkage of the PR form of the phytochrome chromophore. *Journal of the American Chemical Society*. **102**, pp.4821–4828.

Laibach, F. 1943. Arabidopsis thaliana (L.) Heynh. als Objekt für genetische und entwicklungs-physiologische Untersuchungen. *Bot. Arch*. **44**, pp.439–455.

Lambert, K.N., Allen, K.D. and Sussex, I.M. 1999. Cloning and Characterization of an

Esophageal-Gland-Specific Chorismate Mutase from the Phytoparasitic Nematode Meloidogyne javanica. *Molecular Plant-Microbe Interactions*. **12**, pp.328–336.

Laplaze, L., Benkova, E., Casimiro, I., Maes, L., Vanneste, S., Swarup, R., Weijers, D., Calvo, V., Parizot, B., Herrera-Rodriguez, M.B., Offringa, R., Graham, N., Doumas, P., Friml, J., Bogusz, D., Beeckman, T. and Bennett, M. 2007. Cytokinins act directly on lateral root founder cells to inhibit root initiation. *The Plant cell*. **19**, pp.3889–900.

Larkin, J.C., Young, N., Prigge, M. and Marks, M.D. 1996. The control of trichome spacing and number in Arabidopsis. *Development*. **122**, pp.997–1005.

Lechelt-Kunze, C., Meissner, R.C., Drewes, M. and Tietjen, K. 2003. Flufenacet herbicide treatment phenocopies the fiddlehead mutant in Arabidopsis thaliana. *Pest Management Science Pest Manag Sci*. **59**, pp.847–856.

Lee, C.W., Mahendra, S., Zodrow, K., Li, D., Tsai, Y.-C., Braam, J. and Alvarez, P.J.J. 2010. Developmental phytotoxicity of metal oxide nanoparticles to Arabidopsis thaliana. *Environmental Toxicology and Chemistry*. **29**, pp.669–675.

Lee, D.J., Park, J.W., Lee, H.W. and Kim, J. 2009. Genome-wide analysis of the auxin-responsive transcriptome downstream of iaa1 and its expression analysis reveal the diversity and complexity of auxin-regulated gene expression. *Journal of Experimental Botany*. **60**, pp.3935–3957.

Lee, D.L. 2002. *The biology of nematodes*. Taylor & Francis, CRC Press.

Lee, J., He, K., Stolc, V., Lee, H., Figueroa, P., Gao, Y., Tongprasit, W., Zhao, H., Lee, I. and Xing, W.D. 2007. Analysis of transcription factor HY5 genomic binding sites revealed its hierarchical role in light regulation of development. *Plant Cell*. **19**, pp.731–749.

Lee, Y.B., Park, J.S. and Han, S.C. 1972. Studies on the chemical control of white-tip nematode, Aphelenchoides besseyi Christie, before transplanting. *Korean Journal of Plant Protection*. **11**, pp.37–40.

Leister, D., Ballvora, A., Salamini, F. and Gebhardt, C. 1996. A PCR–based approach for isolating pathogen resistance genes from potato with potential for wide application in plants. *Nature Genetics*. **14**, pp.421–429.

Leivar, P., Monte, E., Oka, Y., Liu, T., Carle, C., Castillon, A., Huq, E. and Quail, P.H. 2008. Multiple Phytochrome-Interacting bHLH Transcription Factors Repress Premature Seedling Photomorphogenesis in Darkness. *Current Biology*. **18**, pp.1815–1823.

Leivar, P. and Quail, P.H. 2011. PIFs: Pivotal components in a cellular signaling hub. *Trends*

in Plant Science. **16**, pp.19–28.

Leivar, P., Tepperman, J.M., Monte, E., Calderon, R.H., Liu, T.L. and Quail, P.H. 2009. Definition of early transcriptional circuitry involved in light-induced reversal of PIF-imposed repression of photomorphogenesis in young Arabidopsis seedlings. *Plant Cell*. **21**, pp.3535–3553.

De Ley, P. and Blaxter, M. 2004. A new system for Nematoda: combining morphological characters with molecular trees, and translating clades into ranks and taxa *In*: R. Cook and D. J. Hunt, eds. *Nematology monographs and perspectives*. E.J. Brill, pp.633–653.

De Ley, P. and Blaxter, M. 2002. Systematic position and phylogeny *In*: D. Lee, ed. *The Biology of Nemtodes*. London: Taylor & Francis, pp.1–30.

Leyser, H.M., Pickett, F.B., Dharmasiri, S. and Estelle, M. 1996. Mutations in the AXR3 gene of Arabidopsis result in altered auxin response including ectopic expression from the SAUR-AC1 promoter. *The Plant Journal*. **10**, pp.403–13.

Leyser, H.M.O., Lincoln, C.A., Timpte, C., Lammer, D., Turner, J. and Estelle, M. 1993. Arabidopsis auxin-resistance gene AXR1 encodes a protein related to ubiquitin-activating enzyme E1. *Nature*. **364**, pp.161–164.

Leyser, O. 2018. Auxin Signaling. *Plant physiology*. **176**, pp.465–479.

Li, J. and Chory, J. 1997. A Putative Leucine-Rich Repeat Receptor Kinase Involved in Brassinosteroid Signal Transduction. *Cell*. **90**, pp.929–938.

Li, J., Nagpal, P., Vitart, V., McMorris, T.C. and Chory, J. 1996. A role for brassinosteroids in light-dependent development of Arabidopsis. *Science*. **272**, pp.398–401.

Li, J. and Nam, K.H. 2002. Regulation of Brassinosteroid Signaling by a GSK3/SHAGGY-Like Kinase. *Science*. **295**.

Li, J., Nam, K.H., Vafeados, D. and Chory, J. 2001. BIN2, a new brassinosteroid-insensitive locus in Arabidopsis. *Plant physiology*. **127**, pp.14–22.

Li, Q.F., Wang, C., Jiang, L., Li, S., Sun, S.S.M. and He, J.X. 2012. An Interaction Between BZR1 and DELLAs Mediates Direct Signaling Crosstalk Between Brassinosteroids and Gibberellins in Arabidopsis. *Science Signaling*. **5**, pp.ra72–ra72.

Liang, X., Shen, N.F. and Theologis, A. 1996. Li+-regulated 1-aminocyclopropane-1-carboxylate synthase gene expression in Arabidopsis thaliana. *The Plant Journal*. **10**, pp.1027–1036.

Lichtenthaler, H.K. 1987. Chlorophylls and carotenoids: Pigments of photosynthetic biomembranes. *Methods in Enzymology*. **148**, pp.350–382.

Lin, C., Ahmad, M., Chan, J. and Cashmore, A.R. 1996. CRY2, a second member of the Arabidopsis cryptochrome gene family. *Plant physiology*. **110**, p.1047.

Lin, C., Yang, H., Guo, H., Mockler, T., Chen, J. and Cashmore, A.R. 1998. Enhancement of blue-light sensitivity of Arabidopsis seedlings by a blue light receptor cryptochrome 2. *Proceedings of the National Academy of Sciences of the United States of America*. **95**, pp.2686–90.

Liu, Z.B., Ulmasov, T., Shi, X., Hagen, G. and Guilfoyle, T.J. 1994. Soybean GH3 promoter contains multiple auxin-inducible elements. *The Plant cell*. **6**, pp.645–57.

Ljung, K., Bhalerao, R. and Sandberg, G. 2002. Sites and homeostatic control of auxin biosynthesis in Arabidopsis during vegetative growth. *The Plant Journal*. **28**, pp.465–474.

Ljung, K., Hull, A.K., Celenza, J., Yamada, M., Estelle, M., Normanly, J. and Ran Sandberg, G. 2005. Sites and Regulation of Auxin Biosynthesis in Arabidopsis Roots. *The Plant Cell*. **17**, pp.1090–1104.

Ljung, K., Hull, A.K., Kowalczyk, M., Marchant, A., Celenza, J., Cohen, J.D. and Sandberg, G. 2002. Biosynthesis, conjugation, catabolism and homeostasis of indole-3-acetic acid in Arabidopsis thaliana. *Plant Molecular Biology*. **49**, pp.249–272.

Love, M.I., Huber, W. and Anders, S. 2014. Moderated estimation of fold change and dispersion for RNA-seq data with DESeq2. *Genome Biology*. **15**, p.550.

de Lucas, M., Davière, J., Rodríguez-Falcón, M., Pontin, M., Iglesias-Pedraz, J.M., Lorrain, S., Fankhauser, C., Blázquez, M.A., Titarenko, E. and Prat, S. 2008. A molecular framework for light and gibberellin control of cell elongation. *Nature*. **451**, pp.480–484.

Ludwig-Muller, J. and Cohen, J.D. 2002. Identification and quantification of three active auxins in different tissues of Tropaeolum majus. *Physiologia Plantarum*. **115**, pp.320–329.

Ma, L., Li, J., Qu, L., Hager, J., Chen, Z., Zhao, H. and Deng, X.W. 2001. Light control of Arabidopsis development entails coordinated regulation of genome expression and cellular pathways. *The Plant cell*. **13**, pp.2589–607.

MacMillan, J. 2001. Occurrence of Gibberellins in Vascular Plants, Fungi, and Bacteria.

Journal of Plant Growth Regulation. **20**, pp.387–442.

Maggenti, A. 1981. *General Nematology*. New York, USA: Springer-Verlag.

Magnusson, C. and Golinowski, W. 1991. Ultrastructural relationships of the developing syncytium induced by *Heterodera schachtii* (Nematoda) in root tissues of rape. *Canadian Journal of Botany*. **69**, pp.44–52.

Mandava, N.B. 1988. Plant Growth-Promoting Brassinosteroids. *Annual Review of Plant Physiology and Plant Molecular Biology*. **39**, pp.23–52.

Mapes, C.J. 1965. Structure and function in the nematode pharynx II. Pumping in Panagrellus, Aplectana and Rhabditis. *Parasitology*. **55**, pp.583–594.

Martin, M. 2011. Cutadapt removes adapter sequences from high-throughput sequencing reads. *EMBnet.journal*. **17**, p.10.

Martínez-García, J.F., Huq, E. and Quail, P.H. 2000. Direct Targeting of Light Signals to a Promoter Element-Bound Transcription Factor. *Science*. **288**, pp.859–863.

Masamune, T., Anetai, M., Takasugi, M. and Katsui, N. 1982. Isolation of a natural hatching stimulus, glycinoeclepin A, for the soybean cyst nematode. *Nature*. **297**, pp.495–496.

Mathews, S., Lavin, M. and Sharrock, R.A. 1995. Evolution of the Phytochrome Gene Family and Its Utility for Phylogenetic Analyses of Angiosperms. *Annals of the Missouri Botanical Garden*. **82**, pp.296–321.

Mathews, S. and Sharrock, R.A. 1997. Phytochrome gene diversity. *Plant, Cell and Environment*. **20**, pp.666–671.

Mathre, D.E., Johnston, R.H. and Grey, W.E. 2001. Small Grain Cereal Seed Treatment. *The Plant Health Instructor*.

Mazid, M., Ta, K. and Mohammad F 2011. Role of secondary metabolites in defense mechanisms of plants. *Review Article Biology and Medicine*. **3**, pp.232–249.

McConnell, J.R., Emery, J., Eshed, Y., Bao, N., Bowman, J. and Barton, M.K. 2001. Role of PHABULOSA and PHAVOLUTA in determining radial patterning in shoots. *Nature*. **411**, pp.709–713.

McCormac, A.C. and Terry, M.J. 2002a. Light-signalling pathways leading to the co-ordinated expression of HEMA and LHCB during chloroplast development in Arabidopsis thaliana. *The Plant Journal*. **32**, pp.549–559.

McCormac, A.C. and Terry, M.J. 2002b. Loss of nuclear gene expression during the

phytochrome A-mediated far-red block of greening response. *Plant Physiology*. **130**, pp.402–414.

McCormac, A.C. and Terry, M.J. 2004. The nuclear genes Lhcb and HEMA1 are differentially sensitive to plastid signals and suggest distinct roles for the GUN1 and GUN5 plastid-signalling pathways during de-etiolation. *The Plant Journal*. **40**, pp.672–685.

McMahon Smith, J. and Arteca, R.N. 2000. Molecular control of ethylene production by cyanide in Arabidopsis thaliana. *Physiologia Plantarum*. **109**, pp.180–187.

McSteen, P. and Leyser, O. 2005. Shoot branching. *Annual Review of Plant Biology*. **56**, pp.353–374.

Meher, H.C., Gajbhiye, V.T., Chawla, G. and Singh, G. 2009. Virulence development and genetic polymorphism in Meloidogyne incognita (Kofoid & White) Chitwood after prolonged exposure to sublethal concentrations of nematicides and continuous growing of resistant tomato cultivars. *Pest Management Science*. **65**, pp.1201–1207.

Meskauskiene, R., Nater, M., Goslings, D., Kessler, F., op den Camp, R. and Apel, K. 2001. FLU: a negative regulator of chlorophyll biosynthesis in Arabidopsis thaliana. *Proceedings of the National Academy of Sciences of the United States of America*. **98**, pp.12826–31.

De Meutter, J., Vanholme, B., Bauw, G., Tytgat, T., Gheysen, Greetje and Gheysen, Godelieve 2001. Preparation and sequencing of secreted proteins from the pharyngeal glands of the plant parasitic nematode Heterodera schachtii. *Molecular Plant Pathology*. **2**, pp.297–301.

Mi, H., Huang, X., Muruganujan, A., Tang, H., Mills, C., Kang, D. and Thomas, P.D. 2017. PANTHER version 11: expanded annotation data from Gene Ontology and Reactome pathways, and data analysis tool enhancements. *Nucleic Acids Research*. **45**, pp.D183–D189.

Mitchell-Olds, T. 2001. Arabidopsis thaliana and its wild relatives: A model system for ecology and evolution. *Trends in Ecology and Evolution*. **16**, pp.693–700.

Mobley, E.M., Kunkel, B.N. and Keith, B. 1999. Identification, characterization and comparative analysis of a novel chorismate mutase gene in Arabidopsis thaliana. *Genes*. **240**, pp.115–23.

Mochizuki, N., Tanaka, R., Grimm, B., Masuda, T., Moulin, M., Smith, A.G., Tanaka, A. and

Terry, M.J. 2010. The cell biology of tetrapyrroles: A life and death struggle. *Trends in Plant Science*. **15**, pp.488–498.

Mockaitis, K. and Estelle, M. 2008. Auxin Receptors and Plant Development: A New Signaling Paradigm. *Annual Review of Cell and Developmental Biology*. **24**, pp.55–80.

Möller, B. and Weijers, D. 2009. Auxin control of embryo patterning. *Cold Spring Harbor perspectives in biology*. **1**.

Monthly, C.P. 2014. International news, comment, features and conference reports, Headlines of 2014. *Crop Protection*.

Moon, J., Parry, G. and Estelle, M. 2004. The ubiquitin-proteasome pathway and plant development. *The Plant cell*. **16**, pp.3181–95.

Morris, K.A., Langston, D.B., Davis, R.F., Noe, J.P., Dickson, D.W. and Timper, P. 2016. Efficacy of Various Application Methods of Fluensulfone for Managing Root-knot Nematodes in Vegetables. *Journal of nematology*. **48**, pp.65–71.

Morris, K.A., Langston, D.B., Dickson, D.W., Davis, R.F., Timper, P. and Noe, J.P. 2015. Efficacy of Fluensulfone in a Tomato–Cucumber Double Cropping System. *Journal of Nematology*. **47**, pp.310–315.

Müller-Moulé, P., Nozue, K., Pytlak, M.L., Palmer, C.M., Covington, M.F., Wallace, A.D., Harmer, S.L. and Maloof, J.N. 2016. YUCCA auxin biosynthetic genes are required for Arabidopsis shade avoidance.

Murase, K., Hirano, Y., Sun, T. and Hakoshima, T. 2008. Gibberellin-induced DELLA recognition by the gibberellin receptor GID1. *Nature*. **456**, pp.459–463.

Murashige, T. and Skoog, F. 1962. A Revised Medium for Rapid Growth and Bio Assays with Tobacco Tissue Cultures. *Physiologia Plantarum*. **15**, pp.473–497.

Nagata, N., Min, Y.K., Nakano, T., Asami, T. and Yoshida, S. 2000. Treatment of dark-grown Arabidopsis thaliana with a brassinosteroid-biosynthesis inhibitor, brassinazole, induces some characteristics of light-grown plants. *Planta*. **211**, pp.781–790.

Nagpal, P., Ellis, C.M., Weber, H., Ploense, S.E., Barkawi, L.S., Guilfoyle, T.J., Hagen, G., Alonso, J.M., Cohen, J.D., Farmer, E.E., Ecker, J.R. and Reed, J.W. 2005. Auxin response factors ARF6 and ARF8 promote jasmonic acid production and flower maturation. *Development*. **132**, pp.4107–4118.

Nagpal, P., Walker, L.M., Young, J.C., Sonawala, A., Timpte, C., Estelle, M. and Reed, J.W.

2000. AXR2 encodes a member of the Aux/IAA protein family. *Plant physiology*. **123**, pp.563–74.

Nemhauser, J.L., Mockler, T.C. and Chory, J. 2004. Interdependency of Brassinosteroid and Auxin Signaling in Arabidopsis Jeffrey Dangl, ed. *PLoS Biology*. **2**, p.e258.

Nishimura, T., Hayashi, K., Suzuki, H., Gyohda, A., Takaoka, C., Sakaguchi, Y., Matsumoto, S., Kasahara, H., Sakai, T., Kato, J., Kamiya, Y. and Koshiba, T. 2014. Yucasin is a potent inhibitor of YUCCA, a key enzyme in auxin biosynthesis. *The Plant Journal*. **77**, pp.352–366.

Noe, J.P. and Brannen, P.M. 2015. *Pre- and post-plant application of fluensulfone on blueberry (Vaccinium spp.) for management of replant disease caused by Mesocriconema ornatum*.

Nonhebel, H.M. 2015. Tryptophan-independent indole-3-acetic acid synthesis: Critical evaluation of the evidence. *Plant Physiology*. **169**, pp.1001–1005.

Nonhebel, H.M., Cooney, T.P. and Simpson, R. 1993. The Route, Control and Compartmentation of Auxin Synthesis. *Australian Journal of Plant Physiology*. **20**, p.527.

Normanly, J., Cohent, J.D. and Fink, G.R. 1993. Arabidopsis thaliana auxotrophs reveal a tryptophan-independent biosynthetic pathway for indole-3-acetic acid (auxin/gas chromatography-selected ion monitoring-mass spectrometry). *Biochemistry*. **90**, pp.10355–10359.

Norshie, P.M., Grove, I.G. and Back, M.A. 2016. Field evaluation of the nematicide fluensulfone for control of the potato cyst nematode Globodera pallida. *Pest management science*. **72**, pp.2001–7.

Nozue, K., Harmer, S.L. and Maloof, J.N. 2011. Genomic analysis of circadian clock-, light-,and growth-correlated genes reveals PHYTOCHROME-INTERACTING FACTOR5 as a modulator of auxin signaling in arabidopsis. *Plant Physiology*. **156**, pp.357–372.

Oeller, P.W., Keller, J.A., Parks, J.E., Silbert, J.E. and Theologis, A. 1993. Structural characterization of the early indoleacetic acid-inducible genes, PS-IAA4/5 and PS-IAA6, of pea (Pisum sativum L.). *Journal of Molecular Biology*. **233**, pp.789–798.

Oh, E., Zhu, J.Y., Bai, M.Y., Arenhart, R.A., Sun, Y. and Wang, Z.Y. 2014. Cell elongation is regulated through a central circuit of interacting transcription factors in the Arabidopsis hypocotyl. *eLife*. **2014**.

Ohnishi, T., Godza, B., Watanabe, B., Fujioka, S., Hategan, L., Ide, K., Shibata, K., Yokota, T., Szekeres, M. and Mizutani, M. 2012. CYP90A1/CPD, a Brassinosteroid Biosynthetic Cytochrome P450 of Arabidopsis, Catalyzes C-3 Oxidation. *Journal of Biological Chemistry*. **287**, pp.31551–31560.

Oka, Y. 2014. Nematicidal activity of fluensulfone against some migratory nematodes under laboratory conditions. *Pest Management Science*. **70**, pp.1850–1858.

Oka, Y., Berson, M. and Barazani, A. 2008. MCW-2: A 'true' nematicide belongingto the fluroalkenyl group- *In*: *Proceedings of the 5th International Congress of Nematology*. Brisbane, Australia, pp.313–314.

Oka, Y. and Pivonia, S. 2002. Use of ammonia-releasing compounds for control of the root-knot nematode Meloidogyne javanica. *Nematology*. **4**, pp.65–71.

Oka, Y., Shuker, S. and Tkachi, N. 2013. Influence of soil environments on nematicidal activity of fluensulfone against Meloidogyne javanica. *Pest Management Science*. **69**, pp.1225–1234.

Oka, Y., Shuker, S. and Tkachi, N. 2009. Nematicidal efficacy of MCW-2, a new nematicide of the fluoroalkenyl group, against the root-knot nematode Meloidogyne javanica. *Pest Management Science*. **65**, pp.1082–1089.

Oka, Y., Shuker, S. and Tkachi, N. 2012. Systemic nematicidal activity of fluensulfone against the root-knot nematode Meloidogyne incognita on pepper. *Pest Management Science*. **68**, pp.268–275.

Okada, K., Ueda, J., Komaki, M.K., Bell, C.J. and Shimura, Y. 1991. Requirement of the Auxin Polar Transport System in Early Stages of Arabidopsis Floral Bud Formation. *The Plant Cell*. **3**, pp.677–684.

Okushima, Y., Overvoorde, P.J., Arima, K., Alonso, J.M., Chan, A., Chang, C., Ecker, J.R., Hughes, B., Lui, A., Nguyen, D., Onodera, C., Quach, H., Smith, A., Yu, G. and Theologis, A. 2005. Functional genomic analysis of the AUXIN RESPONSE FACTOR gene family members in Arabidopsis thaliana: Unique and overlapping functions of ARF7 and ARF19. *Plant Cell*. **17**, pp.444–463.

Olszyk, D., Lee, E., Pfleeger, T., Das, M. and Plocher, M. 2008. Comparison of Brassicaceae species for phytotoxicity testing. *Presented at Agronomy/Crop/Soil Science Annual Meeting, Houston, TX, October 05 - 09*.

Oono, Y., Ooura, C., Rahman, A., Aspuria, E.T., Hayashi, K.I., Tanaka, A. and Uchimiya, H.

2003. p-Chlorophenoxyisobutyric Acid Impairs Auxin Response in Arabidopsis Root. *Plant Physiology*. **133**, pp.1135–1147.

Opperman, C.H. and Chang, S. 1991. Effects of Aldicarb and Fenamiphos on Acetylcholinesterase and Motility of Caenorhabditis elegans. *Journal of Nematology*. **23**, pp.20–27.

Opperman, C.H., Taylor, C.G. and Conkling, M.A. 1994. Root-Knot Nematode-Directed Expression of a Plant Root-Specific Gene. *Science*. **263**, pp.221–223.

Ornat, C. and Verdejo-Lucas, S. 2001. A Population of Meloidogyne javanica in Spain Virulent to the Mi Resistance Gene in Tomato *In*: A. E. Robertson, ed. *Plant Disease* [Online]. The American Phytopathological Society, pp.271–276. [Accessed 17 May 2017]. .

Osterlund, M., Hardtke, C., Wei, N. and Deng, X.W. 2000. Targeted destabilization of HY5 during light-regulated development of Arabidopsis. *Nature*. **405**, pp.462–466.

Osterlund, M.T., Ang, L.H. and Deng, X.W. 1999. The role of COP1 in repression of Arabidopsis photomorphogenic development. *Trends in Cell Biology*. **9**, pp.113–118.

Overmyer, K., Tuominen, H., Kettunen, R., Betz, C., Langebartels, C., Sandermann, H. and Kangasjärvi, J. 2000. Ozone-Sensitive Arabidopsis rcd1 Mutant Reveals Opposite Roles for Ethylene and Jasmonate Signaling Pathways in Regulating Superoxide-Dependent Cell Death. *The Plant Cell*. **12**, pp.1849–1862.

Oyama, T., Shimura, Y. and Okada, K. 1997. The Arabidopsis HY5 gene encodes a bZIP protein that regulates stimulus-induced development of root and hypocotyl. *Genes & development*. **11**, pp.2983–95.

Page, D.R. and Grossniklaus, U. 2002. The art and design of genetic screens: Arabidopsis thaliana. *Nature Reviews Genetics*. **3**, pp.124–136.

Page, M.T., McCormac, A.C., Smith, A.G. and Terry, M.J. 2017. Singlet oxygen initiates a plastid signal controlling photosynthetic gene expression. *New Phytologist*. **213**, pp.1168–1180.

Parajuli, G., Kemerait, R. and Timper, P. 2014. Improving suppression of Meloidogyne spp. by Purpureocillium lilacinum strain 251. *Nematology*. **16**, pp.711–717.

Parry, G., Calderon-Villalobos, L.I., Prigge, M., Peret, B., Dharmasiri, S., Itoh, H., Lechner, E., Gray, W.M., Bennett, M. and Estelle, M. 2009. Complex regulation of the TIR1/AFB family of auxin receptors. *Proceedings of the National Academy of Sciences*

of the United States of America. **106**, pp.22540–22545.

Pelagio-Flores, R., Ortíz-Castro, R., Méndez-Bravo, A., Macías-Rodríguez, L. and López-Bucio, J. 2011. Serotonin, a Tryptophan-Derived Signal Conserved in Plants and Animals, Regulates Root System Architecture Probably Acting as a Natural Auxin Inhibitor in Arabidopsis thaliana. *Plant and Cell Physiology*. **52**, pp.490–508.

Pepper, A., Delaney, T., Washburnt, T., Poole, D. and Chory, J. 1994. DET1, a negative regulator of light-mediated development and gene expression in arabidopsis, encodes a novel nuclear-localized protein. *Cell*. **78**, pp.109–116.

Perrot-Rechenmann, C. 2010. Cellular responses to auxin: division versus expansion. *Cold Spring Harbor perspectives in biology*. **2**.

Perry, R. 2002. Hatching *In*: D. Lee, ed. *The Biology of Nemtodes*. New York, USA: Taylor and Francis, CRC Press, pp.147–170.

Perry, R. and Moens, M. 2013. *Plant Nematology* 2nd ed. (R. N. Perry, ed.). Wallingford, UK: CABI Publishing.

Perry, R., Moens, M. and Starr, J. 2009. *Root-knot Nematodes* [Online] (R. Perry, ed.). CABI Publishing. [Accessed 26 May 2017]. .

Perry, R.N. 1983. The effect of potato root diffusate on the desiccation survival of unhatched juveniles of Globodera rostochiensis. *Revue de Nématologie*. **6**, pp.99–102.

Perry, R.N. and Clarke, A.J. 1981. Hatching mechanisms of nematodes. *Parasitology*. **83**, pp.435–449.

Perry, R.N., Clarke, A.J. and Hennessy, J. 1980. The influence of osmotic pressure on the hatching of Heterodera schachtii. *Revue de Nématologie*. **3**, pp.3–9.

Perry, R.N. and Wharton, D.A. 2011. *Molecular and Physiological Basis of Nematode Survival* [Online] (R. N. Perry & D. A. Wharton, eds.). CABI Publishing. [Accessed 26 May 2017]. .

Pertea, M., Pertea, G.M., Antonescu, C.M., Chang, T.C., Mendell, J.T. and Salzberg, S.L. 2015. StringTie enables improved reconstruction of a transcriptome from RNA-seq reads. *Nature Biotechnology*. **33**, pp.290–295.

Phillion, D., Ruminski, P. and Yalamanchili, G.U.P. 1999. Fluoroalkenyl compounds and their use as pest control agents . *USA patent application.*

Pope, C., Karanth, S. and Liu, J. 2005. Pharmacology and toxicology of cholinesterase

inhibitors: uses and misuses of a common mechanism of action. *Environmental Toxicology and Pharmacology*. **19**, pp.433–446.

Popeijus, H., Overmars, H., Jones, J., Blok, V., Goverse, A., Helder, J., Schots, A., Bakker, J. and Smant, G. 2000. Degradation of plant cell walls by a nematode. *Nature*. **406**, pp.36–37.

Potuschak, T., Lechner, E., Parmentier, Y., Yanagisawa, S., Grava, S., Koncz, C. and Genschik, P. 2003. EIN3-Dependent Regulation of Plant Ethylene Hormone Signaling by Two Arabidopsis F Box Proteins. *Cell*. **115**, pp.679–689.

Prigge, M.J., Greenham, K., Zhang, Y., Santner, A., Castillejo, C., Mutka, A.M., O'Malley, R.C., Ecker, J.R., Kunkel, B.N. and Estelle, M. 2016. The Arabidopsis auxin receptor F-box proteins AFB4 and AFB5 are required for response to the synthetic auxin picloram. *G3: Genes, Genomes, Genetics*. **6**, pp.1383–1390.

Prigge, M.J., Platre, M., Kadakia, N., Zhang, Y., Greenham, K., Szutu, W., Pandey, B.K., Bhosale, R.A., Bennett, M., Busch, W. and Estelle, M. 2020. Genetic analysis of the Arabidopsis TIR1/AFB auxin receptors reveals both overlapping and specialized functions | eLife. *elife Sciences*. **9**; **e54740**.

Przemeck, G.K.H., Mattsson, J., Hardtke, C.S., Sung, Z.R. and Berleth, T. 1996. Studies on the role of the Arabidopsis gene MONOPTEROS in vascular development and plant cell axialization. *Planta*. **200**, pp.229–237.

Pufky, J., Qiu, Y., Mulpuri, ·, Rao, V., Hurban, P. and Jones, A.M. 2003. The auxin-induced transcriptome for etiolated Arabidopsis seedlings using a structure/function approach. *Funct Integr Genomics*. **3**, pp.135–143.

Qiao, H., Chang, K.N., Yazaki, J. and Ecker, J.R. 2009. Interplay between ethylene, ETP1/ETP2 F-box proteins, and degradation of EIN2 triggers ethylene responses in Arabidopsis. *Genes & development*. **23**, pp.512–521.

Quareshy, M., Prusinska, J., Li, J. and Napier, R. 2018. A cheminformatics review of auxins as herbicides. *Journal of Experimental Botany*. **69**, pp.265–275.

Rahman Razak, A. and Evans, A.A.F. 1976. An Intracellular Tube Associated With Feeding By Rotylenchulus Reniformis On Cowpea Root. *Nematologica*. **22**, pp.182–189.

Ramos, J.A., Zenser, N., Leyser, O. and Callis, J. 2001. Rapid degradation of auxin/indoleacetic acid proteins requires conserved amino acids of domain II and is proteasome dependent. *Plant Cell*. **13**, pp.2349–2360.

Rathus, E.M. and Landy, P.J. 1961. Methyl Bromide Poisoning. *British Journal of Industrial Medicine*. **18**, pp.53–57.

Ravanel, S., Gakière, B., Job, D. and Douce, R. 1998. The specific features of methionine biosynthesis and metabolism in plants. *Proceedings of the National Academy of Sciences of the United States of America*. **95**, pp.7805–12.

Raven, J.A. and Edwards, D. 2001. Roots: evolutionary origins and biogeochemical significance. *Journal of Experimental Botany*. **52**, pp.381–401.

Redei, G.P. 1975. Arabidopsis as a Genetic Tool. *Annual Review of Genetics*. **9**, pp.111–127.

Reid, J.B., Botwright, N.A., Smith, J.J., O'Neill, D.P. and Kerckhoffs, L.H.J. 2002. Control of Gibberellin Levels and Gene Expression during De-Etiolation in Pea. *PLANT PHYSIOLOGY*. **128**, pp.734–741.

Remington, D.L., Vision, T.J., Guilfoyle, T.J. and Reed, J.W. 2004. Contrasting modes of diversification in the Aux/IAA and ARF gene families. *Plant Physiology*. **135**, pp.1738–1752.

Reynolds, A.M., Dutta, T.K., Curtis, R.H.C., Powers, S.J., Gaur, H.S. and Kerry, B.R. 2011. Chemotaxis can take plant-parasitic nematodes to the source of a chemo-attractant via the shortest possible routes. *Journal of The Royal Society Interface*. **8**, pp.568–577.

Rhoades, H.L. and Linford, M.B. 1961. A study of the Parasitic Habit of Paratylenchus projectus and P. dianthus. *Proceedings of the Helminthological Society of Washington*. **28**, pp.185–190.

Roberts, P.A., Thomason, I.J. and McKinney, H.E. 1981. Influence of Nonhosts, Crucifers, and Fungal Parasites on Field Populations of Heterodera schachtii. *Journal of nematology*. **13**, pp.164–71.

Robinson, A. 2004. Nematode behaviour and migrations through soil and host tissue. Nematode morphology, physiology and ecology. *In*: Z. Chen, S. Chen and D. M. Dickson, eds. *Nematology Advances and perspectives*. Wallingford, UK: CAB International.

Robinson, A. and Perry, R.N. 2011. Behaviour and sensory perception *In*: R. N. Perry and M. Moens, eds. *Plant Nematology*. Wallingford, UK: CAB International.

Robinson, M.P., Perry, R.N. and Atkinson, H.J. 1985. The Effect of Delayed Emergence On

Infectivity of Juveniles of the Potato Cyst Nematode Globodera Rostochiensis. *Nematologica*. **31**, pp.171–178.

Rockwell, N.C., Su, Y.-S. and Lagarias, J.C. 2006. PHYTOCHROME STRUCTURE AND SIGNALING MECHANISMS. *Annual Review of Plant Biology*. **57**, pp.837–858.

Roman, G., Lubarsky, B., Kieber, J.J., Rothenberg, M. and Ecker, J.R. 1995. Genetic analysis of ethylene signal transduction in Arabidopsis thaliana: five novel mutant loci integrated into a stress response pathway. *Genetics*. **139**, pp.1393–409.

Rosso, M.N., Favery, B., Piotte, C., Arthaud, L., De Boer, J.M., Hussey, R.S., Bakker, J., Baum, T.J. and Abad, P. 1999. Isolation of a cDNA Encoding a β-1,4-endoglucanase in the Root-Knot Nematode Meloidogyne incognita and Expression Analysis During Plant Parasitism. *Molecular Plant-Microbe Interactions*. **12**, pp.585–591.

Rousidou, C., Papadopoulou, E.S., Kortsinidou, M., Giannakou, I.O., Singh, B.K., Menkissoglu-Spiroudi, U. and Karpouzas, D.G. 2013. Bio-pesticides: Harmful or harmless to ammonia oxidizing microorganisms? The case of a Paecilomyces lilacinus-based nematicide. *Soil Biology and Biochemistry*. **67**, pp.98–105.

Ruegger, Max, Dewey, E., Gray, W.M., Hobbie, L., Turner, J. and Estelle, M. 1998. The TIR1 protein of Arabidopsis functions in auxin response and is related to human SKP2 and yeast Grr1p. *Genes & Development*. **12**, p.198.

Ruegger, M, Dewey, E., Gray, W.M., Hobbie, L., Turner, J.C. and Estelle, M. 1998. The TIR1 protein of Arabidopsis functions in auxin response and is related to human SKP2 and yeast Grr1p. *Genes & Development*. **12**, pp.198–207.

Ruppert, E.E., Fox, R.S. and Barnes, R.D. 2003. *Invertebrate zoology : a functional evolutionary approach*. Brooks Cole.

De Rybel, B., Audenaert, D., Beeckman, T. and Kepinski, S. 2009. The past, present, and future of chemical biology in auxin research. *ACS Chemical Biology*. **4**, pp.987–998.

Sakamoto, K. and Nagatani, A. 1996. Nuclear localization activity of phytochrome B. *The Plant Journal*. **10**, pp.859–68.

Salinas, K. and Kotcon, J. 2005. In vitro culturing of the predatory soil nematode Clarkus papillatus. *Nematology*. **17**, pp.5–9.

Scanlon, M.J. 2003. The Polar Auxin Transport Inhibitor N-1-Naphthylphthalamic Acid Disrupts Leaf Initiation, KNOX Protein Regulation, and Formation of Leaf Margins in Maize. *Plant Physiology*. **133**, pp.597–605.

Scarpella, E., Barkoulas, M. and Tsiantis, M. 2010. Control of leaf and vein development by auxin. *Cold Spring Harbor perspectives in biology*. **2**.

Schäfer, E. and Nagy, F. 2006. *Photomorphogenesis in plants and bacteria : function and signal transduction mechanisms* [Online] 3rd ed. Dordrecht: Springer. [Accessed 1 June 2017]. .

Schön, A., Krupp, G., Gough, S., Berry-Lowe, S., Kannangara, C.G. and Söll, D. 1986. The RNA required in the first step of chlorophyll biosynthesis is a chloroplast glutamate tRNA. *Nature*. **322**, pp.281–284.

Schreiber, K.J., Austin, R.S., Gong, Y., Zhang, J., Fung, P., Wang, P.W., Guttman, D.S. and Desveaux, D. 2012. Forward chemical genetic screens in Arabidopsis identify genes that influence sensitivity to the phytotoxic compound sulfamethoxazole. *BMC Plant Biology*. **12**, p.226.

Schwechheimer, C., Serino, G., Callis, J., Crosby, W.L., Lyapina, S., Deshaies, R.J., Gray, W.M., Estelle, M. and Deng, X.-W. 2001. Interactions of the COP9 Signalosome with the E3 Ubiquitin Ligase SCF TIR1 in Mediating Auxin Response. *Science*. **292**, pp.1379–1382.

Schwechheimer, C., Serino, G. and Deng, X.-W. 2002. Multiple Ubiquitin Ligase–Mediated Processes Require COP9 Signalosome and AXR1 Function. *The Plant Cell*. **14**, pp.2553–2563.

Sessions, A., Nemhauser, J.L., McColl, A., Roe, J.L., Feldmann, K.A. and Zambryski, P.C. 1997. ETTIN patterns the Arabidopsis floral meristem and reproductive organs. *Development*. **124**.

Shan, X., Yan, J. and Xie, D. 2012. Comparison of phytohormone signaling mechanisms. *Current Opinion in Plant Biology*. **15**, pp.84–91.

Shanks, C.M., Hecker, A., Cheng, C.-Y., Brand, L., Collani, S., Schmid, M., Schaller, G.E., Wanke, D., Harter, K. and Kieber, J.J. 2018. Role of *BASIC PENTACYSTEINE* transcription factors in a subset of cytokinin signaling responses. *The Plant Journal*. **95**, pp.458–473.

Sharbel, T.F., Haubold, B. and Mitchell-olds, T. 2000. Genetic isolation by distance in Arabidopsis thaliana:\rbiogeography and postglacial colonization of Europe. *Molecular ecology*. **9**, pp.2109 –2118.

Sharma, K.K., Singh, U.S., Sharma, P., Kumar, A. and Sharma, L. 2015. *Seed treatments for*

sustainable agriculture-A review [Online]. [Accessed 12 November 2020]. .

Sharrock, R.A. and Quail, P.H. 1989. Novel phytochrome sequences in Arabidopsis thaliana: structure, evolution, and differential expression of a plant regulatory photoreceptor family. *Genes & development*. **3**, pp.1745–57.

Shimada, A., Ueguchi-Tanaka, M., Nakatsu, T., Nakajima, M., Naoe, Y., Ohmiya, H., Kato, H. and Matsuoka, M. 2008. Structural basis for gibberellin recognition by its receptor GID1. *Nature*. **456**, pp.520–523.

Shin, J., Kim, K., Kang, H., Zulfugarov, I.S., Bae, G., Lee, C.H., Lee, D. and Choi, G. 2009. Phytochromes promote seedling light responses by inhibiting four negatively-acting phytochrome-interacting factors. *Proceedings of the National Academy of Sciences of the United States of America*. **106**, pp.7660–7665.

Shiu, S.H. and Bleecker, A.B. 2003. Expansion of the receptor-like kinase/Pelle gene family and receptor-like proteins in Arabidopsis. *Plant physiology*. **132**, pp.530–43.

Sibout, R., Sukumar, P., Hettiarachchi, C., Holm, M., Muday, G.K. and Hardtke, C.S. 2006. Opposite root growth phenotypes of hy5 versus hy5 hyh mutants correlate with increased constitutive auxin signaling. *PLoS Genetics*. **2**, pp.1898–1911.

Sijmons, P.C., Atkinson, H.J. and Wyss, U. 1994. Parasitic Strategies of Root Nematodes and Associated Host Cell Responses. *Annual Review of Phytopathology*. **32**, pp.235–259.

Sijmons, P.C., Grundler, F.M.W., Mende, N., Burrows, P.R. and Wyss, U. 1991. Arabidopsis thaliana as a new model host for plant-parasitic nematodes. *The Plant Journal*. **1**, pp.245–254.

Sikora, R. and Fernandez, E. 2005. Nematodes parasites of vegetables *In*: M. Liuc, R. Sikora and J. Bridge, eds. *Plant Parasitic Nematodes in Subtropical and Tropical Agriculture.* Wallingford, UK: CAB International.

Simon, S. and Petrášek, J. 2011. Why plants need more than one type of auxin. *Plant Science*. **180**, pp.454–460.

Sinclair, S.A., Larue, C., Bonk, L., Khan, A., Castillo-Michel, H., Stein, R.J., Grolimund, D., Begerow, D., Neumann, U., Haydon, M.J. and Krämer, U. 2017. Etiolated Seedling Development Requires Repression of Photomorphogenesis by a Small Cell-Wall-Derived Dark Signal. *Current Biology*. **27**, pp.3403-3418.e7.

Sineshchekov, V.A., Loskovich, A. V., Riemann, M. and Nick, P. 2004. The jasmonate-free

rice mutant hebiba is affected in the response of phyA′/phyA″ pools and protochlorophyllide biosynthesis to far-red light. *Photochemical and Photobiological Sciences*. **3**, pp.1058–1062.

Singh, S., Singh, B. and Singh, A.. 2015. Nematodes: A Threat to Sustainability of Agriculture. *Procedia Environmental Sciences*. **29**, pp.215–216.

Skowyra, D., Craig, K.L., Tyers, M., Elledge, S.J. and Harper, J.W. 1997. F-box proteins are receptors that recruit phosphorylated substrates to the SCF ubiquitin-ligase complex. *Cell*. **91**, pp.209–219.

Smant, G., Stokkermans, J.P., Yan, Y., de Boer, J.M., Baum, T.J., Wang, X., Hussey, R.S., Gommers, F.J., Henrissat, B., Davis, E.L., Helder, J., Schots, A. and Bakker, J. 1998. Endogenous cellulases in animals: isolation of beta-1, 4-endoglucanase genes from two species of plant-parasitic cyst nematodes. *Proceedings of the National Academy of Sciences of the United States of America*. **95**, pp.4906–11.

Smelt, J.H., Crum, S.J.H., Teunissen, W. and Leistra, M. 1987. Accelerated transformation of aldicarb, oxamyl and ethoprophos after repeated soil treatments. *Crop Protection*. **6**, pp.295–303.

Smelt, J.H., Van De Peppel-Groen, A.E., Van Der Pas, L.J.T. and Dijksterhuis, A. 1996. Development and duration of accelerated degradation of nematicides in different soils. *Soil Biology and Biochemistry*. **28**, pp.1757–1765.

Smith, H. and Whitelam, G.C. 1997. The shade avoidance syndrome: multiple responses mediated by multiple phytochromes. *Plant, Cell and Environment*. **20**, pp.840–844.

Smith, M.A., Grimm, B., Kannangara, C.G. and von Wettstein, D. 1991. Spectral kinetics of glutamate-1-semialdehyde aminomutase of Synechococcus. *Proceedings of the National Academy of Sciences of the United States of America*. **88**, pp.9775–9.

Smyth, D.R., Bowman, J.L. and Meyerowitz, E.M. 1990. Early flower development in Arabidopsis. *Plant Cell*. **2**, pp.755–767.

Song, B., Zhao, H., Dong, K., Wang, M., Wu, S., Li, S., Wang, Y., Chen, P., Jiang, L. and Tao, Y. 2020. Phytochrome A inhibits shade avoidance responses under strong shade through repressing the brassinosteroid pathway in *Arabidopsis*. *The Plant Journal*. **104**, pp.1520–1534.

Song, Y. 2014. Insight into the mode of action of 2,4-dichlorophenoxyacetic acid (2,4-D) as an herbicide. *Journal of Integrative Plant Biology*. **56**, pp.106–113.

Spears, J.F. 1968. *THE GOLDEN NEMATODE HANDBOOK Survey, Laboratory, Control, and Quarantine Procedures* [Online]. Washington, D.C: Superintendent of Documents, U.S. Government Printing Office. [Accessed 26 May 2017]. .

Sperling, U., Van Cleve, B., Ve Frick, G., Apel, K. and Armstrong, G.A. 1997. Overexpression of light-dependent PORA or PORB in plants depleted of endogenous POR by far-red light enhances seedling survival in white light and protects against photooxidative damage. *The Plant Journal*. **12**, pp.649–658.

Sperling, U., Franck, F., Van Cleve, B., Frick, G., Apel, K. and Armstrong, G.A. 1998. Etioplast Differentiation in Arabidopsis: Both PORA and PORB Restore the Prolamellar Body and Photoactive Protochlorophyllide–F655 to the cop1 Photomorphogenic Mutant. *The Plant Cell*. **10**, pp.283–296.

Spíchal, L., Rakova, N.Y., Riefler, M., Mizuno, T., Romanov, G.A., Strnad, M. and Schmülling, T. 2004. Two Cytokinin Receptors of Arabidopsis thaliana, CRE1/AHK4 and AHK3, Differ in their Ligand Specificity in a Bacterial Assay. *Plant and Cell Physiology*. **45**, pp.1299–1305.

Ståldal, V., Cierlik, I., Landberg, K., Myrenås, M., Sundström, J.F., Eklund, D.M., Chen, S., Baylis, T., Ljung, K. and Sundberg, E. 2012. The Arabidopsis thaliana transcriptional activator STYLISH1 regulates genes affecting stamen development, cell expansion and timing of flowering. *Plant Molecular Biology*. **78**, pp.545–559.

Starr, J., Mcdonald, A. and Claudius-Cole, A. 2013. *Plant Nematology: Nematode Resistance in Crops.* 2nd ed. (R. Perry & M. Moens, eds.). Wallingford, UK: CABI.

Steenland, K. 1996. Chronic neurological effects oforganophosphate pesticides. *European Journal of Public Health*. **312**.

Steeves, T.A. and Sussex, I.M. 1989. *Patterns in plant development* [Online]. Cambridge University Press. [Accessed 1 June 2017]. .

Stenersen, J. 1979. Action of pesticides on earthworms. Part I: The toxicity of cholinesterase-inhibiting insecticides to earthworms as evaluated by laboratory tests. *Pesticide Science*. **10**, pp.66–74.

Stepanova, A.N., Hoyt, J.M., Hamilton, A.A. and Alonso, J.M. 2005. A Link between Ethylene and Auxin Uncovered by the Characterization of Two Root-Specific Ethylene-Insensitive Mutants in Arabidopsis. *The Plant Cell*. **17**.

Stepanova, A.N., Robertson-Hoyt, J., Yun, J., Benavente, L.M., Xie, D.-Y., Doležal, K.,

Schlereth, A., Jürgens, G. and Alonso, J.M. 2008. TAA1-Mediated Auxin Biosynthesis Is Essential for Hormone Crosstalk and Plant Development. *Cell*. **133**, pp.177–191.

Stephenson, P.G., Fankhauser, C. and Terry, M.J. 2009. PIF3 is a repressor of chloroplast development. *Proceedings of the National Academy of Sciences of the United States of America*. **106**, pp.7654–7659.

Stephenson, P.G. and Terry, M.J. 2008. Light signalling pathways regulating the Mg-chelatase branchpoint of chlorophyll synthesis during de-etiolation in Arabidopsis thaliana *In*: *Photochemical and Photobiological Sciences* [Online]. Royal Society of Chemistry, pp.1243–1252. [Accessed 24 December 2020]. .

Stirling, G. 2011. An Ecological Perspective, a Review of Progress and Opportunities for Further Research. *In*: K. Davies and Y. Spiegel, eds. *Biological Control of Plant-Parasitic Nematodes*. Springer Netherlands., pp.1–38.

Stone, S.L., Williams, L.A., Farmer, L.M., Vierstra, R.D. and Callis, J. 2006. KEEP ON GOING, a RING E3 ligase essential for Arabidopsis growth and development, is involved in abscisic acid signaling. *The Plant cell*. **18**, pp.3415–3428.

Van Straalen, N. and Van Rijn, J. 1998. Eco-toxicological risk assessment of soil fauna recovery from pesticide application. *Review of Environmental Contamination and Toxicology*. **154**, pp.83–41.

Van der Straeten, D., Rodrigues-Pousada, R.A., Villarroel, R., Hanley, S., Goodman, H.M. and Van Montagu, M. 1992. Cloning, genetic mapping, and expression analysis of an Arabidopsis thaliana gene that encodes 1-aminocyclopropane-1-carboxylate synthase. *Proceedings of the National Academy of Sciences of the United States of America*. **89**, pp.9969–73.

Strupp, C., Banas, D.A., Cohen, S.M., Gordon, E.B., Jaeger, M. and Weber, K. 2012. Relationship of metabolism and cell proliferation to the mode of action of fluensulfone-induced mouse lung tumors: analysis of their human relevance using the IPCS framework. *Toxicological sciences : an official journal of the Society of Toxicology*. **128**, pp.284–94.

Sudirman and Webster, J.M. 1995. Effect of Ammonium Ions on Egg Hatching and Second-Stage Juveniles of Meloidogyne incognita in Axenic Tomato Root Culture. *Journal of Nematology*. **27**, pp.346–352.

Suett, D.L. and Jukes, A.A. 1988. Accelerated degradation of aldicarb and its oxidation

products in previously treated soils. *Crop protection*., pp.147–152.

Suzuki, M., Yamazaki, C., Mitsui, M., Kakei, Y., Mitani, Y., Nakamura, A., Ishii, T., Soeno, K. and Shimada, Y. 2015. Transcriptional feedback regulation of YUCCA genes in response to auxin levels in Arabidopsis. *Plant Cell Reports*. **34**, pp.1343–1352.

Swarup, K., Benková, E., Swarup, R., Casimiro, I., Péret, B., Yang, Y., Parry, G., Nielsen, E., De Smet, I., Vanneste, S., Levesque, M.P., Carrier, D., James, N., Calvo, V., Ljung, K., Kramer, E., Roberts, R., Graham, N., Marillonnet, S., Patel, K., Jones, J.D.G., Taylor, C.G., Schachtman, D.P., May, S., Sandberg, G., Benfey, P., Friml, J., Kerr, I., Beeckman, T., Laplaze, L. and Bennett, M. 2008. The auxin influx carrier LAX3 promotes lateral root emergence. *Nature Cell Biology*. **10**, pp.946–954.

Swarup, R., Parry, G., Graham, N., Allen, T. and Bennett, M. 2002. Auxin cross-talk: integration of signalling pathways to control plant development. *Plant Molecular Biology*. **49**, pp.409–424.

Szekeres, M, Németh, K., Koncz-Kálmán, Z., Mathur, J., Kauschmann, A., Altmann, T., Rédei, G.P., Nagy, F., Schell, J. and Koncz, C. 1996. Brassinosteroids rescue the deficiency of CYP90, a cytochrome P450, controlling cell elongation and de-etiolation in Arabidopsis. *Cell*. **85**, pp.171–82.

Szekeres, Miklós, Németh, K., Koncz-Kálmán, Z., Mathur, J., Kauschmann, A., Altmann, T., Rédei, G.P., Nagy, F., Schell, J. and Koncz, C. 1996. Brassinosteroids Rescue the Deficiency of CYP90, a Cytochrome P450, Controlling Cell Elongation and De-etiolation in Arabidopsis. *Cell*. **85**, pp.171–182.

Taiz, L. and Zeiger, E. 2006. *Plant physiology. 4th Edition.* [Online]. Sunderland, Massachusetts: Sinauer Associates, Inc. [Accessed 5 June 2017]. .

Tan, X., Calderon-Villalobos, L.I.A., Sharon, M., Zheng, C., Robinson, C. V., Estelle, M. and Zheng, N. 2007. Mechanism of auxin perception by the TIR1 ubiquitin ligase. *Nature*. **446**, pp.640–645.

Tanaka, K., Nakamura, Y., Asami, T., Yoshida, S., Matsuo, T. and Okamoto, S. 2003. Physiological Roles of Brassinosteroids in Early Growth of Arabidopsis: Brassinosteroids Have a Synergistic Relationship with Gibberellin as well as Auxin in Light-Grown Hypocotyl Elongation. *Journal of Plant Growth Regulation*. **22**, pp.259–271.

Tanaka, R. and Tanaka, A. 2007. Tetrapyrrole Biosynthesis in Higher Plants. *Annual Review*

of Plant Biology. **58**, pp.321–346.

Tao, Y., Ferrer, J.-L., Ljung, K., Pojer, F., Hong, F., Long, J.A., Li, L., Moreno, J.E., Bowman, M.E., Ivans, L.J., Cheng, Y., Lim, J., Zhao, Y., Ballaré, C.L., Sandberg, G., Noel, J.P. and Chory, J. 2008. Rapid Synthesis of Auxin via a New Tryptophan-Dependent Pathway Is Required for Shade Avoidance in Plants. *Cell*. **133**, pp.164–176.

Tepperman, J.M., Zhu, T., Chang, H.-S., Wang, X. and Quail, P.H. 2001. Multiple transcription-factor genes are early targets of phytochrome A signaling. *PNAS*. **98**, pp.9437–9442.

Terry, M.J. and Kacprzak, S.M. 2019. A Simple Method for Quantification of Protochlorophyllide in Etiolated Arabidopsis Seedlings *In*: *Methods in Molecular Biology* [Online]. Humana Press Inc., pp.169–177. [Accessed 31 December 2020]. .

Thakre, S.K. and Ghate, N.N. 1984. Effect of seed soaking with hormones on grain and fodder yield of sorghum and uptake of nutrients by the crop. *PKV Research Journal (India)*.

Thimann, K. V 1939. Auxins and the inhibiton of plant growth. *Biological Reviews*. **14**, pp.314–337.

Thines, B., Katsir, L., Melotto, M., Niu, Y., Mandaokar, A., Liu, G., Nomura, K., He, S.Y., Howe, G.A. and Browse, J. 2007. JAZ repressor proteins are targets of the SCF/COI1 complex during jasmonate signalling. *Nature*. **448**, pp.661–665.

Thomas, B. and Vince-Prue, D. 1997. *Photoperiodism in plants* [Online]. Academic Press. [Accessed 1 June 2017]. .

Tian, Q., Nagpal, P. and Reed, J.W. 2003. Regulation of Arabidopsis SHY2/IAA3 protein turnover. *The Plant Journal*. **36**, pp.643–651.

Tian, Q., Uhlir, N.J. and Reed, J.W. 2002. Arabidopsis SHY2/IAA3 inhibits auxin-regulated gene expression. *The Plant cell*. **14**, pp.301–19.

Timpte, C., Wilson, A.K. and Estelle, M. 1994. The axr2-1 mutation of Arabidopsis thaliana is a gain-of-function mutation that disrupts an early step in auxin response. *Genetics*. **138**, pp.1239–1249.

Tong, H., Xiao, Y., Liu, D., Gao, S., Liu, L., Yin, Y., Jin, Y., Qian, Q. and Chu, C. 2014. Brassinosteroid Regulates Cell Elongation by Modulating Gibberellin Metabolism in Rice. *The Plant Cell*. **26**, pp.4376–4393.

Triantaphylidès, C., Krischke, M., Hoeberichts, F.A., Ksas, B., Gresser, G., Havaux, M., Van

Breusegem, F. and Mueller, M.J. 2008. Singlet oxygen is the major reactive oxygen species involved in photooxidative damage to plants. *Plant physiology*. **148**, pp.960–8.

Trudgill, D.L., Elliott, M.J., Evans, K. and Phillips, M.S. 2003. The white potato cyst nematode (Globodera pallida) - a critical analysis of the threat in Britain. *Annals of Applied Biology*. **143**, pp.73–80.

Tsuchisaka, A. and Theologis, A. 2004. Unique and overlapping expression patterns among the Arabidopsis 1-amino-cyclopropane-1-carboxylate synthase gene family members. *Plant physiology*. **136**, pp.2982–3000.

Tsukaya, H. 2013. Leaf Development. *The Arabidopsis Book*. **11**, p.e0163.

Tytgat, T., De Meutter, J., Gheysen, G. and Coomans, A. 2000. Symposium Sedentary endoparasitic nematodes as a model for other plant parasitic nematodes. *Nematology*. **2**, pp.113–121.

Ueguchi-Tanaka, M., Ashikari, M., Nakajima, M., Itoh, H., Katoh, E., Kobayashi, M., Chow, T., Hsing, Y.C., Kitano, H., Yamaguchi, I. and Matsuoka, M. 2005. GIBBERELLIN INSENSITIVE DWARF1 encodes a soluble receptor for gibberellin. *Nature*. **437**, pp.693–698.

Ulmasov, T., Murfett, J., Hagen, G. and Guilfoyle, T.J. 1997. Aux/lAA Proteins Repress Expression of Reporter Genes Containing Natural and Highly Active Synthetic Auxin Response Elements. *The Plant cell*. **9**, pp.1963–1971.

Unterholzner, S.J., Rozhon, W., Papacek, M., Ciomas, J., Lange, T., Kugler, K.G., Mayer, K.F., Sieberer, T. and Poppenberger, B. 2015. Brassinosteroids Are Master Regulators of Gibberellin Biosynthesis in Arabidopsis. *The Plant Cell*. **27**, pp.2261–2272.

Vahala, J., Schlagnhaufer, C.D. and Pell, E.J. 1998. Induction of an ACC synthase cDNA by ozone in light-grown Arabidopsis thaliana leaves. *Physiologia Plantarum*. **103**, pp.45–50.

Vandenbussche, F., Habricot, Y., Condiff, A.S., Maldiney, R., Van Der Straeten, D. and Ahmad, M. 2007. HY5 is a point of convergence between cryptochrome and cytokinin signalling pathways in Arabidopsis thaliana. *Plant Journal*. **49**, pp.428–441.

Velasquez, S.M., Barbez, E., Kleine-Vehn, J. and Estevez, J.M. 2016. Auxin and cellular elongation. *Plant Physiology*. **170**, pp.1206–1215.

Vercauteren, I., De, J., Engler, A., De Groodt, R. and Gheysen, G. 2002. An Arabidopsis

thaliana Pectin Acetylesterase Gene Is Upregulated in Nematode Feeding Sites Induced by Root-knot and Cyst Nematodes. *Molecular Plant-Microbe Interactions*. **404**.

Vert, G., Walcher, C.L., Chory, J. and Nemhauser, J.L. 2008. Integration of auxin and brassinosteroid pathways by Auxin Response Factor 2. *Proceedings of the National Academy of Sciences of the United States of America*. **105**, pp.9829–34.

Viaene, N., Coyne, D.L. and Davies, K. 2013. *Biological and Cultural Management* [Online] (R. Perry & M. Moens, eds.). Wallingford, UK: CABI Publishing. [Accessed 17 May 2017]. .

Vidal, E.A., Araus, V., Lu, C., Parry, G., Green, P.J., Coruzzi, G.M. and Gutiérrez, R.A. 2010. Nitrate-responsive miR393/AFB3 regulatory module controls root system architecture in Arabidopsis thaliana. *Proceedings of the National Academy of Sciences of the United States of America*. **107**, pp.4477–4482.

Vogel, J.P., Woeste, K.E., Theologis, A. and Kieber, J.J. 1998. Recessive and dominant mutations in the ethylene biosynthetic gene ACS5 of Arabidopsis confer cytokinin insensitivity and ethylene overproduction, respectively. *Proceedings of the National Academy of Sciences of the United States of America*. **95**, pp.4766–4771.

van der Voort, J.R., Kanyuka, K., van der Vossen, E., Bendahmane, A., Mooijman, P., Klein-Lankhorst, R., Stiekema, W., Baulcombe, D. and Bakker, J. 1999. Tight Physical Linkage of the Nematode Resistance Gene Gpa2 and the Virus Resistance Gene Rxon a Single Segment Introgressed from the Wild Species Solanum tuberosum subsp. andigena CPC 1673 into Cultivated Potato. *Molecular Plant-Microbe Interactions*. **12**, pp.197–206.

Voss, G. and Speich, J. 1976. Some properties of cholinesterase of the plant nematode Aphelenchoides ritzema-boosi. *Experientia*. **32**, pp.1498–9.

Wale, S., Platt, H. and Cattlin, N. 2011. Nematodes: potato cyst nematodes. *In*: S. Wale, H. Platt and N. Cattlin, eds. *Diseases, pests and disorders of potatoes*. London, UK: Manson Publishing.

Walsh, T.A., Neal, R., Merlo, A.O., Honma, M., Hicks, G.R., Wolff, K., Matsumura, W. and Davies, J.P. 2006. Mutations in an auxin receptor homolog AFB5 and in SGT1b confer resistance to synthetic picolinate auxins and not to 2,4-dichlorophenoxyacetic acid or indole-3-acetic acid in Arabidopsis. *Plant Physiology*. **142**, pp.542–552.

Wang, B., Chu, J., Yu, T., Xu, Q., Sun, X., Yuan, J., Xiong, G., Wang, G., Wang, Y. and Li, J. 2015. Tryptophan-independent auxin biosynthesis contributes to early embryogenesis in Arabidopsis. *Proceedings of the National Academy of Sciences of the United States of America*. **112**, pp.4821–4826.

Wang, R., Zhang, Y., Kieffer, M., Yu, H., Kepinski, S. and Estelle, M. 2016. HSP90 regulates temperature-dependent seedling growth in Arabidopsis by stabilizing the auxin co-receptor F-box protein TIR1. *Nature Communications*. **7**.

Wang, X., Kota, U., He, K., Blackburn, K., Li, J., Goshe, M.B., Huber, S.C. and Clouse, S.D. 2008. Sequential Transphosphorylation of the BRI1/BAK1 Receptor Kinase Complex Impacts Early Events in Brassinosteroid Signaling. *Developmental Cell*. **15**, pp.220–235.

Wang, Z.-Y., Nakano, T., Gendron, J., He, J., Chen, M., Vafeados, D., Yang, Y., Fujioka, S., Yoshida, S., Asami, T. and Chory, J. 2002. Nuclear-Localized BZR1 Mediates Brassinosteroid-Induced Growth and Feedback Suppression of Brassinosteroid Biosynthesis. *Developmental Cell*. **2**, pp.505–513.

Watson, B.D. 1965. The fine structure of the body-wall and the growth of the cuticle in the adult nematode Ascaris lumbricoides. *Journal of Cell Science*. **3**, pp.75–81.

Wei, N. and Deng, X.-W. 1992. COP9: A New Genetic Locus lnvolved in Light-Regulated Development and Gene Expression in Arabidopsis. *The Plant Cell*. **4**, pp.1507–1518.

Wei, W., Kwokib, S.F., Von Arnitqa, A.G., Lee, A., Mcnellis, T.W., Piekos, B. and Deng ’i ’, X.-W. 1994. Arabidopsis COP8, COP10, and COP11 Genes Are lnvolved in Repression of Photomorphogenic Development in Darkness. *The Plant Cell*. **6**, pp.629–643.

Weijers, D., Schlereth, A., Ehrismann, J.S., Schwank, G., Kientz, M. and Jürgens, G. 2006. Auxin triggers transient local signaling for cell specification in Arabidopsis embryogenesis. *Developmental Cell*. **10**, pp.265–270.

Weiss, D. and Ori, N. 2007. Mechanisms of cross talk between gibberellin and other hormones. *Plant physiology*. **144**, pp.1240–6.

Weller, J.L., Hecht, V., Schoor, J.K.V., Davidson, S.E. and Ross, J.J. 2009. Light regulation of gibberellin biosynthesis in pea is mediated through the COP1/HY5 pathway. *Plant Cell*. **21**, pp.800–813.

Went, F. 1937. *Phytohormones* [Online] (F. W. Went & K. V Thimann, eds.). New York The Macmillan Company. [Accessed 31 May 2017]. .

Went, F.W. 1927. On growth-accelerating substances in the coleoptile of Avena sativa *In*: *Botany meeting of June 26, 1926* [Online]. [Accessed 31 May 2017]. .

Westphal, A. 2011. Sustainable approaches to the management of plant-parasitic nematodes and disease complexes. *Journal of nematology*. **43**, pp.122–5.

WHO 2004. *Deworming for Health and Development: Report of the third global meeting of the partners for parasite control* [Online]. Geneva, Switzerland: World Health Organization. [Accessed 25 May 2017]. .

Williamson, V.M. 1998. Root-knot nematode resistance genes in tomato and their potential for future use. *Annual Review of Phytopathology*. **36**, pp.277–293.

Willige, B.C., Ghosh, S., Nill, C., Zourelidou, M., Dohmann, E.M.N., Maier, A. and Schwechheimer, C. 2007. The DELLA domain of GA INSENSITIVE mediates the interaction with the GA INSENSITIVE DWARF1A gibberellin receptor of Arabidopsis. *The Plant cell*. **19**, pp.1209–20.

Wilson, A.K., Pickett, B.F., Turner, J.C. and Estelle, M. 1990. A dominant mutation in Arabidopsis confers resistance to auxin, ethylene and abscisic acid. *MGG Molecular & General Genetics*. **222**, pp.377–383.

Wilson, M.J. and Jackson, T.A. 2013. Progress in the commercialisation of bionematicides. *BioControl*. **58**, pp.715–722.

Winter, M.D., Mcpherson, M.J. and Atkinson, H.J. 2002. Neuronal uptake of pesticides disrupts chemosensory cells of nematodes. *Parasitology*. **125**, pp.561–565.

Woodward, A.W. and Bartel, B. 2005. A Receptor for Auxin. *The Plant Cell*. **17**, p.2425.

Wyss, U. 1992. Observations on the feeding behaviour of Heterodera schachtii throughout development, including events during moulting. *Fundam. appl. Nematol*. **15**, pp.75–89.

Wyss, U. 1997. Root Parasitic Nematodes: An Overview *In*: C. Fenoll, F. M. W. Grundler and S. A. Ohl, eds. *Cellular and Molecular Aspects of Plant-Nematode Interactions* [Online]. Springer Netherlands, pp.5–22. [Accessed 25 May 2017]. .

Wyss, U., Munch, A. and Grundler, F.M.W. 1992. The Parasitic Behaviour of Second-Stage Juveniles of Meloidogyne Incognita in Roots of Arabidopsis Thaliana. *Nematologica*. **38**, pp.98–111.

Wyss, U. and Zunke, U. 1986. Observations on the behaviour of second stage juveniles of Hetero inside host roots. *Revue de Nématologie*. **9**, pp.153–165.

Xie, D.-X., Feys, B.F., James, S., Nieto-Rostro, M. and Turner, J.G. 1998. COI1: An Arabidopsis Gene Required for Jasmonate-Regulated Defense and Fertility. *Science*. **280**, pp.1091–1094.

Xu, F., He, S., Zhang, J., Mao, Z., Wang, W., Li, T., Hua, J., Du, S., Xu, P., Li, L., Lian, H. and Yang, H.Q. 2018. Photoactivated CRY1 and phyB Interact Directly with AUX/IAA Proteins to Inhibit Auxin Signaling in Arabidopsis. *Molecular Plant*. **11**, pp.523–541.

Yamaguchi, S. 2008. Gibberellin Metabolism and its Regulation. *Annual Review of Plant Biology*. **59**, pp.225–251.

Yang, C., Xie, F., Jiang, Y., Li, Z., Huang, X. and Li, L. 2018. Phytochrome A Negatively Regulates the Shade Avoidance Response by Increasing Auxin/Indole Acidic Acid Protein Stability. *Developmental Cell*. **44**, pp.29-41.e4.

Yang, H.Q., Wu, Y.J., Tang, R.H., Liu, D., Liu, Y. and Cashmore, A.R. 2000. The C termini of Arabidopsis cryptochromes mediate a constitutive light response. *Cell*. **103**, pp.815–827.

Yang, S.F. and Hoffman, N.E. 1984. Ethylene Biosynthesis and its Regulation in Higher Plants. *Annual Review of Plant Physiology*. **35**, pp.155–189.

Yang, X., Lee, S., So, J.H., Dharmasiri, S., Dharmasiri, N., Ge, L., Jensen, C., Hangarter, R., Hobbie, L. and Estelle, M. 2004. The IAA1 protein is encoded by AXR5 and is a substrate of SCF TIR1. *Plant Journal*. **40**, pp.772–782.

Yi, C. and Deng, X.W. 2005. COP1 - From plant photomorphogenesis to mammalian tumorigenesis. *Trends in Cell Biology*. **15**, pp.618–625.

Zaki, M.H., Moran, D. and Harris, D. 1982. Pesticides in groundwater: the aldicarb story in Suffolk County, NY. *American journal of public health*. **72**, pp.1391–5.

Zaman, M., Kurepin, L. V, Catto, W. and Pharis, R.P. 2015. Enhancing crop yield with the use of N-based fertilizers co-applied with plant hormones or growth regulators. *Journal of the Science of Food and Agriculture*. **95**, pp.1777–1785.

Zawislak, K. and Tyburski, J. 1992. The tolerance of root, industrial and fodder crops to continuous cultivation. *Acta Academiae Agriculturae ac Technicae Olstenensis, Agricultura*. **55**, pp.149–162.

Zemlyanskaya, E. V., Omelyanchuk, N.A., Ubogoeva, E. V. and Mironova, V. V. 2018. Deciphering auxin-ethylene crosstalk at a systems level. *International Journal of Molecular Sciences*. **19**.

Zhang, H., He, H., Wang, Xuncheng, Wang, Xiangfeng, Yang, X., Li, L. and Deng, X.W. 2011. Genome-wide mapping of the HY5-mediated genenetworks in Arabidopsis that involve both transcriptional and post-transcriptional regulation. *Plant Journal*. **65**, pp.346–358.

Zhang, H., Rider, S.D., Henderson, J.T., Fountain, M., Chuang, K., Kandachar, V., Simons, A., Edenberg, H.J., Romero-Severson, J., Muir, W.M. and Ogas, J. 2008. The CHD3 remodeler PICKLE promotes trimethylation of histone H3 lysine 27. *Journal of Biological Chemistry*. **283**, pp.22637–22648.

Zhang, X., Garreton, V. and Chua, N.-H. 2005. The AIP2 E3 ligase acts as a novel negative regulator of ABA signaling by promoting ABI3 degradation. *Genes & development*. **19**, pp.1532–43.

Zhang, Y., Li, C., Zhang, J., Wang, J., Yang, J., Lv, Y., Yang, N., Liu, J., Wang, X., Palfalvi, G., Wang, G. and Zheng, L. 2017. Dissection of HY5/HYH expression in Arabidopsis reveals a root-autonomous HY5-mediated photomorphogenic pathway.

Zhang, Z.-Q. 2013. Animal biodiversity: An outline of higher-level classification and survey of taxonomic richness. *Zootaxa*. **3703**, pp.1–82.

Zhao, B. and Li, J. 2012. Regulation of Brassinosteroid Biosynthesis and Inactivation. *Journal of Integrative Plant Biology*. **54**, pp.746–59.

Zhao, Y. 2010. Auxin biosynthesis and its role in plant development. *Annual review of plant biology*. **61**, pp.49–64.

Zobel, R.W. 1974. Control of morphogenesis in the ethylene-requiring tomato mutant, diageotropica. *Canadian Journal of Botany*. **52**, pp.735–741.